The Development and Evaluation of Novel Monoclonal Antibodies Directed against Folate Pathway Components

Amy Elizabeth Quinn

A Thesis Submitted for the Degree of Doctor of Philosophy from the School of Clinical and Laboratory Sciences at Newcastle University, Newcastle Upon Tyne.

SCHOOL OF CLINICAL AND LABORATORY SCIENCES
NORTHERN INSTITUTE FOR CANCER RESEARCH

2008

Declaration

I hereby declare that as the author of this thesis, all the work reported was performed by myself. This thesis is original and has not been submitted for any other qualification.

Signed

Amy Elizabeth Quinn

Acknowledgements

I would like to thank my supervisors - Drs. Mik Pinkney and Nigel Piggott for their help, support and encouragement throughout this project; I also extend my thanks to Dr. Ian Milton for sponsorship of this project and use of the facilities at Leica Biosystems, Newcastle and Drs Craig Robson and Nicola Lawson for their generous offer of support when I needed it most.

I would like to acknowledge everyone, both at Leica and Newcastle University who have assisted me with training and techniques and everyone who has provided me with reagents and cell lines essential for successful completion of my project. I would also like to thank Mike Cole for his assistance with the statistical analysis of my data.

I would like to acknowledge my family, closest friends and my husband David for all their support and positive encouragement throughout – without them I could have never got through this.

This project was a BioNET industrial collaborative project funded and sponsored by Newcastle University and Leica Biosystems Newcastle (formerly Novocastra laboratories).

Publications

Smith, A.E., Pinkney, M., Piggott, N.H., Calvert, A.H., Milton, I.D. & Lunec, J. (2007) A Novel Monoclonal Antibody for Detection of FR-α in Paraffin Embedded Tissues. Hybridoma 26: (5) 281-288.

Quinn, A.E., Pinkney, M., Piggott, N.H., Calvert, A.H., Milton, I.D. & Lunec, J. (2009)

A Novel Monoclonal Antibody for detection of FPGS in Paraffin Embedded Tissues. Hybridoma 28: (6) 415-421

Nutt, J.E., Razak, A.R., O'Toole, K., Black, F., Quinn, A.E., Calvert, A.H., Plummer, E.R., Lunec, J. (2010) the role opf folate receptor alpha (FRalpha) in the response of malignant pleural mesothelioma to pemetrexed-containing chemotherapy. British Journal of Cancer 102: (3) 553-560.

Abstracts and Presentations

Smith, A.E., Pinkney, M., Piggott, N., Kucukmetin, A., Edmondson, R., Calvert, A.H. & Lunec, J.

The Development and Evaluation of a Novel Monoclonal Antibody
to FR-α Suitable for Use on Paraffin Embedded Samples.
Poster Presentation – Quinquennial Review of CRUK groups at the NICR, Oct 2006, Translational Research.

Amy E. Smith, Michael Pinkney, Nigel H. Piggott, Ali Kucukmetin, Richard Edmondson, Hilary Calvert, Ian D. Milton & John Lunec.

Novel Monoclonal Antibodies to Folate Receptor Alpha and Folylpolyglutamate Synthetase for use on Paraffin Embedded Samples.

Amerian Association for Cancer Research Meeting. April 2007 - Late Breaking Poster Session.

Abstract

Folates are essential in the *de novo* nucleotide biosynthetic pathway, folate receptor alpha (FR-α) is a folate transporter which is an attractive target for anticancer drug design due to its limited expression in normal tissues. It has great potential to direct therapies toward pathologic cells whilst minimizing toxicity in normal tissues. The enzyme folylpolyglutamate synthetase (FPGS) polyglutamates folates and folate analogues, trapping them within the cell and increasing their affinity as substrates for subsequent enzymatic reactions. Expression of folate biochemical pathway components, such as FR-α and FPGS, may be indicators of malignancy and also determine response to antifolate chemotherapeutics and other folate pathway targeted therapies currently being evaluated. Knowledge of their expression in tumours may enable optimal use by identifying responsive subgroups of patients. In spite of their importance in the diagnosis and treatment of cancer, the lack of monoclonal anti-FR-α and FPGS antibodies suitable for immunohistochemistry (IHC) analysis of formalin fixed, paraffin embedded biopsy samples or Western blot analysis has limited research in this area.

The aim of this project was to generate and fully characterize monoclonal antibodies to detect specific expression of these proteins in formalin fixed, paraffin embedded tissues for use on archival tissue and samples collected prospectively in connection with clinical trials of antifolates.

Novel monoclonal antibodies with specificity for sensitive detection of FR-α and FPGS in paraffin-embedded tissues were developed. ELISA and Western blot analysis confirmed specific reactivity of both antibodies to the recombinant protein, a single 40kD protein in whole cell lysates from cell lines known to express FR-α, and a single 60kD protein from cells expressing FPGS. Epitope mapping experiments confirmed specificity restricted to a linear epitope present in the protein target sequences.

IHC analysis of FR-α in a panel of normal tissues demonstrated predominantly membrane with cytoplasmic staining limited to some ovarian epithelia (inclusion cysts), placental trophoblasts and proximal kidney tubules; FPGS demonstrated a wider pattern of expression. FR-α analysis of a panel of malignant and benign tissues demonstrated limited expression with variable intensities of staining and patterns of membrane and cytoplasmic

reactivity between cases. In the majority of malignant ovarian tumours, including an archival tissue microarray (TMA) of 167 tumour samples, membrane staining was observed in 89% of cases. FPGS analysis on a panel of benign and malignant tissues demonstrated frequent and high cytoplasmic expression in a range of tumours compared to normal adjacent tissue.

The archival ovarian cancer TMA analysis showed a significant association between high expression of FR-α and poor patient survival ($p=0.012$, Cox regression) indicating a role for FR-α as a prognostic marker and potential therapeutic target for ovarian cancer and other cancers with expression of FR-α, detectable via the use of our antibody on FFPE tumour samples.

Abbreviations

5-FU	5-fluorouracil
αα	Amino acid
ABC	Streptavidin Biotin complex
AGE	Agarose gel electrophoresis
ALL	Acute lymphoblastic leukaemia
AMP	Adenosine monophosphate
AP	Alkaline phosphatase
APS	Ammonium persulphate
APES	Aminopropyl-tri-ethoxy-silane
AT	Adenine thymine
ATP	Adenosine triphosphate
AICAR	Aminoimidazole carboxamide ribonucleotide
AICARFT	Aminoimidazole carboxamide ribonucleotide formyltransferase
BCIP	5-bromo-4chloro-3-indolylphosphate
BLAST	Basic local alignment search tools
BP	Base pairs
BPB	Bromophenol blue
BSA	Bovine serum albumin
C_1	Single carbon fragments
CBC	Comparative biology centre
CIAP	Calf intestine alkaline phosphatase
CIT	Citrate
CO_2	Carbon dioxide
DAB	Diaminobenzidine tetrachloride

DCC	Dextran coated charcoal
DEPC	Diethylpyrocarbonate
DHF	Dihydrofolate
DHFR	Dihydrofolate reductase
DMF	Dimethyl formamide
DMSO	Dimethyl sulphoxide
DNA	Deoxyribonucleic acid
dNDP	Deoxynucleotide diphosphate
dNTP	Deoxynucleotide triphosphates
dsDNA	Double stranded deoxyribonucleic acid
dTMP	Deoxythymidine monophosphate
DTT	Dithiothrietol
dUMP	Deoxyuridine monophosphate
dUTP	Deoxyuridine triphosphates
EBI	European bioinformatics institute
ECL	Enhanced chemiluminescence
ELISA	Enzyme linked immunosorbent assay
ER	Oestrogen receptor
FACS	Fluorescence activated cell sorting
$FADH_2$	Flavin adenine dinucleotide
FBP	Folate binding protein
FCS	Foetal calf serum
fDUMP	Fluorodeoxyuridine monophosphate
FFPE	Formalin fixed, paraffin embedded
FPGH	Folylpolyglutamate hydrolase

FPGS	Folylpolyglutamate synthetase
FR	Folate receptor
FR-α	Folate receptor alpha
GAR	Glycinamide ribonucleotide
GARFT	Glycinamide ribonucleotide formyl transferase
GMP	Guanosine monophosphate
GPI	Glycophosphatidylinositol
GTP	Guanosine triphosphates
GST	Glutathione s transferase
HAT	Hypoxanthine, aminopterin, thymidine
HF	High-folate
HGPRT	Hypoxanthine-guanine phosphoribosyl transferase
HRP	Horseradish peroxidase
IF	Immunofluorescence
Ig	Immunoglobulin
IHC	Immunohistochemistry
IMP	Inosine monophosphate
IP	Intraperitoneal
IPTG	Isopropyl-D -thiogalactopyranoside
IV	Intravenous
LF	Low-folate
MAb	Monoclonal antibody
MPM	Malignant pleural mesothelioma
mRNA	Messenger ribonucleic acid
MS	Methionine synthase

MTA	Multitargeted antifolate
MTX	Methotrexate
NADH	Nicotinamide adenine dinucleotide
NADPH	Nicotinamide adenine dinucleotide phosphate
NBT	Nitroblue tetrazolium
NF	Normal-folate
NHL	Non-Hodgkin lymphoma
NRS	Normal rabbit serum
NSCLC	Non-small-cell lung cancer
OD	Optical density
OSE	Ovarian surface epithelium
PA	Polyacrylamide
PAGE	Polyacrylamide gel electrophoresis
PBS	Phosphate buffered saline
PCR	Polymerase chain reaction
PCS	Polycloning site
PEG	Polyethylene glycol
RE	Restriction endonuclease
RFC	Reduced folate carrier
RNA	Ribonucleic acid
RNR	Ribonucleotide reductase
RT	Reverse transcriptase
RTPCR	Reverse transcription polymerase chain reaction
SHMT	Serine hydroxy methyltransferases
SDS	Sodium dodecyl sulphate

SDS-PAGE	Sodium dodecyl sulphate polyacrylamide gel electrophoresis
TAXI	Tetracycline, ampicillin, X-Gal, IPTG
TBS	Tris buffered saline
T/E	Tris/EDTA
TEMED	Tetramethyl ethylene diamine
TFB	Transformation buffer
THF	Tetrahydrofolate
T_m	Melting temperature
TMA	Tissue microarray
TMP	Thymidine monophosphate
TS	Thymidylate synthase
Tx	Thioredoxin
UMP	Uridine monophosphate
UTP	Uridine triphosphate
WB	Western blot
WT	Wild type
X-Gal	5-bromo-4-chloro-3indolyl β-D-galactosidase

Hypothesis

Folate biochemical pathway components such as FR-α and FPGS are predicted to be determinants of response to novel antifolate drugs such as pemetrexed and other folate receptor targeted cancer therapies. Such drugs are showing promise in current cancer chemotherapy trials and knowledge of their level of expression in tumours will enable their optimal use by identifying responsive subgroups of patients. This thesis describes the development and validation of specific monoclonal antibodies to facilitate this.

To be practical for the analysis of protein biomarkers in multicentre clinical trials, antibodies are required which can be used on FFPE tissue, which is readily processed in local routine histology laboratories. To date, FR-α and FPGS antibodies suitable for immunohistochemical analysis of FFPE samples are not commercially available. A major aim of this project is to rectify this situation by the production of antibodies directed against both proteins. The antibodies generated may be of particular use as companion diagnostics to facilitate the screening ofpatients to establish the predictive value and significance of FR-α and FPGS expression for the therapeutic response to antifolates, in the context of multicentre clinical trials. In addition, the antibodies may also be used to predict response of other folate receptor targeted drug delivery systems and therapies currently under investigation.

The antibodies developed in this project were evaluated on cultured tumour cell lines and panels of archival FFPE normal tissue and tumour samples, including a tissue microarray of 167 ovarian tumour samples to ensure the patterns of immunoreactivity were consistent with previous published data and to test the hypothesis that FR-α and FPGS may be markers of poor prognosis in ovarian tumours with high expression.

It is also hypothesised that FR-α expression may be altered via changes in extracellular conditions or via the action of hormones. The antibody validation experiments were also complimented by *in vitro* studies to determine whether alteration of extracellular folate concentration or treatment of breast and ovarian tumour cell lines with anti-oestrogens such as tamoxifen increases FR-α expression and potentially sensitises the cells to antifolates such as pemetrexed which are hypothesised to be internalized via FR-α.

Aims and Expectations

- To produce monoclonal antibodies directed against FR-α and FPGS, for which there is an identifiable market as research tools and potential companion diagnostic/ prognostic markers of response in conjunction with the use of antifolate cancer chemotherapy agents and other agents currently being investigated.
- Evaluate their ability to detect expression of these proteins by immunohistochemical analysis of FFPE tissue samples.
- Evaluate the suitability of the antibodies for detection of FR-α and FPGS proteins by Western blotting of sodium dodecyl sulphate (SDS) polyacrylamide gel electrophoresis (SDS-PAGE) separations of tissue protein extracts.
- Epitope map the antibodies to ensure their specificity for the target.
- Assess the expression levels of FR-α and FPGS on ovarian cancer patient samples and evaluate their utility as prognostic markers.
- Determine whether extracellular folate concentration changes and antioestrogens alter the expression of FR-α. This would have implications for the response to FR-α targeted therapies.
- Evaluate the suitability of the antibodies for application in other techniques such as IF and FACS and identify any potential neutralizing properties they may possess.

Table of Contents

Declaration II

Signed II

Acknowledgements III

Publications III

Abstracts and Presentations IV

Abstract V

Abbreviations VII

Hypothesis XII

Aims and Expectations XIII

Table of Contents XIV

List of Tables XXX

Chapter One 1

1. General Introduction 1

1.1. The Immune System 1

1.1.1. Innate Immunity 1

1.1.2. Adaptive Immunity 2

1.1.3. B-Lymphocytes 2

1.2. Antibodies 3

1.3. Antigens 4

1.4. Polyclonal Antibodies 5

1.5. Monoclonal Antibodies 5

1.6. Metabolism 7

1.7. Folates 8

1.7.1. The Folate Pathway 9

1.8. Folate Transport 12

1.8.1. The Reduced Folate Carrier 12

1.8.2. Folate Receptors (FR's) 13

1.8.3. Folate Receptor Alpha Expression 18

1.8.4. Regulation of Folate Receptor Alpha Expression 20

1.8.5. Folate Receptor Alpha and Cancer 21

1.8.5.1. Selection of Patients for Folate Receptor Alpha Targeted Therapies 23

1.9. Folylpolyglutamate Synthetase 24

1.10. Summary 26

1.11. Research Plan 27

Chapter Two 29

2. Antigen Design and Preparation 29

2.1. General Introduction 29

2.2. Recombinant Protein Expression Systems 29

2.2.1. The pET Expression System 30

2.3. Aims and Objectives 34

2.4. Materials and Methods 35

2.4.1. Antigen Design 35

2.4.1.1. Homology Searches 35

2.4.1.2. BLAST Searches 35

2.4.2. Target Sequence Selection 35

2.4.3. Restriction Mapping 36

2.4.4. Oligonucleotide Primer Design 36

2.4.5. Oligonucleotide Primer Synthesis 37

2.4.5.1. Oligonucleotide Primer Quantitation 37

2.4.6. RNA Preparation 38

2.4.7. Complementary DNA Preparation/RT-PCR 38

2.4.8. The Polymerase Chain Reaction (PCR) 39

2.4.9. Agarose Gel Electrophoresis 41

2.4.9.1. Preparation of DNA Size Markers 41

2.4.9.2. Agarose and Running Buffer Preparation 42

2.4.10. Gel Extraction/ Fragment Preparation 42

2.4.11. Preparation of pGEM T-easy plasmid construct 42

2.4.12. pGEM T-Vector Ligations 43

2.5. Protein Expression 44

2.5.1. Preparation of Growth Media 44

2.5.1.1. 2YT Media 44

2.5.1.2. 2YT Agar 44

2.5.2. Overnight *E.coli* cultures 44

2.5.3. Novablue *E.coli* Non-Expression Host 45

2.5.4. Competent *E.coli* Preparation 46

2.5.5. Transformation of pGEM T Easy Constructs into Novablue *E.coli* 46

2.5.6. Selection Plates 47

2.5.7. Colony Screening Procedure and Plasmid Isolation 47

2.5.7.1. Plasmid Minipreparations 47

2.5.8. Restriction Digestion of Plasmid DNA 47

2.5.9. Automated DNA Sequencing 49

2.5.10. Expression of FR-α and FPGS Recombinant Proteins 49

2.5.10.1. Subcloning in to pET Expression Vectors 49

2.5.10.2. Preparation of the Insert for Subcloning 55

2.5.10.3. Preparation of pET vectors 55

2.5.10.4. Ligation of DNA fragments into pET constructs 56

2.5.10.5. Transformation into Novablue E.coli 56

2.5.10.6. Screening Transformant Colonies 56

2.5.11. Transformation into an Expression Host 57

2.5.11.1. E.coli BL21 (DE3) plysS and Tuner (DE3) plysS 57

2.5.11.2. Transformation into E.coli BL21/Tuner 57

2.5.12. Fusion Protein Expression 58

2.5.12.1. Small Scale Fusion Protein Induction 58

2.5.13. SDS Polyacrylamide Gel Electrophoresis 58

2.5.13.1. Large Scale Fusion Protein Induction 59

2.5.14. Sonication of Large Scale Products 60

2.5.15. His-Bind Column Chromatography 60

2.5.15.1. Soluble Columns 60

2.5.15.2. Insoluble Columns 61

2.5.15.3. Protein Assay 61

2.5.16. Refolding of Insoluble Protein Fractions 62

2.5.17. Refolding by Dialysis 62

2.5.18. Refold Columns 63

2.6. Results - Antigen Design 63

2.6.1. Amino Acid and Gene Sequences 63

2.6.2. Target Sequence Selection 63

2.6.3. Primer Design 64

2.6.4. Amplification of FPGS2 and FR-α DNA 65

2.6.5. Amplification of FPGS3 cDNA 66

2.6.6. Fragment Preparations and Restriction Digests 67

2.6.7. pET Cloning 70

2.6.8. Expression of FR-α and FPGS Recombinant Proteins in *E.coli* 70

2.6.9. Large Scale Recombinant Protein Expression 73

2.6.10. Recombinant FR-α and FPGS Protein Purification 73

2.6.10.1. FPGS2 73

2.6.10.2. FR-α 74

2.6.10.3. FPGS3 76

2.7. Discussion 78

2.7.1. Recombinant Protein Production 78

Chapter Three 81

3. Antibody Production 81

3.1. Hybridoma Technology 81

3.1.1. Cell Fusion Technique 81

3.1.2. Antibody Screening and Characterisation 83

3.1.3. Epitope Mapping 84

3.2. Aims and Objectives 87

3.3. Materials and Methods 88

3.3.1. Mouse Immunisation Schedule 88

3.3.2. Growth of Cell Lines 89

3.3.3. Protein Estimation 90

3.3.4. Western Blotting (WB) 91

3.3.5. Assessment of Bleeds via Western Blot 92

3.3.6. Immunohistochemistry 94

3.3.6.1. Indirect Avidin-Biotin (ABC) Technique Immunohistochemistry 96

3.3.6.2. Novolink™ Polymer Immunohistochemistry 97

3.3.6.3. Bleed Assessment via Immunohistochemistry 97

3.3.7. NS-1 Myeloma Cell Culture 98

3.3.8. Cell Fusion Procedure 99

3.3.8.1. Fusion Preparation 99

3.3.8.2. Splenocyte Preparation 99

3.3.8.3. NS-1 Myeloma Cells 99

3.3.8.4. Fusion in PEG 100

3.3.9. Enzyme Linked Immunosorbent Assay (ELISA) 100

3.3.9.1. Screening for Specific Hybridoma Colonies via ELISA 100

3.3.9.2. ELISA Screening of Hybridomas against Fusion Protein Tags 102

3.3.10. Screening ELISA Positive Hybridomas via IHC 102

3.3.11. Cloning Hybridomas via Limiting Dilution 102

3.3.11.1. Assessment of 1st and 3rd Clones via Western Blot Analysis 103

3.3.12. Freezing Down Cells 103

3.3.13. Weaning into R20 Medium 104

3.4. Antibody Validation and Characterisation 104

3.4.1. Characterisation of Weaned Clones via Immunohistochemistry 104

3.4.2. Characterisation of Weaned clones via Western Blot Analysis 104

3.4.3. Further Characterisation 105

3.4.4. Epitope Mapping 105

3.5. Results – Hybridoma Technology 107

3.5.1. Mouse Immunisation and Polyclonal Assessment 107

3.5.1.1. FPGS Immunisations/Polyclonal Assessment 107

3.5.2. FR-α Immunisations/Polyclonal Assessment 109

3.5.2.1. Western Blot Studies to Identify the Cause of Cross-Reactivity 111

3.5.3. Production of Anti FR-α and FPGS Antibodies 114

3.5.3.1. Anti FPGS Antibody Generation 114

3.5.4. FPGS Expression via Western Blot Analysis 115

3.5.4.1. FPGS Extended Panel 116

3.5.4.2. FPGS Leukaemia Panel 118

3.5.5. FPGS Expression in Normal and Inflamed Tissues 118

3.5.6. FPGS Expression in Benign and Malignant Tissues 121

3.5.7. FPGS Further Characterisation 124

3.5.8. FPGS Epitope Mapping 125

3.5.8.1. Anti FR-α Antibody Generation 126

3.5.8.2. FR-α Expression via Western Blot Analysis 128

3.5.8.3. FR-α Extended Panel 128

3.5.8.4. FR-α Leukaemia Panel 130

3.5.9. FR-α Expression in Normal and Inflamed Tissues 130

3.5.10. FR-α Expression in Benign and Malignant Tissues 132

3.5.11. FR-α Further Characterisation 135

3.5.12. FR-α Epitope Mapping 136

3.5.13. mOV 18 Epitope Mapping 137

3.5.14. LK26 Epitope mapping 138

3.6. Discussion 139

3.6.1. FPGS Antibody Development 139

3.6.1.1. FPGS WB Analysis 139

3.6.1.2. FPGS IHC Analysis 141

3.6.1.3. FPGS Epitope Mapping 141

3.6.2. FR-α Antibody Development 142

3.6.2.1. FR-α WB Analysis 143

3.6.2.2. FRα IHC Analysis 145

3.6.2.3. FR-α Epitope Mapping 146

Chapter Four 150

4. Ovarian Tissue Microarray Analyses 150

4.1. Ovarian TMA Study Aims and Objectives 151

4.2. Ovarian TMA Study Materials and Methods 151

4.2.1. Assessment of TMA IHC Staining- Scoring System Used 152

4.2.2. Statistical Analysis 153

4.2.2.1. Kaplan-Meier Survival Plots and Log-Rank Test 153

4.3. Ovarian TMA Study - Results 154

4.3.1. FR-α and FPGS Images and Scoring 154

4.3.2. Statistical Analysis of Overall Survival 162

4.3.2.1. Overall Survival and FR-α Score 1, 2 and Mean 164

4.3.2.2. Overall Survival and FPGS Score 1, 2 and Mean 166

4.3.2.3. Overall Survival Multivariate Analysis 166

4.3.3. Statistical Analysis of Time to Relapse 167

4.3.3.1. Relapse Free Survival and FR-α Score 1, 2 and Mean 169

4.3.3.2. Relapse Free Survival and FPGS Score 1, 2 and Mean 171

4.3.4. Relapse Free Survival Multivariate Analysis 171

4.3.4.1. Correlations between FR-α, FPGS and Other Prognostic Variables 172

4.4. Discussion 176

Chapter Five 182

5. Cell Studies 182

5.1. Cell Studies - Aims and Objectives 184

5.2. Oestrogen Regulation Study – Materials and Methods 185

5.2.1. Culture and Treatment of Cells 185

5.3. Oestrogen Regulation Study - Results 186

5.4. Oestrogen Regulation Study – Discussion 187

5.5. Extracellular Folate Concentration Study – Materials and Methods 188

5.6. Extracellular Folate Concentration Study – Results 189

5.6.1. FPGS 189

5.6.2. FR-α 190

5.7. Extracellular Folate Concentration Study – Discussion 190

5.8. mOV18 Comparative Study –Materials and Methods 191

5.9. mOV18 Comparative Study - Results 192

5.10. mOV18 Comparative Study – Discussion 195

5.11. Breast Cancer Case Study – Materials and Methods 195

5.12. Breast Cancer Case Study – Results 196

5.13. Breast Cancer Case Study - Discussion 197

5.14. Immunofluorescence Studies – Materials and Methods 197

5.15. Immunofluorescence Studies - Results 198

5.16. Immunofluorescence Studies - Discussion 201

6. Concluding Remarks and Future Direction 203

References 208

List of Figures

Figure 1-1: Antibody structure. 4

Figure 1-2: Diagrammatic representation of the structure of the folic acid molecule. 9

Figure 1-3: General overview of the folate metabolic pathway.. 11

Figure 1-14: Diagrammatic representation of the RFC.. 13

Figure 1-15: GPI anchor structure.. 14

Figure 1-16: The organisation of human FR genes. 16

Figure 1-17: Diagrammatic representation of the folate receptor potocytosis mechanism... 17

Figure 2-1: The control elements of the pET system. 32

Figure 2-2: Overview of the recombinant protein production methods used for the generation of recombinant FR-α and FPGS 33

Figure 2-3: Primer Tm calculation. 37

Figure 2-4: Steps involved in PCR reactions. 40

Figure 2-5: T-Easy Vector Map. 43

Figure 2-6: Photograph of blue-white selection plate. 45

Figure 2-7: Common RE's generating both blunt and sticky ends. 48

Figure 2-8: pET 21 Vector map. 51

Figure 2-9: pET 41 Vector map 53

Figure 2-10: pET32 Vector map 54

Figure 2-11: FR-α target region. 64

Figure 2-12: FPGS target region. 64

Figure 2-13: FR-α and FPGS PCR products. 66

Figure 2-14: FPGS nested PCR product. 67

Figure 2-15: FR-α and FPGS restriction digests. 68

Figure 2-16: Typical DNA sequencing chromatogram trace obtained. 69

Figure 2-17: FPGS small scale inductions. 71

Figure 2-18: FR-α pET21 small scale inductions. 72

Figure 2-19: FR-α pET41 small scale inductions 72

Figure 2-20: FPGS insoluble fractions. 74

Figure 2-21: FR-α insoluble fractions. 75

Figure 2-22: FR-α refolded fractions. 76

Figure 2-23: FPGS dialysed protein. 77

Figure 3-1: Overview of de novo and nucleotide salvage pathways in mammalian cells. 83

Figure 3-2: Overview of MAb production 86

Figure 3-3: Semi-dry blotting apparatus. 93

Figure 3-4: Indirect ABC technique immunohistochemistry. 95

Figure 3-5: Novolink™ polymer methodology. 97

Figure 3-6: Positive ELISA plate. 101

Figure 3-7: AP WB of FPGS polyclonal bleed. 108

Figure 3-8: Polyclonal and monoclonal comparison. 108

Figure 3-9: FR-α polyclonal bleed. 110

Figure 3-10: FPGS polyclonal bleed. 115

Figure 3-11: FPGS extended panel WB. 116

Figure 3-12: FPGS extended panel (2) WB. 117

Figure 3-13: FPGS leukaemia panel WB. 118

Figure 3-14: FPGS normal panel. 120

Figure 3-15: FPGS tumour panel.. 123

Figure 3-16: FPGS pre-treatment evaluation. 124

Figure 3-17: FPGS epitope mapping. 125

Figure 3-18: FPGS epitope. 126

Figure 3-19: FR-α bleed evaluation. 127

Figure 3-20: FR-α extended panel WB. 128

Figure 3-21: FR-α extended panel (2) WB. 129

Figure 3-22: FR-α leukaemia panel WB. 130

Figure 3-23: FR-α normal panel. 132

Figure 3-24: FR-α tumour panel (1). 134

Figure 3-25: FR-α pre-treatment selection. 135

Figure 3-26: FR-α epitope mapping. 136

Figure 3-27: FR-α epitope. 137

Figure 3-28: mOV18 epitope mapping. 137

Figure 3-29: mOV18 epitope. 138

Figure 3-30: LK26 epitope mapping. 138

Figure 4-1: Photograph of the OVCA TMA slides. 154

Figure 4-2: Photograph of OVCA1 stained with FR-α. 155

Figure 4-3: Photograph of twelve TMA cell cores (x1) stained with FR-α. 156

Figure 4-4: Photograph of eight TMA cores (x4) stained with FR-α. 157

Figure 4-5: Photograph of OVCA1 stained with FPGS. 158

Figure 4-6: Twelve TMA cell cores (x1) stained with FPGS. 159

Figure 4-7: Photograph of eight TMA cores (x4) stained with FPGS. 160

Figure 4-8: FR-α membrane staining. 161

Figure 4-9: FPGS cytoplasmic staining. 161

Figure 4-10: FR-α Kaplan-Meier analysis (1). 164

Figure 4-11: FR-α Kaplan-Meier analysis (2). 165

Figure 4-12: FR-α Kaplan-Meier analysis (3). 165

Figure 4-13: FPGS Kaplan-Meier analysis (1). 166

Figure 4-14: FR-α Kaplan-Meier analysis (4). 169

Figure 4-15: FR-α Kaplan-Meier analysis (5). 170

Figure 4-16: FR-α Kaplan-Meier analysis (6). 170

Figure 4-17: FPGS Kaplan-Meier analysis (2). 171

Figure 4-18: Statistical analysis of the relationship between FR-alpha IHC score 1 and the other prognostic variables. 174

Figure 4-19: Statistical analysis of the relationship between FPGS IHC score 2 and the other prognostic variables. 175

Figure 5-1: FR-α oestrogen regulation WB. 186

Figure 5-2: FPGS extracellular folate concentration WB. 189

Figure 5-3: FR-α extracellular folate concentration WB. 190

Figure 5-4: FR-α mOV18 comparative study.. 194

Figure 5-5: FR-α Breast cancer IHC case study. 196

Figure 5-6: IF comparative study WB.. 200

List of Tables

Table 2-1: RT-PCR Components 39

Table 2-2: PCR Mixture Components 40

Table 2-3: Standard Conditions used in PCR reactions. 41

Table 2-4: Reagents used in T-vector ligations. 44

Table 2-5: Reagents used for restriction digests. 49

Table 2-6: Reagents used for restriction digestion in preparation for subcloning 55

Table 2-7: Reagents used for pET vector digestion 55

Table 2-8: Reagents used for ligations 56

Table 2-9: FR-α and FPGS forward and reverse primers. 65

Table 2-10: FPGS Nested PCR primer sequences. 67

Table 2-11: FR-α primer sequences. 70

Table 2-12: Summary of some of the recombinant proteins generated in this project. 77

Table 3-1: Mouse immunisation schedules employed in this study. 89

Table 3-2: Human cell lines used for characterisation of FR-α and FPGS antibodies. 90

Table 3-3: Immunostaining for wild-type FPGS NN 3.2 on normal and inflamed tissues. 119

Table 3-4: Immunostaining for FPGS on a range of benign and malignant tissues 122

Table 3-5: Immunostaining for wild-type FR-α BN 3.2 on normal and inflamed tissues..... 131

Table 3-6: Immunostaining for FR-α on a range of benign and malignant tissues 133

Table 4-1: Summary of statistical analysis of overall survival 163

Table 4-2: Summary of statistical analysis of time to relapse 168

Table 4-3: Summary of the correlations between FR-α/FPGS and the other prognostic variables. 173

Chapter One

Chapter One

1. General Introduction

1.1. The Immune System

The immune system is the body's defence system against foreign agents, infectious organisms and cancerous cells. It has the capacity to generate an enormous variety of cells and molecules which act in synergy to specifically recognise and eliminate countless foreign organisms.

The immune response can be broadly divided into two phases – immune recognition and response. Immune recognition is extremely specific and can identify subtle chemical differences which distinguish one pathogen from the next. Furthermore, this recognition system is able to discriminate between foreign molecules and the body's own cells and proteins.

Once a pathogen has been recognized, the immune system recruits a variety of cells and molecules to generate an effector response. Subsequent exposure to the same pathogen evokes immunological memory, characterised by a heightened immune reaction and a more rapid response (Goldsby, Kindt, Osborne, & Kiuby, 2003).

1.1.1. Innate Immunity

Immunity itself can also be segregated into two broad categories; the less specific component, innate immunity, provides the first line of defence against infection and prevents the penetration and spread of many infectious agents. Innate immunity is nonspecific and does not improve with repeated exposure, but does provide broad reactivity against various frequently encountered foreign pathogens.

Components of the innate immune system include a variety of anatomic, physiological, biochemical, inflammatory and cellular barriers including skin, mucosa, lysozymes, complement and phagocytes (Goldsby et al., 2003).

1.1.2. Adaptive Immunity

Adaptive immunity differs from innate immunity as it is able to recognise and selectively eliminate foreign pathogens. Adaptive immune responses differ between individuals as they are reactions to specific antigenic challenges.

The antigenic specificity of the adaptive immune system allows it to distinguish subtle differences among antigens and is capable of generating tremendous diversity in its recognition molecules. Immunologic memory allows the adaptive immune response to confer lifelong immunity to many pathogens after just one initial exposure.

Adaptive immunity is not independent of innate immunity and both systems work intimately together. Immune responses can be divided into cell mediated and humoral responses. Cell mediated immunity can be transferred only by the administration of T-lymphocytes from an immune individual; in contrast humoral immunity refers to transient immunity that can be transferred to a non-immune individual by the administration of serum antibodies from an immune individual (Goldsby et al., 2003). As this project is concerned with the humoral branch of the immune response this branch only will subsequently be discussed.

1.1.3. B-Lymphocytes

B-lymphocytes mature in the bone marrow and each cell expresses a membrane bound antibody molecule. As a B-cell matures, random rearrangements of gene segments encoding an antibody molecule generate a vast number of B-cells with different antigenic specificities. Naive B-cells circulate and, upon first encounter with a pathogen whose antigen matches the membrane bound antibody, divide rapidly and differentiate into clones of antigenically committed mature B-lymphocyte daughter cells with a single, distinct specificity. Each cell clone recognises a discrete, identical site of amino acids (epitope) on an antigen. Epitopes can be both linear and conformational in nature. Memory B-cells are identical to the naive cell, expressing the same membrane bound antibody but have a longer lifespan. Plasma cells are B cells containing no membrane bound antibody but produce antibody in a secreted form, and have a finite lifespan of only a few days (Goldsby et al., 2003).

1.2. Antibodies

Antibodies function as the effectors of the humoral immune response by binding to antigen and neutralising it or facilitating its elimination. When an antigen is coated with antibody it can be eliminated in two ways:

- It can crosslink several antigens, forming clusters for digestion by phagocytosis; this occurs via activation of the complement system and results in lysis of the foreign organism.
- Antibodies can also 'coat' (opsonise) an organism, thus neutralising it and preventing it from binding to host cells (Guyton & Hall, 1997) .

Antibodies (also termed Immunoglobulins, Ig's) are glycoproteins residing in the serum fraction of blood (Tiselius, 1939) and have a common structure of four peptide chains, consisting of two identical light chains and two identical heavy chains; these are linked to each other by disulphide bonds and various noncovalent linkages to form a heterodimer (Figure 1-1). Similar interactions link the two heavy and light chains to form a dimer of dimers, forming the basic 4 chain structure of an antibody molecule (Guyton & Hall, 1997).

Approximately the first 110 amino acids of the amino terminal region of a light or heavy chain can show great variation among antibodies and it is this region which is responsible for their defined specificity. The light chains contain a constant and a variable domain and are classified as either κ or λ, based upon small differences in their polypeptide structure. Each antibody contains two light chains which are always identical, but it is the heavy chains which determine the antibody subclass (isotype). There are five types of mammalian Ig heavy chain: α, δ, ε, γ and μ; these chains are found in IgA, IgD, IgE, IgG and IgM antibodies respectively (Jaton & Riesen, 1976). Each heavy chain contains a constant and a variable region, the constant region being almost identical in all antibodies of the same class. Each isotype differs in its biological properties, function and location. Igs can be further divided into sub classes/ isotypes based upon minor differences in the sequences of α and γ heavy chains: α1, α2, γ 1, γ2, γ3 and γ4 giving rise to immunoglobulins IgA1, IgA2, IgG1, IgG2, IgG3 and IgG4 respectively. IgG is the major Ig present in the serum and provides the majority of antibody based immunity to pathogens (Goldsby et al., 2003).

Digestion of an antibody molecule with the enzyme papain produces three antibody fragments; two identical with antigen binding activity, denoted Fab fragments with a MW of 45,000 Da, and one fragment with no antigen binding activity, denoted the Fc fragment with a MW of 50,000 Da (Figure 1-1).

Figure 1-1: Antibody structure. Each heavy and light chain in an Ig molecule contains an amino terminal variable (V) region (pale blue, yellow respectively), the remainder of the molecule the constant (C) regions (dark blue and purple) exhibit limited variation, defining the two light and five heavy chain subclasses. The Fc and Fab/ Fab^2 regions are also depicted (Abcam).

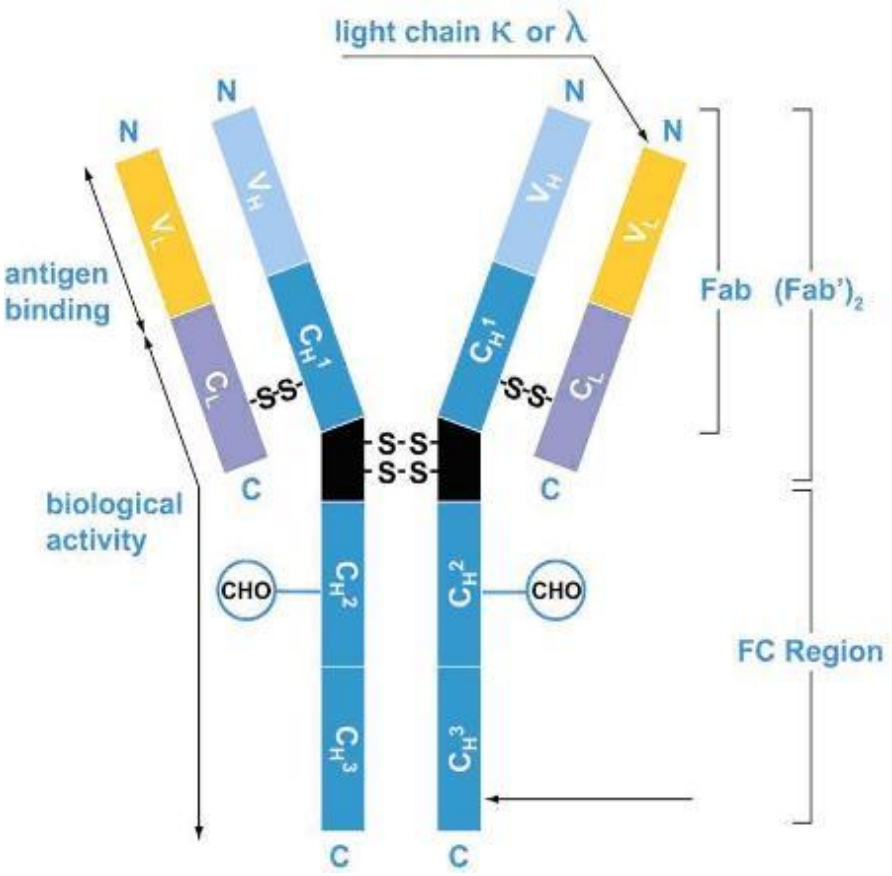

1.3. Antigens

Substances which are recognised by the B-cell antibody are termed antigens; the basic principle of any immunological technique is that an antibody will combine with its specific antigen to give an exclusive complex of Ab/Ag. Classically, an antigen is defined as any substance which elicits an immune response in a susceptible animal and is capable of binding with the specific antibodies generated. Antigens are usually of a high molecular

weight and are commonly proteins or polysaccharides although nucleic acids, lipids and peptides have also been reported to function as antigens (Goldsby et al., 2003).

For an efficient Ag/Ab interaction to occur the epitope must be exposed and available for binding, alterations in the conformation of epitopes through tissue processing, fixation, reduction and pH changes may affect the binding. It is for this reason antibodies are often effective for one particular immunological technique such as immunohistochemistry (IHC) but are unsuitable for application in a different technique such as Western blot (WB) or immunoprecipitation of native proteins.

1.4. Polyclonal Antibodies

Prior to 1975, the only antibodies available were polyclonal in nature. Polyclonal antibodies refer to antibodies present in the crude serum of an immunised animal, capable of recognising a number of different immunogenic epitopes of the administered immunogen. These antibodies may be of different subclasses. It will also contain other, sometimes large amounts of undesirable immunoglobulins produced via the animals immune response and, depending on the immunogenicity of the administered antigen may make up as little as 5% of the total immunoglobulin present. The presence of such antibodies increases the risk of cross reactivity and anomalous results and variability between batches often leads to inconsistencies in results. However, despite the drawbacks these antibodies are often used as they are quick and inexpensive to produce, requiring little skill or technical expertise. They are particularly useful when amplification of a signal from a target protein with low expression is required as they recognise multiple epitopes on one protein.

1.5. Monoclonal Antibodies

Monoclonal antibodies, in contrast are slow and expensive to produce and require high technology and extensive technical skills in order to produce successful antibodies. Large quantities of specific antibodies can be produced and their specificity ensures that only one epitope is recognised on an antigen, this is extremely useful when observing subtle protein alterations and the antibodies are less likely to cross react with other proteins and generally produce less background cross reaction. Once a hybridoma is established a constant and

renewable antibody source is generated and all batches are identical, eliminating the problem of batch variability associated with polyclonal antibodies. Monoclonal antibodies are only one subclass, usually IgG, allowing for selection of an appropriate secondary antibody for detection.

Monoclonal antibodies (MAbs) have revolutionised immunology, their ability to discriminate between antigens has had a major impact upon numerous research areas including cancer, virology and inflammatory diseases. MAbs have several different roles and may be used in all stages of cancer therapy from the diagnosis, monitoring and finally also in the treatment of the disease. MAbs are produced by a specialised cell fusion technique, the methodology of which will be discussed in detail in section 3.1. The resultant antibodies generated are derived from stable fusion cells which can be grown in culture secreting genetically identical antibodies.

Their precise antigen specificity and ability to distinguish fine structural antigenic differences between proteins overcome the problems with cross reaction associated with polyclonal antisera and make them powerful biochemical tools. In addition to their therapeutic potential they are also extremely versatile in molecular biology, with application in ELISA, IHC, Western blotting (WB) and immunofluorescence (IF); convenient labelling with fluorescent or electron dense particles allow their application in both fluorescence and electron microscopy.

As therapeutic agents, MAbs can be used directly to react with antigens on the surface of cancer cells and may enhance the immune response. They can be selected to act against growth factor receptors, inhibiting tumour growth. In addition they can be conjugated to anticancer drugs, radioisotopes or other toxins; upon binding to their antigen they can then selectively target the agent they are carrying to the tumour cells.

Animal antibodies may elicit an immune response themselves in an individual. Many antibody therapies also require humanisation of the antibody before they can be used in order to reduce the likelihood of an immune reaction (Schroff, Foon, Beatty, Oldham, & Morgan, 1985).

MAbs have had tremendous success to date, particularly in haematologic malignancies and in a number of solid tumours. To date the FDA have approved 21 MAb products, with six of

these being approved specifically for their use in cancer. The first MAb to receive FDA approval was Rituximab, a humanised MAb directed against CD20, a B-cell antigen expressed to a high degree in B cell malignancies, it is indicated for the treatment of low-grade lymphomas refractory to conventional therapy (Hainsworth, 2000; Hainsworth et al., 2000). Other MAbs include Trastuzumab (Herceptin®), a humanised McAb targeting the HER-2/neu antigen expressed in 25-35% of breast cancers and Edrecolomab targeting the 17-1A antigen seen in colon and rectal malignancies (Hainsworth et al., 2000; Haller, 2001).

MAbs also have application outside of cancer therapy, including Palivisumab, used in the treatment of respiratory syncitial virus and Infliximab, which targets tumour necrosis factor alpha (TNF-α), used in the treatment of Crohns disease and arthritis (Alkan, 2004).

The 'magic bullet' approach to cancers is the ultimate aim in cancer therapies, to selectively target the tumour whilst protecting normal tissues from any of the toxic effects. MAb's by their very nature have the potential to do just this, making them extremely attractive current and future tools in the fight against cancers.

1.6. Metabolism

Glucose and other food molecules taken in from the diet are catabolised via controlled, stepwise oxidation processes, in order to provide chemical energy in the form of ATP and NADH.

The products of glycolysis, the citric acid cycle and oxidative phosphorylation occur in the cytosol, mitochondrial matrix and mitochondrial membrane respectively and serve as the starting material for each subsequent reaction.

As well as catabolic reactions, the intermediate products from both glycolysis and the citric acid cycle are used to produce small molecules used as raw materials in various biosynthetic pathways. One of such pathways is the synthesis of activated precursors, which ultimately form new DNA.

Nucleotides, needed to form both RNA and DNA are synthesized via specialised biosynthetic pathways; carbon and nitrogen atoms present in purine and pyrimidine bases are derived from amino acids; deoxyribose and ribose sugars are derived from glucose (Alberts et al., 2002).

Nucleotides play a central role in almost all biochemical processes carried out within the human body. Not only are they the monomeric components of DNA and RNA, but they also drive many free energy requiring reactions, regulate numerous metabolic pathways, mediate hormone signals and are essential coenzymes in a number of enzymatic reactions. Almost every cell in the human body can synthesize nucleotides *de novo* and from the degradation products of nucleic acids, reflecting their vital importance (Voet & Voet, 2004).

1.7. Folates

Folate is derived from the latin word 'folium' meaning leaf, it is found in high concentrations in green, leafy vegetables and was first isolated from spinach in 1941 (Mitchell, Snell, & Williams, 1941).

Folate is the generic term given to a large family of B vitamins with similar biological activity. Folates exist in various oxidation states, the most oxidised and stable of which is folic acid (pteroylmonoglutamate, PteGlu, Figure 1-2), used in nutritional supplements and food fortification. Naturally occurring folates are also used as pharmaceutical agents in the treatment of various cancers and anaemia (Fitzpatrick, 2003).

Folic acid and its various coenzymes facilitate the transfer of single carbon (C_1) fragments from donor molecules and are involved in methylation reactions, including purine and pyrimidine nucleotide biosynthesis, amino acid conversions such as the conversion of serine to glycine, catabolism of histidine to glutamic acid and the conversion of homocysteine to methionine (Fitzpatrick, 2003).

The chemical structure of folate is comprised of a para-amino benzoic acid linked at one end to a 2-amino, 4-hydroxy- pteridine ring (pteroic acid) and at the other end to a variable number of glutamic acid moeties, typically 1-9 residues (Figure 1-2). The pteridine ring is the component of the molecule which can be altered in its oxidation state at the N^5 and N^{10} positions. This ring cannot be synthesized endogenously by mammalian cells and must be obtained from exogenous sources via the diet or from intestinal microflora (Berg, Tymoczko, & Stryer, 2002; Rosenblatt, 1995).

Figure 1-2: Diagrammatic representation of the structure of the folic acid molecule. a) P-amino benzoic acid is linked at one end to 6 methyl pteridin, forming pteroic acid and at the other end to a variable number of glutamic acid moieties, forming the whole folic acid molecule. b) The structure of the polyglutamic acid molecule, three residues are represented but up to nine residues can be attached to the folic acid molecule (Polonen, 2000).

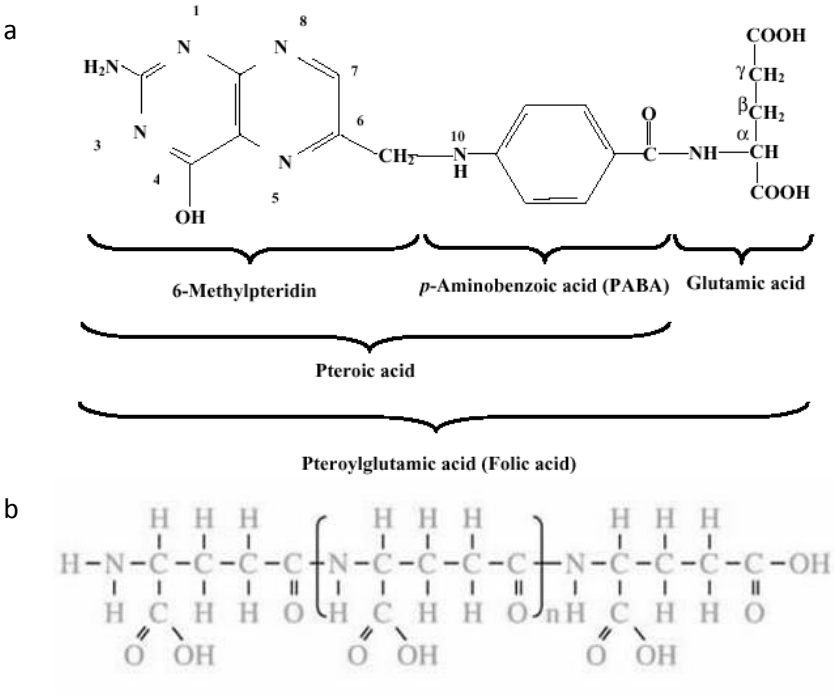

1.7.1. The Folate Pathway

Folates taken in from the diet are absorbed through the intestine in the monoglutamyl form, primarily as N^5-methyl tetrahydrofolate (THF). Transport through the membrane is facilitated by both receptor and carrier mediated mechanisms via the folate receptor (FR) and reduced folate carrier (RFC) respectively. Once inside the cell monoglutamyl folates are polyglutamated via the action of the enzyme folylpolyglutamate synthetase (FPGS, Figure 1-3). These steps will be discussed in more detail in section 1.9.

N^5-methyl THF is converted into its more versatile cofactor N^5,N^{10}-methylene THF via the action of the enzyme serine hydroxymethyl transferase (SHMT). Demethylation of 5-methyl THF can also occur via the vitamin B^{12} dependent reaction with methionine synthase (MS), yielding THF (Figure 1-3). N^5,N^{10}-methylene THF is a key substrate, as its cellular concentration is thought to regulate the flux of this substrate into the different branches of

the pathway and is a more useful intracellular form of the vitamin that can be used in nucleotide biosynthesis (Green, MacKenzie, & Matthews, 1988; Matthews, 1984).

Once inside the cell THF can be directed into one of three major branches in the pathway contributing towards:

- Methionine synthesis and hence DNA Methylation
- Purine synthesis
- Thymidine synthesis

Figure 1-3: General overview of the folate metabolic pathway. Folates[1] are transported into cells predominantly by the RFC[2] and also by the FR[3]. FPGS[4] catalyses the polyglutamation of folates. SHMT[5] aids in the conversion of 5-methyl THF to 5,10 methylene THF, MS[6] also yields THF from the catalysis of homocysteine to methionine. THF can aid in purine synthesis via GARFT[7] and AICARFT[8], yielding THF and thymidine synthesis via the action of TS[9], yielding DHF and dTMP, the resultant DHF being recycled back to THF via the action of DHFR[10].

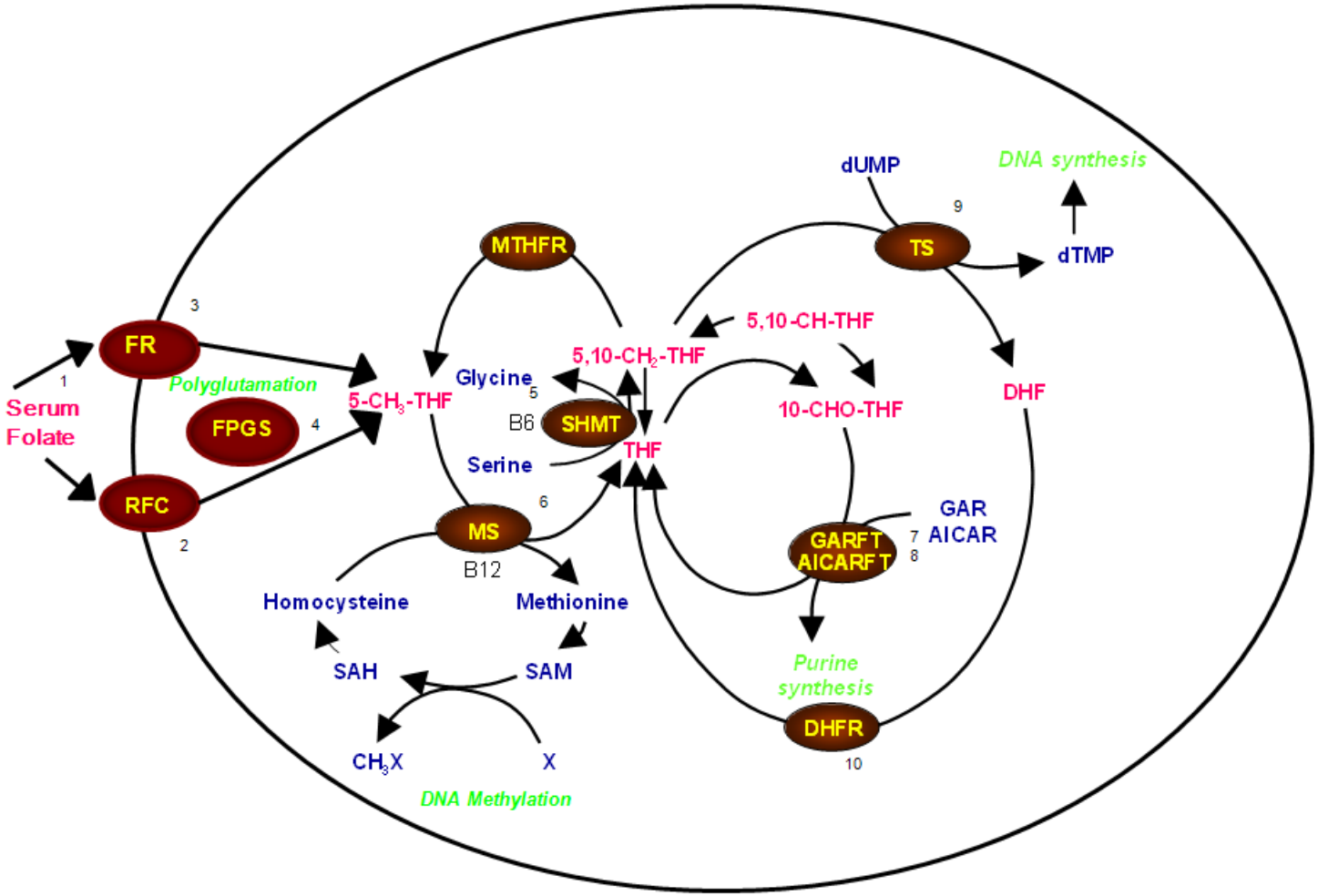

1.8. Folate Transport

The mechanisms by which folates are transported across cell membranes has been an area of research interest for many years. The mechanisms of cellular transport in tumours have been well studied and are commonly found to differ in tumours when compared with normal tissue.

Normal adult tissues have been found to exhibit two major cellular transport mechanisms, each with a differential affinity for various oxidation states of folates and folyl coenzymes. These transport systems can be distinguished by their preferences for folates as substrates, as well as by differences in temperature and pH dependence (Lucock, 2000).

The folate transport systems may be divided into two separate categories; the membrane channels or carriers which vectorialy transport the molecules, and the receptors, endocytic vesicles which are internalised. Both bind folates and some antifolate chemotherapy agents with high affinity and specificity (Brzczinsca, Winska, & Balinska, 2000). Although these methods are distinct from one another and function independently, both systems appear to deliver folate to the same intracellular compartment and their role in folate metabolism appear similar (Brzczinsca et al., 2000). More recently, the ubiquitously expressed proton coupled folate transporter, a low pH, carrier mediated mechanism of folate transport has also been identified. This mechanism was initially thought to be related to that of the RFC but recent work has identified it as genetically distinct from this mechanism. This transport mechanism may be an additional route of folate/antifolate uptake relevant to cells at low pH (Qiu et al., 2006; Zhao & Goldman, 2007).

1.8.1. The Reduced Folate Carrier

The RFC is a member of the major facilitator superfamily of transport carriers and is a high capacity bi-directional transporter for both natural folate compounds and antifolate chemotherapeutics. It is similar in structural homology to the glucose transporter and possesses thiol groups vital to its transport function. Transport via the RFC is temperature dependent, sodium independent and is characterized by a neutral pH optimum (Brzczinsca et al., 2000).

A study by Whetstine *et al* (2002) characterised the RFC gene and found it to be ubiquitously expressed in normal tissues. This is the major route of transport of folate into the cell (Whetstine, Flatley, & Matherley, 2002). It is located on the plasma membrane and contains twelve transmembrane domains with both the C and N terminal regions being located in the cytoplasm (Figure 1-4). The transport kinetic properties of the RFC indicate a poor affinity for folic acid (Ki =

~200μM) for reduced folate cofactors and methotrexate (MTX) (Antony, 1996; Brzczinsca et al., 2000; Henderson, 1990).

Folate metabolism is responsible for the conversion of homocysteine to methionine, important in the biosynthesis of S-adenosylmethionine, a methyl donor. Subsequently this is responsible for the methylation of CpG islands by DNA methyltransferases. If this biosynthetic pathway is impaired it may lead to either hypo- or hypermethylation, this may in turn adversely affect expression of the RFC (Odin et al., 2003).

Figure 1-4: Diagrammatic representation of the RFC. Note the twelve transmembrane domains which loop between the inner and outer surfaces of the cell membrane, a large cytoplasmic loop inside the cell and cytoplasmic N and C terminal regions (Sadlish, Williams, & Flintoff, 2002).

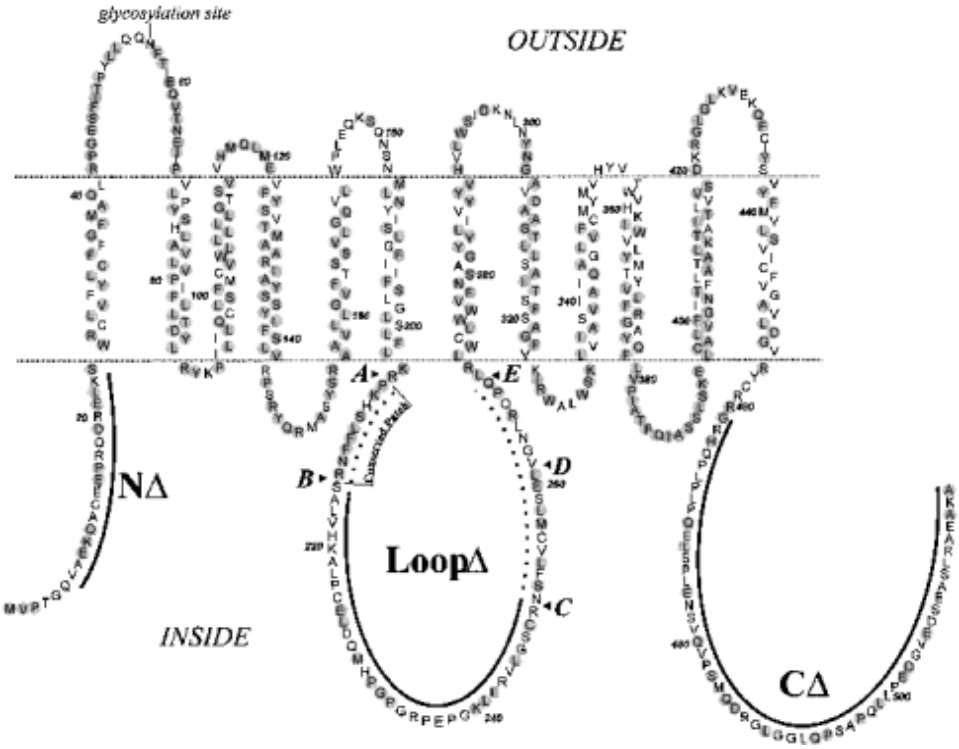

1.8.2. Folate Receptors (FR's)

Folate receptors have been an intense area of research, particularly in the last decade due to their unique pattern of distribution in normal tissues. The expression of folate receptors may have become redundant due to the ubiquitous expression of the high capacity RFC, however, there are a small number of normal tissues in which folate receptor expression is present. It is thought such tissues may serve to acquire folates from biological fluids where the folate concentration is very low (Elnakat & Ratnam, 2004). Much of the research aimed at folate receptors is concerned with

the use of folate receptors as target for cancer treatment including small molecules such as antifolates or antibody therapies and the utility of folate receptors as a marker of prognosis or companion diagnostic for subgroups of cancers with their expression.

Folate receptors are glycopolypeptides which are normally attached to the cell membrane via a glycophosphatidylinositol (GPI) anchor. GPI anchored proteins are attached to the external surface of the cell membrane by glycolipid moeties and are not directly accessible from the cytosolic face of the membrane (Figure 1-5).

This feature makes the receptor inaccessible to circulating folates and antifolates. (Mayor & Reizman, 2004). Also termed folate binding proteins (FBP), they bind a range of folyl coenzymes, including folic acid and N^5-methyl-THF with a high affinity (Ki = 0.09-0.24nM) (Antony, 1996; Elnakat & Ratnam, 2004).

Figure 1-5: GPI anchor structure. General core structure consists of ethanolamine phosphate in an amide linkage to the C-terminus of the protein, three mannose residues (orange), glucosamine (blue) and phosphatidylinositol (purple) (Mayor & Reizman, 2004).

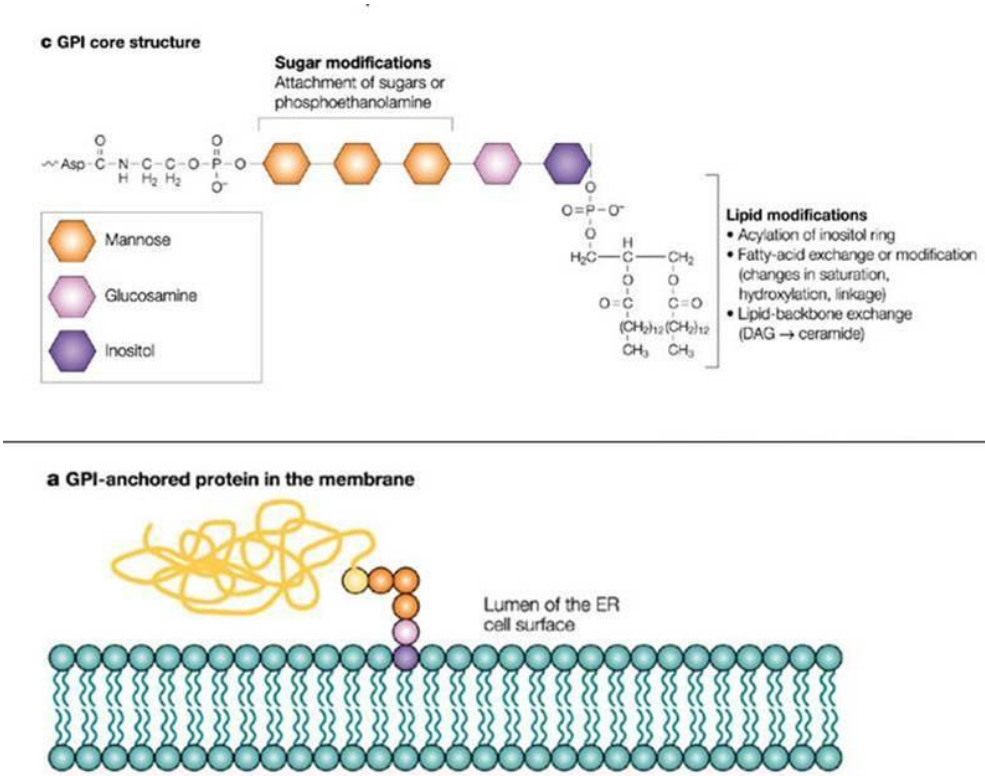

FR's have a mass of approximately 38-40 kDa and are members of the FOLR gene family, consisting of FOL1, FOL2 and FOL3 genes which encode the homologous isoforms FR-α, β and γ (Figure 1-6). All isoforms share highly conserved sequences in approximately 75% of the gene but differ in the

5’ untranslated region. This may account for the difference in tissue expression and biochemical properties observed between isoforms (Antony, 1992; Saiwaka, Price, Hance, Chen, & Elwood, 1995).

The two membrane associated forms of FR (α and β) are attached to the cell membrane surface and are capable of transporting folate into the cell by carrier mediated endocytosis but the majority of normal tissues virtually lack its expression (Elwood et al., 1997).

FR-β has been found to be expressed in placenta and haematopoetic cells but not in other tissues. (Ratnam, Marquardt, Duhring, & Freisheim, 1989; Ross et al., 1999). Furthermore, FR-β found to be expressed on the surface of haematopoetic progenitor and stem cells has not been found to be functional for folate binding, indicating folate transport in such cells is also largely due to the RFC (Reddy et al 1999).

A third member, FR γ, the product of the FOL3 gene is a secretory protein as it lacks the signal required for the formation of a GPI anchorage site, it has been found primarily in normal haematopoetic and leukaemic cells. As its levels are virtually undetectable in normal human serum it may potentially be of use as a serum marker for lymphoid malignancies (Antony, Kane, Portillo, Elwood, & Kolhouse, 1985). These isoforms have now been characterised from several species (Antony, 1996).

More recently a fourth member, FR-δ has been identified through database mining although its function and tissue expression has yet to be identified (Elnakat & Ratnam, 2004; Takimoto, 1997).

The chromosomal location of the FR genes, including FR-δ has been determined to be 11q13.3-11q14 and the FR’s are thought to be structurally similar to riboflavin binding proteins. From comparative cDNA sequences FR’s β and γ are closer in similarity than FR-α, indicating the gene encoding FR-α was diverged earlier in evolution (Elnakat & Ratnam, 2004). As this project is concerned with the generation of antibodies directed against FR-α, the RFC and other FR isoforms will not be discussed further.

Figure 1-6: The organisation of human FR genes. The numbers are indicative of the exon lengths in base pairs. P indicates the location of the promoter regions, adjacent to which are the Sp1 and ets binding sites which drive the basal promoter activity (Elnakat & Ratnam, 2004).

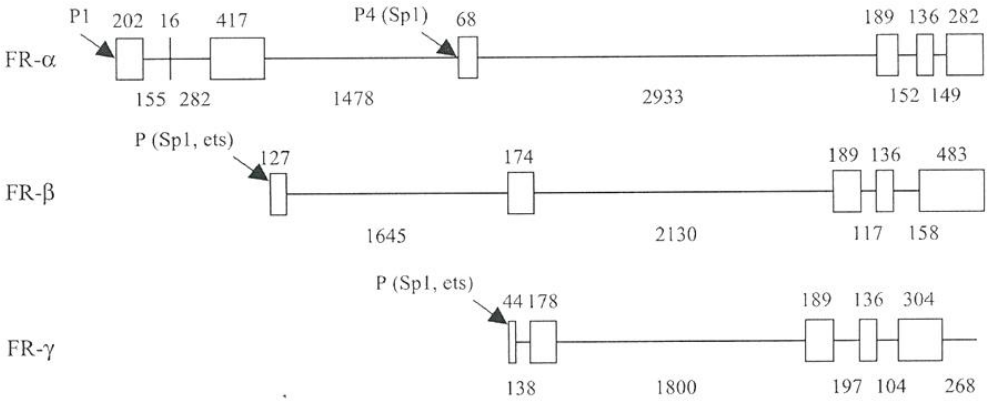

There is no homology between the RFC and the membrane anchored FR proteins that would suggest any structural or functional similarity between the carriers and, although their functional role appears to be similar, their transport kinetics and affinity for folate differ significantly (Elnakat & Ratnam, 2004).

Membrane-associated forms of the receptor are fully capable of transporting folate into the cell, although the RFC is the primary folate uptake pathway utilized by normal cells (Elnakat & Ratnam, 2004). A number of theories exist as to the mechanism of folate uptake by FR's.

The first reports indicated that FR's are recycled via a mechanism termed potocytosis (Figure 1

-7). This mechanism was proposed from the observation that FR-α recycled between an intracellular, acid resistant pool to an extracellular, acid-sensitive pool (Kamen, Wang, Streckfuss, Peryea, & Anderson, 1988). FR's are clustered on the cell membrane surface and have been reported to be preferentially associated with uncoated vesicular structures known as caveolae (membrane invaginations). These are characterised by the presence of caveolin – a marker protein. Caveolin 1 binds to cholesterol and is thought to play an essential role in internalisation and recycling of the FR, whereby the folate-bound receptor complex is internalised by the caveolae. Increased acidification of the closed compartment would dissociate the folate from the receptor and transport it into the cytosol with the energy generated from the acidic gradient. The closed invagination in the cell membrane would then reopen to expose the receptors for the next

cycle (Rothberg, Ying, Kolhouse, Kamen, & Anderson, 1990). Subsequent studies have indicated that the caveolar hypothesis may not be necessary for folate transport and have demonstrated that GPI-anchored proteins are distributed diffusely across the surface of the cell membrane, requiring cross-linking for subsequent clustering into caveolae. They also established that this was not achieved by folate binding (Mayor, Rothberg, & Maxfield, 1994). Some studies, however still argue that efficient delivery of folate into the cytosol is dependent upon caveolae (Ritter, Fajardo, Matsue, Anderson, & Lacey, 1995).

Figure 1-7: Diagrammatic representation of the folate receptor potocytosis mechanism. The lowering of intracellular pH releases the anionic folate from the carrier. This lowering is achieved by acidification via an H+ pump which then causes the folate to dissociate from the receptor. It is then subsequently released from the vesicle into the milieu of the cytosol. The FR is then recycled back up to the plasma membrane, this process has been reported to take between 30 minutes and 5 hours (Kamen & Smith, 2004; Rothberg et al., 1990).

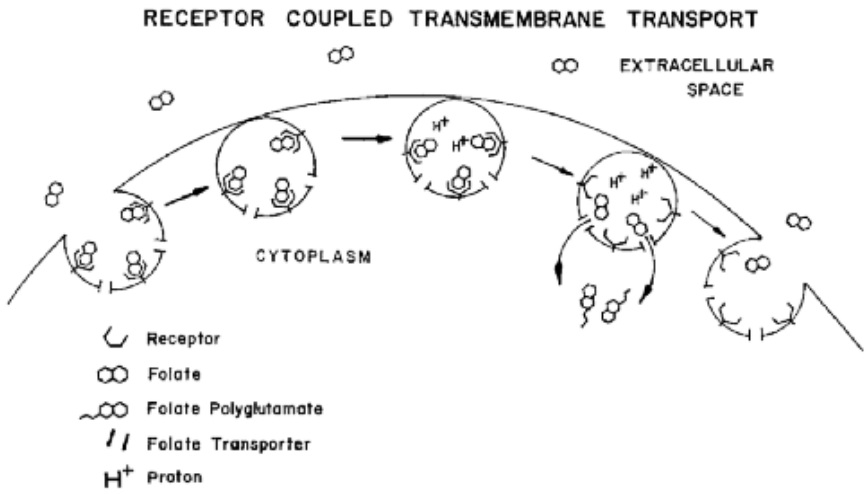

More recently the lipid-raft endocytosis theory has been proposed as an FR-α transport mechanism. This involves membrane domains rich in lipids, GPI anchored proteins and signalling proteins clustered into large platforms that are able to segregate various membrane components. Lipid rafts are thought to regulate a number of different processes including lipid sorting, protein trafficking, cell polarisation and signal transduction (Le Roy & Wrana, 2005; Simons & Ikonen, 1997). A number of studies have now indicated the role of this transport mechanism in FR mediated folate uptake, describing the potocytosis mechanism to be more akin to the PCFT. Recently, a number of proteins crucial to the cycling of FR's have been identified and may provide more information on functional regulation of FR's, although the exact mechanism is still to be

elucidated (Elnakat et al., 2009; Le Roy & Wrana, 2005; Mayor, Sabharanjak, & Maxfield, 1998; Sabharanjak & Mayor, 2004).

The proposed transport systems are present in normal tissue, although are largely restricted to luminal surfaces and areas not directly accessible to the bloodstream. The mechanisms described are relatively inefficient, low-capacity modes of folate transport utilised by normal cells, likely to be due to their restricted expression. If FR's are overexpressed in malignant cells, however, they may be an additional relevant transport route of folate, antifolate and other folate targeted therapies (Lucock, 2000; Theti & Jackman, 2004)

The accumulated folate in the cytoplasm is regulated once it is released from the receptor. Slowly proliferating cells or folate depleted cells only take up folate until the cytoplasm has accumulated physiological levels of the polyglutamates, after which the process is inhibited through FPGH modulation, although the receptor remains functional and is not destroyed by the process (Brzczinsca et al., 2000).

1.8.3. Folate Receptor Alpha Expression

The expression profiles of FR-α described by Weitman *et al* were obtained by immunohistochemical analysis with the use of two murine monoclonal antibodies, mOV18 and mOV19, which were generated against an ovarian tumour membrane preparation. The mOV18 antibody; developed as an ovarian cancer marker and the LK26 antibody, raised against a choriocarcinoma cell line were both subsequently discovered to recognise FR-α, however for immunohistochemical staining they only work in a limited fashion on freshly frozen tissue sections and are unsuitable for use in other applications such as WB, or IHC analysis of paraffin embedded tissue (Coney et al., 1991).

Although there are many limitations with the use of these antibodies they have still been used in various studies to provide a large amount of information on the distribution of FR-α in normal and malignant tissues. Results from the use of the mOV 18 and 19 antibodies and mRNA studies have indicated that FR-α expression is limited to the epithelia of the choroid plexus, proximal kidney tubules, fallopian tube, uterus, epididymis, acinar cells of the breast, thyroid and trophoblasts in the placenta where they facilitate maternal to foetal transport of folate (Mangiarotti et al., 2001). IHC analysis on frozen sections have also indicated expression in bronchial glands, alveolar epithelium of lung, oesophagus, stomach, pancreas and thyroid with varying levels of expression (Mantovani et al., 1994). Expression in proximal kidney tubules has been reported both in human

proximal tubule cell lines and in intact rat kidney used to follow both uptake and trafficking of fluorescent conjugates of folic acid. These studies have indicated a role for FR-α in the salvage and reabsorption of folates that have escaped into the urine. This study also contra-indicated the fate of folate in neoplastic cells where cytosolic release of folates is readily observed (Reddy & Low, 1998), explaining the absence of toxicity of folate conjugates to the kidney (Morshed, Ross, & McMartin, 1997, Sandoval, 2004). In the placenta, folates are proposed to play a role in the accumulation of folates in the foetal circulation (Yasuda et al., 2008). In the CSF their role is thought to be similar through their expression in the choroid plexus (Ramaekers & Blau, 2004; Wollack et al., 2007).

Many studies have examined FR-α expression and ability to bind folate in malignant tissues by various methods, including microarray analysis and radioligand binding assays. Much attention has focused upon ovarian and endometrial cancers as these tumour types express FR-α most consistently. Although the receptor has been found to be downregulated in mucinous adenocarcinomas of the ovary, FR-α has been found to be consistently expressed in non-mucinous adenocarcinomas of the ovary, uterine adenocarcinoma, testicular choriocarcinoma, ependymal brain tumours and non functioning pituitary adenoma (Garin-Chesa et al., 1993; Ross, Chaudhuri, & Ratnam, 1994; Weitman et al., 1992a, {Ross, 1994, Garin-Chesa, 1993). It has been reported to be expressed in MPM and less frequently in breast, colon and renal carcinomas. As well as identification of the presence of FR-α in such tumours, the ability to bind folate has also been demonstrated (Elnakat & Ratnam, 2004).

Wu *et al* (1999) used a quantitative *in situ* hybridisation method to examine the expression levels of mRNAs for FR-α in paraffin embedded tissue sections of a number of different ovarian, uterine and cervical cancers. Different patterns of FR regulation were observed between the different tissue types as well as in differentiation and malignancy. Differentiation of the germinal epithelium into mucinous tumours was found to be associated with the down regulation of FR-α. However, FR-α expression was found to be retained in malignant serous tumours of the ovary (Wu, Gunning, & Ratnam, 1999).

Recently Yang *et al* (2007) found that FR-α mRNA is frequently overexpressed in osteosarcoma samples via the use of the reverse transcriptase polymerase chain reaction (RT-PCR). 75% of the tested samples (84/107) were found to contain detectable FR-α mRNA with 29.9% containing higher levels than that of the control ovarian cancer cell line SKOV-3 (Yang et al., 2007).

1.8.4. Regulation of Folate Receptor Alpha Expression

In recent years, a number of transcriptional/post-transcriptional mechanisms have been studied as potential contributors to the unique tissue specificity patterns of FR genes. The investigation of such regulatory mechanisms could potentially be clinically advantageous as selective over expression may enhance the efficacy of FR-targeted therapies and the relevance of FR-α as a diagnostic marker.

Several studies have examined the effect of folate concentration on receptor expression and have found that variations in the extracellular and hence intracellular folate concentration can modulate FR-α expression in a variety of cells. *In vitro* data has consistently indicated that FR-α protein was regulated by folate concentration in culture medium with cells grown in low folate conditions having up to a 4 fold increase in FR-α expression compared to cells grown in standard culture medium. This increase has also been shown to be reversed by the addition of folic acid or reduced folate coenzymes to the medium (Kane et al., 1988; Kelemen, 2006). Modulation of FR-α in this way may enhance tumour response to folate targeted therapies taken in by this route.

Reports that various steroid hormones may alter FR-α expression support the requirement for further investigation. This type of regulation would be of value in folate receptor targeted treatments as it is hypothesised that the major limitation of this type of treatment is the variability of FR-α expression levels in tumours. Any means of specifically increasing FR-α expression would be of great potential in enhancement of such therapies and in the enhancement of diagnostic imaging. Concomitant use of both antioestrogens and antifolates in oestrogen expressing tumours may also have a synergistic effect and potential clinical relevance.

Kelley *et al* (2003) reported that folate receptor levels are generally relatively low in oestrogen receptor positive ovarian and cervical tumour cell lines and have hypothesized that FR-α expression may be regulated by oestrogens. A negative correlation between FR-α expression levels and oestrogen receptor status in primary breast cancers has been observed, suggesting FR-α may be regulated via this nuclear receptor. The study reported transcriptional repression of FR-α by the oestrogens and derepression by antioestrogens such as Tamoxifen (Kelley, Rowan, & Ratnam, 2003).

Similarly Tran *et al* (2005) reported enhancement of FR-α expression via the glucocorticoid receptor (GR) agonist Dexamethosone which was inhibited by a GR antagonist. Treatment of HeLa (cervical carcinoma) cells with dexamethasone resulted in a progressive increase in expression of

both FR-α mRNA detected by real-time PCR and FR-α protein detected by WB using FR-specific rabbit antiserum. This enhancement was not, however observed in FR negative cells (Tran, Shatnawi, Zheng, Kelley, & Ratnam, 2005).

Other studies identifying potential modulators of FR expression include retinoic acid dependent upregulation of FR-α (Bolton, Wood, Kennedy, Don, & Mattick, 1999), variant hepatocyte nuclear factor 1 activation of the FR-α P1 promoter (Tomassetti et al., 2003), caveolin downmodulation relating to overexpression of FR-α (Bagnoli et al., 2000), ethanol related upregulation of FR's (Romanoff, Ross, & Mc Martin, 2007) and translational upregulation of FR's via increased intracellular homocysteine concentration (Antony et al., 2004).

1.8.5. Folate Receptor Alpha and Cancer

FR-α is the most widely studied folate receptor isoform and is also the most highly expressed, although, as described previously its expression is largely restricted to the apical membrane of polarised epithelial cells where it is not supplied with folate in the circulation. This is in contrast to its constitutive expression in certain specific malignancies where it is accessible via the vascular system.

FR-α protein has been characterised as a marker of ovarian carcinoma, as it is overexpressed in more than 90% of non-mucinous ovarian carcinomas (Campbell, Jones, Foulkes, & Trowsdale, 1991). Its expression is usually absent on normal ovarian epithelial cells but appears to be stable in ovarian cancers and has been shown to increase in its expression with disease progression (Mangiarotti et al., 2001). As the expression of FR-α appears to be related to malignant transformation, it is an active area of research, particularly as its expression in most normal cells is restricted, which makes it an attractive candidate for novel, experimental tumour targeted therapies.

Another interesting area of research is the role of FR-α in tumour progression. It has been found that tumours with negative expression grow more slowly and that transfection of functional FRα can cause cells to grow more rapidly. This may be due to the nanomolar concentrations at which FR-α can take up folates, which may be too low for effective uptake via the RFC which takes up folates in the micromolar range (Ebel et al., 2007).

Folate receptor targeted therapies currently being developed cover three broad categories; small molecule therapies including the antifolate class of chemotherapeutics, immunotherapies via the

use of FR targeted antibodies and TS inhibitors and folate conjugates, including both therapeutic agents and carriers. All such therapies require a disgnostic test in order to select for patients who may potentially benefit from the therapy, particularly in the case of FR-α which is a key determinant of response but its expression is limited.

As folate plays a major role in the growth and replication of normal cells, its components are highly relevant targets for anticancer drug design. The effectiveness and cytotoxicity of these drugs are thought to be due to their inhibition of both DNA and RNA synthesis. Antifolates (antimetabolites), typically analogues of folates and TS inhibitors are the major classes of drug relevant to folate receptor targeted therapies.

Natural folates and the classical antifolates are known to be taken up primarily via the RFC, although FR-α is an additional route relevant to some antifolates, particularly when the extracellular folate concentration is low (Theti & Jackman, 2004). The RFC is ubiquitously expressed and is the major cause of patient intolerability to such drugs with a lower concentration of drug reaching the tumour and causing toxicity in normal tissue. Antifolates specifically directed to FR-α would therefore be extremely promising, as the targeted approach would potentially deliver a higher concentration of drug to the tumour cells and result in lower toxicity to normal tissue (Jackman, Theti, & Gibbs, 2004; Wang, Zhao, & Goldman, 2003).

Pemetrexed was developed in 1992 and is termed a multitargeted antifolate due to its ability to inhibit the folate dependent enzymes TS, DHFR, GARFT and AICARFT (Exinger et al., 2003). Pemetrexed has been found to have a high affinity for FR-α indicating this may be an additional, relevant route of uptake into the cell which may overcome drug resistance often seen with antifolates, although the primary route of uptake is via the RFC (Exinger et al., 2003; Wang et al., 2003).

Other antifolates which have shown an affinity for FR-α are the TS inhibitors ZD9331 and CB300638 and the GARFT inhibitor lometrexol, particularly CB300638 which is an FR-α targeted TS inhibitor (Gibbs et al., 2005; Theti & Jackman, 2004). Such drugs may be of particular relevance to tumours overexpressing FR-α and some have even been designed as such, given that RFC mediated antifolate drug delivery and its associated toxicities are impossible to avoid with current antifolates.

Two anti FR-α antibodies are currently being tested in clinical trials, the mOV18 antibody, which has shown promise in phase I trials with complete remissions being observed in 5/15 patients, with the remission being sustained in 1 patient almost 3 years post follow up and minimal side effects (Crippa et al., 1994).

A humanised MAb, MORAb-003 (farletuzumab) has also been developed and has shown success in both phase I and II clinical trials. It was originally derived from the LK26 antibody, also a human anti- FR-α antibody suitable for use on frozen tissue and has been tested, both as a monotherapy and in combination with chemotherapy with promising results (Armstrong, 2009; Ebel et al., 2007; Konner et al., 2010).

Folate conjugation aims to exploit FR mediated endocytosis by delivering the conjugated agent directly to the site of FR-α expressing tumours. A number of chemotherapeutic agents have been conjugated to folate with promising results, various types of drug carrier have also been conjugated to folates including liposomes, lipid nanoparticles and micelles. They have the potential to increase the load of cytotoxic drug to the tumour site and may allow it to be retained more readily than simple folate conjugates (Zhao, Li, & Lee, 2008).

Other relavant therapies currently being investigated are folate conjugated anti T-cell receptor antibodies, which have previously been found to specifically target tumour cells for lysis, suggesting these conjugates may have value as immunotherapeutic agents (Kranz, Partrick, Brigle, Spinella, & Roy, 1995). Recently, dendritic cells transfected with FR-α mRNA have been used for the treatment of relapsed metastatic ovarian cancer with promising results (Hernando et al., 2007).

1.8.5.1. Selection of Patients for Folate Receptor Alpha Targeted Therapies

There are a number of methods of assessing FR-α expression such as IHC on frozen tissue (Campbell et al., 1991) and imaging with folate conjugated radioisotopes (Zhao et al., 2008). It has also been suggested a simple blood test may potentially allow for selection of suitable patients due to the identification of functional soluble FR-α present in serum being higher in ovarian cancer patients than healthy volunteers (Basal et al., 2009; Mantovani et al., 1994).

However, the standard and most routinely used method of detecting the level of expression of FR in tumours would be measuring the levels on FFPE tumour samples collected by biopsies. An

antibody suitable for this use would therefore be extremely promising as a potential companion disgnostic to all the therapies described.

1.9. Folylpolyglutamate Synthetase

FPGS catalyses the ATP dependent formation of an amide bond between the γ-carboxyl group of naturally occurring folates and the amino group of glutamic acid. The enzyme has both cytosolic and mitochondrial forms, differing only by the presence of a 42 residue amino terminal leader peptide sequence in the mitochondrial form. Up to seven glutamate residues can be added to monoglutamate compounds allowing them to be retained in the cell. This reaction occurs in both natural folates and antifolates. This is essential for the survival of all proliferating mammalian cells and it plays a central role in the action of antifolates, as polyglutamation increases both intracellular drug concentration and affinity for subsequent enzymatic reactions (Freemantle, Taylor, Krystal, & Moran, 1995; Odin et al., 2003).

The FPGS gene spans 12 kilobases in length and the protein itself is approximately 60kDa, the cytosolic form differs from the mitochondrial form by a mass of 1 kDa. Both isoforms are derived from the same gene and the leader sequence is thought to be required for tracking and penetration into the mitochondria. Mitochondrial forms are thought to be involved in mitochondrial C_1 metabolism whereas cytosolic forms are required for establishment of normal cytosolic folate pools (Chen et al., 1996; Sanghani, Sanghani, & Moran, 1999).

As the action suggests, FPGS is expressed in any cell undergoing sustained proliferation and is also expressed in a number of differentiated tissues. Expression of FPGS activity is regulated by a proliferation dependent mechanism by which rapidly dividing cells express higher enzymatic activity than quiescent cells. Folate binding has also been shown to activate FPGS enzyme activity (Barredo & Moran, 1992; Egan et al., 1995; Sun, Cross, Bognar, Baker, & Smith, 2001). In addition, the folate binding domain of FPGS has been reported to be strikingly similar to that of DHFR (Sun, Bognar, Baker, & Smith, 1998).

To date there is no known IHC data available on this particular protein, although mRNA gene expression studies have been carried out. Often mRNA and protein levels do not correlate and similarly a decrease in FPGS activity is not always associated with a decrease in FPGS mRNA, indicating that alteration in FPGS expression may occur at the post-transcriptional level (Leclerec et al 2001).

FPGS mRNA transcript levels have been found to be high in various tumours, in particular B-lineage leukaemias. High levels of expression have also been observed in normal gut, bone marrow stem cells, liver and kidney. In the same study human heart and skeletal muscle were found to express very high levels of FPGS specific mRNA. Human brain and, surprisingly, placental tissue were found to have a low level of FPGS message. This enzyme, however, has not been found to be appreciably expressed in other normal adult tissues (Freemantle & Moran, 1997). These findings agree with a study carried out in 2001 by Leclerec *et al*, who also found high FPGS mRNA expression levels in human skeletal muscle, heart, liver and kidney (Leclerec & Barredo, 2001).

A study by Odin *et al* (2003) found gene expression levels of FPGS to be significantly higher in colorectal tumour biopsies compared with normal adjacent mucosa. They concluded that the level of expression is also an independent prognostic marker, as patients with low levels of FPGS had shorter tumour specific survival than patients with a high level. They suggested the low level may indicate a folate deficient state that could increase aggressiveness of the tumour (Odin et al., 2003).

Modulation of FPGS in order to increase sensitivity to antifolates is an interesting area of research, although few studies have investigated this. Sohn *et al* (2004) investigated FPGS modulation on chemosensitivity to 5-FU and MTX in colon cancer cells transfected with sense/antisense FPGS cDNA. They found FPGS overexpressing cells to confer growth advantage over those cells treated with antisense cDNA and significant increase in sensitivity to 5-FU. No difference in chemosensitivity was observed with MTX (Sohn et al., 2004). Further studies in this area using different cell lines and antifolates would be interesting.

As FPGS is paramount in catalysing the activation of antifolate compounds, specific anti-FPGS monoclonal antibodies suitable for use on formalin fixed and paraffin embedded samples may enable us to predict the degree of response tumours may have to such drugs, enabling more informed decisions to be made with regard to the choice of treatment and identification of those patients most likely to respond to antifolate chemotherapy. In addition it would greatly aid in clarification of FPGS expression profiles which, to date have largely relied on mRNA data which is not always representative of the protein expression levels in the same tissue (Leclerec et al 2001).

1.10. Summary

The folate pathway components FR-α and FPGS are highly relevant targets, particularly in ovarian cancer and other tumour types with high expression. The dual role of FR-α as both a promising target for cancer therapy and its association with poor prognosis makes it particularly interesting. Cancer therapies currently being developed aim to offer the 'magic bullet approach' to cancer therapy, targeting the tumour and minimizing toxicity to normal tissues. A number of therapies are currently preclinical and clinical trials. Potential modulators of FR-α expression have also been identified and have the potential to upregulate expression of FR-α in tumour cells, enhancing the efficiacy of folate targeted therapies. A number of methods are currently being developed to determine the expression of FR-α in tumours, which would aid in the selection of patients who may benefit from FR targeted therapies. Antibodies directed against FR-α and FPGS, suitable for use on FFPE tumour samples would greatly assist with this highly relevant area of research and allow suitable patients to be selected routinely and with ease in hospital pathology labs without the need for complex detection methods. It is thus a major aim of this project to generate antibodies suitable for this application.

1.11. Research Plan

Year 1:

Stage 1: Select regions from FR-α and FPGS protein sequences and amplify via PCR from cDNA prepared from mRNA derived from cell lines, clone the product into a T-vector. Sequence fidelity would then be assessed via automated DNA sequencing from Lark Technologies. The insert would then be subcloned into both pET21b and pET41b expression plasmids. pET41b plasmids have been shown to increase the solubility of proteins due to the presence of a GST tag, this tag is also highly immunogenic and may aid in stimulating the mouse immune response later in the project. Initial subcloning would be performed using NovaBlue *E.coli*, this host lacks T7 polymerase, and this step reduces plasmid instability. The plasmid would then be transformed into the inducible T7+ lysogenic expression host BL21plysS or Tuner strain. Purification of the resultant recombinant protein will be achieved via his-bind chromatography.

Stage 2: Laboratory female BalbC mice would be immunised with the antigens prepared in stage 1. Responding animals would be sacrificed after an immunisation schedule and the primed B-cells from the spleen would be fused with NS-1 myeloma cells to establish specific hybridomas. The specific reactivity of the secreted antiodbodies will be assessed via ELISA, IHC and Western blotting.

Year 2: Evaluation of antibodies for immunohistochemistry on paraffin and frozen tumour samples, Western blotting and ELISA; Epitope mapping of selected antibodies; Analysis of FR-α and FPGS expression in tumour biopsy samples, including a large archival collection of ovarian tumour samples in tissue microarray form and correlation of expression with clinical and histopathological data, including oestrogen receptor expression, and prognostic significance for response and survival in univariate and multivariate analysis.

Year 3: *In vitro* cell studies on breast and ovarian tumour cell lines to test for the ability to modulate the expression of FR-α by oestrogen and anti-oestrogen treatment and the consequence for response to folate receptor targeted therapies. Assessment of antibodies for application in other techniques such as IF and FACS. Evaluation of any neutralizing properties the antibodies may possess. Preparation of thesis.

Chapter Two

Chapter Two

2. Antigen Design and Preparation

2.1. General Introduction

Prokaryotic host expression systems have been used widely in molecular biology to produce recombinant proteins for a wide range of different applications. One such application is the immunisation of animals for monoclonal antibody production.

Both monoclonal and polyclonal antibodies have important clinical applications in the detection, diagnosis and treatment of cancers. They are also important tools for the study of protein expression in both normal and tumour tissues. Antibodies can be directed against a wide range of different antigens such as recombinant proteins (soluble or refolded), synthetic peptides, nucleic acids and carbohydrates.

The generation of a suitable recombinant protein or synthetic peptide which can be used for the induction of an immune response in laboratory animals is the first step in antibody production. Both prokaryotic (bacterial) (Rosenberg et al., 1987; Studier & Moffatt, 1986) and eukaryotic expression systems (Luckow & Summers, 1988) may be utilized to produce a suitable antigen.

2.2. Recombinant Protein Expression Systems

Prokaryotic expression systems are commonly used for the production of recombinant eukaryotic proteins and have several advantages, including the ease of cell culture, inducible protein expression, rapid cell growth and subsequent protein expression, ability to express large regions of the protein of interest and high protein yield. It offers advantage over more complex eukaryotic systems when required for antigen generation and subsequent immunisation for antibody production. Prokaryotic hosts lack complex post-translational modification processes which can often lead to masking of linear epitopes (Baneyx, 1999). This may be of particular value when attempting to generate antibodies suitable for both IHC and WB analysis. The fusion proteins produced via this method can be purified by affinity chromatography and the antigens produced are often successful. If the protein produced is insoluble, simple methods are available to solubilise and refold the protein, although this may pose a problem if the protein produced is required for functional or enzymatic studies, as recovery of functional proteins from insoluble

inclusion bodies is not always possible (Singh & Panda, 2005). The pET prokaryotic expression systems using *E.coli* as a host were selected for use in this project in order to generate recombinant FR-α and FPGS for subsequent immunisation, which will be discussed in more detail in the following chapter.

Eukaryotic expression systems include protein expression via yeast, mammalian and insect cells. The advantage of eukaryotic expression systems are the high levels of protein expression and ease of purification. Some systems even secrete the protein into the media, allowing for continuous expression of a protein without lysing the cells. As eukaryotic proteins are being produced by eukaryotic cells there are no problems associated with incorrect protein folding and the post translational modifications remain intact. These are important for functional protein studies and the analysis of protein-protein interactions. The major disadvantage of eukaryotic expression is the slow rate of protein production as eukaryotic cells do not grow as rapidly as prokaryotic cells (Mattanovich, Gasser, Hohenblum, & Sauer, 2004).

Synthesis of peptides is another method of generating an antigen for immunisation and is particularly useful when a unique sequence is required from proteins with high sequence homology They are also useful where a particular epitope target is required for antibody production such as an antibody directed against a phosphorylated region of a protein. The disadvantages of peptides are their instability and lack of immunogenicity. They often have to be conjugated to larger compounds, decreasing the likelihood of an immune response to the peptide target. They are also more difficult to use as screening antigens in later stages of antibody production, as peptides are more likely to degrade. It often requires many attempts to generate an antibody to a peptide, so it is also potentially time consuming. In our experience this has not been found to be as successful as generation of antibodies to recombinant protein antigens. For this reason the recombinant protein method was used in preference to generation of a peptide target.

2.2.1. The pET Expression System

The pET expression vector system is one of the most commonly used *E.coli* expression systems, it is used for subcloning regions of cDNA and subsequent expression of corresponding recombinant protein regions in *E.coli* host strains (Rosenberg et al., 1987; Studier & Moffatt, 1986). The pET system relies on high level inducible expression from the bacteriophage T7 promoter in specialised

bacterial hosts in which the production of T7 RNA polymerase is under the control of an inducible lac promoter (Figure 2-1). The system also allows convenient tagging of proteins with 6 histidine motifs to facilitate purification of proteins by immobilised nickel ion chromatography and the production of fusion proteins tagged with sequences that often enhance solubility of the target protein. The pET expression system is of particular value when expression of large protein target regions and high levels of recombinant protein are required.

Target DNA is subcloned into pET plasmids, once cloned they are under the control of the bacteriophage T7 promoter which controls the transcription and expression of the protein. Expression can therefore be induced by transformation into an *E.coli* host carrying a T7 RNA polymerase gene. Initially the plasmid is transformed into a non-expression host such as Novablue, which does not contain the T7 RNA polymerase gene. This step reduces plasmid instability caused by potentially toxic protein production in the host and increases the yield of recombinant plasmid. After this step the plasmid is then transferred into an expression host containing a copy of the T7 RNA polymerase gene (Figure 2-2).

Figure 2-1: The control elements of the pET system. A recombinant plasmid is transferred to *E.coli* containing a copy of the gene encoding T7 RNA polymerase. These hosts are also lysogens of bacteriophage DE3, a lambda derivative containing the LacI gene, lac UV5 promoter and the T7 RNA polymerase gene. Once the DE3 lysogen is formed, the only promoter able to direct the transcription of the T7 RNA polymerase gene is the UV5 promoter, inducible by IPTG. Addition of IPTG induces production of T7 RNA polymerase, transcribing target DNA in the plasmid (Novagen Catalogue).

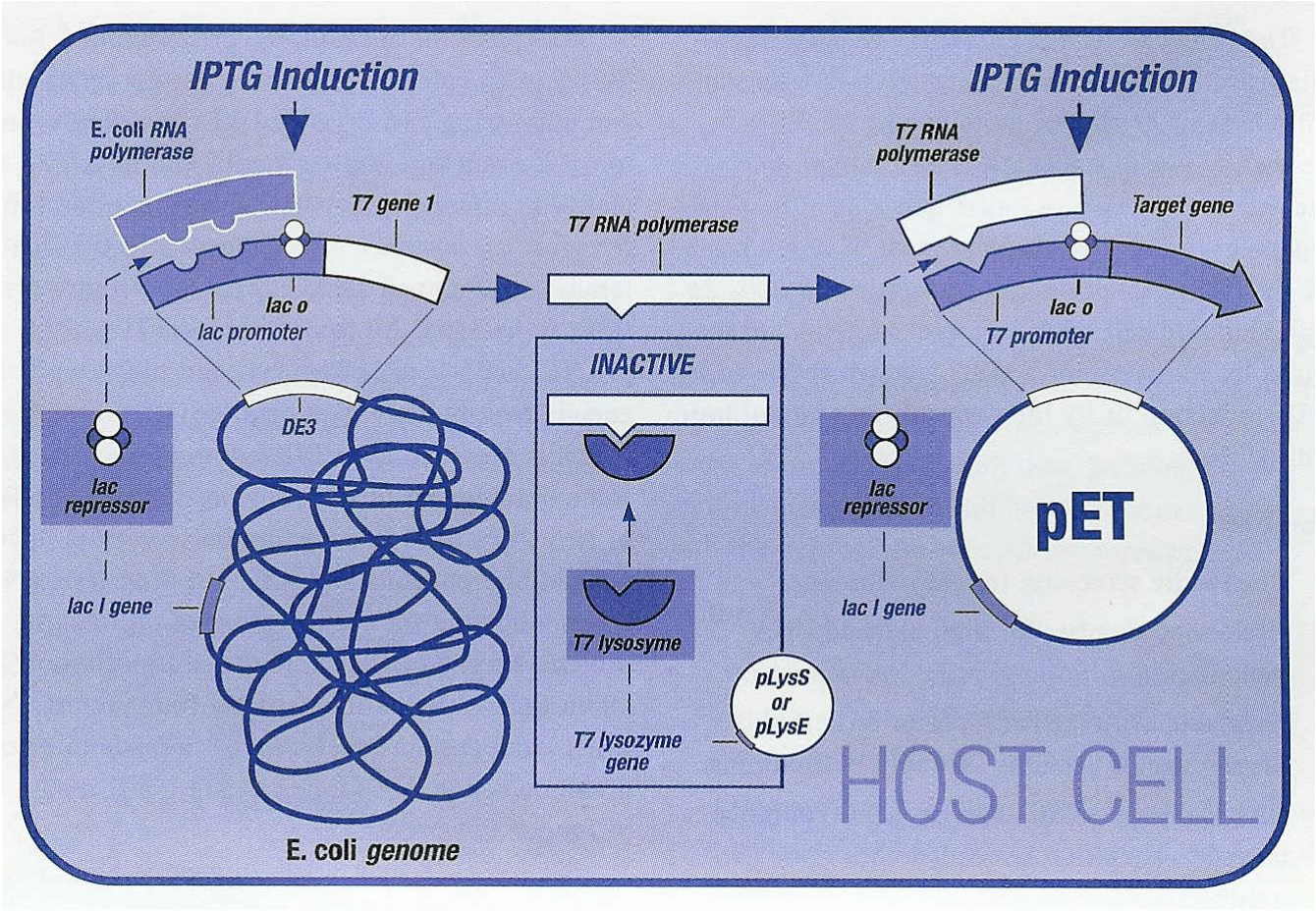

Figure 2-2: Overview of the recombinant protein production methods used for the generation of recombinant FR-α and FPGS. Suitable target sequences were selected using bioinformatics tools to ensure targets were unique, primers were designed and synthesised and DNA was created from mRNA via RTPCR and PCR. The DNA was cloned into a non expression vector and propagated in a non-expression host then subcloned into a pET expression vector and expressed in an *E.coli* expression host. Resultant proteins were purified and stored in preparation for immunisation.

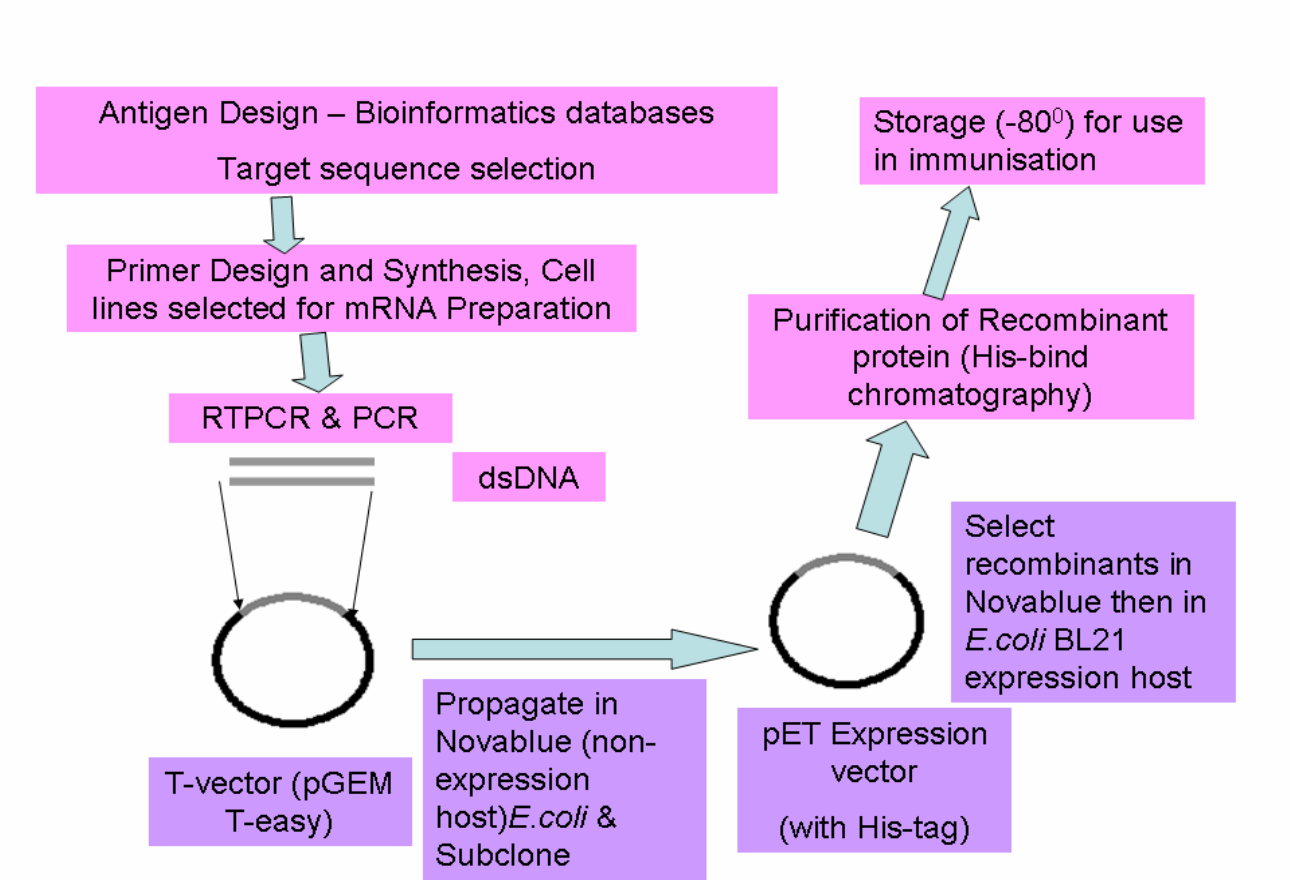

2.3. Aims and Objectives

The aim of this part of the project was to generate suitable recombinant FR-α and FPGS proteins which could subsequently be used as immunogens for the production of anti FR-α and FPGS antibodies. The schedule in this part of the project was as follows:

- Identify the known coding sequences for both proteins and perform homology searches, selecting target sequences based on the information.
- Design and generate suitable FR-α and FPGS primers for amplification of cDNA prepared from cell lines known to express the proteins and to prepare the insert for cloning.
- Use pGEM T vectors to clone the insert and check sequence fidelity via automated sequencing.
- Excise the fragment from the T-vector and subclone into pET21b and 41b expression plasmids.
- Expand and purify the pET-fragment constructs in a non expression strain of *E.coli* and transform into a suitable expression host to express his-tagged recombinant FR-α and FPGS.
- Purify the resultant recombinant protein via his-bind (nickel affinity) column chromatography.

2.4. Materials and Methods

2.4.1. Antigen Design

2.4.1.1. Homology Searches

Literature and bioinformatic database searches were performed to elucidate the known full-length amino acid and base sequences for each protein of interest (FR-α and FPGS). The sequences were found using links and tools on the European Biomatics Institute (EBI) website at http://srs.ebi.ac.uk (1997-2003 LION Bioscience AG). FR-α and FPGS were listed under accession numbers P15328 and Q05932 respectively.

Homology tools were then used to identify any similarities between the protein sequences and to identify any other homologous sequences. This would reduce the possibility of any potential antibody cross reactivity later in the project.

2.4.1.2. BLAST Searches

Basic Local Alignment Search Tools (BLAST) (Gish & States, 1993) are similarity search programs designed to identify any sequences which show significant alignments. It can detect relationships between sequences common to humans and also inter-species relationships.

The BLAST program was accessed via the National Center for Biotechnology Information (NCBI) website at http://www.ncbi.nlm.nih.gov/BLAST/Blast.cgi.

2.4.2. Target Sequence Selection

The primary aim of target sequence selection was to identify unique regions within the FR-α and FPGS sequences for the generation of highly specific antibodies by avoiding regions of homology with other proteins using the programs described above.

In addition, compliance with GMM risk assessment procedures was also necessary. This involved avoidance of any key active site residues, anchorage points and other motifs required for biological activity. This allowed the project to be performed at containment class I.

The aim was to select as much of the sequence as possible whilst concomitantly observing the above regulations.

2.4.3. Restriction Mapping

Restriction maps for each cDNA protein coding region were also obtained in order to determine the positions of all restriction sites throughout both the FR-α and FPGS sequences. This was performed in order to enable appropriate selection of restriction sites to engineer into the terminals of the forward and reverse primers which would be used to amplify the regions selected, use of a restriction site already present in the target sequence would result in truncation of the protein and thus were avoided. The restriction maps were obtained from Harvard education at http://pga.mgh.harvard.edu/cgi-bin/map.cgi. The maps obtained also provided information on unique restriction sites and restriction sites not found within the protein sequence. This assisted in selection of appropriate restriction sites.

2.4.4. Oligonucleotide Primer Design

Complementary primers were designed, *E.coli* codon usage was considered at this stage as translation may be impaired if the codon usage is found to be low, which may result in failure of subsequent steps. Rectification of this may involve alteration of a limited number of bases or movement of primers to avoid unfavourable codon usage. The primers were designed to base pair with mRNA sequences derived from cell lines known to express the protein, flanking the regions of interest. Information on the protein expression in various cell lines was found from the National Cancer Institute website at http://dtp.nci.nih.gov/mtweb/.

Restriction sites were engineered into the 5’ end of each forward and reverse primer to allow for subcloning into the polycloning site of pET expression vectors.

As well as addition of restriction sites the primers had to be designed to ensure the proteins would be translated in the correct reading frame, engineering an extra base into the primer sequence is often required to ensure this occurs. A guanine residue was also engineered into the 5’ end of the restriction site as they are the most efficient residues for acquiring non-template derived adenine residues which *Taq* polymerase commonly adds to the sequence during transcription. This is of significance as initial cloning involved placement of the fragment into a T-vector which will be discussed in detail in section 2.4.11.

GC rich areas of the sequence were also avoided if at all possible as they often cause problems with self complementation in PCR.

The melting temperatures (T_m) of each forward and reverse primer pair were also calculated to ensure they were similar, to ensure both primers would anneal under the selected conditions.

Figure 2-3: Primer T_m calculation. Approximate T_m values were estimated according to the following general rule:

$$4^o (G+C) + 2^o (A+T) = T_m$$

2.4.5. Oligonucleotide Primer Synthesis

Primers were synthesised using an automated synthesiser, (Applied Biosystems) the method used to add each base was the phosphoramidite method (Caruthers 1987). Prior to each synthesis the machine was prepared according to the manufacturers instructions and various visual safety checks performed. The resultant primer solutions were removed from the machine in glass vials containing ammonium hydroxide. The solution was transferred into plastic screw cap 1.6ml microfuge tubes, sealed and incubated at 56^{o}C overnight to remove protective groups. The primers were then placed at -20^{o}C for 15 minutes to reduce the volatile state of ammonia. 400µl primer solution was removed and treated with 40µl Sodium acetate (NaAc, 2M, pH 4.0-4.8) to remove the ammonium hydroxide. 1.2ml 100% ethanol was then added and the DNA precipitated for 15 minutes at -80^{o}C, then centrifuged (Eppendorf 5702, 10 minutes, 14000 RPM) to pellet the DNA. The supernatant was removed and the pellet washed in 100µl 70% ethanol, spun down again and dried in a 65^{o}C hot block. Once dry the pellet was resuspended in 150µl RNase free water treated with 0.1% DEPC.

2.4.5.1. Oligonucleotide Primer Quantitation

Primer concentrations were calculated using an automated calculator. 10µl primer was added to 990µl dH_2O to make a 1/100 dilution and placed in a cuvette. The machine was blanked according to the manufacturer's instructions and the absorbance at 260nm measured (Genequant II DNA/RNA Calculator, Pharmacia Biotech). The primer concentration was given in pmol/µl (µmol/l). For each primer solution measured, a stock solution of 7.5µM was prepared and stored at -20^{o}C.

2.4.6. RNA Preparation

The human ovarian carcinoma cell lines SKOV-3 and IGROV-1 were selected for RNA extraction as, from the NCBI data, they were found to have high levels of both FR-α and FPGS mRNA. The cells, which grew as a monolayer, were maintained in appropriate culture medium: RPMI 1640 (Sigma, UK), 10% foetal bovine serum (Sigma, UK) and 2mM L-glutamine (Sigma, UK) with 5% CO_2 in a 37^{o}C incubator. Cells were harvested at approximately 75% confluence (~10^7 cells) via the use of trypsin-EDTA (Sigma, UK), washed three times in phosphate buffered saline (PBS) and pelleted via centrifugation (Eppendorf 5702, 2000 RPM, 6 mins). The pellet was resuspended in 200µl PBS and stored at -20^{o}C prior to RNA extraction. mRNA was extracted from both cell lines using an RNA preparation kit (RNeasy, Qiagen) and extraction of total RNA was carried out according to the manufacturer's instructions. The quality of the RNA was assessed by agarose gel electrophoresis (see 2.4.9) and spectrophotometry.

2.4.7. Complementary DNA Preparation/RT-PCR

Reverse transcription of mRNA is necessary as eukaryotic genes cannot be translated directly by bacterial cells due to the presence of introns. Eukaryotic organisms have the ability to remove non-coding introns after transcription via enzymatic splicing. As bacteria lack these necessary enzymes, they are unable to translate eukaryotic genes in their native form. Amplification of DNA segments can be performed by obtaining spliced mRNA transcripts from the eukaryotic cytoplasm and converting it back to a DNA copy lacking introns. This is achieved using the enzyme reverse transcriptase (RT), also known as RNA dependent DNA polymerase. The resultant complementary DNA (cDNA) template can then be used for the polymerase chain reaction.

cDNA was prepared from SKOV-3 and IGROV-1 mRNA by RT-PCR. 0.5ml microcentrifuge tubes were assembled containing the following components:

Table 2-1: RT-PCR Components

Reagent	Volume (µl)
RNA (1-2µg)	3
Reverse Primer (7.5µM)	4
MgCl2 (25mM Fermentas)	4
Dimethyl Sulphoxide (DMSO) (Sigma)	1
10x RT Buffer (100mM Tris pH 8.3, 0.5µM KCl, 15mM MgCl2, 0.1% gelatine, 20mM DTT) (Promega)	2
RNase free H_2O	3
RNasin (10U/µl, Promega)	0.5
dNTP's (10mM, Promega)	2
Reverse Transcriptase (20U/µl, Promega)	0.6

The mixture was overlaid with 40µl mineral oil to avoid evaporation and pulse spun to ensure mixing of the components. Reverse transcription was performed in a mini thermal cycler (MS Research Mini-Cycler), this machine was programmed for chain extension at 42^{o}C for 30 minutes, enzyme denaturation at 95^{o}C for 5 minutes and a 4^{o}C cooling temperature, left for a minimum of 15 minutes. The cDNA was stored at -20^{o}C until required.

2.4.8. The Polymerase Chain Reaction (PCR)

PCR is an enzyme based technique used to amplify a segment of DNA which lies between two regions of a known base sequence. The cDNA produced via RT-PCR is denatured via heating in the presence of two oligonucleotide primers engineered to anneal to the 5' and 3' ends of the sequence of interest and a pool of the four dNTP's. The mixture is then cooled to allow the primers to anneal and amplification is achieved via the action of *Taq* DNA polymerase. This cyclic mechanism of heat denaturation, annealing and amplification can be repeated many times (Figure 2-4). *Taq* polymerase can be added to the PCR mixture before heat denaturation, it can also be added once the annealing temperature is achieved; this is known as a 'hot start'. *Taq* polymerase is purified from the thermophilic bacterium *Thermus Aquaticus* which resides in hot springs in temperatures above 100^{o}C. Its DNA polymerase is thermostable and is not affected by the heat denaturation step, it is for this reason it is commonly used in PCR reactions.

Figure 2-4: Steps involved in PCR reactions. DNA is denatured to separate the double stranded helical structure (step 1), annealing is then achieved by addition of Taq polymerase to the mixture of primers and a pool of dNTP's and cooled (step 2); amplification/ synthesis (step 3) is achieved via a cyclic mechanism of heat denaturation, annealing and amplification which may be repeated many times (Britannica encyclopaedia 1998).

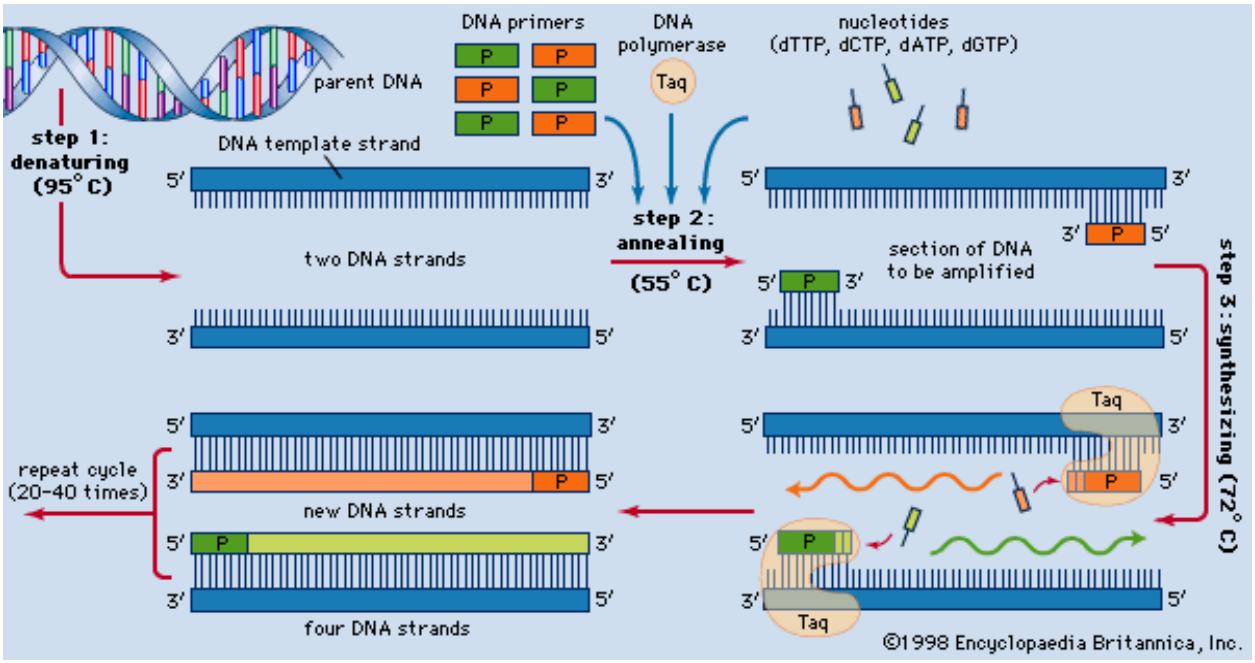

PCR was performed according to the method of Mullis *et al*. A sterile 0.5ml centrifuge tube was used in the PCR reactions, 10µl of cDNA from both the SKOV-3 and IGROV-1 RT reactions were added to the tube along with various other reaction components used to hybridise to the cDNA and prime elongation (Mullis et al., 1986).

Table 2-2: PCR Mixture Components

Reagent	Vol (µl)
cDNA from RT Reaction	10
Forward Primer (7.5 µm)	2
$MgCl_2$ (25 mM, Fermentas)	2
Dimethyl Sulphoxide (DMSO) (Sigma)	4
10x RT Buffer(100mM Tris pH 8.3, 0.5µM KCl, 15mM MgCl2, 0.1% gelatine, 20mM DTT) (Promega)	4
RNase free H_2O	27.5
Taq Polymerase (1u/µl, Fermentas)	0.5

Again the mixture was overlaid with mineral oil to avoid evaporation and pulse spun to ensure all reagents were mixed. PCR was performed in a thermal mini-cycler via a programmed reaction. (MS Research Mini-Cycler)

The following program was used in the PCR reaction.

Table 2-3: Standard Conditions used in PCR reactions.

Step	Temperature	Time	Reason
1	95^{o}C	1 minute	Denaturation of cDNA
2	55^{o}C	1 minute	Primer annealing
3	72^{o}C	1 minute	DNA synthesis
4	95^{o}C	30 seconds	Denaturation
5	55^{o}C	30 seconds	Primer re-annealing
6	72^{o}C	1 minute	DNA synthesis Repeat steps 4-6 30 times
7	72^{o}C	10 minutes	Pick up A's for T- vector, complete synthesis
8	4^{o}C	Overnight	

The resultant PCR product was held at 4^{o}C and stored at -20^{o}C. A 7µl sample of both PCR products was analysed by agarose gel electrophoresis to observe the result of the reactions.

2.4.9. Agarose Gel Electrophoresis

Agarose gel electrophoresis is used to separate DNA molecules on the basis of their size and is commonly used following PCR reactions to assess the success of the amplification, concentration and size of the PCR product generated. The resolution is dependent upon the concentration of agarose, the buffering system used, mass charge ratio and relative electrophoretic mobility of the fragments when an electric current is applied to the gel.

2.4.9.1. Preparation of DNA Size Markers

A stock solution of DNA markers were prepared by addition of 20µl loading buffer (0.35% Orange G, 30% glycerol, 10mM EDTA) and 40µl dH_2O to 10µl of a 123 base pair ladder (Sigma, UK). Markers were stored at -20^{o}C until required. 6µl was loaded on to each gel. 7µl PCR reaction mixture was added to 3µl loading buffer and loaded on to the gel.

2.4.9.2. Agarose and Running Buffer Preparation

1.7% agarose gels were used for separation and detection of PCR fragments. Gels were prepared by melting 1.7g agarose powder (Helena Biosciences) in 100mls Tris-Boric acid-EDTA buffer (TBE buffer; 0.09M Tris-Borate, 0.002M EDTA, pH 7.4). The solution was allowed to cool to 56^{o}C before addition of 1µl ethidium bromide (EtBr) (125µg/ml, Sigma).

The gel was poured into a gel casting tray with a comb to form wells for sample loading. Once set the gel was submerged in an electrophoresis tank containing TBE buffer, the samples and markers were loaded and the gel electrophoresed for approximately 20 minutes at 120 volts.

The DNA was visualised by staining with EtBr which, was added to both the gel running buffer and agarose, EtBr is a DNA intercalating agent and binds to DNA between the bases of the double helix. The labelled DNA can then subsequently be visualised via the use of an ultraviolet light transillumanator (UV-dual intensity transilluminator, UVP Ltd. UK) as EtBr has fluorescent properties under these conditions.

2.4.10. Gel Extraction/ Fragment Preparation

PCR products were excised from agarose gels via the use of a scalpel and purified using a column based method using a QIA quick spin gel extraction kit (Qiagen). Protocols were followed according to the manufacturers instructions.

Once eluted the purified samples were analysed by gel electrophoresis to observe the purity and yield of the fragment and then stored at -20^{o}C until required.

2.4.11. Preparation of pGEM T-easy plasmid construct

Use of cloning vectors is a convenient way to facilitate insertion of PCR fragments into pET expression vectors. Adenine residues are commonly added to PCR products by *Taq* polymerase. For this reason T-vectors (Promega pGEM, T Easy), plasmids containing a thymidine residue at each end of the cloning site are first used to carry the fragment of interest. They are prepared by cutting Promegas pGEM -5zf vector with EcoRV and adding 3' terminal thymidine residues to both ends, this overhanging thymidine base binds more easily to the adenine tail on the PCR product. In addition to this pGEM T Easy vectors also possess the β lactamase enzyme gene which causes bacterial ampicillin resistance, allowing for selection of *E.coli* which contain the plasmid only. Furthermore the T7 and SP6 RNA polymerase promoters flank the polycloning site which is within

the α peptide coding region of the LacZ gene for β galactosidase. Bacterial colonies utilise this enzyme to metabolise galactose into lactose and glucose (Figure 2-5). Insertional inactivation of this gene allows selection of recombinants via blue/white screening.

The advantage of cloning into a T-vector before cloning into a pET expression vector is the ease with which the fragment can be cloned via AT cloning. An alternative strategy would be to digest the PCR product with restriction enzymes and to clone directly into appropriately digested pET vectors. However, pET vectors have low copy numbers and it is difficult to produce a DNA miniprep of sufficient quantity/quality for DNA sequencing. Cloning the PCR products into the higher copy-number pGEM T-easy plasmids is the preferred method as it facilitates the sequencing of the amplified DNA from a single miniprep. Universal M13 sequencing primers will anneal to the sites flanking the polycloning site of the pGEM T-easy vector, further facilitating sequencing.

Figure 2-5: T-Easy Vector Map. Note the polycloning site, containing a number of different restriction sites within the LacZ gene used in blue-white selection. This plasmid also contains the gene for ampicillin resistance (Novagen catalogue).

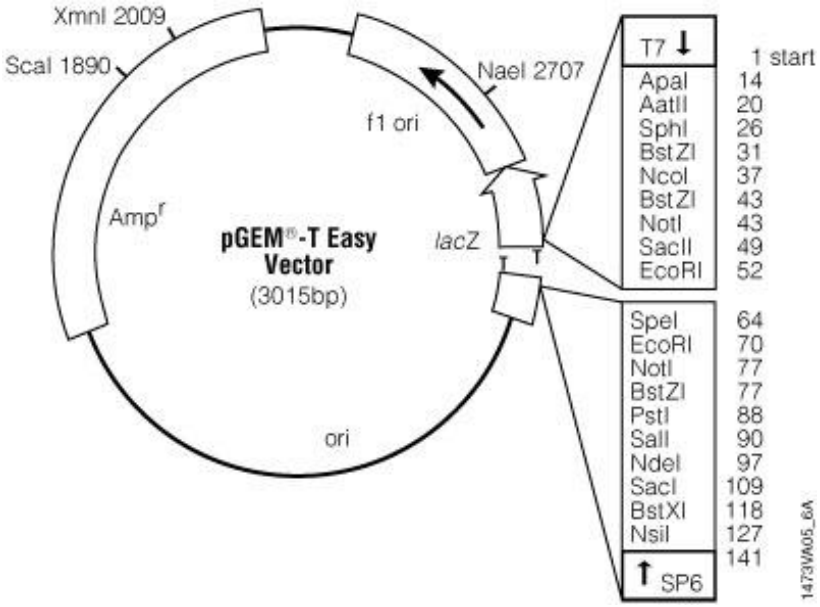

2.4.12. pGEM T-Vector Ligations

T-vector ligations were carried out in 1.6ml microfuge tubes.

To the tube the following components were added;

Table 2-4: Reagents used in T-vector ligations.

Reagent	Volume (µl)
Vector (Promega pGEM 50ng/µl)	1
Insert (Fragment Preparation)	1 or 2 depending upon yield
10x Ligation buffer (400 mM Tris-HCl pH 7.8, 100 mM MgCl2, 100 mM DTT, 5 mM ATP) (Fermentas)	1
RNase free dH_2O	Vol to make total vol = 10µl
T4 DNA Ligase (Fermentas 1000u/µl)	1

Samples were overlaid with mineral oil and ligations incubated overnight at 16^{o}C. Samples were stored at -20^{o}C until required.

2.5. Protein Expression

2.5.1. Preparation of Growth Media

2.5.1.1. 2YT Media

16g Tryptone Difco (Becton Dickinson), 10g yeast extract (Becton Dickinson) and 5g sodium chloride (BDH) were dissolved in 1 litre of distilled water. The media was aliquoted into 200ml bottles and sterilised by autoclaving before use.

2.5.1.2. 2YT Agar

3g Bacto-agar (Becton Dickinson) was added to a 200ml aliquot of 2YT media. The 2YT agar was then melted and sterilized via boiling, then allowed to cool.

2.5.2. Overnight *E.coli* cultures

Novablue stock cultures are routinely grown in the biological safety laboratory on tetracycline plates. Bacterial cell culture was performed in biological safety cabinets employing aseptic techniques. 20ml universals containing 5ml 2YT and 10µl tetracycline (15mg/ml, Kramel Biotech) were inoculated with a single colony (1µl) stock Novablue *E.coli* and grown overnight at 37^{o}C in an orbital incubator.

2.5.3. Novablue *E.coli* Non-Expression Host

Novablue *E.coli* is a K-12 bacterial cloning strain commonly used in general purpose bacterial cloning. It has high plasmid transformation efficiency and gives a high yield of good quality plasmid DNA from standard minipreps. Wild type *E.coli* strains possess the LacZ gene encoding the α and β subunits of β galactosidase. As described earlier, this enzyme breaks down galactose, it is also able to break down a chromogenic analogue of galactose; X-gal (5-bromo-4-chloro-3-indolyl-B-D-galactoside). When this compound is metabolised it yields a blue compound. Bacterial colonies with an intact LacZ gene therefore appear blue in media supplemented with X-gal (Figure 2-6).

Novablue *E.coli* are modified to lack the genes encoding the α-subunit if this protein and thus cannot synthesize functional β-galactosidase. pGEM vectors carry the gene encoding the α-subunit, creating an intact gene in Novablue *E.coli* containing the plasmid, these cells are able to synthesize functional β-galactosidase. These cells are therefore able to form blue colonies on X-gal supplemented agar plates. The LacZ gene in the pGEM vector has been engineered to contain a polycloning site within the gene encoding the α-subunit of β-galactosidase. If the plasmid contained an insert the LacZ gene would fail to function correctly. It would be unable to metabolise X-gal to the blue product and the colonies would remain white (Figure 2-6). This allows identification of *E.coli* with a plasmid containing an insert from *E.coli* containing the plasmid which has recircularised without an insert. Only a very small proportion of host cells actually take up plasmid DNA. In addition, Novablue *E.coli* possess tetracycline resistance properties, this in combination with the ampicillin resistance gene carried by the plasmid allow for continual selection and reduce the frequency of false positive white colonies.

Figure 2-6: Photograph of blue-white selection plate. White colonies indicate the plasmid contains an insert as the colonies are unable to metabolise X-gal. Blue colonies retain this ability and metabolise X-gal, appearing blue.

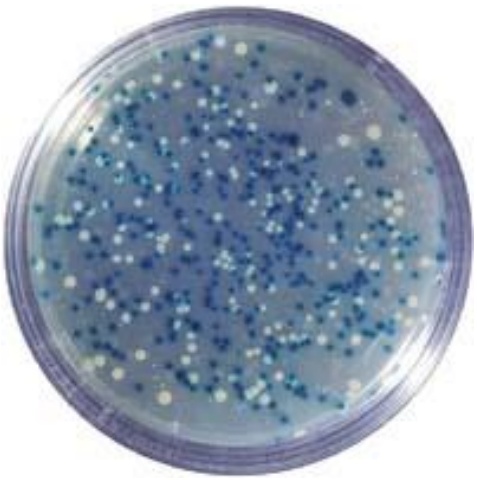

2.5.4. Competent *E.coli* Preparation

Transformation of plasmids into *E.coli* is achieved by inducing a transient competent state into the host cells, this state enables them to take up exogenous DNA.

A centrifuge tube containing 50ml pre warmed 2YT medium containing 100µl tetracycline (15mg/ml) was inoculated with 500µl overnight culture (see previous section), The culture was incubated at 37^{o}C in an orbital incubator and continually monitored until an optical density (OD) of 0.4 at 550nm was achieved (WPA CO210 Digital Colorimeter). At this point the cells are in mid-log phase and are growing exponentially. The centrifuge tube containing the culture was stored on ice for 20 minutes to halt cell growth. The cells were then centrifuged at 4^{o}C for 10 minutes at 3000 RPM (MS Falcon C1300). The supernatant was discarded and and the cells resuspended in 8mls pre-chilled transformation buffer (TFB) (3.73g KCl, 4.4g MnCl2, 0.735g CaCl2, 0.4g hexamine cobalt chloride, 5ml 1M 2-[N-morpholino] ethanesulfonic acid (MES) pH 6.3, made up to 500ml with distilled water). The cells were then centrifuged again at 4^{o}C for 10 minutes at 3000 RPM. The supernatant was discarded and the cells resuspended in 2mls TFB and 70µl DMF (Sigma) was added. This mixture was stored on ice for 5 minutes after which 70µl 2.25M dithiothreitol (DTT) was added and incubated for a further 10 minutes on ice. Finally a further 70µl DMF was added and the cells incubated on ice for a minimum of 1 hour before use. After this time the cells were competent and ready for transformation.

2.5.5. Transformation of pGEM T Easy Constructs into Novablue *E.coli*

A 10µl volume of ligation mix was added to 200µl competent Novablue *E.coli* and incubated on ice for 45 minutes. The cells were then heat shocked at 42^{o}C for 90 seconds in a water bath, they were then transferred to ice for 2 minutes. After the addition of 800µl 2YT to each sample the cells were incubated at 37^{o}C for 1 hour in a dry hot block. The cells were centrifuged for 3 minutes at 2000 RPM (Microfuge, Beckman Coulter), sufficient supernatant was discarded to leave 100µl residual volume. The pellet was resuspended in this small volume and spread over the surface of a TAXI selection plate. The plates were allowed to dry and were then inverted and incubated overnight at 37^{o}C.

2.5.6. Selection Plates

TAXI plates are used for blue/white selection of transformants, they also contain antibiotics for screening out non transformants.

- T = Tetracycline
- A = Ampicillin
- X = X-Gal
- I = IPTG

Preparation of TAXI plates 2YT agar was prepared as described in section 2.5.1, a 200ml volume was melted and cooled to approximately 56^{o}C before addition of 400µl tetracycline (15mg/ml), 400µl ampicillin (25mg/ml, Sigma), 1ml X-gal (2%) and 80µl 1M IPTG (isopropylthiogalactoside, Q-Biogene). The agar was then mixed and poured into approximately 12 petri plates and allowed to cool in a biological safety cabinet. Plates were stored inverted at 4^{o}C until required.

2.5.7. Colony Screening Procedure and Plasmid Isolation

2.5.7.1. Plasmid Minipreparations

12 white colonies were picked from each TAXI selection plate used for transformation and used to prepare 5ml overnight cultures (5mls 2YT, 10µl Tetracycline, 10µl Ampicillin). The cultures were incubated overnight at 37^{o}C in an orbital incubator. 12 colonies were selected as blue-white selection is not always specific and false positives may occur.

Plasmid DNA was isolated via the use of a Qiagen QIAprepR Miniprep kit. First 1.5ml of each overnight culture was transferred into a micro-centrifuge tube and centrifuged for 3 minutes at 13000 RPM. The supernatant was discarded and protocols were then followed according to the manufacturers instructions. The principle of the method is based upon alkaline lysis of the bacterial cells, adsorption of plasmid DNA on to silica in the presence of high salt then washing and elution of plasmid DNA. Minipreps were stored at -20^{o}C until required.

2.5.8. Restriction Digestion of Plasmid DNA

Bacterial restriction endonucleases (RE's) are commonly used to both prepare and recover DNA fragments by 'cutting' DNA at specific sequences. (Smith, 1979) The sequences recognised by RE's

are commonly 4-6 bases in length and are highly specific to each particular RE. The nomenclature applied to RE's uses abbreviations, with the first letter being derived from the genus name and the second two letters from the species name. Additional letters and/or numbers are added for identification of the specific enzyme (Smith & Nathans, 1973). Cleavage of the DNA strands can give rise to either 'blunt' ends where both strands terminate in a base pair or 'sticky' ends (cohesive termini) where cleavage is staggered and results in an overhang of unpaired nucleotides (Figure 2-7). The RE's used in this project were used to excise the fragments of interest from the T-vector in order to confirm the presence of the DNA insert, the RE's used also produced sticky ends in order for them to be able to form bonds with the complementary region on the plasmid in subsequent steps.

Figure 2-7: Common RE's generating both blunt and sticky ends. AluI and HaeIII (top) generate blunt ends, BamHI, HindIII and EcoRI (bottom) generate sticky ends.

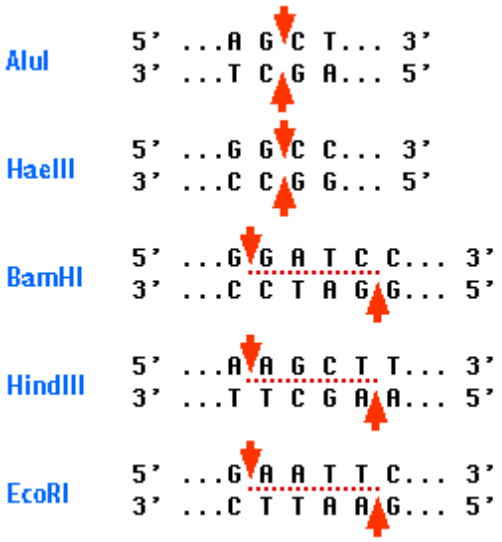

In both instances double digests were performed to liberate the cloned insert from the plasmid DNA as both sequences were engineered with different RE sites on their forward and reverse primers. FR-α contained SacI and XhoI restriction sites and FPGS contained BamHI and HindIII restriction sites named RE1 and RE2 as described in Table 2.5. Engineering two different RE sites in to the primers allows for directional cloning so the insert is in its desired orientation. The double digestion mixture was prepared as described below. The mixture was then incubated in a dry hot block at 37^{o}C for 30 minutes. 7µl of each digest was added to 3µl loading buffer and resolved via

1.7% agarose gel electrophoresis using 123 bp markers as a reference, 2 combs were placed in each agarose gel.

Table 2-5: Reagents used for restriction digests.

Reagent	Volume (µl)
Miniprep	5
10X Buffer (Appropriate colour) (Red - FPGS 10mM Tris-HCl pH8.5, 10mM MgCl2, 100mM KCl, 0.1 mg/ml BSA. Yellow –FR-α 33mM Tris-Acetate pH 7.9, 10mM Mg Acetate, 66mM Potassium acetate, 0.1 mg/ml BSA)	1
RE1 (10U/µl)	0.5
RE2 (10U/µl)	0.5
H_2O	3

2.5.9. Automated DNA Sequencing

The previous step allowed confirmation of the presence of the insert, a second step was also added in order to confirm the identity of the insert. The sequences of the inserts were fully characterised via automated dye-terminator DNA sequencing using the universal M13 forward and reverse primers. This was used to ensure the complete target sequence had been cloned into the pGEM vector. 20µl samples of miniprep DNA were sent to Lark Technologies (Essex, UK) for sequencing.

2.5.10. Expression of FR-α and FPGS Recombinant Proteins

2.5.10.1. Subcloning in to pET Expression Vectors

A wide variety of pET vectors are now available for use with *E.coli* host expression systems for protein production. Production of proteins via the use of both simple pET expression vectors and vectors containing water soluble tags were used. Use of vectors containing tags encoding water soluble protein sequences such as glutathione s-transferase (GST) and thioredoxin (Tx) assist with solubility of potentially insoluble proteins.

pET 21 was selected as it is a relatively simple vector, it is an expression vector under the control of T7 RNA polymerase. It contains ampicillin resistance, a polycloning site for cloning the insert and a C-terminal His-tag, used for purification (Figure 2-8). The protein produced from this type of vector is favoured in mouse immunisation schedules as it does not contain any 'tag' (with the exception of the His-tag), this allows for easier screening in hybridoma technology stages, which will be discussed in more detail in the following chapter. However, experience in this lab has shown that proteins produced in such vectors are not always easy to purify, particularly with insoluble proteins which may also be cysteine rich. As they do not contain a large tag, the protein does not always appear to be immunogenic to the animal, particularly if small regions were targeted. Short, untagged sequences are often degraded to nothing in *E.coli* cells and are undetectable via SDS PAGE. For this reason both pET 21, 41 and 32 vectors were selected for generation of recombinant proteins as all targets were small and relatively cysteine rich. Water soluble tags may aid in the solubility and improve immunogenicity of short sequences as they potentially contain motifs which may solicit the help of T-cells.

Figure 2-8: pET 21 Vector map (Novagen catalogue).

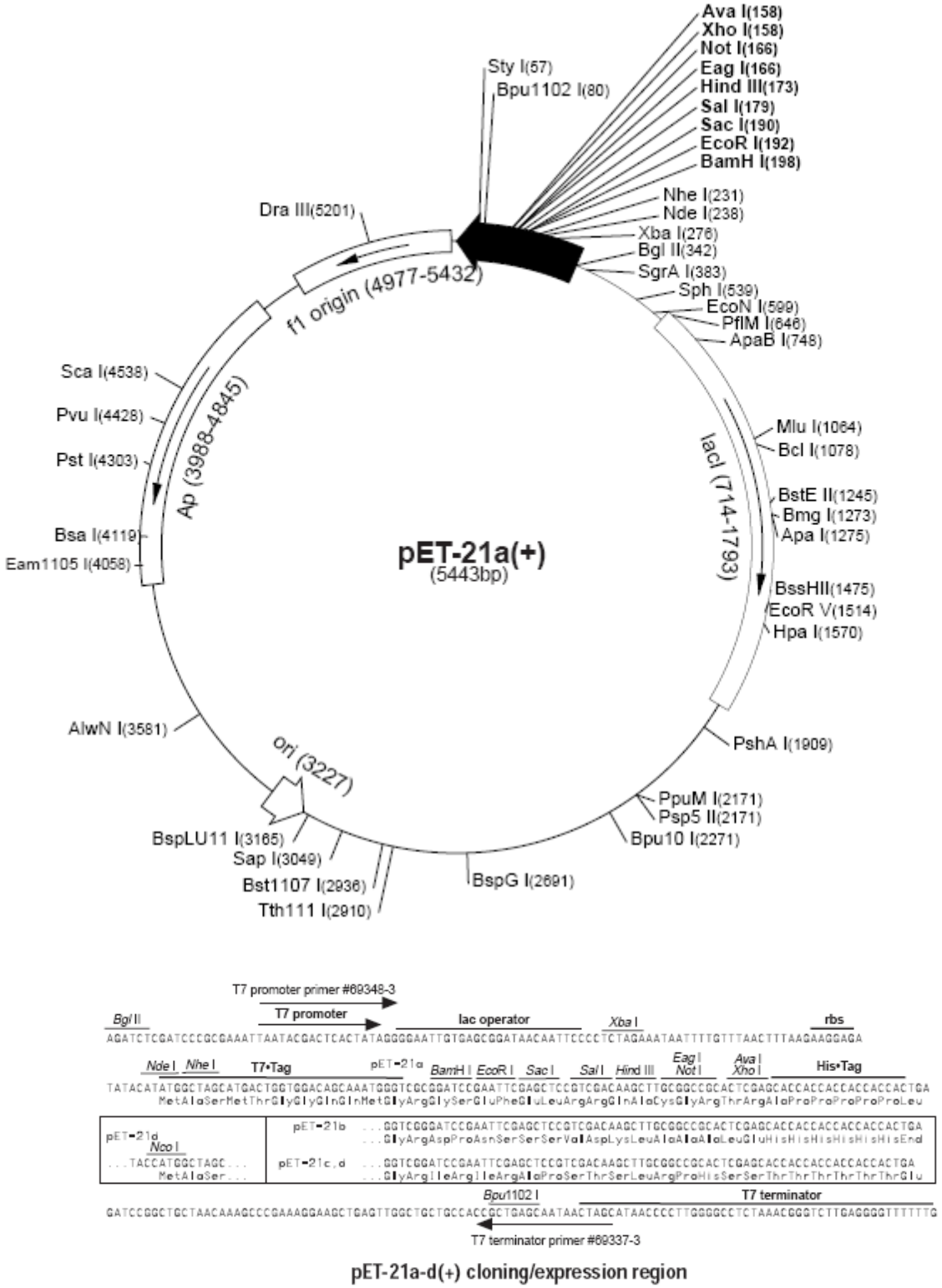

pET-21a-d(+) cloning/expression region

pET 41 vectors were selected as an adjunct to the pET 21 vector. pET41 vectors possess all the features of the pET 21 system, although kanamycin resistance replaces ampicillin resistance. In addition it has a GST fusion tag, this has been reported to enhance the production and solubility of the fusion protein produced. As the proteins we intended to produce were likely to be insoluble this was deemed a suitable vector to use. The GST tag may also stimulate the mouse immune system due to the large size of the tag. This has inherent advantages and disadvantages as it may increase the affinity of the antibody due to a stronger immune response but may also decrease the number of antibodies being produced to the protein as they may recognise the GST construct in addition to the protein. In addition pET32 vectors were also used, they are similar to pET41 but contain a thioredoxin (TX) tag in place of the GST tag and possess ampicillin resistance.

Figure 2-9: pET 41 Vector map (Novagen catalogue)

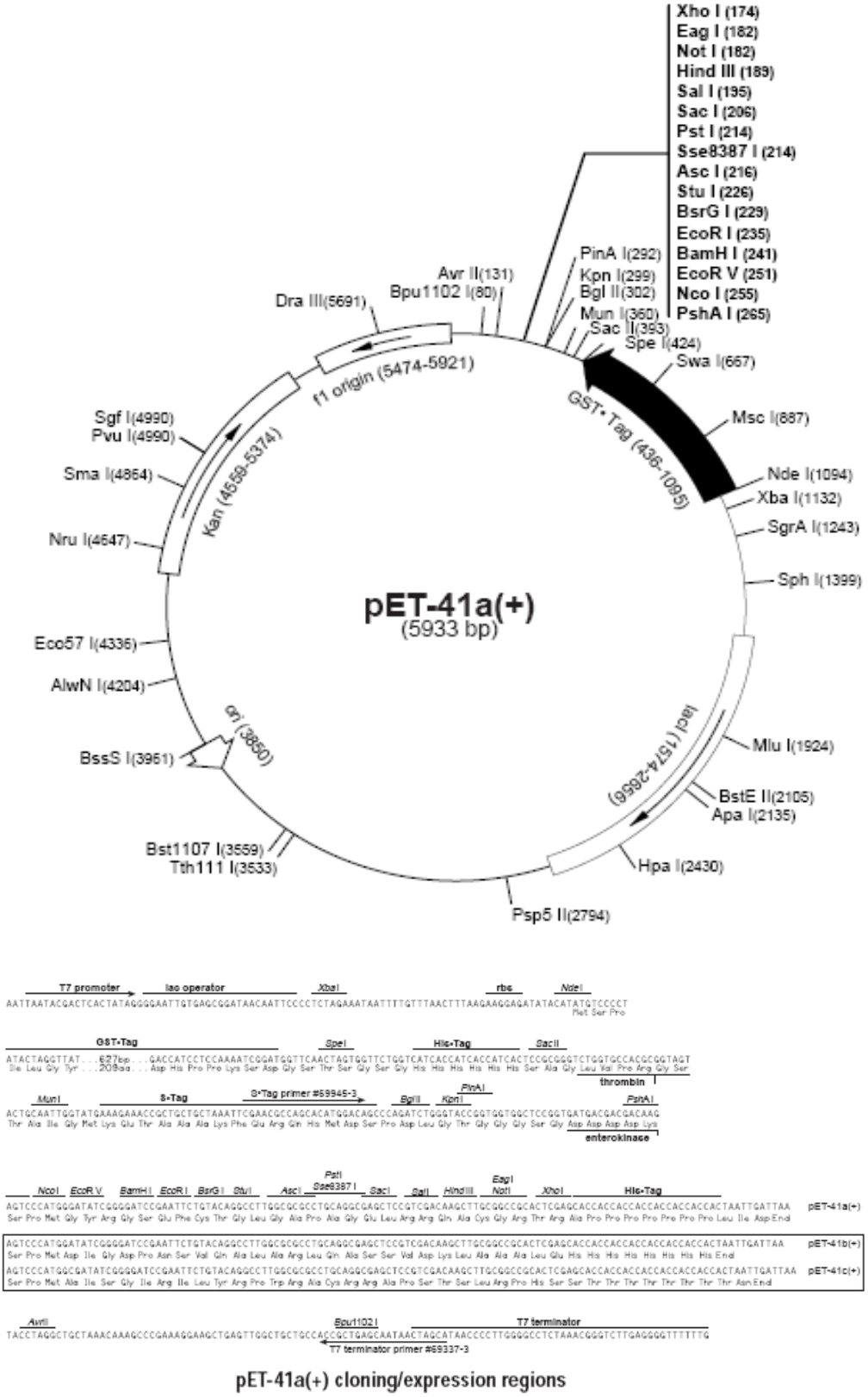

pET-41a(+) cloning/expression regions

Figure 2-10: pET32 Vector map (Novagen catalogue)

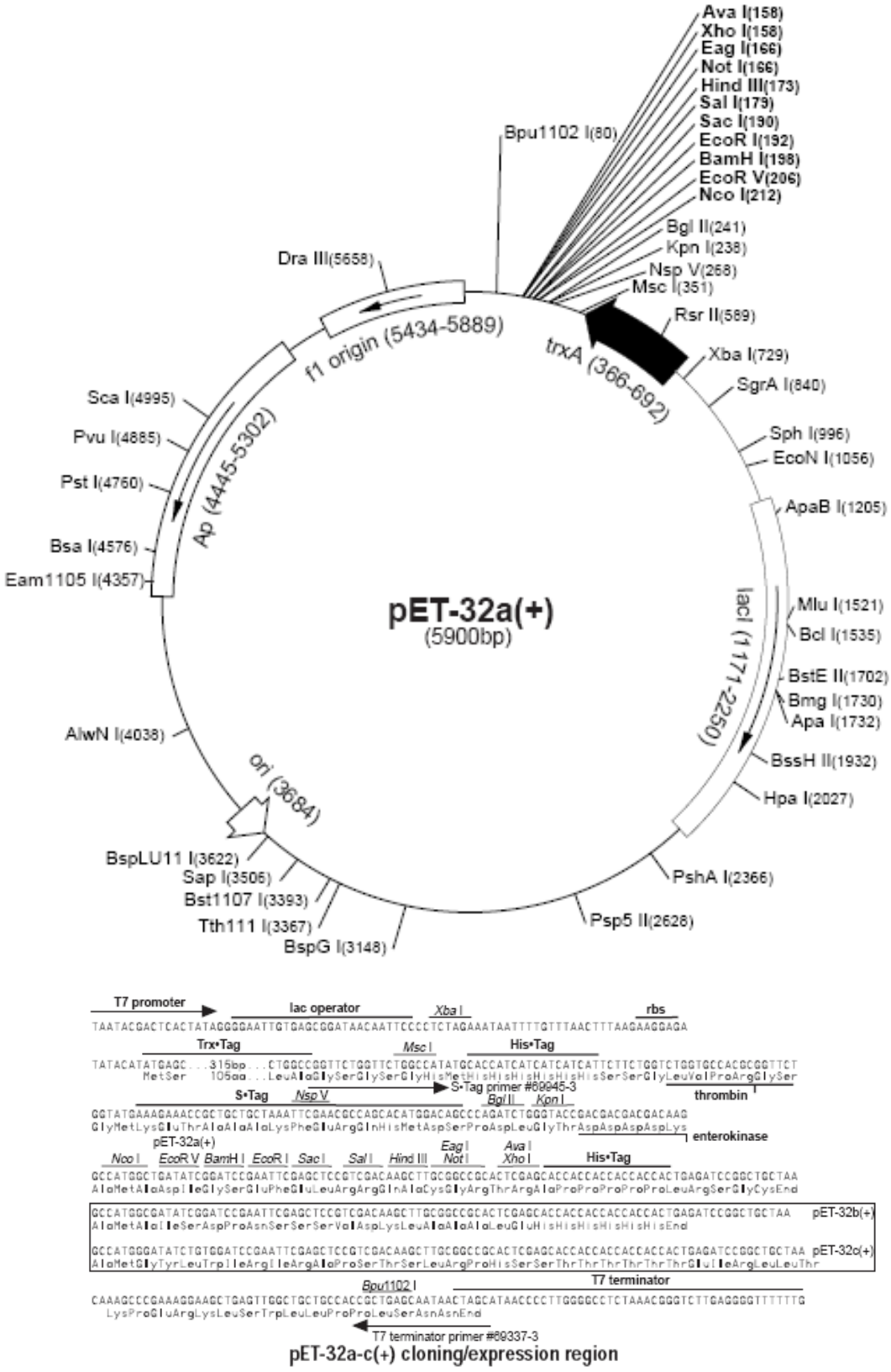

2.5.10.2. Preparation of the Insert for Subcloning

Double restriction digests via the use of the same RE's detailed in section 2.5.8 were performed in order to excise the inserts from the pGEM plasmids using the following reagents.

Table 2-6: Reagents used for restriction digestion in preparation for subcloning

Reagent	Volume (µl)
Miniprep (4µg)	20
10X Buffer (Appropriate colour)	3
RE1 (10U/µl)	1
RE2 (10U/µl)	1
H_2O	Volume to make total = 30

The mixture was incubated at 37^{o}C for 1 hour and samples were analysed via 1.7% agarose gel electrophoresis. The whole sample was added to 6µl loading buffer. Following electrophoresis the band was extracted from the gel and a fragment preparation made using the Qiagen kit as previously described.

2.5.10.3. Preparation of pET vectors

The pET vectors used were prepared by digestion of the neat vector with the appropriate restriction enzymes in order to produce the appropriate sticky ends required for cloning of the FR-α and FPGS fragments.

Table 2-7: Reagents used for pET vector digestion

Reagent	Volume (µl)
Neat Vector (pET21, 41 or 32)	2
RE1 (10U/µl)	1
RE2 (10U/µl)	1
10X Buffer (appropriate colour)	2
H_2O	Volume to make total = 20

Vectors were incubated for one hour then treated with 2µl calf intestine alkaline phosphatase (CIAP, Promega 1U/µl) to remove 5' phosphate groups and prevent the vector recircularising. A clean up kit (Novagen) was then used to remove all traces of reagents and other contaminants,

following this the entire sample was run on an agarose gel and a fragment preparation performed, vectors were stored at -20^{o}C until required.

2.5.10.4. Ligation of DNA fragments into pET constructs

Ligations were performed in a similar way to that of pGEM ligations. In both cases the vectors used were already prepared and needed no preparation before the ligations were performed.

Table 2-8: Reagents used for ligations

Reagent	Volume (µl)
dH_2O	6
Fragment Prep	1
pET 21/41	1
10 X Ligase buffer (Fermentas, 400mM Tris-HCl, 100mM $MgCl_2$, 100mM DTT, 5mM ATP pH7.8)	1
T4 DNA Ligase (Fermentas, 1U/µl)	1

The samples were overlaid with oil to prevent evaporation and incubated at 16^{o}C overnight.

Overnight Novablue cultures were also prepared as previously described.

2.5.10.5. Transformation into Novablue E.coli

The pET constructs were first transformed into the non-expression host Novablue. Novablue cells were prepared and transformed as described previously for pGEM transformations. Selection of transformants was made following overnight incubation at 37^{o}C on 2YT agar plates. pET 21 and 32 colonies were grown on agar containing ampicillin (50µg/ml) and pET41 colonies grown on agar containing kanamycin (30µg/ml).

2.5.10.6. Screening Transformant Colonies

As blue-white selection is not present at this stage, all colonies appear white. 12 colonies from each plate were selected and grown overnight in 5ml broth cultures with the appropriate antibiotic. The plasmid DNA was subsequently purified from 1.5ml aliquots of each culture using the standard Qiagen minipreparation protocol described previously.

The plasmid DNA was again double restriction digested as described previously and the electrophoretic mobility compared with 123 base pair markers assessed using 1.7% agarose gel electrophoresis. This allowed differentiation between plasmid – insert constructs from empty vectors which had lost the insert. Orientation of the insert was not performed due to the presence of different restriction sites at either end of the insert.

2.5.11. Transformation into an Expression Host

2.5.11.1. E.coli BL21 (DE3) plysS and Tuner (DE3) plysS

Both the above *E.coli* strains are λDE3 lysogens that carry a chromosomal copy of the T7 RNA polymerase gene under the control of the lacUV5 promoter. The addition of isopropyl β-D-1-thiogalactopyranoside (IPTG) brings about production of a T7 RNA polymerase which can then transcribe genes cloned downstream of the T7 lac promoter in pET plasmids. Both strains possess the pLysS plasmid, which carries a chloramphenicol resistance gene and encodes the gene for T7 lysozyme. T7 lysozyme inhibits T7 RNA polymerase and the plasmid produces enough of this enzyme to inhibit the basal (pre-induction) level of T7 RNA polymerase. This prevents 'leaky' expression of the target gene. This enzyme also aids cell lysis following protein expression.

Furthermore *E.coli* Tuner strains are lacZY deletion mutants of BL21, the lacY (lac permease) mutation causes the IPTG to enter the cells uniformly. This produces a homogenous, concentration dependent induction and has been found to be effective in increasing the solubility of previously insoluble proteins. This is due to the IPTG entering more slowly, allowing protein production to proceed at a slower rate, lowering the possibility of recombinant proteins being segregated into insoluble inclusion bodies. These features make these strains of *E.coli* particularly suited to large scale protein expression.

2.5.11.2. Transformation into E.coli BL21/Tuner

Both BL21 and Tuner are routinely cultured in 2YT media. Competent cells were prepared and transformed as previously described for the Novablue *E.coli*. 1µl of each plasmid miniprep was added to 100µl competent cells and transformed. Following transformation recombinants were selected for by culture on plates containing ampicillin for pET 21 constructs and kanamycin for pET 41 constructs. Transformant colonies were selected for small and large scale protein production.

2.5.12. Fusion Protein Expression

2.5.12.1. Small Scale Fusion Protein Induction

Colonies were picked from the transformation plates and cultured at 37^{o}C in an orbital incubator in 5mls 2-YT media with the appropriate antibiotic (50µg/ml). The absorbance at 550nm was monitored until it reached 0.4 (mid-log phase). At this point a 1ml sample was removed and incubated at 37^{o}C, this was used as the pre-induction sample, a 10µl sample was also removed to provide an overnight culture for large scale induction. To the remainder of the culture 10µl 1M IPTG was added and incubated for 3 hours at 37^{o}C. Following induction 1ml samples were taken and centrifuged, along with the uninduced sample (13000 RPM, 3 minutes). The cell pellets from both the pre and post induction cultures were resuspended in 150µl SDS Laemmli sample buffer (40% dH_2O, 5% 2-mercaptoethanol, 2%SDS, 20% glycerol, 25% Tris 250mM pH 6.8, 0.1% bromophenol blue).

2.5.13. SDS Polyacrylamide Gel Electrophoresis

The pre and post induction samples in SDS Buffer were boiled in a water bath to denature the proteins and 10µl added to each well, they were resolved electrophoretically via the use of 12% polyacrylamide gels. The gels were stained with Coomassie blue, the molecular weight of the induced protein was confirmed in relation to standard molecular weight markers. Once successful induction was confirmed, large scale protein induction could be carried out.

SDS PAGE was carried out via the use of a Bio-Rad Mini-Protean casting unit, which was assembled according to the manufacturers instructions. The gel consisted of a lower 12% resolving gel and an upper 4% stacking gel. The stacking gel allows concentration of the loaded sample and improves resolution on entry into the lower gel. The 12% resolving gel was prepared as follows; 3mls 30% acrylamide mix, 1.85ml dH_2O, 5mls 750mM Tris pH 8.8, 50µl 20%SDS. The solution was stored at 4^{o}C. When required, 100µl 10% w/v ammonium persulfate (APS), and 10µl N,N,',N'-tetramethylethylenediamine (1% v/v) (TEMED, Sigma) was added and poured between the glass plates of the casting gel, 2cm beneath the top of the glass. It was then overlaid with water to ensure there was an even meniscus. Once polymerised the water was decanted and the stacking gel was added. (1ml 30% acrylamide mix, 3.89mls dH_2O, 5mls 125mM Tris pH 6.8) 50µl APS and 5µl TEMED were added to activate and the stacking gel loaded on top of the resolving gel. The comb was then placed in between the glass plates, ensuring no air was trapped between the plates, and the gel was allowed to polymerise. Once polymerised, the comb was removed and the

wells washed with distilled water to remove any unpolymerised acrylamide. The gels were then placed in the electrophoresis tank and the reservoirs filled with Tris-glycine electrophoresis buffer (25mM Tris pH 8.3, 192mM glycine, 0,1% SDS).

The samples were added along with 6µl markers (Bio-Rad Precision plus dual colour protein standards) and electrophoresed for approximately 30 minutes at 240 volts or until the dye front had reached the bottom of the gel. After completion gels were removed from the glass plates and the stacking gel excised and discarded. Gels were then either stained for visualisation of the protein bands or transferred to nitrocellulose filters for Western blots.

The gels were stained with Coomassie blue and fixed with methanol and glacial acetic acid. This was achieved by immersion of the gel in a solution containing 0.25% (w/v) Coomassie blue, 40% methanol and 10% glacial acetic acid for a minimum of 1 hour at room temperature with gentle agitation. The gels were then destained with a destain solution containing 40% methanol and 10% glacial acetic acid to remove excess background staining. The bands were visible and were compared with known molecular weight protein standards. The gels were photographed then discarded.

2.5.13.1. Large Scale Fusion Protein Induction

The purpose of large scale induction is to produce a larger quantity of recombinant protein for immunisation. The 10µl sample taken from the small scale induction was grown in a 5ml overnight culture with the appropriate antibiotic (50µg/ml). The next day this was added to 500µl pre-warmed 2-YT media with 1ml appropriate antibiotic (50µg/ml). The culture was incubated for approximately 3 hours at 37^{o}C in an orbital incubator until an OD of 0.4 at 550nm was reached. The flasks were then induced with 500µl 1M IPTG and incubated for a further 3 hours. The cultures were then harvested and separated from the culture medium via centrifugation. (3000RPM, 40 minutes) The supernatant was discarded and the pelleted cells resuspended in 10mls 1X His-bind buffer (5mM imidazole, 500mM NaCl, 20mM Tris-HCl pH 7.9). The suspension was transferred into a 25ml universal and a few granules of lysozyme (Sigma) were added to aid in disruption of the bacterial cell membranes. The universals were stored at -20^{o}C overnight or until required for processing.

2.5.14. Sonication of Large Scale Products

After overnight storage the bacterial cell walls were disrupted by first thawing the mixture then sonicating (MSE Soniprep 150 Sonicator). The cells were sonicated 12 times for 1 minute each time with 1 minute intervals on an amplitude setting of 12 microns. The lysate was then centrifuged in polycarbonate centrifuge tubes at $4^{o}C$ for 20 minutes at 27,000G. The supernatant (containing the soluble fraction) was decanted into a fresh universal and filtered (0.45µM filters) in preparation for column chromatography, this method was employed initially as immunisation with soluble proteins has in the past been more successful in obtaining high quality antibodies, which may be due to the protein being more immunologically active. The insoluble fraction (pellet) was resuspended in 10mls His-Bind Buffer containing 8M urea (5mM imidazole, 500mM NaCl, 20mM Tris-HCl pH 7.9, 8M Urea). This was placed on a roller in an attempt to solubilise the pellet.

2.5.15. His-Bind Column Chromatography

2.5.15.1. Soluble Columns

Fusion proteins are designed and consideration is given to purification of the protein at the design stage. The strategy commonly employed to facilitate this purification is to fuse the target gene to a sequence capable of selectively recognising a matrix bound ligand. In this case pET 21, 41 and 32 were selected as they encode a hexahistidine tag. This is then translated via the use of *E.coli* to form 6 consecutive histidine residues

This type of chomatography is dependent upon the hexahistidine tag present on the recombinant protein binding to nickel ions on a column. During purification the His-tag sequence binds to divalent cations ($Ni^{2+)}$ immobilised on agarose His-bind metal chelation resin (Novagen). The unbound proteins are washed away and the protein of interest is eluted using an imidazole elution buffer.

5mls of an even suspension of His-Bind resin (Novagen) were added to a 5ml polypropylene column. The resin was left to settle by gravity and once the storage buffer (20% ethanol) had washed away, the column was washed with 10mls deionised water and charged with 10mls charge buffer (5mM $NiSO_4$). Binding of nickel to the resin was observed via the change of column colour from white to blue. The free nickel was washed away and the column equilibrated with 10mls binding buffer (5mM imidazole, 500mM NaCl, 20mM Tris-HCl pH 7.9). The column was allowed to run until all the solution had reached the top of the column before adding the next solution,

continuous flow was ensured and it was never allowed to run dry. At this stage the protein fraction was added, either the soluble fraction or solubilised pellet (refolded by dialysis - see section 2.5.17) was allowed to flow through, followed by a further 10 mls His-Bind buffer. The column was the washed with 10mls wash buffer (60mM imidazole, 500mM NaCl, 20mM Tris-HCl pH 7.9). The bound protein was then eluted with 10ml elute buffer (1M imidazole, 500 mM NaCl, 20 mM Tris-HCl pH 7.9). 0.5ml fractions were collected in 1.5ml microcentrifuge tubes, 12 in total were collected for quality and quantitative analysis. After use the nickel was removed from the column by adding 10mls 200mM EDTA and then washing with deionised water. As the columns could be used more than once, they were stored in the fridge until required.

2.5.15.2. Insoluble Columns

The same method as the above method was employed when running an insoluble column, the insoluble fraction was centrifuged (15 mins 27,000 G) and the supernatant decanted and filtered via the use of a 0.45 µM filter. His-bind buffer was added to reduce the molar concentration of the protein solution from 8M to 6M. Following this the protocol was followed as above, however all solutions used contained 6M urea in addition to the other components.

2.5.15.3. Protein Assay

The concentration of the eluted protein fractions was determined via the use of a Bradford protein microassay. 10µl samples from each fraction were added to 790µl dH_2O and 200µl Bradford dye reagent concentrate (BioRad) compared with a blank containing 200µl Bradford reagent and 800µl dH_2O, the OD was measured at 590nm at room temperature. The total protein concentration in each fraction was determined by comparison with a standard curve of BSA standard controls.

10µl samples were taken from fractions containing significant concentrations of protein (more than 0.4mg/ml) and were mixed with an equal volume of SDS sample buffer and analysed via SDS-PAGE to determine the molecular weight and purity of the protein.

After this had been confirmed the protein fractions with the highest concentration of protein were pooled together and re-assayed to determine the total protein fraction concentration. A freeze thaw test was performed on a small sample of the protein and re assayed to ensure the protein

was suitable for freezing down. Once confirmed the proteins were split into 200µg aliquots and stored at -80^{o}C until required.

2.5.16. Refolding of Insoluble Protein Fractions

It is common for proteins overexpressed in *E.coli* host strains to be insoluble and to be segregated into insoluble inclusion bodies within the cell. In order to recover immunologically active protein, the inclusion bodies need to be solubilised refolded and purified.

The pellet was solubilised in binding buffer with 8M urea and left on a roller for at least 24 hours or longer if necessary. As the pellet was solubilised under denaturing conditions (urea) the denaturing agent was then be gradually removed to allow the protein to refold and gain its antigenicity, this step was vital as the immunisation of mice relies upon the protein being recognised by the murine immune system and mice cannot be injected with urea. Refolding was achieved via either successive dialysis, (performed after running the insoluble fraction on an insoluble column) reducing the molarity of the denaturant gradually whilst keeping the constituents of the dialysis buffer constant or via refolding of the insoluble protein and reducing the denaturant concentration whilst bound to the column.

2.5.17. Refolding by Dialysis

12cm lengths of 5-24/32 visking tubing (Medicell International) were cut and rinsed in distilled water to separate the two layers. Medi clips were used to secure the end of the tubing and the insoluble fraction added to the tubing. Another clip was used to secure the end once filled with the protein. 500mls of a 4M urea 10mM Tris-HCl solution (pH 8.0) was prepared and the dialysis tubing was placed in the solution, which was left for 3 hours at room temperature with constant magnetic stirring. Buffer changes were performed, halving the molar concentration of urea each time from 4M, 2M, 1M, 0.5M, 0.25M, 0.125M, 60mM, and 30mM, after which the dialysed protein was washed twice in a 10mM Tris-HCl solution. Once dialysis was completed the protein was recovered from the tubing and the solution was then Bradford assayed to determine the concentration of protein present and frozen down if necessary.

2.5.18. Refold Columns

Another method employed to reduce the urea concentration and attempt to isolate the protein was by use of a refold column. The same procedure applied to insoluble columns was followed with a number of additional steps. After loading of His-Bind buffer, the insoluble fraction was added to the column followed by an additional 10mls His-Bind buffer + 6M urea. A further 10mls His-Bind buffer + 4M urea were added to the column, after which 10mls His-Bind buffer and 2M urea were added. Finally, 10mls His-Bind buffer, wash buffer and elution buffer, all without urea were added successively to the column and the fractions collected as normal.

2.6. Results - Antigen Design

2.6.1. Amino Acid and Gene Sequences

Links on the EMBL-EBI website located FR-α and FPGS base and amino acid sequences, which were listed under accession numbers P15328 (257 amino acids, 29819 Da) and Q05932 (587 amino acids, 65609 Da) respectively. FPGS was found to have both a mitochondrial and cytosolic from, differing only in the presence of a leader peptide sequence in the mitochondrial form, responsible for tracking and penetration into mitochondria.

BLAST searches revealed no significant homology between the sequences, or similarity to any other human sequences for either FR-α or FPGS.

2.6.2. Target Sequence Selection

One target region for FR-α was selected and two targets for FPGS (Figure 2-11 and Figure 2-12). The lengths of each sequence were 189 amino acids on FR-α and 228 and 167 amino acids on FPGS targets 1 and 2 respectively, the target sequences were selected in accordance with GMM risk assessments described in section 2.4.2. The sequences on FR-α avoided a serine residue (S-234), known to be involved in the formation of a GPI anchor to the cell membrane, this ensured the recombinant protein would be unable to bind lipid membranes. It is well documented that sequences with a high number of cysteine residues are incorrectly folded when expressed in *E.coli*, due to disulphide bond scrambling. As the region we were intending to clone contained 13 cysteine residues we predicted the recombinant form of the protein would be safe.

Although FPGS is also cysteine rich, its active soluble form has been produced in *E.coli* . Therefore the same risk assessment could not be used for this protein. The sequences selected on FPGS

avoided three key active site residues located at the C-terminal domain and the ATP binding site, which is critical to enzyme function as it catalyses the conversion of folates to polyglutamate derivatives. These measures ensured the recombinant protein would be inactive.

Figure 2-11: FR-α target region. 189 amino acid FR-α target region selected (purple), note avoidance of n-terminal signalling sequence (black) and serine 234 (red).

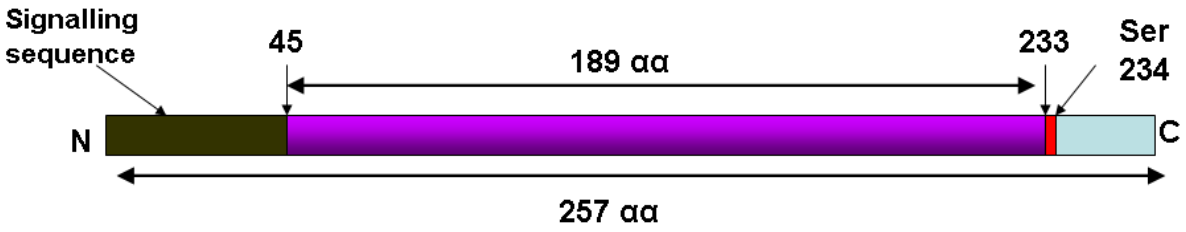

Figure 2-12: FPGS target region. Two FPGS target sequences selected (purple) - one 228 amino acid region denoted FPGS2 (left) and one 167 amino acid region denoted FPGS3 (right), note the avoidance of the ATP binding site and three key active site residues (red).

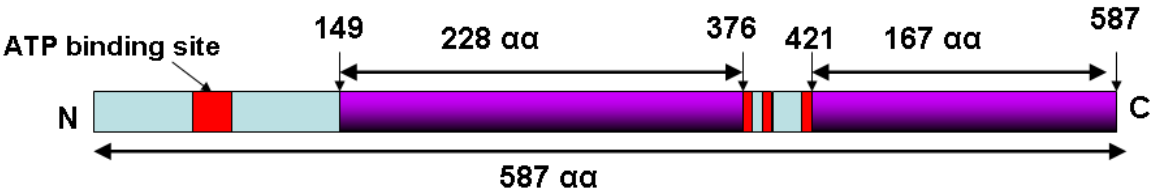

2.6.3. Primer Design

Primers were designed, considering the *E.coli* codon usage and restriction sites were added to the ends of the primers. SacI (GAGCTC) and XhoI (CTCGAG) were selected as the restriction sites to be added to FR-α forward and reverse primers. BamHI (GGATCC) and HindIII (AAGCTT) were selected for both targets on the FPGS primers respectively (Table 2-9).

SacI, XhoI and HindIII restriction enzyme sites were selected as they were not present in the target sequence, BamHI was present in the FPGS sequence but primers were designed to begin after this site for ease with cloning, for this reason the targets on FPGS were termed FPGS2 and FPGS3 as FPGS1 was the initial design planned to begin before the BamHI site (Table 2-9). The primers were synthesized, concentrations calculated and 7.5µm solutions made.

RNA preparations were made for RT-PCR, the ovarian tumour cell lines SKOV-3 and IGROV-1 were used for this purpose.

Table 2-9: FR-α and FPGS forward and reverse primers.

Primer	Sequence
FR-αF	5'GGAGCTCTGAAAAGCCAGGCCCGGAGGACAAGT3'
FR-αR	5'GCTCGAGCATGGCTGCAGCATAGAACCTCGC3'
FPGS2 F	5'GGGATCCGCCTGAGCTCTTCACCAAG3'
FPGS2R	5'GAACCTTCAGGTACCAGGTACCAGGTGAAGGGGCCC3'
FPGS3F	5' GGGATCCGGCGGCCCTGCTGAAGCT3'
FPGS3R	5' GAAGCTTCTGGGACAGTGCGGGCTCCAG3'

2.6.4. Amplification of FPGS2 and FR-α DNA

RT-PCR was carried out to produce both FR-α and FPGS2 cDNA, initially using the mRNA extracted from the ovarian tumour cell line SKOV-3. Both FPGS and FR-α cDNA was then amplified via PCR using both forward primers and the product fractionated and visualised via agarose gel electrophoresis. In both cases a fluorescent band of DNA was observed between the 492 and 615 bp marker for FR-α and between the 615 and 738bp marker for FPGS (Figure 2-1), these correlated with the approximate sizes of 567 and 684 bases respectively.

Figure 2-13: FR-α and FPGS PCR products. Photographic image of 1.7% agarose gel showing fluorescent bands of ethidium bromide bound PCR products prepared from the SKOV-3 cell line when exposed to UV light. The circles show the PCR product produced from FR-α (left, 567bp) and FPGS2 (right, 684bp).

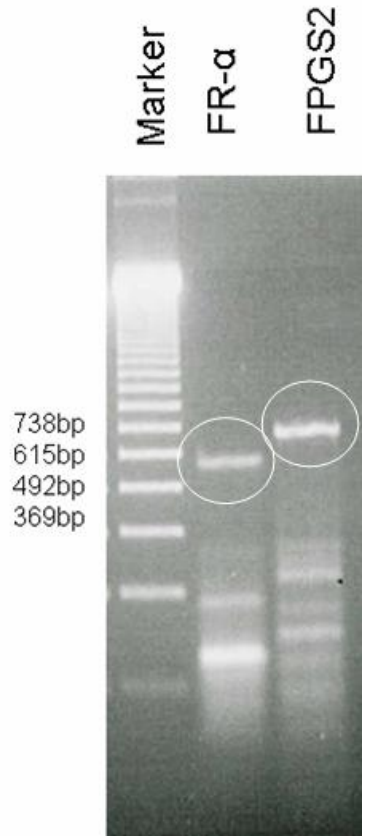

2.6.5. Amplification of FPGS3 cDNA

FPGS3 required optimisation of the PCR reaction in order obtain a band. Various strategies were performed in order to obtain the required product. The annealing temperature was first increased in an attempt to increase specificity of primer-mRNA complementation, this was without success. The ovarian tumour cell line IGROV-1 was then tried as the RNA source, again without success. A two-stage hemi nested PCR was then performed using the forward primer from FPGS2 and the FPGS3 reverse primer in the first round (as this is part of the same protein), the second round was a template PCR reaction using the FPGS3 forward and reverse primers and serial dilutions of the template. In this case bands were obtained but were the incorrect length. As this sequence is relatively GC rich it was inferred that the problem may be due to the primers self complementing each other. For this reason it was decided new primers were to be designed outside of the target region to carry out a full nested PCR (Table 2-10). In the first round the new primers were used to

amplify the target sequence. In the second round the original forward and reverse primers were used and this was found to be successful. Both cell lines were used and both were successful, however when cloned into the T-vector and sent for sequencing the product amplified from the IGROV-1 cell line was found to contain errors which may have been significant, therefore, the product amplified from the SKOV-3 cell line was pursued (Figure 2-14). Errors were found in both sequences, likely to be due to errors arising from the two-stage PCR reaction, however only one was deemed significant.

Table 2-10: FPGS Nested PCR primer sequences.

Primer	Sequence
FPGS3F Nested	5' GAGGTTCGAGTCTTGCTCTTCAATG3'
FPGS3R Nested	5' GGAAAGCCAAAAACAAAAGGCACCTA3'

Figure 2-14: FPGS nested PCR product. Photographic image of 1.7% agarose gel, 2nd Round Nested PCR using SKOV-3 cell line as the RNA source. The neat preparation was used as this contains the highest concentration of PCR product. Note the band (arrowed) corresponds to the 123bp standards at 500 bases.

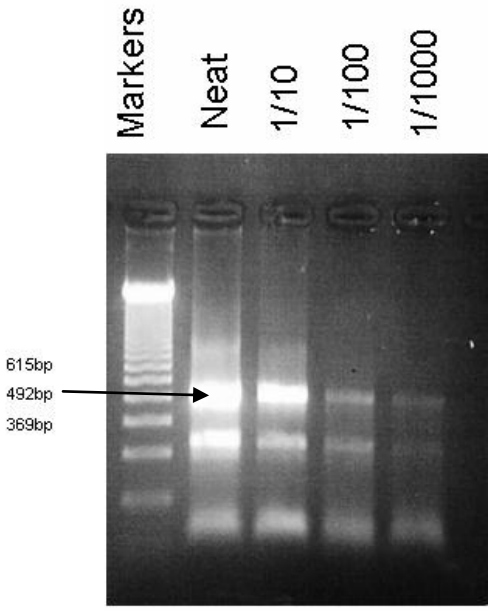

2.6.6. Fragment Preparations and Restriction Digests

Following PCR the bands were excised from the gel, fragment preparations prepared and ligated into pGEM T Easy vectors. They were then transformed into Novablue *E.coli*, grown on TAXI selection plates (to select for the presence of the pGEM vector) and plasmid minipreparations (minipreps) were prepared.

Restriction digests were performed on the plasmid minipreps using the appropriate RE's for each construct. They were then analysed on an agarose gel to differentiate between those vectors containing inserts and those only possessing an empty vector (Figure 2-15).

Figure 2-15: FR-α and FPGS restriction digests. Photographic example of 1.7% agarose gel showing restriction digests for FR-α (left) and FPGS2 minipreps (right). FR-α vectors were digested with SacI and XhoI restriction enzymes, FPGS2 vectors were digested with BamHI and HindII restriction enzymes. Again bands corresponding to 567 bases (FR-α) and 684 bases (FPGS2) were observed.

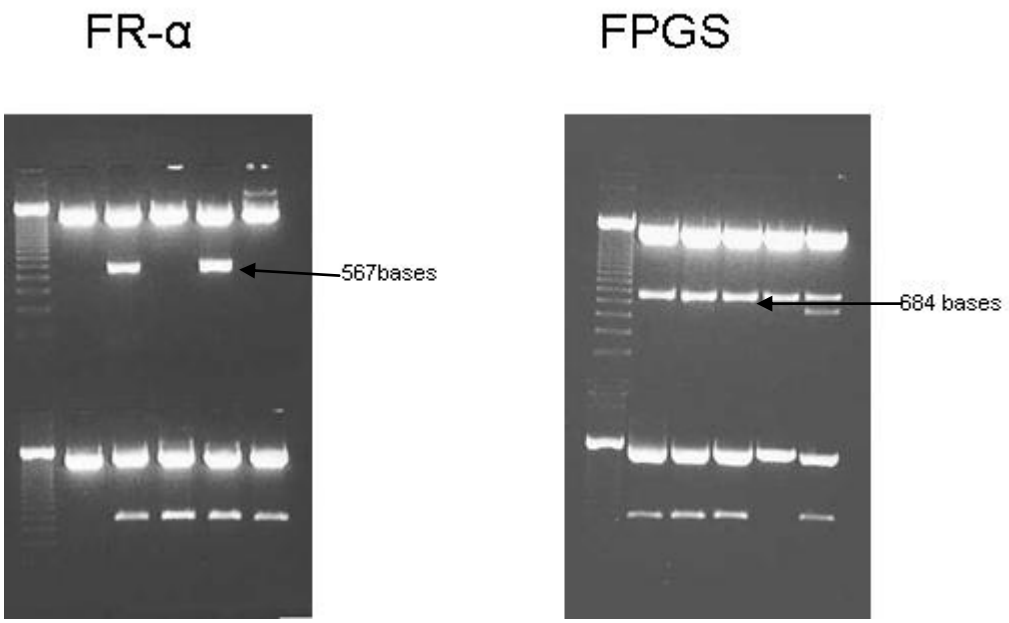

One positive miniprep was selected from each gel and a sample sent to Lark Technologies (Essex, UK) for automated sequencing. Accuracy in this technique is maintained for approximately 380 bases downstream of primer binding. Bases denoted N were unidentified by the sequencer.

The following image shows a typical trace obtained (Figure 2-16), approximately 60 bases of the initial sequence represents the polycloning region of the pGEM plasmid, after which the added bases and restriction sites engineered into the primer, followed by the target sequence. The sequences were analysed to ensure they correlated with the published sequences, once complete identity and conformity was ensured, the FR-α and FPGS2 fragments were ligated into pET 21 and pET 41 expression vectors.

Figure 2-16: Typical DNA sequencing chromatogram trace obtained. Each of the four colours represents a signal given by a base, adenine (green); thymine (orange), cytosine (blue) and guanine (black).

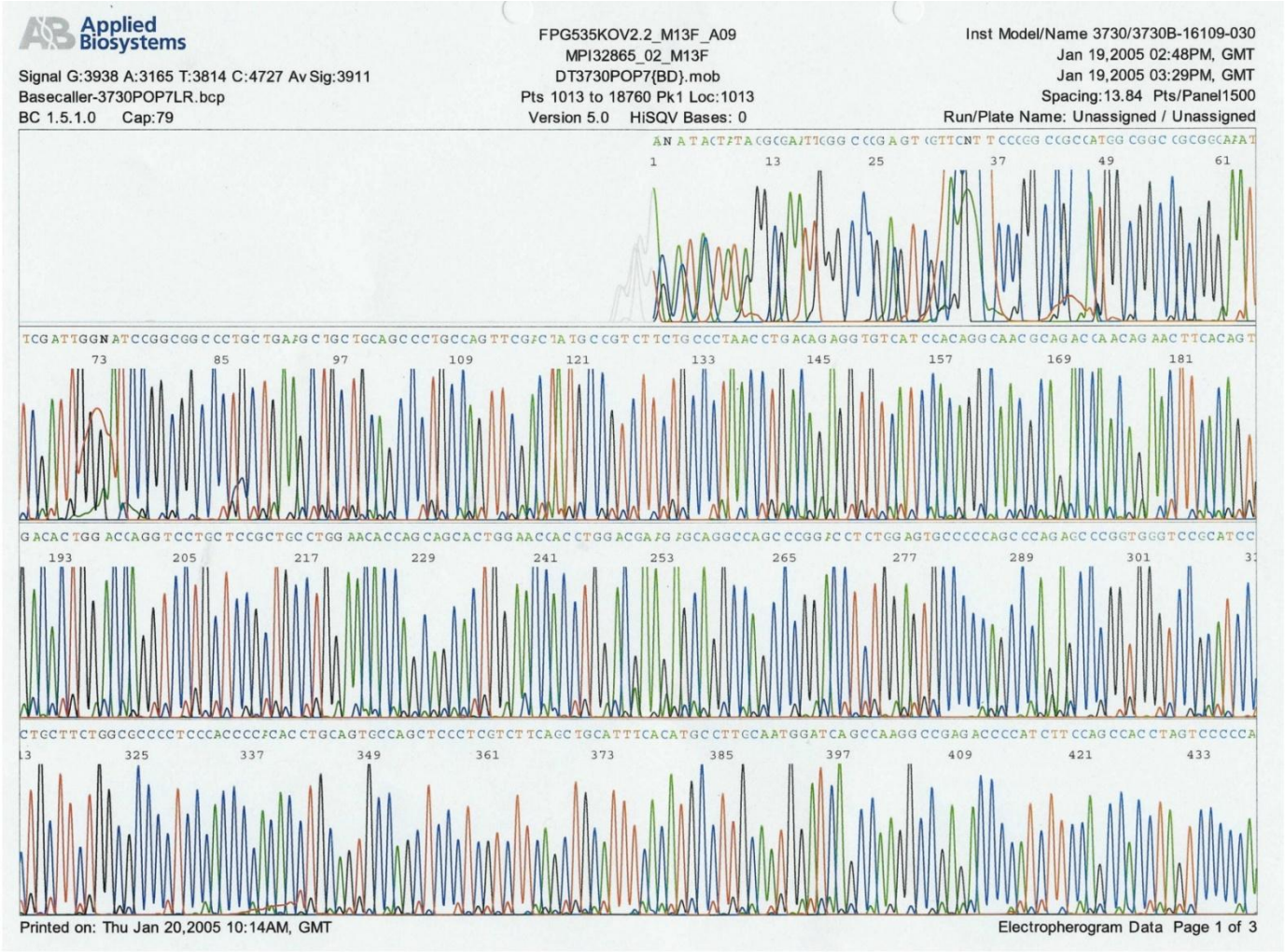

The FPGS2 sequence was analysed and the sequence was found to be correct. The FR-α sequence, however contained a base substitution 16 amino acids downstream of the forward primer. The substitution resulted in a stop codon, transformation using this miniprep would have resulted in a truncated protein. It was inferred that the error may lie in the cell line and all minipreps may contain the error. Two methods were developed to rectify this problem.

A long primer was designed which corrected the stop codon (Denoted FR-α F2).

A new primer was designed which began after the stop codon (Denoted FR- α F3).

Table 2-11: FR-α primer sequences.

Primer	Sequence
FR-α F2	5'GGAGCTCTGAAAAGCCAGGCCCGGAGGACAAGCTGCATGAGCAGTGTCGTCCGTGGC GTAAGAATGCCTGCTGT3'
FR-α F3	5' GGAGCTCT AAGAATGCCTGCTGTTCTACCAACAC3'

2.6.7. pET Cloning

Once sequences were checked and found to be correct they were ligated into both pET 21 and pET 41 vectors, which had been pre-cleaved with the appropriate restriction enzymes and transformed into Novablue *E.coli*. Minipreparations were prepared as described earlier, restriction digested and screened via 1.7% agarose gel electrophoresis to ensure the selected miniprep contained an insert.

2.6.8. Expression of FR-α and FPGS Recombinant Proteins in *E.coli*

One positive plasmid miniprep was selected for each target and was used for transformation into BL21 (DE3) pLysS or Tuner expression hosts. One colony from each plate was selected and small scale inductions were performed as previously described. Both pre and post induction samples were resolved via SDS-PAGE and visualised via staining with Coomassie blue (Figures 2-17, 2-18

and 2-19). The molecular weights of the FPGS2 protein in pET 21 and pET 41 constructs were calculated to be 28 kDa and 58 kDa respectively.

The molecular weights of FR- α and FR- αF2 in pET 21 and pET 41 constructs were calculated to be 23.1 kDa and 55 kDa respectively.

The molecular weights of FPGS3 in pET 21 and pET 41 constructs were calculated to be 21.3 kDa and 51.7 kDa respectively.

The following photographs are examples of some of the small scale inductions carried out.

Figure 2-17: FPGS small scale inductions. 12% (v/v) polyacrylamide gel. FPGS2 pET 21 and 41 small scale inductions illustrating pre and post IPTG induction samples. (PI – pre induction, I – post induction) The bands circled at approximately 28 and 58 kDa marked with a white circle indicate the induced protein bands.

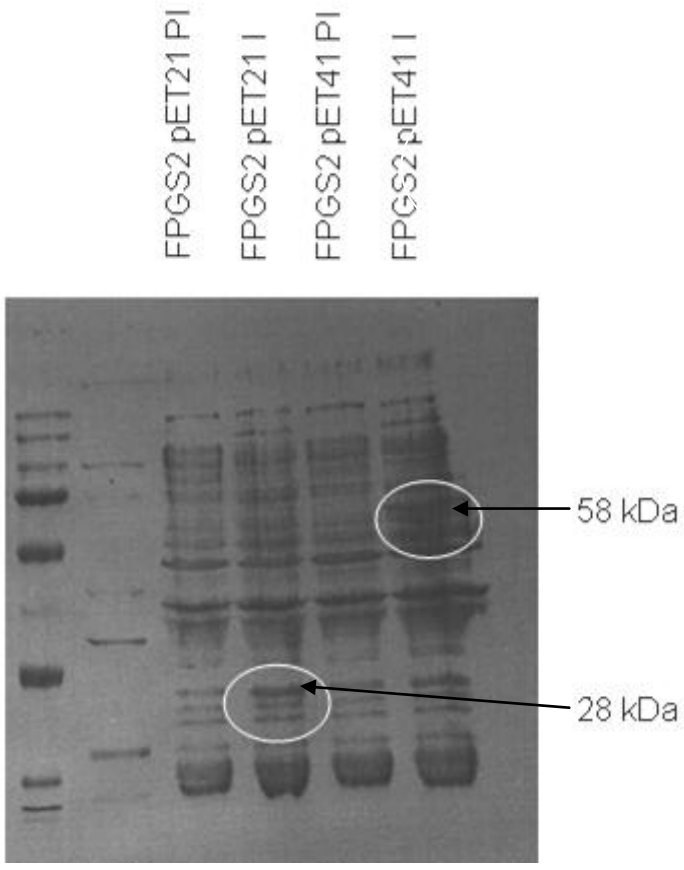

Figure 2-18: FR-α pET21 small scale inductions. 12% (v/v) Polyacrylamide gel. FR-α and FR-α F2 pET 21 BL21 small scale inductions illustrating pre and post IPTG induction samples. The bands marked with a white circle at approximately 23kDa indicate the induced protein band.

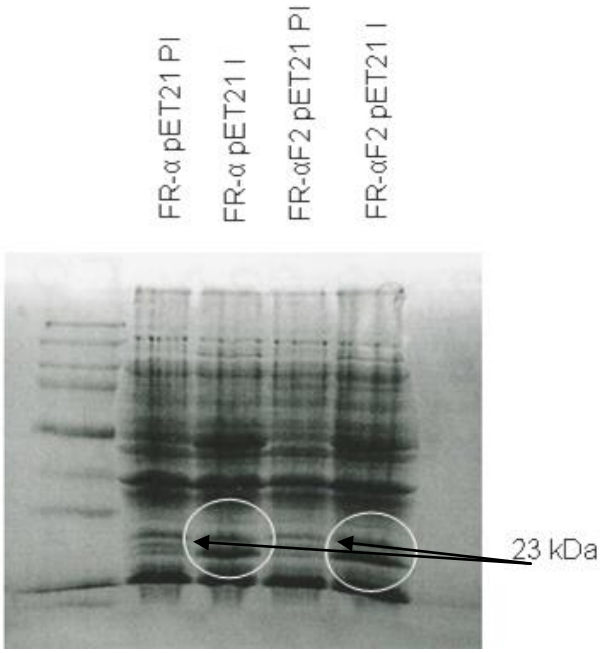

Figure 2-19: FR-α pET41 small scale inductions. 12% (v/v) Polyacrylamide gel. FR-α and FR-α F2 pET 41 BL21 small scale inductions illustrating pre and post IPTG induction samples. The bands marked with a white circle at approximately 55kDa indicate the induced protein band.

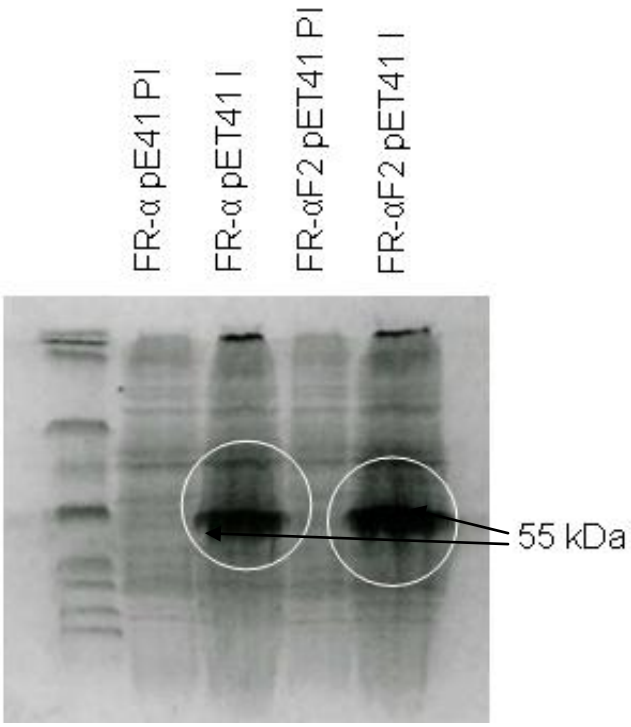

2.6.9. Large Scale Recombinant Protein Expression

Following confirmation from small scale inductions that a protein of the expected approximate molecular weight was expressed, large scale inductions were carried out. Typically two large flasks (500ml cultures) were used to carry out the large scale induction for each protein. The BL21 strain was used to generate FPGS2 recombinant proteins, both BL21 and Tuner strains were used for FR-α and Tuner alone for FPGS3 (after unsuccessful BL21 purification) in an attempt to increase solubility.

2.6.10. Recombinant FR-α and FPGS Protein Purification

2.6.10.1. FPGS2

FPGS2 large scale inductions were defrosted, sonicated and separated into soluble and insoluble fractions. They were then purified using His-Bind chromatography on a soluble column. The quality and quantity of the purified protein were assessed by SDS-PAGE and Bradford Assay. Finally the fractions were pooled to create the protein to be used in subsequent immunisations.

Recombinant FPGS-2 protein was initially purified from the pET 41 soluble fraction, however, in the hybridoma generation stage a significant issue with cross reactivity of the soluble protein was highlighted which will be discussed in more detail in section 3.5.2.1. This resulted in purification of the insoluble pET41 fraction to be purified via insoluble His-bind column chromatography and used for immunization (Figure 2-20). In addition, generation of a new FPGS2 pET32b construct was subsequently purified and used as a screening antigen in subsequent stages of the project. The molecular weight of the new FPGS2 pET32 recombinant protein was calculated as 45kDa.

The FPGS2 pET21 construct did not yield sufficient protein to be used for immunisation and was discontinued. A summary of the FPGS recombinant proteins produced is detailed in Table 2-12.

Figure 2-20: FPGS insoluble fractions. 12% (v/v) Polyacrylamide gel. FPGS2 32b BL21 insoluble fractions collected via His bind chromatography (lanes 1-9) which were subsequently pooled together to generate one sample, dialysed and used both for immunisation and as a screening antigen.

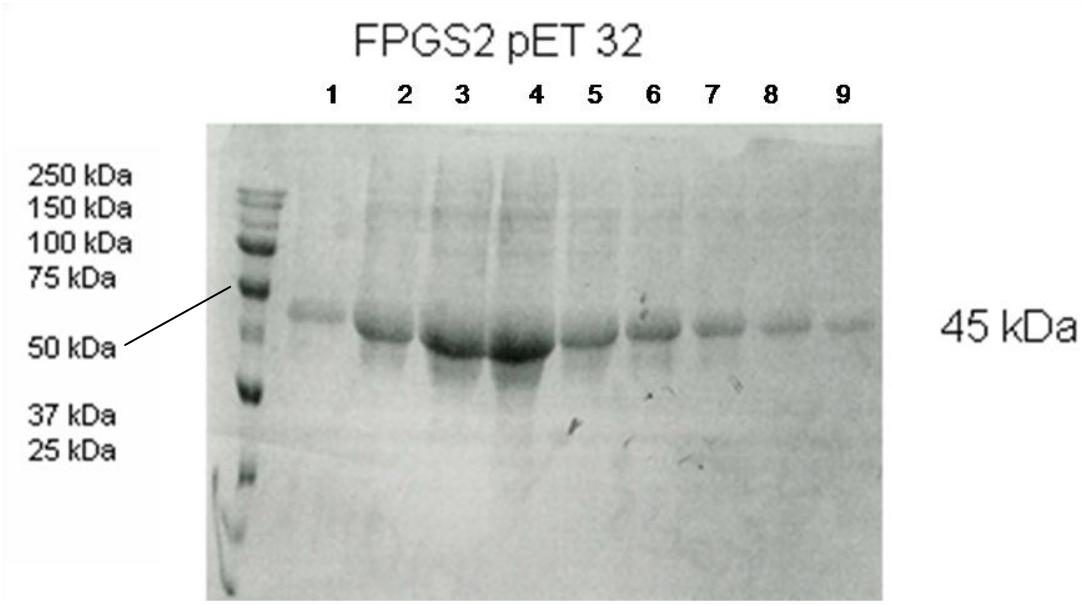

2.6.10.2. FR-α

Recombinant FR-α and FR-α F2 large scale protein induction samples were also purified from the soluble fraction as described above for FPGS2, in light of the cross reactivity problem associated with FPGS and the likelihood of the same occurring with FR-α it was decided that the insoluble fractions of FR-α and FR-αF2 would be purified and used for immunisation (Figure 2-21). Despite one of the initial plasmid minipreparations containing a stop codon 16 bases into the coding sequence, others generated at the same time did not contain the error as first thought, as another miniprep was sent to Lark technologies for sequencing and was found to contain no errors. It was decided that as both FR-α and FR-αF2 fractions were essentially the same, the only difference being the primers used that these fractions could safely be pooled together to generate a large stock of recombinant FR-α. In addition to this a pET32 construct was generated as a screening antigen, the insoluble fraction was purified via the use of a refold column (Figure2-22). Again this was to overcome previous problems with cross reaction which will be discussed in more detail in section 3.5.2.1. The molecular weight of the new FR-α pET32 recombinant protein was calculated to be 39.3 kDa.

The FR-αF3 primers were not used as this would have only generated a truncated version of the successful FR-α and FR-αF2 proteins and protein production via the use of these primers was therefore discontinued.

The FR-α pET21 construct did not yield sufficient protein for immunisation and attempts to produce this protein were also stopped. A summary of the FPGS recombinant proteins produced is detailed in Table 2-12.

Figure 2-21: FR-α insoluble fractions. 12% (v/v) Polyacrylamide gel. FR-α pET 41 Tuner insoluble fractions (lanes 1-10) which were subsequently pooled together into one sample, dialysed and used both for immunisation and as a screening antigen.

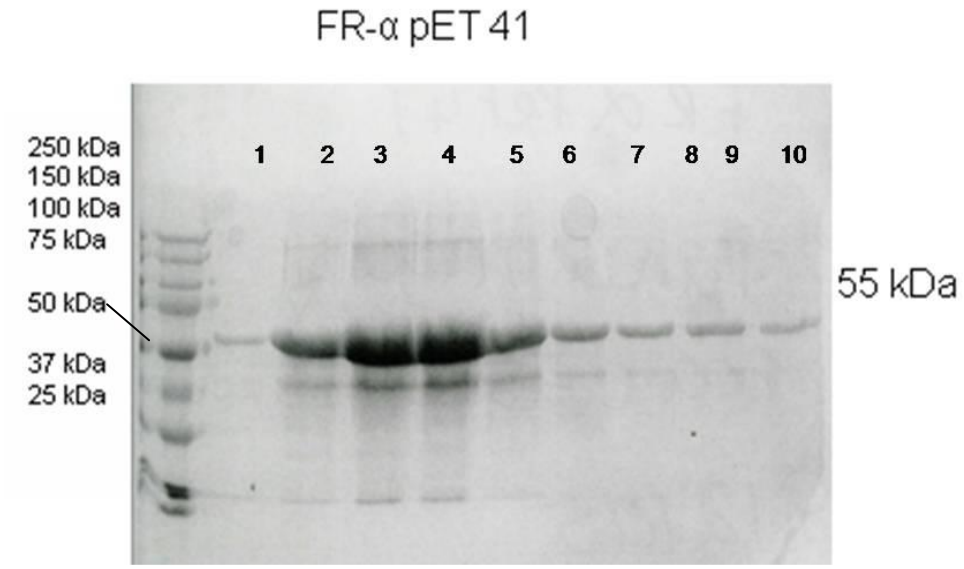

Figure 2-22: FR-α refolded fractions. 12% (v/v) Polyacrylamide gel. FR-α pET 32 refolded fractions (lanes 1-8) which were refolded via the refold column method (see section 2.5.18).

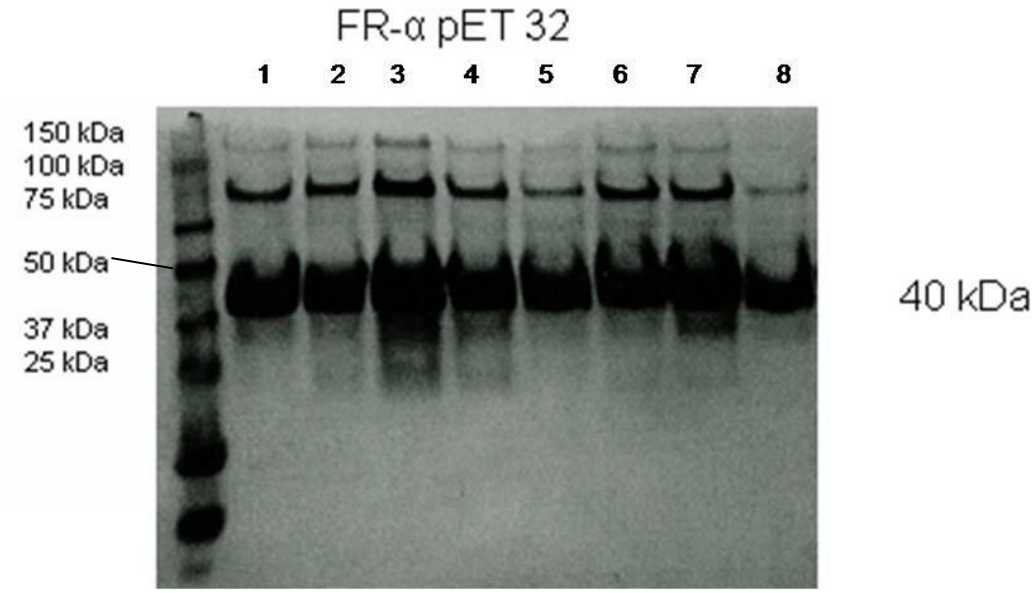

2.6.10.3. FPGS3

FPGS3 recombinant protein was not identified in the soluble fraction and His-Bind chromatography was carried out on an insoluble column in order to purify the protein. The fractions were pooled and dialysed, the quality and quantity of the resultant protein was again assessed via SDS-PAGE and Bradford assay (Figure 2-23). A summary of the FPGS recombinant proteins produced is detailed in Table 2-12. All proteins were stored in 200µg aliquots at -80^{o}C until required for immunisation.

Figure 2-23: FPGS dialysed protein. 12% (v/v) Polyacrylamide gel. FPGS3 pET 41 recombinant protein, refolded by dialysis.

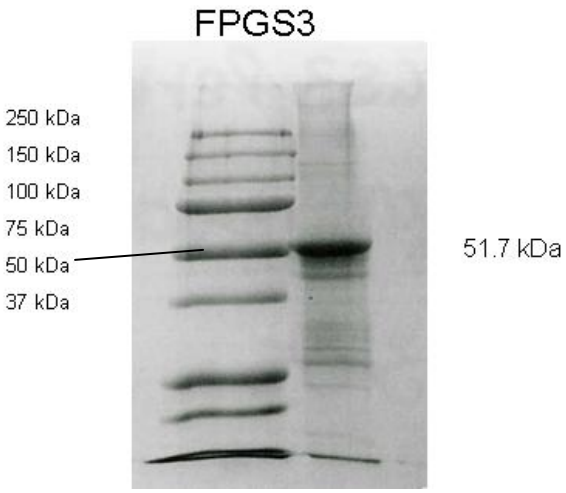

Table 2-12: Summary of some of the recombinant proteins generated in this project.

Protein/ Target	Vector	Tag	*E.coli* Strain	Soluble/ Insoluble	Refold Method	Use for protein
FPGS1	NA	NA	NA	NA	NA	Abandoned at design stage
FPGS2	pET21	His	BL21	Soluble	NA	Insufficient yield for immunisation
FPGS2	pET41	His, GST	BL21	Soluble	NA	Used for immunisation – abandoned after 3rd cloning
FPGS2	pET41	His, GST	BL21	Insoluble	Dialysis	Used for immunisation/screening
FPGS2	pET32	His, Tx	BL21	Insoluble	Dialysis	Used for immunisation/screening
FPGS3	pET41	His, GST	Tuner	Insoluble	Dialysis	Used for immunisation – subsequently failed
FR-α	pET21	His, Tx	BL21	Soluble	NA	Insufficient yield for immunisation
FR-α	pET41	His, GST	BL21	Soluble	NA	Used for immunisation
FR-α (and F2)	pET41	His, GST	Tuner	Insoluble	Dialysis	Pooled and used for immunisation/screening
FR-α	pET32	His, Tx	Tuner	Insoluble	Refold column	Used for screening
FRα3	NA	NA	NA	NA	NA	Abandoned as would generate truncated protein

2.7. Discussion

2.7.1. Recombinant Protein Production

Antibodies suitable for immunohistochemical analysis of paraffin embedded tissue samples are extremely useful as much of the tissue obtained from tumour samples is readily obtainable for storage and transportation in this form. To date, there are no known commercially available FPGS antibodies and only one known commercially available antibody capable of recognising FR-α. The mOV 18 and 19 antibodies which have been found to recognise FR-α only do so in a limited fashion, identify only the native protein conformation and are unsuitable for analysis on paraffin embedded samples and Western blotting. In addition, mOV19 is no longer commercially available. As they are only suitable for analysis on frozen tissue sections, their application is limited. Thus it was one of the aims of this project to rectify this situation and produce a panel of antibodies which can be used in wider applications.

The first step in monoclonal antibody production was to focus upon molecular biology techniques to produce a suitable immunogen which could subsequently be used to immunise mice to produce monoclonal antibodies, which will be discussed in detail in section 3.1.

The recombinant protein expression method used is currently the method of choice for the production of immunogenic proteins. Using the methods described earlier, we were able to successfully produce all three recombinant proteins from target sequences with relatively few complications.

The aims of this particular section of the project were satisfied as all three recombinant proteins have been successfully expressed and purified via the use of recombinant protein expression techniques. These proteins were subsequently used for immunisation of mice for generation of anti FR-α and FPGS antibodies. In addition, recombinant proteins for FR-α and FPGS2 have been generated in pET32 vectors which may be used for immunisation or as screening antigens, as the protein target sequence remains the same and the sequences differ only in the tagged and vector flanking regions. This will avoid any problems relating to antibody cross reaction. The importance of this will also be discussed in detail in the following chapter.

The stop codon in the FR-α sequence was inferred to be an error arising from the cell line used. This was the reason for the design of the FR-αF2 and FR-αF3 primers. It was later discovered, however, that this was not the case, as one of the other minipreps was sent for sequencing and was found to be correct. In hindsight a different miniprep could have been sent earlier for

sequencing before design and preparation of new primers was considered. The protein might then have been produced more quickly; however valuable experience was gained in the design of primers and the methods involved in recombinant protein production. Additionally, valuable PCR troubleshooting experience was gained from the problems encountered with the FPGS3 primers.

The proteins were produced using pET 32 and pET 41 vectors. It would have been useful to have purified a protein in the pET 21 construct to observe the difference in antibody yield with and without a GST protein present. However all proteins were too insoluble without the presence of the tag, the yields in the soluble fractions were negligible and when refolding was attempted the proteins precipitated into solution rapidly, both on refold columns and by dialysis.

All proteins produced had degradation to some degree, which may have been caused by the overgrowth of *E.coli* cultures. This was not deemed to be a disadvantage as it may allow for many different protein species to be presented to the murine immune system. Degradation may have been reduced by inducing the large scale induction samples at an earlier stage in the growth. This was not however deemed necessary as undegraded protein has not, in the past, always been required to produce successful antibodies.

In summary, the aims of this part of the project were achieved, the next stage being dependent upon the immune response produced by the mice to the protein.

Chapter Three

Chapter Three

3. Antibody Production

3.1. Hybridoma Technology

Antibodies are commonly produced via the immunisation of laboratory animals, typically mice and rats, with an antigen emulsified in an adjuvant solution. Antigens are typically proteins although peptides, nucleic acids and carbohydrates have also been used. The two most commonly used adjuvants are Freunds complete and incomplete adjuvants. Freunds complete adjuvant contains mineral oil and an additional component, the cell walls of mycobacterium which serve as non-specific stimulators of the murine immune response (Freund, 1956; Freund & Mc Dermott, 1942). Adjuvants are used as they strongly enhance the immune response via a number of different mechanisms including retention of the immunogen at the site of administration, stimulation of an immune response at the injection site and protection against antigen catabolism, all resulting in promotion of subsequent immune reactions. The animal immune system identifies the antigen as 'non-self' and an immune response is generated, this involves the clonal expansion of B-cells which differentiate to form plasma cells, able to secrete antibody of a single defined specificity. Plasma cells sequester in secondary lymphoid organs, particularly the spleen where antibodies are secreted and circulate in the blood and lymph, serving to recognise and opsonize any foreign antigens encountered. If collected, these plasma cells would be an ideal source of antibody; however these cells are unable to survive *in vitro* for any period of time and are unsuitable for use as an antibody source.

3.1.1. Cell Fusion Technique

Many attempts had been made to produce antibodies with single known specificity, however, until the development of hybridoma technology all attempts had failed (Berry, 2005). In 1975 Georges Kohler and Cesar Milstein developed a method of generating monoclonal antibodies by successful fusion of antibody secreting B-cells from the spleen of an immunised mouse with a mouse B-cell tumour (myeloma) cell line. This was achieved via somatic cell hybridisation, resulting in a cell which had the immortal characteristics of a myeloma cell and the genetic predisposition to secrete specific antibodies. The resultant cells may be maintained indefinitely *in vitro* and are able to secrete antibodies into the culture supernatant (Kohler, Howe, & Milstein,

1976; Kohler & Milstein, 1975, 1976). Initially the Sendai virus was used in an attempt to generate hybrid cells with little success. (Harris & Watkins, 1965). Later Polyethyleneglycol (PEG) was found to be an effective method of cell fusion due to its ability to partially disrupt cell membranes, causing lipid exchange between cells and integration of cell membranes and is now the standard fusing agent employed in fusion techniques (Kohler & Milstein, 1976).

Cell fusion is a random process, creating multinucleate cells amongst which are the few binucleate cells (hybridomas) of one myeloma cell and one B-cell. When the hybrid cells divide, the nuclei initially form a mononuclear cell with tetraploid chromosomes, the additional two sets of chromosomes are then lost, resulting in a diploid hybrid cell. All cells resulting from the fusion are cultured in media containing hypoxanthine, aminopterin and thymidine (HAT), which is selective for hybrid cells only and depends upon the fact that mammalian cells synthesize their nucleotides via two different pathways as shown in Figure 3-1.

As reviewed in Chapter 1, the *de novo* pathway requires glutamine and aspartate as substrates for purine and pyrimidine nucleotides which are in turn involved in DNA synthesis. Synthesis involves the transfer of a methyl of formyl group from an activated form of tetrahydrofolate. The antifolate aminopterin blocks this pathway thus inhibiting DNA synthesis via the *de novo* pathway. The cultured cells are forced to utilise the salvage pathway in which nucleotides are synthesized via the action of the enzymes hypoxanthine-guanine phosphoribosyl transferase (HGPRT) and thymidine kinase (TK), (Figure 3-1).

The P3-NS-1/1-Ag-1 (NS-1) variant of the mouse myeloma cells are commonly used in the fusion process as they only produce a κ light chain, reducing the amount of contaminating antibody present. In addition, they are deficient in the enzyme HGPRT, which is used in the nucleotide salvage pathway. The aminopterin present in the HAT media blocks the *de novo* pathway, cultured cells such as NS-1 cells and NS-1-NS-1 hybrids which are deficient in this enzyme will not survive. Despite possessing an intact HGPRT gene, splenocytes and splenocyte-splenocyte hybrids have a finite lifespan of 1-2 weeks in culture and thus cannot survive alone. The only cell type able to survive in these conditions are the hybridomas, which are HGPRT positive as they contain a copy of the gene from the splenocyte. They are also able to survive in culture due to possessing the immortal properties of a myeloma cell line.

Figure 3-1: Overview of *de novo* and nucleotide salvage pathways in mammalian cells. Aminopterin inhibits the *de novo* synthesis of dATP, dGTP, dCTP and dTTP. If this is blocked, the two salvage pathways are activated via the action of the enzymes HGPRT and TK.

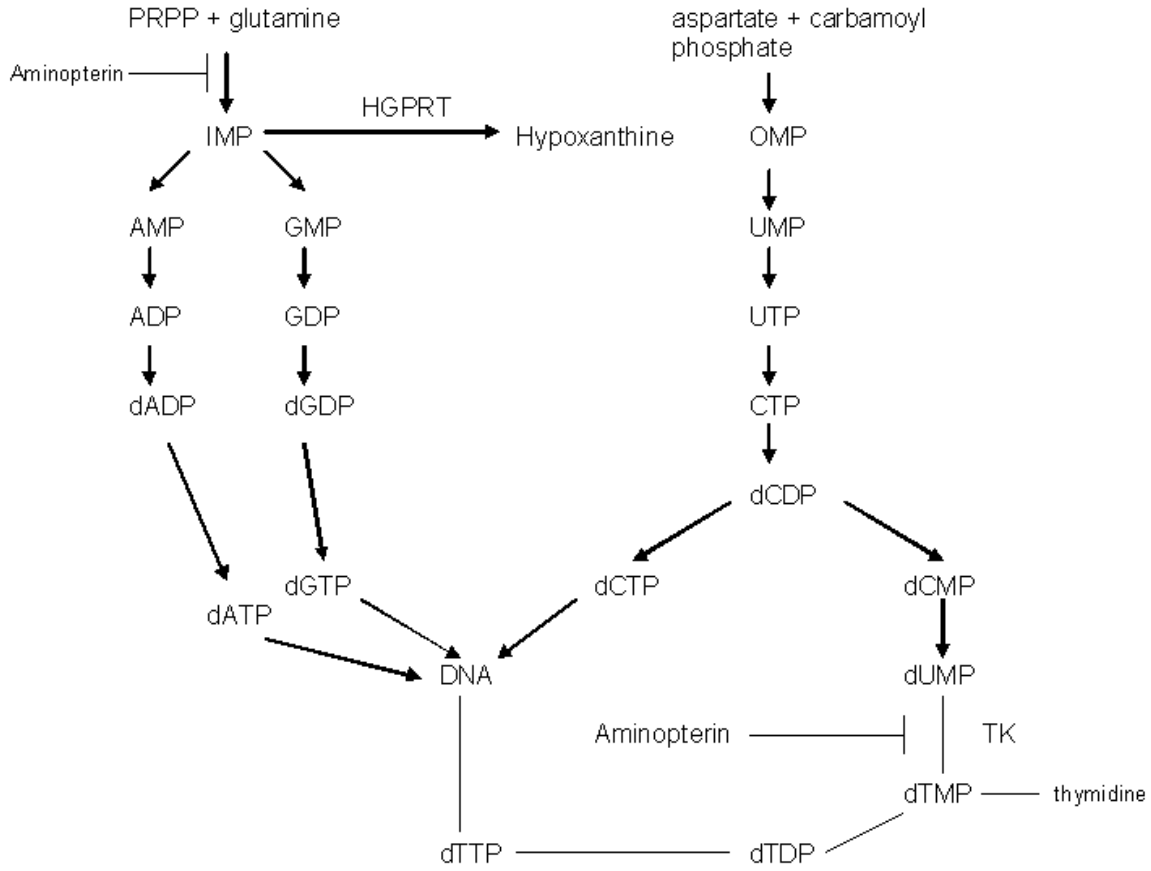

3.1.2. Antibody Screening and Characterisation

The key aspect of monoclonal antibody generation is the screening protocol which must be performed in order to select the specific antibody of choice. A number of different procedures are performed in order to screen hybridoma culture supernatants to detect bound monoclonal antibody. Taking advantage of the specific nature of the antibodies, fluorescent, enzyme linked or otherwise tagged antibodies can be used in order to visualise the results. The most common screening techniques used are ELISA, WB and IHC. The major advantage of such assays is the speed at which they can be performed, their reliability and accuracy. Initial screening of fusions is extremely important as it is on the basis of this result that hybridoma colonies are selected. ELISA assays are often selected for initial fusion screening as it is regarded as a rapid, highly sensitive assay and allows screening of the large numbers of hybridomas generated by fusions. Qualitative results provide a simple positive or negative result for each supernatant sample and the margin

between positive and negative samples is determined via the use of positive and negative controls. Secondary screening via immunohistochemical analysis on paraffin embedded sections and via WB on cell lines and tissue extracts can also be performed to confirm specificity of the antibody.

The hybridomas are then subsequently 'cloned' by limiting dilution three times, to eliminate any cells which have lost their ability to secrete antibody which may exhibit growth advantage over the desired cell population, and to ensure the probability that population of antibody secreting cells are derived from one single cell (Figure 3-2).

After successful generation of antibodies, their specificity can then be assessed by both IHC and WB analysis on normal, tumour and cell line panels to ensure they are specific for the target protein.

A number of different cell line pellets including, ovarian, breast, colorectal and MPM malignancies were obtained both from Novocastra and Newcastle University. In addition, a panel of leukaemia cell lines kindly donated by Dr. Sally Coulthard were also included. As FPGS mRNA has been reported to be expressed in a number of cell types, particularly cells of lymphoid origin, it was thought that further investigation of FPGS expression in leukaemia cells would be interesting and would fully characterise the antibody (Leclerec & Barredo, 2001; Nair & Mc Guire, 2005).

3.1.3. Epitope Mapping

Epitope mapping is a versatile technique as it can be used for a number of different applications; it enables antibody specificity to be defined and may predict the occurrence of cross-reaction. It can also be used in development of assays, to define sites of protein modification, to probe protein structures, elucidate their functions and may also be used as a model for protein-protein interactions. Epitope mapping can be performed by a number of different techniques for different applications, each with their own inherent advantages and disadvantages. Mapping methods include peptide arrays, phage displays of random peptide libraries, expressed protein fragments via molecular biology, partial proteolysis and mass spectrometry.

The antigen binding site of an antibody is termed the paratope, where the region of an antigen that binds to the paratope is termed the epitope, interactions between the antibody and antigen are hydrophobic and electrostatic in nature and are noncovalent (Ramos-Vara, 2005).

Eptiope mapping was planned in order to bring closure to this part of work, depending upon the time available the method used to perform epitope mapping may have varied. If possible, epitope mapping was also planned for the mOV 18 and LK26 antibodies to observe any similarities/differences between the epitopes recognised. This would be dependent upon the method of epitope mapping selected. Epitope mapping is not routinely carried out to characterise antibodies but in this study it was performed as it was necessary to confirm our antibodies recognised an epitope present in the target sequence.

Figure 3-2: Overview of MAb production. Following immunisation, splenocytes were fused with NS-1 myeloma cells and incubated for 7-10 days and screened by ELISA to select for hybridomas secreting antibody. Positive hybridomas were picked and screened via IHC and WB and cloned three times (7-10 days minimum for each round of cloning) to ensure they were monoclonal.

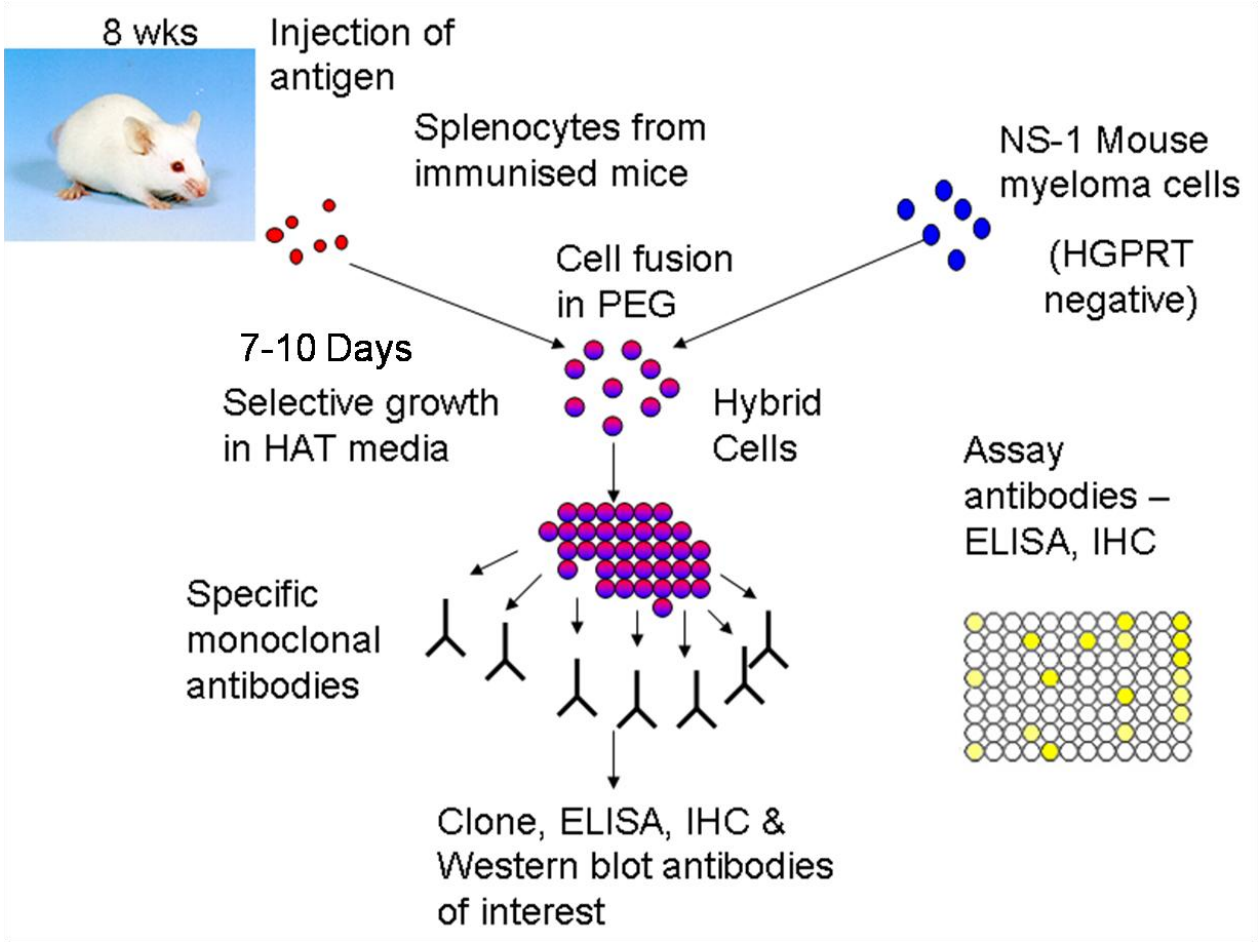

3.2. Aims and Objectives

The aim of this part of the project was to develop specific antibodies to the FR-α and FPGS protein targets and fully characterise the antigen specificity of the antibodies via ELISA, WB and IHC.

- Immunise three sets of five female, Balb C mice with an optimal concentration of recombinant protein targets FR-α, FPGS2 and FPGS3 generated previously.
- Assess the immune response of the mice bleeds via WB and IHC.
- Perform cell fusions on the splenocytes of the most responsive mice with NS-1 myeloma cells to generate hybridomas.
- Isolate and characterise the specific monoclonal antibodies via ELISA, WB and IHC.
- Clone positive hybridomas three times, assessing the antibody specificity by ELISA and WB at each stage on control tissues and cell lines.
- Stability testing of positive hybridomas at different temperatures.
- Weaning of positive hybridomas into non-supplemented media.
- Full characterisation of the antibodies on panels of normal and tumour tissue
- Further characterisation of the antibodies via WB analysis on cell line panels derived from cell lysates grown in culture.
- Epitope mapping of the antibodies to identify the region of the target sequence recognised.

3.3. Materials and Methods

3.3.1. Mouse Immunisation Schedule

The immunisation schedule employed in this project was selected according to current guidelines already in place at Novocastra Laboratories, as much success has already been seen via the use of these methods. Many factors influence a successful immune response, including injection site, adjuvant used and chemical nature/solubility of the immunogen.

For both the FR-α and the FPGS immunogens, five 6-7 week old female Balb/C mice, weighing 20-40 g, supplied by Charles Rivers, were immunised subcutaneously with a mixture of 150-180µg antigen (20µg/mouse plus extra material to account for losses during processing), 400µl PBS and approximately 480µl Freunds complete adjuvant. The mixture was emulsified using a double – hub emulsification needle and PBS containing 2% Tween 80 added to make the total volume 1.4 ml. All five mice were immunised with 200µl solution and the excess discarded. The 5 mice were identified by labelling their ears as follows:

- LN, (Left Notch).
- RN, (Right Notch).
- BN, (Both Notch).
- NN, (No Notch).
- 2RN (2 Right Notch).

On day 14, all 5 mice received a second subcutaneous booster immunisation of 20µg/mouse of recombinant protein, in Freund's incomplete adjuvant.

On day 28, all 5 mice received an intraperitoneal (IP) immunisation of 20µg/mouse of recombinant protein diluted in PBS solution only and on day 35 approximately 0.2 ml of blood was taken from the tail vein of each mouse and tested via ELISA to assess the antibody response. This procedure was performed at the Comparative Biology Centre, Newcastle University (CBC). Administration of the immunogen intraperitoneally generates a strong immune response as it drains directly into the thoracic lymphatic system and major veins where they have immediate, direct exposure to the immune system, particularly the spleen.

On day 42, all 5 mice received a second IP booster immunisation of 20µg/mouse of recombinant protein diluted in PBS and on day 49, approximately 0.2 ml of blood was taken from the tail vein of each mouse and stored at -20^{o}C. These bleeds were tested for specificity to both FR-α and FPGS via WB and IHC. Multiple inoculations were performed and repeated in order to expose the animals to a large amount of antigen, whilst concomitantly lowering the risk of hypersensitivity reactions which may cause animal death.

Any mice found to produce specific antibody received an intravenous (IV) booster injection of 20µg of recombinant protein in PBS solution 5 days prior to fusion. This was performed in order to boost blastogenesis in the immune system maximally, the primary site being in the spleen (Table 3-1). The mice were humanely sacrificed on the day of fusion by dislocation of the neck. Immunisations, ELISA screening and sacrifices were carried out by trained staff at the CBC.

Table 3-1: Mouse immunisation schedules employed in this study.

Injection No	No of Mice/Project	Procedure/ Adjuvant	Site	Immunogen (µg/mouse)	Schedule Day
1	5	Freunds Complete adjuvant	Subcutaneous	20	0
2	5	Freunds Incomplete Adjuvant	Subcutaneous	20	14
3	5	PBS Tween	Intraperitoneal	20	28
4	5	PBS Tween	Intraperitoneal	20	42
5	5	PBS	Intravenous	20	5 days before fusion

3.3.2. Growth of Cell Lines

Frozen aliquots of cell lines were kindly donated by Dr. Sally Coulthard, Dr. Joyce Nutt and Dr. Jane Margetts at Newcastle University in addition to the use of various cell lines already stored and prepared at Novocastra Laboratories. The following cell lines were used in the characterisation of the expression of the FR-α and FPGS antibodies. The cell lines, origin and culture conditions are shown in Table 3-2.

Table 3-2: Human cell lines used for characterisation of FR-α and FPGS antibodies. Cell lines, types and designations used in further WB studies using FR-α and FPGS antibodies.

Cell Line	Type	Culture Conditions (2mM L-glutamine, 10% FBS, 5% CO_2, 37°C)
IGROV-1	Human ovarian epithelial carcinoma	RPMI-1640 monolayer
OVCAR-3	Human ovarian epithelial carcinoma	RPMI-1640 Bovine Insulin (0.01 mg/ml)
SKOV-3	Human ovarian carcinoma	RPMI-1640 monolayer
SW626	Human ovarian adenocarcinoma	RPMI-1640 monolayer
PA-1	Human ovarian teratocarcinoma	RPMI-1640 monolayer
HeLa	Human cervical carcinoma	RPMI-1640 monolayer
BT20	Human breast ductal carcinoma	RPMI-1640 monolayer
HBL100	Human normal breast epithelia	RPMI-1640 monolayer
MCF7	Human breast adenocarcinoma	RPMI-1640 monolayer
MSTO-211H	Human lung mesothelioma	RPMI-1640 monolayer
NCI-H28	Human lung mesothelioma	RPMI-1640 monolayer
NCI-H226a	Human lung mesothelioma	RPMI-1640 monolayer
A549	Human lung alveolar basal epithelial cell carcinoma	Dulbeccos Modified Eagles media monolayer
HT29/219	Human colon epithelial carcinoma	RPMI-1640 monolayer
CaCo2	Human colon epithelial adenocarcinoma	Dulbeccos Modified Eagles media monolayer
HCT116	Human colon epithelial carcinoma	Dulbeccos Modified Eagles media monolayer
Bristol 8	Human B-lymphoblastoid line	RPMI 1640 suspension
A375	Human epithelial malignant melanoma	RPMI-1640 monolayer
SJSA	Human osteosarcoma	RPMI 1640 suspension
SHSY5Y	Human neuroblastoma	Dulbeccos Modified Eagles media monolayer
Jurkat	Human T-cell acute lymphoblastic leukaemia (ALL)	RPMI-1640 suspension
Molt 4	Human T-cell ALL	RPMI-1640 suspension
CCRF-CEM	Human T-cell ALL	RPMI-1640 suspension
TK6	Human lymphoblastoid thymidine kinase heterozygote	RPMI 1640 suspension
PFI-285	Human T-cell lymphoma	RPMI 1640 suspension
Pre-B	Human pre-B cells	RPMI 1640 suspension
ECR-293	Human embryonic kidney	Dulbeccos Modified Eagles medium monolayer

3.3.3. Protein Estimation

Cell lines were cultured as described in Table 3-2. All protein lysates were prepared from the different cell lines in exactly the same way. The protein concentration present in each sample was estimated by an automated analyser.

A confluent monolayer or suspension of each cell line was grown in a $75cm^2$ flask (approx $8x10^5$ cells/ml) and the media removed by decanting. The cells were washed in Dulbeccos PBS (Sigma) to

remove any non adherent cells/cell debri, non cell associated proteins and contaminant from the cell monolayer/suspension. The adherent cells were then incubated for 15 minutes in 15ml non-enzymatic cell dissociation solution (0.2M EDTA, Sigma) and washed off with a 10ml pipette and PBS. Trypsin was not used as it may have sheared the receptors from the cell surface. Cell suspensions were centrifuged for 5 minutes at 300G, the supernatant discarded and washed in a further 10ml PBS and centrifuged again. 100µl cell lysis buffer/10^7 cells (62.5 mM tris pH 6.8, 10% glycerol, 2% (w/v) SDS) was added to each cell pellet to lyse the cells. Samples were then sonicated to break the cells down further and boiled at 100^{o}C for 10 minutes prior to protein estimation.

Protein estimation was performed in a 96 well microtitre plate and was carried out using a Pierce protein assay kit (Pierce, Rockford IL) according to the manufacturers instructions. The unknown protein concentrations of the cell lysates were compared to that of known albumin protein standards and the results read via the use of a Spectromax 250 Microplate spectrophotometer system (Molecular Devices Corporation) according to the standard operating procedures. The unknown protein concentrations were determined and the volume of lysate to ensure all samples were loaded with equal amounts of protein calculated. The samples were stored at -20^{o}C until required.

3.3.4. Western Blotting (WB)

WB allows the identification of proteins recognised by specific antibodies which recognise linear, rather then conformational epitopes as WB is typically performed under denaturing conditions.

The target recombinant proteins and appropriate cell lysates are first electrophoretically separated via SDS-PAGE and then transferred onto a nitrocellulose membrane. This is then probed with the antibody of interest to assess the specificity of binding to the required epitope present in the antigen, corresponding to the correct molecular weight, as determined by known molecular weight markers (see section 2.5.13 for SDS-PAGE method).

A number of detection methods are commonly used in WB, including colourimetric, chemiluminescence, radioactive and fluorescent detection. Two techniques were utilised in this study. The colourimetric alkaline phosphatase (AP) method and the horse radish peroxidise (HRP) enhanced chemiluminescence (ECL) method. AP is conjugated to the secondary antibody and upon reaction with a suitable substrate an insoluble dye is precipitated onto the membrane, staining it.

This technique is simple to perform, although is regarded as less sensitive than other methods. ECL is considered to be one of the most sensitive detection methods, relying on a substrate which luminesces when exposed to the reporter conjugated to the secondary antibody (HRP in this case). The light is captured on photographic film; this does not degrade with time so a permanent record can be kept.

3.3.5. Assessment of Bleeds via Western Blot

12% SDS polyacrylamide (PA) gels were prepared, recombinant proteins and cell line extracts at a concentration between 0.2-0.5 µg/µl were electrophoresed for 45 minutes at a constant voltage (170V), together with suitable molecular weight markers (Bio-Rad precision plus dual colour protein standards). Satisfactory separation was judged by the visualisation of the bromophenol blue dye and viewing the progress of the pre-stained standards reaching the base of the PA gel.

The gels were then equilibrated in ice-cold transfer buffer (0.025M Tris, 20% methanol, 0.1% SDS, pH 8.6) for five minutes. Six sheets of blotting paper and one piece of nitrocellulose paper (Hybond-C, Amersham) were cut into rectangles, slightly larger than the gel and soaked in transfer buffer. Three sheets of blotting paper were placed in the semi-dry blotter (Hoeffer TE70) stacked on top of each other, a sheet of nitrocellulose paper was added and then the gel. A further three sheets of blotting paper were placed on top of the stack, taking care to exclude any air bubbles. The semi-dry blotter was then run at a constant current of 60 mA for 30 minutes for one gel (or 120 ma for 2 gels), as shown in Figure 3-3.

.

Figure 3-3: Semi-dry blotting apparatus. The nitrocellulose gel underlaid with blotting paper was sandwiched between blotting paper and placed in a semi dry blotter to facilitate transfer of the protein bands to the membrane.

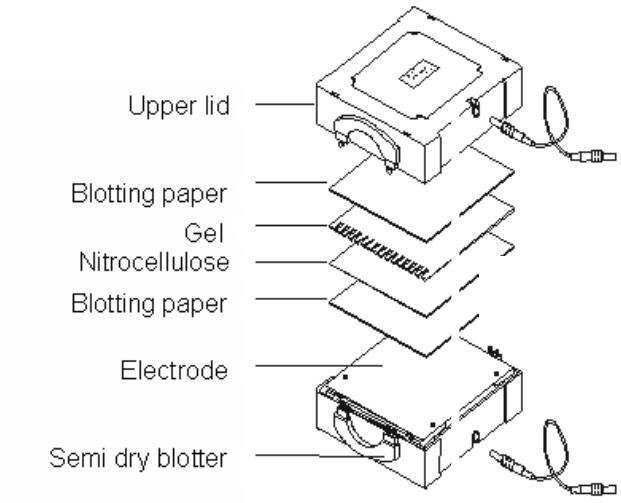

The transferred proteins were visualised by incubation with Ponceau S red reversible stain (Sigma) for 2 minutes, followed by destaining in distilled water. The protein tracks were cut into strips, washed in PBS-tween (PBSt) rinse buffer and labelled NN, LN, RN, 2RN and BN. The strips were placed in blocking solution (10% (w/v) skimmed milk in PBSt) to block free binding sites and reduce non specific binding and incubated at room temperature for 1 hour or overnight at 4^{o}C.

Each individual strip was then incubated at room temperature for 1 hour with the appropriate bleed, diluted 1/250 in 10% foetal calf serum (FCS) (Sigma) in PBSt. The pre-immune bleeds were used as a negative control. The AP detection method was considered to be the most suitable detection method for WB of bleeds as ECL results are difficult to interpret due to excessive background.

The strips were washed in several changes of PBSt rinse buffer and placed in rabbit anti-mouse alkaline phosphatase (RAMAP) secondary antibody (Amersham), diluted 1/500 in 10% foetal calf serum, for 1 hour at room temperature. The strips were washed again in several changes of PBS rinse buffer, and then washed twice in alkaline phosphatase buffer (100mM NaCl, 5mM $MgCl_2$, 100mM diethanolamine, pH 9.5). The antigen-antibody-antibody complex on the nitrocellulose paper was then visualised by placing the strips in developer solution (10ml AP buffer, 33µl nitrobluetetrazolium (NBT, 100mg/ml), 66µl 5-bromo4-chloro3-indolyl phosphate (BCIP, 50mg/ml) (Sigma), until the bands could be visualised. The chromagen cleavage reaction was terminated by

briefly placing the strips in 10% acetic acid prior to air drying. The membrane was then scanned to generate an electronic image and stored, protected from the light.

3.3.6. Immunohistochemistry

Immunohistochemistry is used to identify tissue components via the use of both polyclonal and monoclonal antibodies. This technique has a long history, the first concepts of which were described in 1941 via the use of an antibody containing a fluorescent group (Coons, Creech, & Jones, 1941). The technique was used throughout the 1970's, gaining application in the identification of proteins on formalin fixed paraffin embedded tissue samples, although at this time the applications were limited as not all proteins in samples were identified. This is largely due to masking of epitopes caused by tissue processing. In 1991, Shi and colleagues identified a high temperature unmasking method to expose target epitopes in fixed tissues; this revolutionised immunohistochemistry as the sensitivity of the technique was greatly increased and many antibodies previously regarded as being of little use in fixed tissue were found to be of much greater value (Shi, Key, & Kalra, 1991).

It has been hypothesized that heating tissue sections to temperatures in excess of $100^{O}C$ causes disruption of cross links formed between formalin and the proteins tertiary or quaternary structure. These cross links are considered to be responsible for the masking of epitopes commonly seen. It may also restore antigens altered via acetylation or methylation. Dependent upon the degree of cross linkage, epitope retrieval solutions with differing pH may be used in order to optimise this technique.

IHC is extremely useful as it is able to provide information upon protein expression levels in tissues and cellular localisation. In addition, it can be used to confirm the presence or absence of cellular markers and based upon their location within the cell can often aid in the elucidation of the function of particular proteins. IHC is able to detect relatively low levels of protein in tissues, although it is not as sensitive as ELISA or WB analysis.

Various detections may be used in IHC, the techniques used in this study are the indirect streptavidin-biotin (ABC) technique as described in Figure 3-4 and the newer, more sensitive Novolink™ bench polymer kit (Novocastra laboratories, Figure 3-5). The basic methodology and detection method used in both methods are similar, although a polymer replaces the secondary antibody and avidin-biotin complex in the Novolink™ method. The advantages of the polymer kit

are the ease and efficiency of the steps involved and the increased sensitivity of a polymer based detection kit.

Figure 3-4: Indirect ABC technique immunohistochemistry. The primary antibody binds to the target (step 1) and a secondary biotinylated conjugate antibody binds to the complex (step 2). Biotin molecules are recognised by streptavidin, which is conjugated to a horseradish peroxidise (HRP) enzyme. Each streptavidin binds four biotin molecules and a macromolecule complex is formed (step 3). Addition of a chromogenic substrate such as 3'3-diaminobenzidine tetrahydrochloride (DAB) causes the HRP to cleave it into an insoluble brown product which is precipitated at the site of formation.

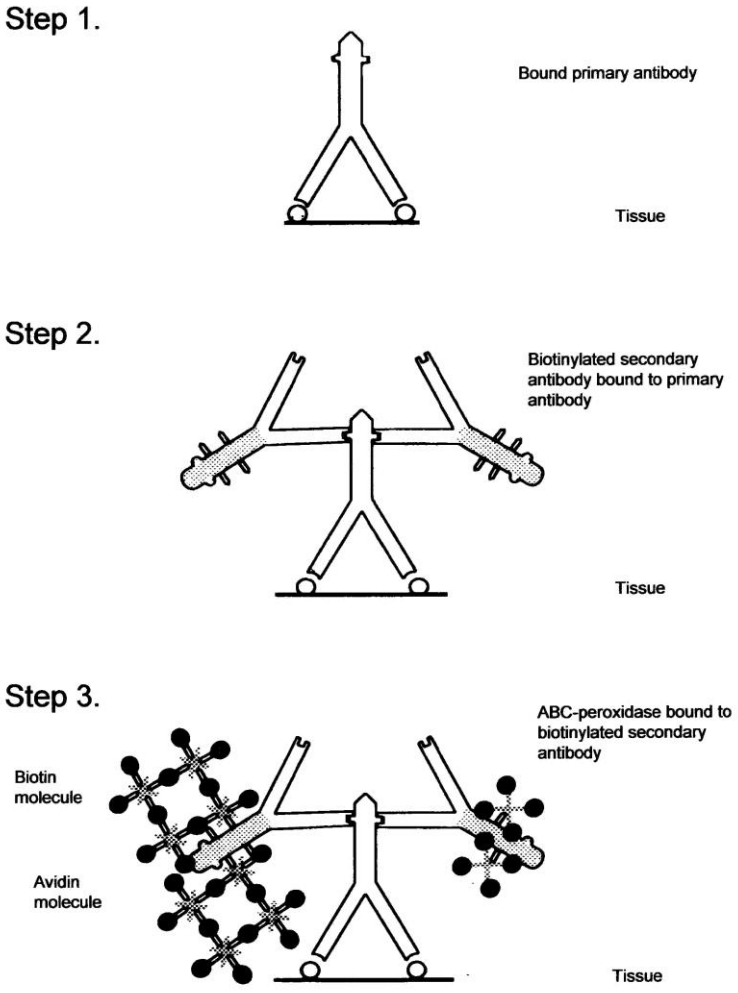

3.3.6.1. Indirect Avidin-Biotin (ABC) Technique Immunohistochemistry

IHC was carried out according to the method described by Hsu and colleagues (1981). 5 µm sections of paraffin embedded tissue were cut using a microtome (Leica Biosystems) and placed onto 3-aminopropyltriethoxysaline (APES) coated slides. Sections were incubated at 37^{O}C overnight, then baked at 60^{O}C for 60 minutes, then deparaffinized in xylene and rehydrated through graded alcohols (100%, 90% and 70% ethanol in dH_2O). Endogenous peroxidase activity was neutralised by incubating in a mixture of 3% H_2O_2 in methanol at room temperature for 10 minutes. The sections were washed in running tap water pre-treated with the appropriate reagent at a given pH in a pressure cooker for 1 minute at maximum pressure in order to expose antigenic epitopes. The sections were once again washed in tap water and placed in tris-buffered saline (TBS) buffer, (140mM NaCl, 50mM Tris-HCl pH 7.6) for 5 minutes. In order to block any non-specific tissue binding sites, the sections were incubated with 10% normal rabbit serum (NRS) in TBS buffer for 10 minutes at RT. Excess blocking serum was removed and replaced with the appropriate dilution of bleed/primary antibody and the sections were incubated at 25°C for 60 minutes. Following incubation, sections were washed in TBS for 5 minutes and covered with biotinylated rabbit anti-mouse secondary antibody (Novocastra Laboratories), diluted 1/500 with 10% NRS in TBS buffer and the sections were incubated at 25°C for 30 minutes. Following incubation sections were washed in TBS buffer for 5 minutes and then covered with peroxidase-conjugated ABC complex (Novocastra Laboratories) diluted in TBS buffer and incubated again at 25°C for 30 minutes. After a final wash in TBS buffer, bound peroxidase was visualised using 3'3-diaminobenzidine tetrachloride (DAB) chromogen. The sections were washed in tap water, counterstained with haematoxylin, dehydrated through graded alcohols, cleared and mounted in a mixture of Distyrene, Plasticizer and Xylene (DPX) (Sigma), (Figure 3-4).

3.3.6.2. Novolink™ Polymer Immunohistochemistry

Figure 3-5: Novolink™ polymer methodology. Steps and methodology employed via the use of the Novolink™ polymer kit. N.B. Antigen retrieval was performed in a pressure cooker as previously described prior to the blocking steps.

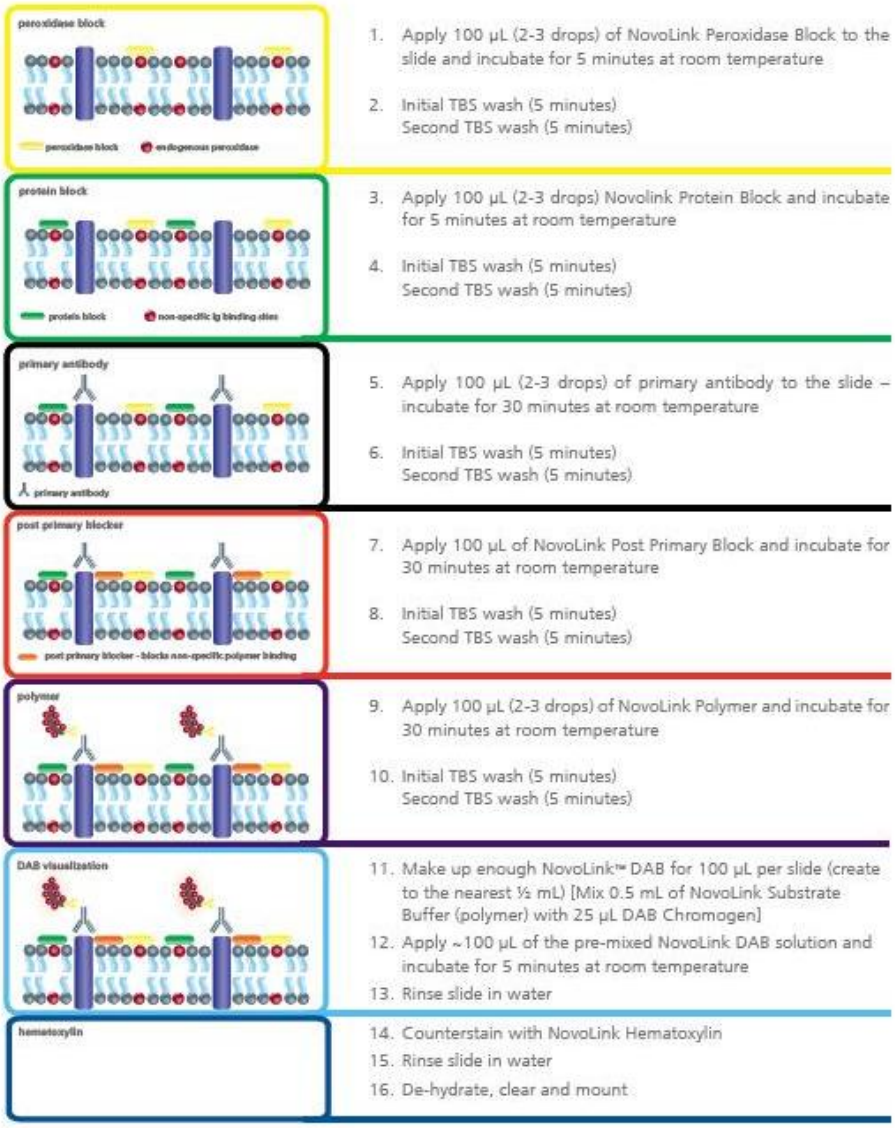

3.3.6.3. Bleed Assessment via Immunohistochemistry

All 5 bleeds, diluted 1:400 with 10% NRS in TBS, were tested on ovarian and colon adenocarcinoma, normal colon and placental FFPE samples obtained from Novocastra archives using IHC with the indirect ABC IHC technique and the Novolink polymer testing kit. The pre-treatments used were high temperature citrate (200mM citric acid, 500mM NaOH, pH 6.0) and Tris/EDTA (10mM Tris, 1mM EDTA, pH 9.0) unmasking in a pressure cooker at high pressure for 1 minute and the enzyme based proteinase-K bench unmasking technique. The unmasking solution

that gave the most specific staining was chosen and used in subsequent experiments. Mice with positively responding sera were selected for the final IV injection and subsequent fusion.

3.3.7. NS-1 Myeloma Cell Culture

As described earlier, NS-1 cells are immortal cancer cell line variants of mouse cell myelomas which have lost the ability to both synthesize and secrete immunoglobulin (Ig) heavy chains. They are therefore ideal candidates for hybridoma development as they do not produce contaminating antibody.

Cell culture was performed in a Class II tissue culture hood using aseptic techniques, typical culture medium for myeloma cells is RPMI 1640 (Sigma), 20% (v/v) FCS (Sigma), 2mM L-glutamine (Sigma), 2.5ml penicillin/streptomycin (500 µg/ml) (Sigma), also known as R20 medium. The media was stored at 4^{O}C when not in use and from the date of production it had a shelf life of one month. Media was pre-warmed to 37^{O}C in a water bath prior to use.

Five days prior to cell fusion, a cryovial containing 1 x 106, P3-NS-1/1-Ag-1 azaguanine selected myeloma cells, was removed from liquid nitrogen and thawed rapidly in a 37^{O}C water bath. The cells were re-suspended in 10 ml R20 medium and centrifuged for 5 minutes at 125g. Following centrifugation, the supernatant was discarded and the cells were re-suspended in 10 mls R20 medium and transferred to a 162cm² flask, where a further 30 ml of R20 was added. The cells were stored in a 37^{O}C incubator with 5% CO_2. Cell growth was monitored daily by microscopic examination until approximately 80% cell density was achieved. Upon reaching this density (typically 2-3 days) the NS-1 cells were counted using a haemocytometer and trypan blue (Sigma) was used to measure cell viability. A minimum of $2X10^7$ cells with a viability greater then 90% was required in order to proceed with the cell fusion.

Typically, cells were fed once every 2-3 days by subculturing 1ml of the cell suspension into approximately 30mls R20 media and expanded up to approximately 80mls two to three days prior to cell fusion.

3.3.8. Cell Fusion Procedure

3.3.8.1. Fusion Preparation

One week after selection for IV, the positively responding mouse, as determined by WB and immunohistochemical bleed assessment was sacrificed at the CBC and collected approximately 30 minutes before commencement of fusion. Prior to fusion, 5ml of HAT medium (Sigma), and 10% (v/v) BM-Condimed H1 (Boehringer-Mannheim, UK) and 15% Foetal Calf Serum (Sigma), was added to 190 ml of R20 medium (fusion medium) in a 75cm^2 flask and warmed to 37^{O}C in a water bath. Condimed contains a mixture of growth factors and cytokines, including Interleukin-7 (IL-7) which markedly stimulates growth of hybridoma cells in culture and aids in the production of hybrids secreting antibody. A vial containing 4 ml of 50% PEG 1500 in 75 mM Hepes (Sigma) and a universal containing 50 ml of R20 medium was also placed in the water bath.

3.3.8.2. Splenocyte Preparation

The mouse was drenched in 70% alcohol before being placed into the sterile hood. The mouse was laid on its right side and using sterile scissors, the fur and skin was cut along the abdomen and the spleen excised. All bound fat and additional tissue was removed and the spleen was washed in a petri dish containing approximately 10mls warm, sterile R20 medium. The spleen was then transferred to a further petri dish containing approximately 10 ml of R20 medium. Using sterile forceps and a seeking tool, splenocytes were gently teased out of the splenic capsule and into the medium, taking care not to disrupt the capsule itself. Once the majority of the splenocytes were removed the splenic capsule and mouse were discarded. The cell suspension was slowly passed up and down several times through a large 18 gauge needle. This large needle was then exchanged for a smaller 25 gauge needle and the process was repeated in order to produce a single cell suspension whilst avoiding rupture of the splenocytes.

3.3.8.3. NS-1 Myeloma Cells

Before preparing the cell suspension, an appropriate volume of NS-1 cells were calculated, in order to provide 2x10^7 cells necessary for the fusion, using a haemocytometer. The volume of media, containing 2x10^7 NS-1 cells was transferred into a 50 ml universal and centrifuged for 5 minutes at 125G. The supernatant was discarded and the cell pellet gently tapped to dislodge the cells.

3.3.8.4. Fusion in PEG

The splenocyte single cell suspension prepared in the syringe was slowly added to the universal containing the NS-1 cells and the mixture of both cells (NS-1:Spleen cells approx 1:8) was centrifuged again at 125 G. The supernatant was discarded and the cell pellet gently tapped to resuspend both types of cell into the residual medium. The cells were placed into a small $37^{O}C$ water bath where they remained throughout the fusion procedure. The universal was continually rotated and 2ml of PEG 1500 (Sigma) was added to the cell mixture over 1 minute taking care not to immerse the pipette tip into the cell suspension. 1ml of R20 media was then added over 1 minute with the tip of the pipette placed firmly against the bottom of the universal. Subsequently, 2x 10 mls R20 medium were added over 4 minutes with the tip placed just under the meniscus. The cell mixture was decanted into the $75cm^2$ flask containing the fusion medium prepared earlier. The suspension was plated out at 200 µl/well into twelve 96 well sterile culture plates, leaving the final column on the 12th plate free for controls, and incubated at $37^{O}C$, 5% CO_2 for 7 days. After approximately 7 days the plates were examined microscopically to identify hybridoma colonies.

3.3.9. Enzyme Linked Immunosorbent Assay (ELISA)

ELISA is a solid phase binding assay used in a variety of applications, including determination of the antigenic constituent of hybridoma supernatants by antigen-antibody interactions between the recombinant protein used for immunisation and the antibodies generated resulting from fusions. A secondary antibody is typically conjugated to an enzyme. In this case AP was conjugated to the secondary antibody which cleaved a colourless P-nitrophenyl phosphate substrate to the yellow cleavage product monophosphonitrophenol, the absorbance of which could then be measured by a spectrophotometer (450nm).

3.3.9.1. Screening for Specific Hybridoma Colonies via ELISA

After approximately 7 days, the 12 fusion plates were screened by ELISA to detect any specific anti-FR-α and FPGS antibodies. 100µl of the appropriate recombinant protein, at a concentration of 1 µg/ml in coating buffer (15mM Na_2CO_3, 35mM $NaHCO_3$, pH 9.6) were added to each well of twelve 96 well ELISA plates and incubated either at $37^{O}C$ for 2.5 hours or overnight at $4^{O}C$. The plates were washed three times with PBSt, pH 7.2 to remove any unbound antigen, using a hand operated plate washer (Dynatech Laboratories, UK). 50µl PBSt with 1% NRS was added to each

well to reduce any background resulting from pH variability between wells. 50µl of primary supernatant from the fusion plates was then added to the corresponding ELISA plate via the use of a 96 channel pipette transplater with sterile 96 tip transplate cartridge (Transtar, UK). A positive control, using the corresponding positive bleed, diluted 1:1000 and 1:5000 in PBSt and a negative control of PBSt only, was also added to the final column on the 12th plate and the plates were incubated at 37^{O}C for 1.5 hours.

After washing to remove any unbound antibody, the plates were incubated at 37^{O}C for 1.5 hours with 100µl/ well AP conjugated rabbit anti-mouse IgG (Sigma) diluted 1/2000 in PBSt. After the final washing step to remove any unbound secondary antibody the plates were incubated with 100µl/well AP tablets (Sigma) dissolved in AP buffer (100mM diethanolamine, 100mM NaCl, 5mM $MgCl_2$, pH 9.5) at a concentration of 1 mg/ml for 15 minutes or until the colour developed (Figure 3-6). 50µl of 3M NaOH was added to each well to stop the reaction and the optical density of the plates were then read on an MRX plate reader (Dynex Technologies) at 450 nm. Positive wells were identified, using the positive controls as a guide and hybridomas in the corresponding wells from the original fusion plates were picked off using a 10 µl pipette and transferred to a new 96 well ELISA plate. A positive response was determined by an optical density (OD) above the OD of the control at 1/5000. The positive hybridomas were then supplemented with R20/condimed medium and left to grow overnight at 37^{O}C.

Figure 3-6: Positive ELISA plate. Photograph of an ELISA plate showing positive wells (yellow).

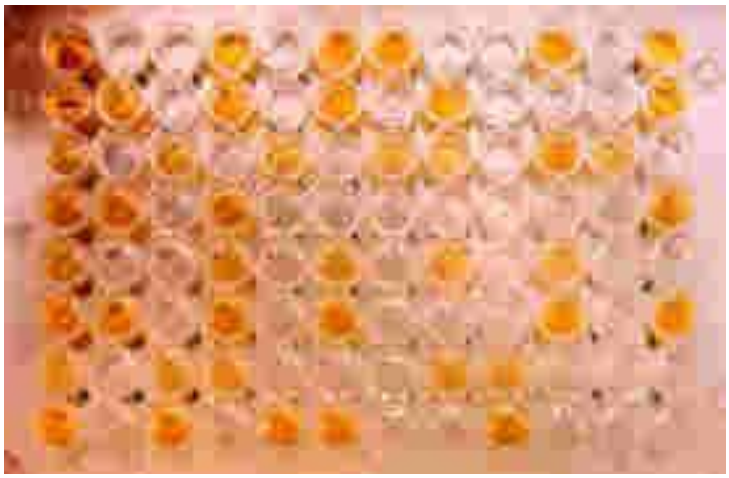

3.3.9.2. ELISA Screening of Hybridomas against Fusion Protein Tags

As the amino acid sequences of FR-α and FPGS were cloned into pET32a-Tx and pET41b-GST tagged vectors respectively, the ELISA positive hybridomas were screened against both TX and GST proteins by ELISA as previously described to ensure any hybridomas secreting antibodies recognising either protein were identified and discarded. Any cells recognising the 'tag' were located to the corresponding wells on the culture plate were removed. All remaining positive hybridomas were supplemented with R20/condimed medium and left to grow overnight at 37^{O}C.

3.3.10. Screening ELISA Positive Hybridomas via IHC

ELISA positive hybridoma supernatants were screened by IHC on FFPE tissue sections obtained from the Novocastra archives, using the standard indirect ABC technique and Novolink Polymer kit as described in section 3.3.6. The unmasking methods, as determined from the bleed assessment were citrate pH 6 for FR-α and Tris EDTA pH9 for FPGS hybridomas.

At this stage the sections were scored as either negative, 1+ (weak), 2+ (moderate) or 3+ (strong) using a light microscope and specific hybridomas were transferred to a 24 well plate and given the appropriate volume of R20/condimed medium and left to grow

3.3.11. Cloning Hybridomas via Limiting Dilution

The ELISA and IHC positive hybridomas were cloned to ensure that the antibody secreting hybridomas were from single parent cells and thus monoclonal in origin. This also ensured the antibody secreting cells were not contaminated with more rapidly growing non-secreting cells which often exhibit growth advantage over cells secreting antibody.

Two 96 well plates were prepared for each positive hybridoma by addition of 200 µl R20/condimed medium to each well and pre-warming at 37^{O}C. The calculated volume containing 1000 cells from each positive hybridoma was then diluted in 4mls R20/condimed medium and 100µl of cell suspension was then seeded into the first 2 columns of each 96 well plate. It was then serially diluted across the plates by transferring 100 µl of cell suspension from rows 1 and 2 to rows 3 and 4 respectively, continuing across to the end of the plate. Excess cell suspension was discarded and the plates were incubated at 37^{O}C until sufficient growth had been achieved, typically 7-10 days; the hybridomas were then screened by ELISA.

Positive wells towards the right of the plate (typically one or two hybridomas per cloning plate) were selected to be grown for IHC analysis to ensure the antibody gave specific tissue staining.

In order to produce a monoclonal antibody, this cycle of screening via ELISA and IHC and cloning procedures needed to be repeated a minimum of three times to ensure the hybridoma clones were statistically 99.99% monoclonal. The cells were also frozen down before cloning at each stage to ensure a stock of hybridoma was available to return to if necessary in case of failure of cloning or contamination.

3.3.11.1. Assessment of 1st and 3rd Clones via Western Blot Analysis

ECL WB was used to assess 1st and 3rd clones in addition to IHC analysis to confirm specific reactivity with both the recombinant protein and cell lines known to express the protein. The methods were performed as described in section 3.3.4. The more sensitive ECL detection method was used to assess clones.

After addition of the primary antibody and washing steps, an HRP labelled anti-mouse IgG secondary antibody (Amersham) at a dilution of 1/2000 in PBSt/ 10% foetal calf serum was added to the membrane and incubated for 1 hour at room temperature. After several washes in rinse buffer the antibody reaction was revealed using a chemiluminescence ECL detection kit (Amersham) according to the manufacturer's instructions. After addition of the appropriate volume of reagents the membranes were wrapped in cling film (Saran wrap) and placed in an x-ray film cassette with a sheet of autoradiography film (Kodak) in a dark room and exposed for the appropriate length of time. The exposed film was then developed in an automatic x-ray film processor (XOgraph X4, Xograph Imaging Systems Ltd, Gloucestershire).

3.3.12. Freezing Down Cells

Before and after each cloning procedure, cell samples were frozen down and stored in liquid nitrogen. 1ml of cell solution was placed into a centrifuge tube and centrifuged for 5 minutes at 125G. The supernatant was discarded and 0.5 ml of freeze mix (90% FCS, 10% dimethyl sulphoxide (DMSO, Sigma) was added to the cell pellet. The mixture was then transferred to a freezing vial, labelled and placed in a cryo-freezing container at -80^{o}C for no longer than one week prior to being transferred to liquid nitrogen.

3.3.13. Weaning into R20 Medium

Positively responding clones were transferred into 6 well plates and weaned into R20 medium by slowly decreasing the percentage of R20/condimed medium. Throughout the weaning process, a well containing cells in R20/condimed medium was grown in the event that the weaned cells could not survive in the lower concentrations of condimed medium. The weaning process duration can range from 2 weeks to a few months depending upon the hybridomas response to the reduction in condimed. Once the cells were successfully weaned into R20, approximately 50 ml of cell suspension was grown in a 75 cm^2 tissue culture flask, frozen down and stored in liquid nitrogen, and approximately 70 ml of cell suspension was grown in a 162cm^2 tissue culture flask as a pre-production batch and left to overgrow for further testing.

3.4. Antibody Validation and Characterisation

3.4.1. Characterisation of Weaned Clones via Immunohistochemistry

Once the clones had been weaned into basic R20 media, they were tested via IHC using the Novolink polymer kit on large panels of formalin fixed, paraffin embedded normal and tumour tissues in order to fully assess the expression of the proteins on a wide variety of tissues. A panel of normal and tumour samples were obtained from Novocastra archives. In addition, any tumour samples stored in the Novocastra tissue archives thought to be of interest were also added to the panel. Archival ovarian adenocarcinoma samples collected in connection with clinical trials of pemetrexed which had appropriate ethical approval for use in this study were also added to the panel as ovarian cancer is the main focus in this study. The results of these panels could then be compared with literature on known expression of the proteins to assess the specificity of the antibody.

3.4.2. Characterisation of Weaned clones via Western Blot Analysis

WB was performed on an extended panel of both positive and negative cell lines to further characterise the antibodies and support the IHC studies as described in section 3.3.4. A large cell line panel was used to assess the FPGS antibody as there was no IHC data to compare it to and thus it relied heavily on the data obtained from WB analysis for characterisation.

3.4.3. Further Characterisation

In addition to IHC and WB analysis, the FR-α and FPGS antibodies were also assessed for their suitability for use with no pre-treatment and alternative pH pretreatments to ensure the selected pretreatment was still the most suitable. They were assessed for use with PBS buffer as this is commonly used in America and in addition they were assessed for use on the automated Bond IHC system. Most of these tests were performed to ensure the antibody was suitable as a marketable product both in the UK and worldwide. Once all criteria had been satisfied the antibodies were isotyped (Isostrip Mouse Isotyping Kit) according to the manufacturers instructions and sent for review by both the managing director and Dr. Gary Hoffman, a consultant pathologist who analysed the staining on the sections and the appropriate literature. Once satisfied the antibody was specific for the target it was signed off and transferred to the production department where additional stability tests would be performed in preparation for mass production.

3.4.4. Epitope Mapping

Finally, epitope mapping via the use of a peptide array was used to fully characterize the antibodies and identify the epitope present on the target sequence. It was decided to use the Cancer Research UK (CRUK) resource to generate the peptide array immobilised on a cellulose membrane to map the FR-α and FPGS antibody epitopes. This technique used a multipeptide synthesiser (Intavis) on which arrays of up to 600 peptides could be generated. The FR-α and FPGS target sequences were sent to CRUK and overlapping peptides of 12 amino acids in length, overlapping by one residue each time were generated and immobilised on to the membranes.

The advantage of use of this resource is the ease of the methods used, applying a simple WB based technique for detection of positive peptides, it is also extremely fast and highly accurate results are obtained. The disadvantages of this method are that peptide array generation is costly and the coding sequence must be known. It was decided to use this technique primarily due to time limitations as other techniques may take as long as 6 months to complete and the results of this experiment would be valuable for completion and conclusion of this part of the work.

Two FPGS membranes were received and three FR-α membranes, suitable for use with five different antibodies in total. It was decided to use one of the membranes to map the mOV 18 antibody in addition to the FR-α antibody to observe the similarities/differences between the epitope recognition sites. The additional membrane was used to map the LK26 antibody.

The membranes were treated in the same way to the techniques used in WB as described in section 3.3.4, beginning with the blocking step.

After treatment and development the membranes were stained with Ponceau S, an anionic sodium salt of a diazo dye which binds to the basic amino groups of proteins in an acid solution. It binds to primarily histidine, arginine and to a lesser extent lysine residues. Not all peptides react with the dye as not all sequences contain these amino acids, however it was possible to accurately infer the position of the other peptide spots based upon the positions of the visible peptides (Thompson-Hayner, Driscoll, Ferayorni, Spies-Karotkin, & Jauregui, 1982).

3.5. Results – Hybridoma Technology

3.5.1. Mouse Immunisation and Polyclonal Assessment

3.5.1.1. FPGS Immunisations/Polyclonal Assessment

Five mice were successfully immunised with soluble FPGS2 pET41 protein, as this was the initial project it was decided that all mice should be fused as a training exercise. However, further studies highlighted a problem and all immunised mice subsequently failed, this will be discussed in detail later in this chapter. The initial five mice appeared to have responded well, LN appearing to have the best response via WB. The best responding mouse was then assessed via IHC on ovarian and colon adenocarcinomas, term placenta and normal colon to assess the polyclonal response, using Tris-EDTA for antigen retrieval. The staining observed was cytoplasmic and punctuate and was inferred to be correct as there was no IHC data to compare it to. For this antibody WB results were heavily relied upon as confirmation that the staining seen was correct. The staining was thought to be correct as it was in the correct compartment within the cell and punctuate staining was indicative of the type of staining expected from a cytoplasmic/mitochondrial enzyme (Figure 3-8). A single band was observed via WB at 60 kDa so it was thought that the positive staining confirmed by a band at the correct molecular weight was confirmation of antibody specificity (Figure3-7). Fusions were performed on all five mice, two clones reached the third and final cloning stage before a cross reactivity issue and a gap in the screening procedure were identified, this is discussed in detail in section 3.5.2.1. The following figures show the staining and WB immunoreactivity observed, however, these clones were discarded at the final stage.

Figure 3-7: AP WB of FPGS polyclonal bleed. FPGS2 pET 41 polyclonal bleed. Note the band at the expected MW of FPGS at 60 kDa and absence of band in the pre immune bleed. (-C - negative control lane, LN – Left Notch bleed).

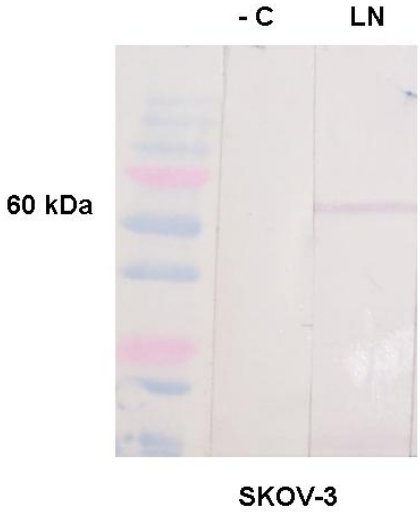

Figure 3-8: Polyclonal and monoclonal comparison. IHC photographs of a paraffin embedded ovarian adenocarcinoma sample stained with FPGS2 pET 41 LN bleed and third clone. Note the cytoplasmic punctuate staining seen which was the expected FPGS staining pattern.

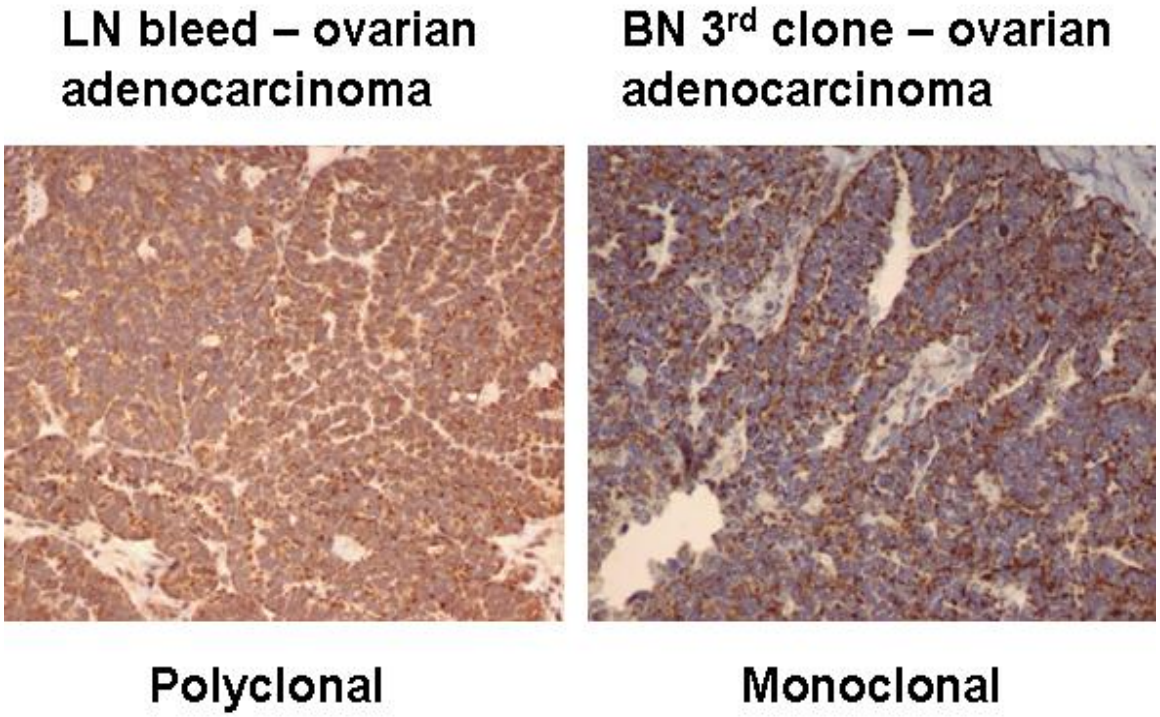

A further five mice were successfully immunised with FPGS3 pET 41 refolded protein, all five mice were found to show a very weak response via both IHC and WB.

Given the problems highlighted above, five mice were also immunised with FPGS2 pET 32 refolded protein, as it was found that immunisation with refolded rather than soluble proteins appeared to eliminate the cross reaction problem described in section 3.5.2.1. All mice appeared to have responded via WB and IHC, 2RN giving the strongest and most specific response. All mice were selected for fusion.

In total 15 mice were immunised for the FPGS project and 15 fusions were performed.

3.5.2. FR-α Immunisations/Polyclonal Assessment

Initially five mice were successfully immunised with FR-α pET41 soluble protein, the polyclonal assessment indicated only one strongly positively responding mouse (BN) so a further five were immunised with FR-αF2 soluble protein. This was performed before the FPGS cross reactivity problem was observed. Upon the bleed assessment for FR-αF2 it was observed that a single band at 60 kDa appeared to be present on these WB's. As the expected molecular weight for FR-α is 40 kDa this was the first indication that there may be a problem with the antibodies and initiated an investigation into determination of the specificity of the antibodies via WB studies, described in the following section. At first it was thought the proteins may have somehow become mixed up, however subsequent tests ruled this out. In light of this problem highlighted with the FPGS protein/antibodies and the possibility that it may also be affecting the FR-α samples, a further five mice were immunised with the FR-α pET 32 refolded construct as this was thought to prevent previous cross reaction problems. Again, in total 15 mice were immunised and 15 fusions performed for the FR-α project. In the FR-α pET 41 immunisations, bleed BN was selected for further IHC analysis, citrate buffer (pH6) was found to be the most suitable antigen retrieval solution and IHC analysis on normal colon and ovarian adenocarcinoma showed membrane/cytoplasmic punctuate staining (Figure 3-9). On further analysis this staining pattern was seen to be strikingly similar to that of the staining observed for the FPGS2 bleeds.

Figure 3-9: FR-α polyclonal bleed. IHC photograph of FR-α pET 41 NN polyclonal bleed on normal colon (top) and ovarian adenocarcinoma (bottom) x20. Note the membrane/cytoplasmic punctuate staining and the similarity in staining with the FPGS LN bleed previously shown.

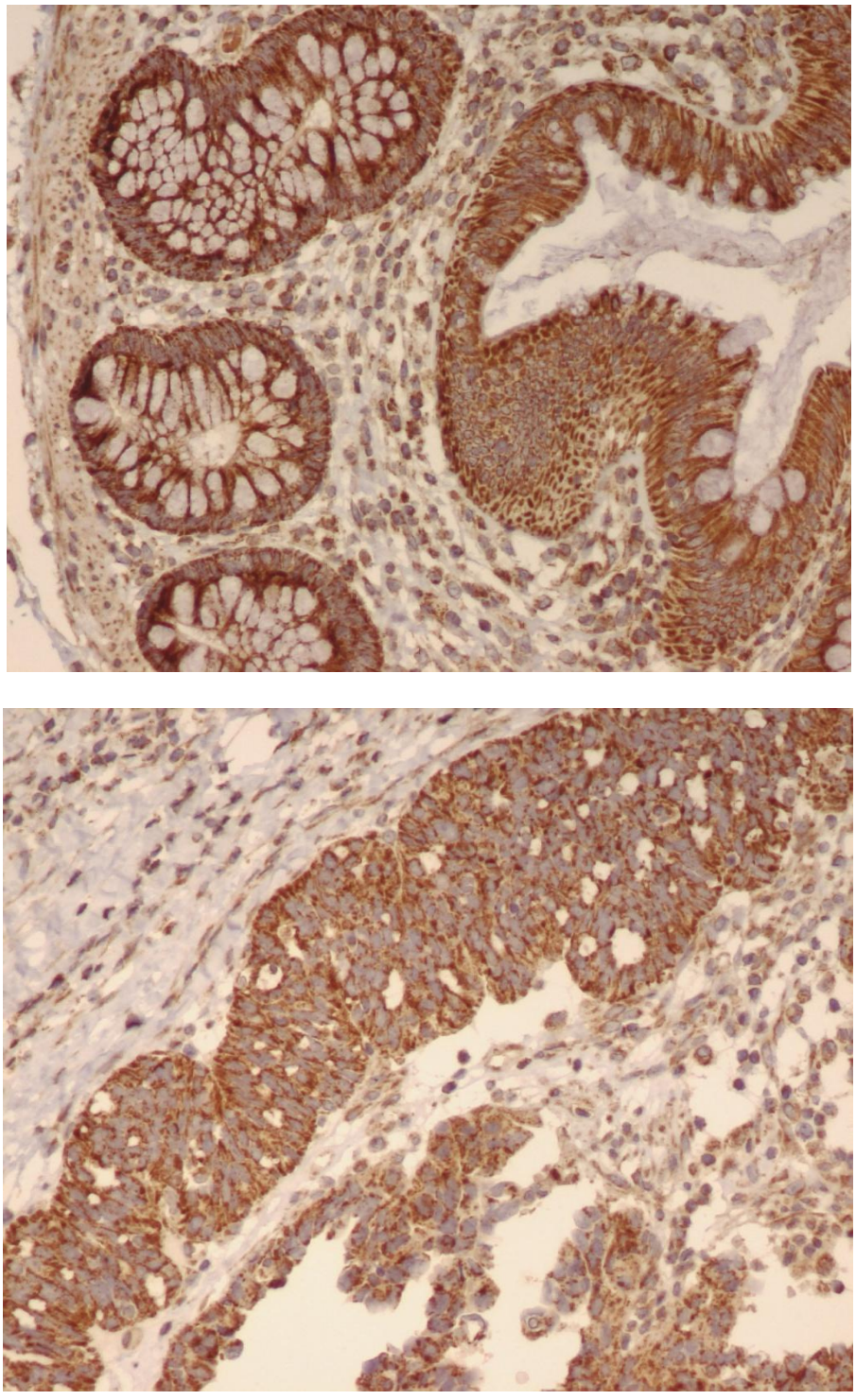

3.5.2.1. Western Blot Studies to Identify the Cause of Cross-Reactivity

The first indication of a cross reactivity problem was the assessment of the FR-αF2 bleeds which all appeared to have single band reactivity with a 60 kDa protein. As the expected size of FR-α was 40 kDa and each bleed was producing a specific single band it appeared there may be a problem. It is unusual for a bleed to give a single band under normal circumstances as many bands are usually present due to the polyclonal nature of the serum. The first time this occurred with the FPGS protein it was considered to be fortunate, however, concerns were raised when it also occurred when the FR-α bleeds were assessed.

This had not been highlighted earlier due to the fact that the correct molecular weight for FPGS is, in fact 60 kDa. It was decided that the FPGS antibodies, which by this stage were 3rd clones, should be tested via WB studies to ensure they were recognising the correct protein.

At this stage it was thought that the immunoreactivity of both proteins may be due to either an error in molecular biology where the proteins may have become mixed up, this may have occurred at Novocastra or at the CBC during immunisation. Another hypothesis was cross reaction due to the same polylinker region being present in both protein constructs.

The first step in investigation of this was to test this hypothesis and collect recombinant protein samples in different constructs previously developed at Novocastra.

Proteins generated in the following constructs were collected;

- pET 41 (GST)
- pET 21 (Simple vector with no tag)
- pET 32 (Tx)
- pET 41s (GST with different flanking regions)
- pET 32s (Tx with different flanking regions)

A simple ELISA was initially performed, coating an ELISA plate with each of the above proteins and adding the FPGS2 BN 3rd clone. This was inconclusive as reactivity was observed with the both the FPGS2 pET41 and FR-α pET 41 soluble proteins but only weak reactivity with the other protein

constructs. This may have indicated that the proteins were mixed up but further studies were required.

WB was then performed using the same proteins; AP gave a very weak signal so it was decided to use ECL. The result was surprising as it appeared that a single, 60 kDa band of immunoreactivity was present in all the protein samples tested to varying degrees. As the target sequences were different, the vector flanking regions of each construct were aligned to determine whether there were similarities. Again, this proved inconclusive as the flanking regions differed significantly. The most similar flanking region was in the pET 32 construct tested, however the signal did not appear to be any stronger with this protein. As this band was in other proteins which could not have been mixed up, the possibility of the proteins contaminating one another was not explainable in light of this result, although the strongest reactivity was still seen with both the FR-α and FPGS pET41 soluble constructs. In fact, strongest reactivity was observed between the FR-α pET41 soluble protein and the FPGS antibody. Similarly when another BLAST search was performed, aligning the FR-α and FPGS sequences, no regions of homology were identified. It was then hypothesized that the antibodies may just have a very high affinity for 'sticky proteins', ovalbumin and bovine serum albumin are known to be extremely 'sticky' and had not been produced using vectors so they were tested but no signal was observed for either protein.

Recombinant enterokinase enzyme was used to cleave the proteins into two fragments to identify which region of the proteins the cross reaction occurred, as it cleaved the proteins before the tag, it could be determined whether the epitope being recognised by the FPGS antibody is from the vector sequence alone or part of the protein and vector sequence. Bands were observed throughout the whole sequence, although it wasn't clear how well the enterokinase enzyme kit had worked as the protein was degraded. An anti GST antibody was used and gave a signal in the cleaved protein where there was no signal using the FPGS antibody at the corresponding molecular weight so it could be concluded the cross reaction was not due to the tagged region.

Another theory may have been that this was a WB artefact so two methods were applied to test this theory. Both the FR-α and FPGS soluble pET41 proteins were tested against dilutions of antibody to determine whether one signal reduced as the dilution of antibody increased, however both signals stayed as strong as each other so the artefact theory was rejected.

The possibility of the positive signal being an artefact caused by the presence of SDS was also examined. A 'dot blot' WB was performed with no SDS present and the proteins in their native

conformation. Again, all protein samples were tested but a signal was only observed corresponding to the FR-α and FPGS soluble pET41 proteins.

While the blotting studies were being performed, it had been decided that new recombinant proteins prepared in different vectors should be generated as screening antigens, as this cross reaction problem had highlighted a gap in the screening protocol not previously observed. FR-α and FPGS pET 32 constructs were successfully generated although this time they could not be produced in their soluble form and required refolding.

Once these proteins were prepared they were tested with the FPGS clone and surprisingly, neither protein showed any immunoreactivity with the FPGS antibody. As the target region was the same it was concluded that all projects should be discarded as the results obtained could not be considered accurate. Although not tested, it is now hypothesized that as both proteins are cysteine rich, the *E.coli* may have produced soluble stress proteins, possibly a heat shock protein which contaminated the soluble protein fractions in both the FR-α and FPGS pET41 soluble recombinant proteins. The protein produced is likely to be microbial heat shock protein 60 (HSP60), similar to the human equivalent, produced in response to stress (Chen et al., 1998; Kaufmann et al., 1991). Although not previously reported, this theory would also explain the reason for signals being observed at varying levels in other protein samples, possibly dependent upon the number of cysteine residues and relating to the level of stress placed upon the cells to produce the proteins. As the main focus of the project was the generation of antibodies this was not investigated any further and focus was placed upon new immunisation schedules, using the new recombinant proteins with the target regions only for screening as this would ensure only the target region was in common. This may also be supported by the absence of signal in the GST protein as this is a water soluble protein which is not cysteine rich and would not have caused the *E.coli* cells as much stress to produce.

Similar problems have been seen at Novocastra previously, although the reason for the observations were unknown, a 27 kDa protein thought to be Heat shock protein 27 (HSP27) had been found to commonly contaminate soluble protein samples and was taken into consideration when producing recombinant proteins of 27kDa. It is unfortunate that in this case the contaminant happened to be the same molecular weight as the target which misled us to believe the results observed were correct.

The new constructs were found to be successful, this may be due to the fact that they required refolding, as the new proteins were produced in an insoluble form, soluble stress proteins would not have contaminated the samples.

3.5.3. Production of Anti FR-α and FPGS Antibodies

3.5.3.1. Anti FPGS Antibody Generation

An antibody to FPGS2, clone NN3.2 was successfully generated resulting from fusion of mouse BN with refolded recombinant FPGS2 pET32 protein. Unfortunately an antibody to the second target was not generated successfully. All five mice showed a weak response and subsequently the hybridomas generated failed as the response was proven to be too weak, although fusions were performed using all five mice.

The ELISA screening of the fusion was performed using the FPGS2 pET 41b refolded protein sample which had previously been generated and purified. This approach safeguards against producing cross reactive or artefactual antibodies in two ways: Firstly, the only region in common to both the immunising and screening fusion proteins is the target region. Reactivity with the fusion partner (GST or Tx) or with flanking vector sequences will therefore be automatically screened out. Secondly, the use of refolded, insoluble material circumvents the problem that may be caused by any highly immunogenic soluble contaminants such as the postulated soluble 60kDa shock response protein. Following the successful BN fusion, 15 hybridomas were identified which reacted in ELISA with recombinant FPGS pET 41 refolded antigen. From these, subsets were selected producing characteristic patterns of heterogeneous cytoplasmic immunostaining on sections of paraffin wax embedded ovarian adenocarcinoma and colon carcinoma (Figure 3-10).

Figure 3-10: FPGS polyclonal bleed. IHC photograph of FPGS pET 32 NN polyclonal bleed on normal colon (top) and ovarian adenocarcinoma (bottom) x20. Note the cytoplasmic staining and the difference between the staining seen with this bleed compared with the cross reactive bleed shown previously (Figure 3-8).

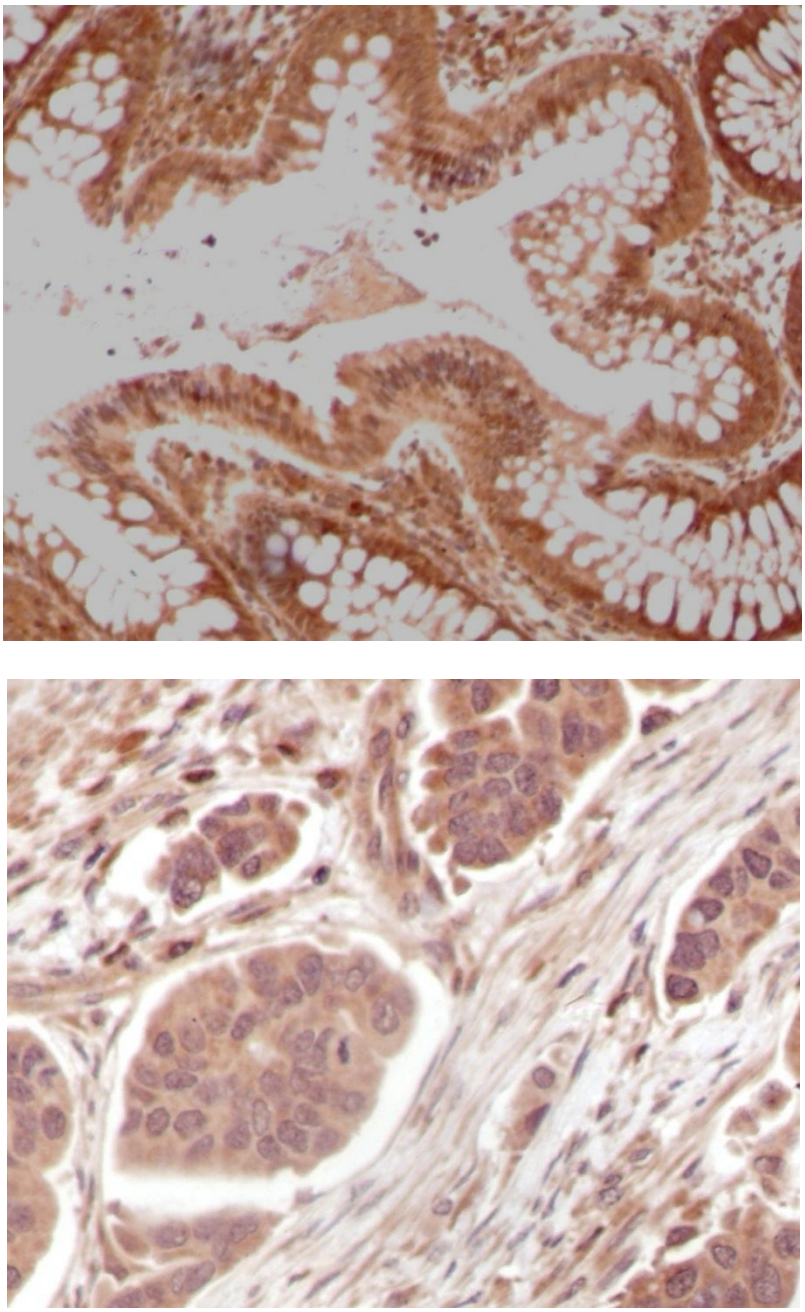

3.5.4. FPGS Expression via Western Blot Analysis

The selected FPGS antibodies were tested for their ability to react specifically with the human FPGS protein in a large panel of various different cell lines by WB as shown in section 3.5.4. The FPGS antibody produced from clone BN3.2 detected a single band of approximately 60 kDa in the majority of cell lines tested with varying levels of expression observed. An antibody to β-actin was used to correct for variations in loading between samples.

3.5.4.1. FPGS Extended Panel

Figure 3-11: FPGS extended panel WB. Representative WB (n=3) showing detection of FPGS WT protein on a panel of cell lines via use of the generated FPGS NN3.2 antibody. An antibody to β-actin (42kDa) was used as a loading control to correct for variations in loading between samples.

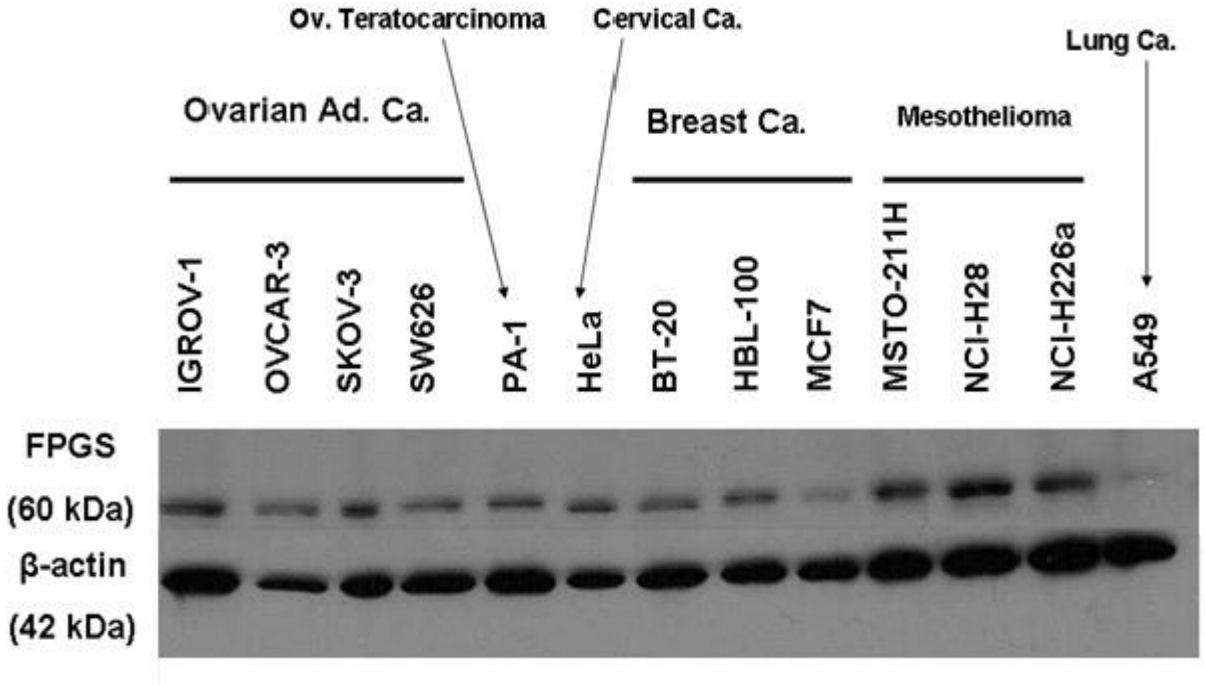

Moderate expression was observed in all samples tested with the exception of the A-549 lung carcinoma and MCF7 breast cancer cell lines which displayed weaker expression of FPGS relative to the other samples. Slightly higher expression of FPGS was seen in the mesothelioma samples tested, although loading of these samples also appeared to be slightly higher.

Figure 3-12: FPGS extended panel (2) WB. Representative WB (n=3) showing detection of FPGS WT protein by WB on a panel of cell lines via use of the generated FPGS NN3.2 antibody. An antibody to β-actin was used as a loading control to correct for variations in loading between samples.

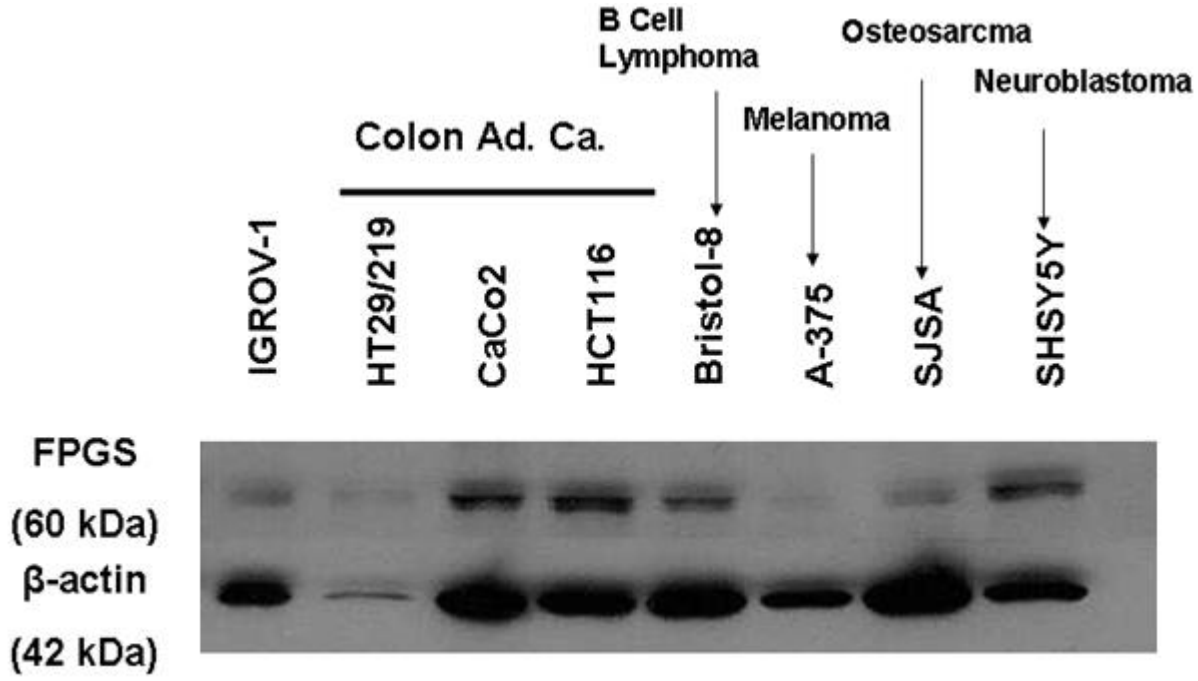

Weak expression was observed in the A-375 melanoma and SJSA osteosarcoma samples tested, moderate expression was seen in the colon adenocarcinoma, B-cell lymphoma and neuroblastoma samples tested.

3.5.4.2. FPGS Leukaemia Panel

Figure 3-13: FPGS leukaemia panel WB. Representative WB (n=3) showing detection of FPGS WT protein by WB on a panel of cell lines via use of the generated FPGS NN3.2 antibody. An antibody to β-actin (42kDa) was used as a loading control to correct for variations in loading between samples.

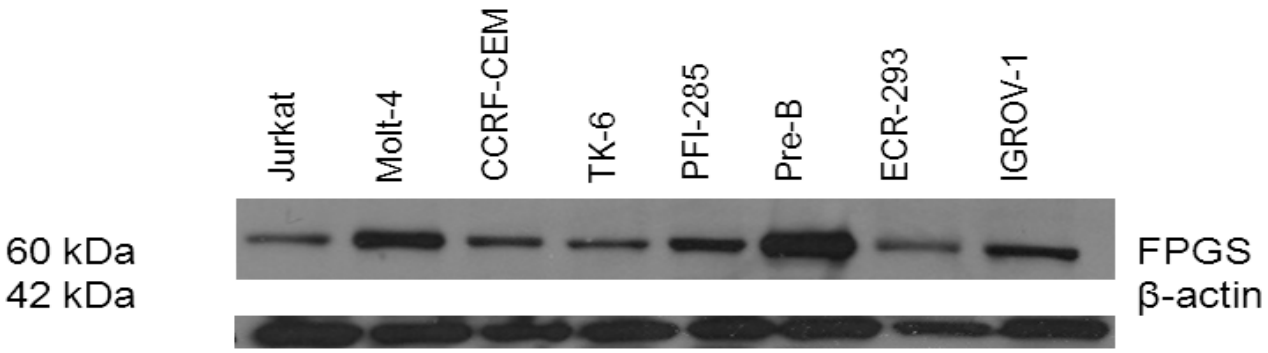

Expression was observed in all samples tested, moderate expression was observed in leukaemia cell lines Jurkat, CCRF-CEM, TK6, PFI-285, embryonic kidney ECR-293 (Figure 3-13) and the ovarian carcinoma IGROV-1 positive control. Stronger expression was seen in Pre-B and Molt 4 cells.

3.5.5. FPGS Expression in Normal and Inflamed Tissues

Immunoreactivity with the NN3.2 FPGS MAb was detected in a wide range of normal and inflamed human tissues. Positively staining samples included colon, kidney, liver, myocardium, tonsil, bone marrow and stomach. Negative samples included cerebellum and spinal cord (Figure 3-14).

The reactivity of FPGS antibody, clone NN3.2, on a panel of normal and inflamed tissues is summarised in Table 3-3.

Table 3-3: Immunostaining for wild-type FPGS NN 3.2 on normal and inflamed tissues.

Tissue	Morphological Features	FPGS cytoplasmic staining intensity
Adrenal	Medulla Cortex Zona Granulosa	Strong Weak Negative
Inflamed appendix	Lamina Propria/Crypts Submucosa	Moderate Weak-Negative
Bowel, large	Brush Border/Crypts Smooth Muscle	Moderate-Strong Moderate
Bowel, small	Villi/Crypts Smooth Muscle	Moderate Weak-Negative
Brain, cerebellum	All elements	Negative
Cervix	Epithelium.Glands Endothelium	Weak-Negative Weak
Gall bladder	Submucosa Muscle Layers	Moderate-Weak Weak
Kidney	Glomeruli Convoluted tubules Kidney vasculature	Negative Weak Negative
Kidney	Glomeruli Convoluted tubules Kidney vasculature	Weak-Negative Moderate Weak
Liver	Hepatocytes/Parenchynal Cells Endothelium	Moderate-Weak Weak
Inflamed lung, peripheral	Alveolar Macrophages All elements	Moderate-Weak Negative
Muscle, skeletal	All elements	Negative
Myocardium	Muscle Endothelium	Strong-Moderate Weak
Ovary	Stroma/connective tissue Ovary vasculature	Weak Weak-Negative
Placenta (term)	Syncito/Cytotrophoblasts Mesenchymal cells Placental vasculature	Moderate-Strong Moderate Moderate
Inflamed skin	All elements	Moderate-Weak
Spinal cord	All elements	Negative
Testis	Seminiferous tubules Sertoli/Leydig Cells	Negative Weak
Inflamed tonsil	Follicles Epithelia	Strong Moderate-Weak
Ulcerative colitis	All elements	Moderate
Umbilical cord	All elements	Weak-Negative
Uterus (endometrium)	All elements	Moderate

Figure 3-14: FPGS normal panel. Cytoplasmic immunohistochemical staining for FPGS using clone NN 3.2 in paraffin embedded normal tissues: a) adrenal gland; strong reactivity in the medulla, weaker reactivity in the cortex and negativity in the zona granulosa (x20); b) gall bladder; moderate- weak reactivity in the submucosa and weak reactivity in the muscle layers (x10); c) kidney; moderate reactivity in the tubules, weak/negative reactivity in the glomeruli and weak reactivity in the vascular structures (x10); d) liver; moderate-weak reactivity in hepatocytes, parencymal cells and endothelium (x10); (e) myocardium; strong-moderate reactivity in muscle and weak reactivity in endothelium (x20); f) placenta; moderate-strong reactivity in trophoblast layers, moderate reactivity in vasculature and mesenchymal cells (x40); g) ileum; moderate reactivity in villi/crypts, weak reactivity in smooth muscle layers (x20); h) colon; moderate-strong reactivity in brush border/crypts, moderate reactivity in smooth muscle layers (x40).

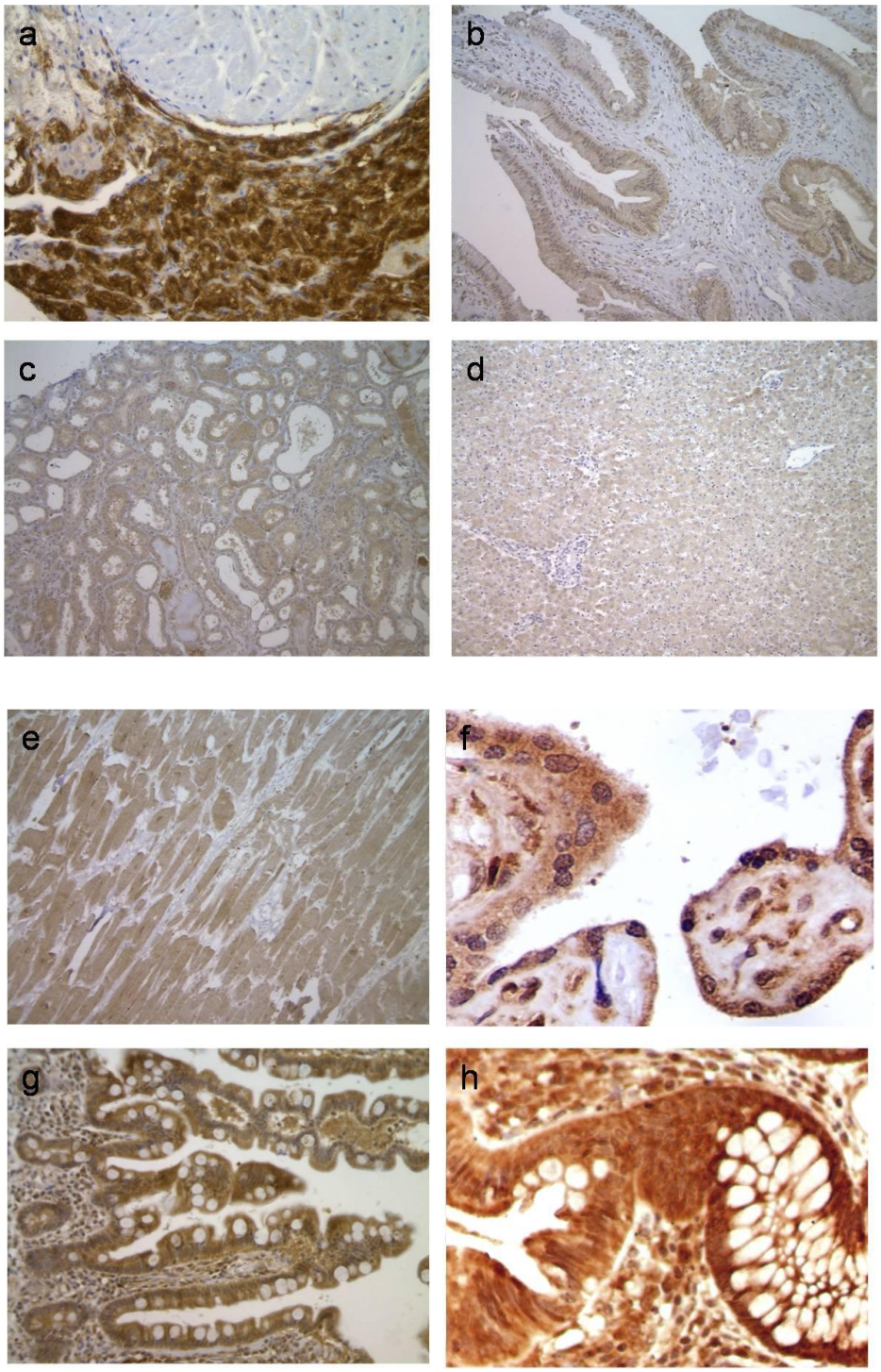

3.5.6. FPGS Expression in Benign and Malignant Tissues

The reactivity of the FPGS antibody, clone NN3.2, on a panel of formalin-fixed and paraffin-embedded tumour tissues samples is described in Table 3-4, this panel included tumour tissue microarrays (TMA's). The staining pattern of FPGS cytoplasmic positivity within each case was also heterogeneous. Strongly positive cytoplasmic staining for FPGS in tumour cells was noted in the majority of samples tested; lower staining intensity was also observed in adjacent normal tissue and mixed germ cell choriocarcinoma, fibrothecoma, gangliobeuroma and solitary fibrous tumour omentum (Figure 3-15).

Table 3-4: Immunostaining for FPGS on a range of benign and malignant tissues

Tissue	FPGS cytoplasmic staining intensity
Bone Marrow	Moderate
Bone Marrow	Moderate-Weak
GIST	Weak-Negative
Hairy Cell Leukaemia	Negative
B-cell Lymphoma	Moderate (cell aggregates)- Weak
B-cell Lymphoma	Strong (cell aggregates)
Liver	Moderate-Weak
Breast carcinoma	Moderate-Weak
Melanoma	Strong-Weak
Melanoma	Weak
Mesothelioma	Strong-Moderate (n=2)
Mesothelioma	Moderate
Mesothelioma	Weak-Negative
Breast Carcinoma	Moderate-Weak
Breast Carcinoma	Strong-Weak
Ovary Serous carcinoma	Weak-Negative (n=3)
Ovary Serous carcinoma	Weak-Moderate
Ovary Serous carcinoma	Moderate-Negative (n=2)
Ovary Adenocarcinoma	Weak-Negative
Ovary Adenocarcinoma	Moderate-Weak (n=2)
Ovary Adenocarcinoma	Moderate
Ovary Adenocarcinoma	Strong (n=2)
Ovary Adenocarcinoma	Strong-Moderate (n=2)
Colon Adenocarcinoma	Strong-Moderate
Colon Adenocarcinoma	Weak-Negative
Cholangiocarcinoma	Strong-Moderate
Placenta A (term)	Weak-Negative
Placenta B (mid-term)	Weak-Negative
Placenta	Moderate
Hepatoma	Strong-Moderate
Fibrothecoma	Negative
Ovary Clear cell	Strong-Weak
Ovary thecoma	Moderate
Ovary granulosa	Weak-Negative
Gangliobeuroma	Negative
Squamous Carcinoma of Cervix	Strong
Bladder transitional cell carcinoma	Strong
Bladder Transitional Cell Carcinoma	Weak-Negative
Pancreatic Adenocarcinoma	Negative
Gastric adenocarcinoma	Weak
Renal cell carcinoma	Negative
Renal cell carcinoma	Weak-Negative
Prostate adenocarcinoma	Moderate-Weak
Prostate adenocarcinoma	Strong-Moderate
Thyroid papillary carcinoma	Strong-Moderate
Thyroid follicular adenocarcinoma	Moderate
Liver cell adenocarcinoma	Moderate-Weak
Adrenal Oncocytoma	Moderate
Desmoplastic SRCT	Strong-Moderate
Ewings Sarcoma	Weak-Negative
Basal Cell carcinoma	Strong

Figure 3-15: FPGS tumour panel. Cytoplasmic immunohistochemical staining for FPGS using clone NN3.2 in a selection of paraffin embedded benign and tumour tissues) a) Colon adenocarcinoma; strong reactivity in tumour (x20); b) colon adenocarcinoma; strong reactivity in tumour (x40) c) B-cell lymphoma; moderate reactivity in tumour cell aggregates (x20); d) Bone marrow; moderate reactivity in cell aggregates (x20); e) breast carcinoma; moderate-weak reactivity in tumour (x10); f) mesothelioma; strong-moderate reactivity in tumour (x10); g) ovarian adenocarcinoma moderate reactivity in tumnour islands (x10); h) ovarian adenocarcinoma; strong-moderate reactivity in tumour islands (x10).

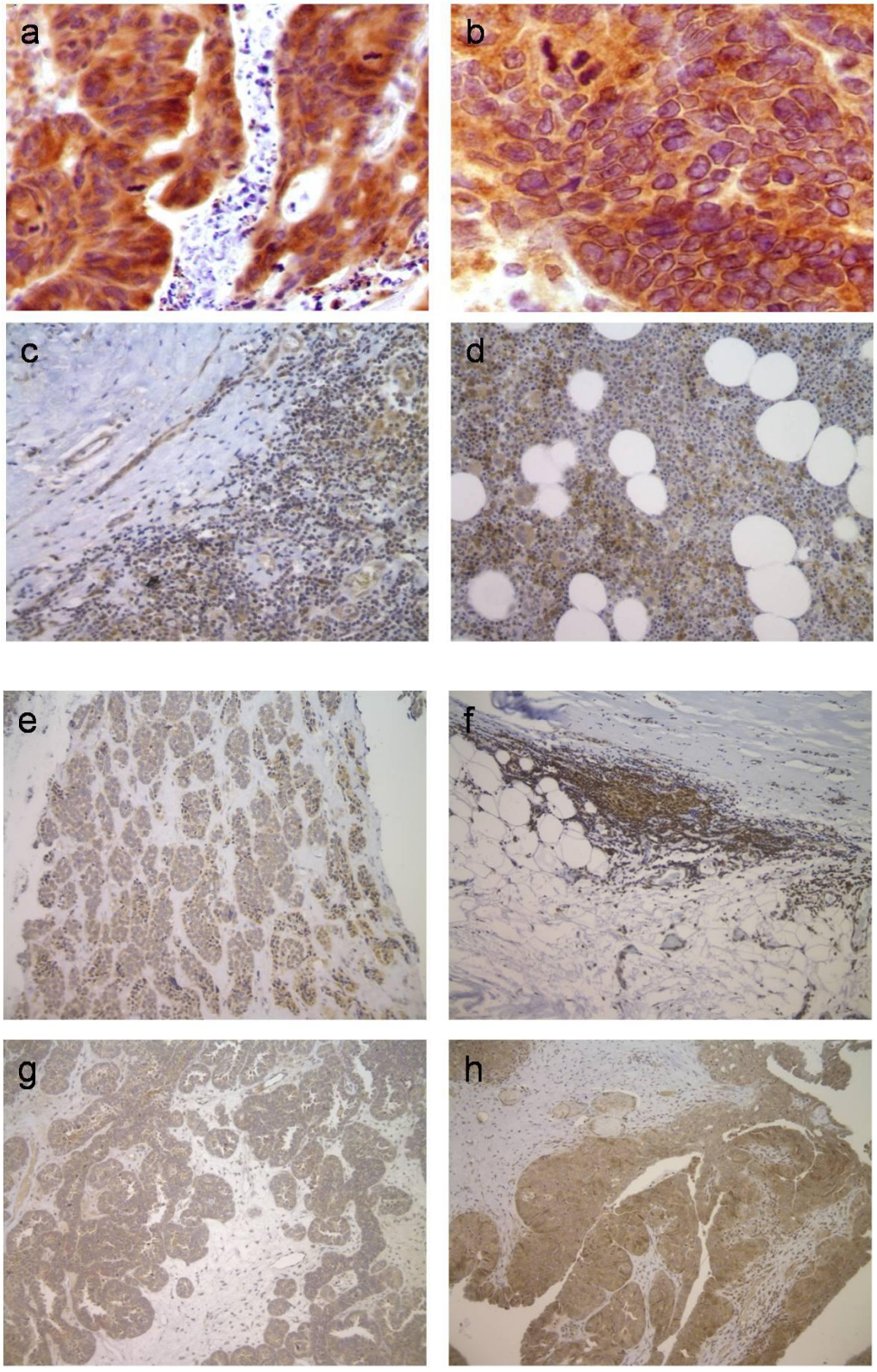

3.5.7. FPGS Further Characterisation

The FPGS antibody was found to be suitable for use with both TBS and PBS buffers, it was also found to be suitable for use with both the ABC, Novolink™ polymer kit and a Bond Max™ automated immunostainer (Leica Biosystems, UK). Tris-EDTA was confirmed to be the best method of unmasking as Citrate produced too little unmasking, as did proteinase K. No unmasking was found to produce no staining at all (Figure 3-16). The antibody isotype was determined to be Ig G1 κ.

Figure 3-16: FPGS pre-treatment evaluation. Immunohistochemical staining for FPGS using clone NN3.2 in a selection of paraffin embedded ovarian adenocarcimoma samples with different pretreatments. Citrate (Cit) a,d&g; Tris EDTA (TE) b,e&h; No pre-treatment (NP) c,f&i. Note the lack of staining in the NP samples, weak staining in the CIT samples and optimal staining seen in the TE treated samples.

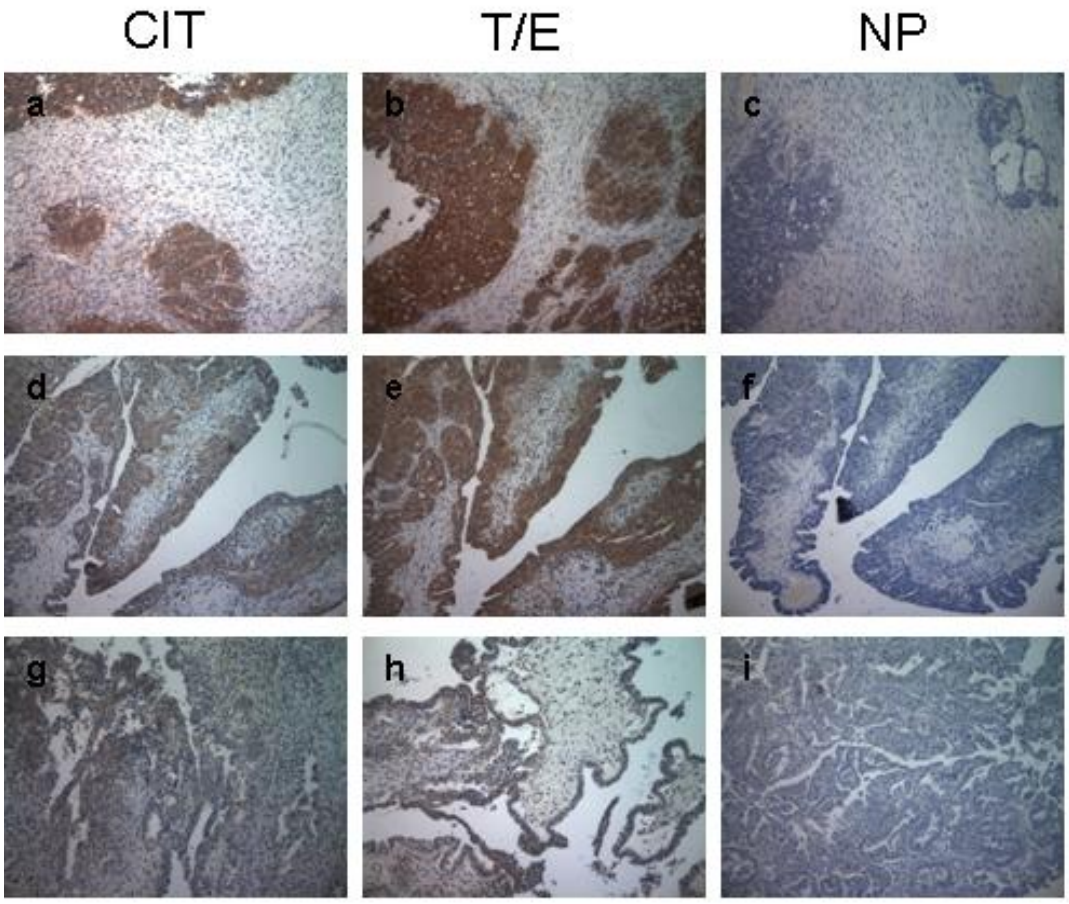

3.5.8. FPGS Epitope Mapping

Figure 3-17: FPGS epitope mapping. FPGS membrane (top) and the same membrane stained with Ponceau-S (bottom) to observe the location on the peptide array recognised by clone NN 3.2.

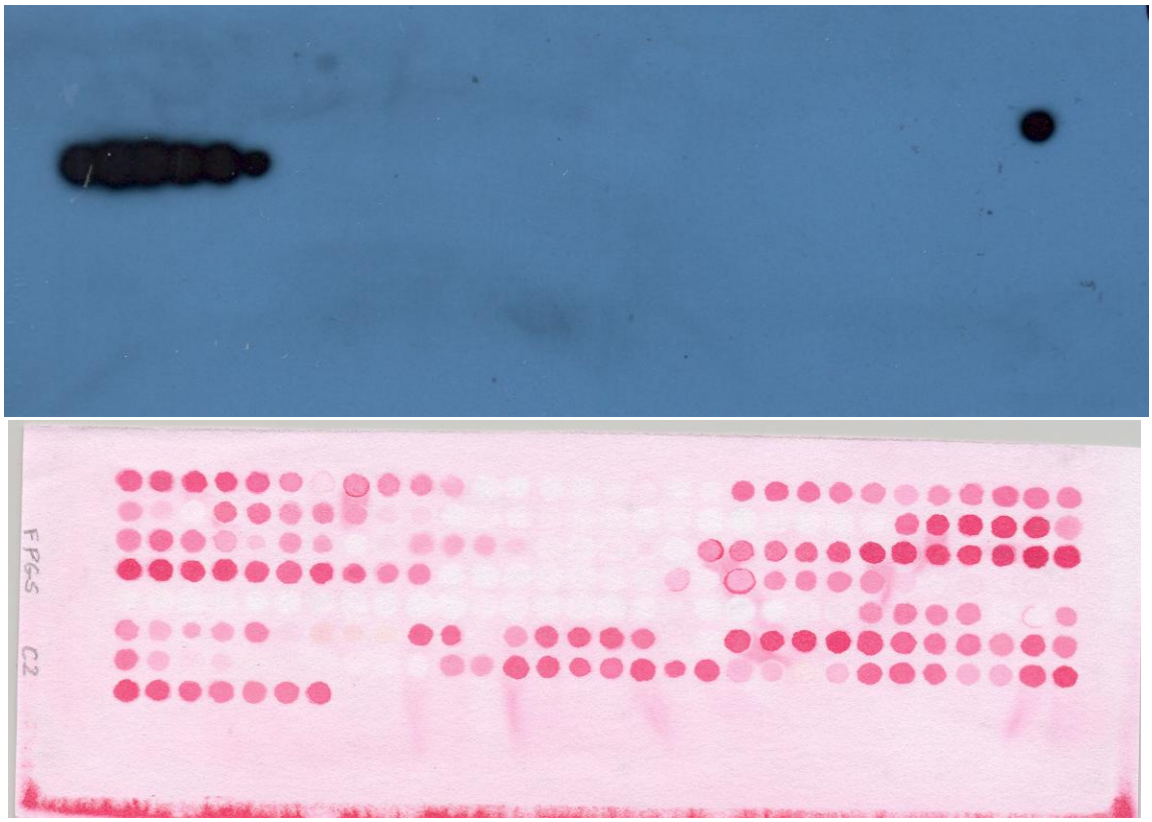

Seven peptides reacted with the NN 3.2 antibody, corresponding to the following peptides on the array as determined from the data sheet provided with the membranes. One peptide was positive (N29), followed by two negative peptides (N30, O1), the final six peptides showing reactivity were consecutive (O2-O8) (Figure 3-18).

Figure 3-18: FPGS epitope. Peptide sequences corresponding to the spots showing reactivity with the FPGS NN 3.2 antibody. Positive sequences are shown in blue and negative adjacent peptides in red. Most likely epitope is shown in green.

N29	E-K-I-A-W-Q-K-G-G-I-F-K
N30	K-I-A-W-Q-K-G-G-I-F-K-Q
O 1	I-A-W-Q-K-G-G-I-F-K-Q-G
O 2	A-W-Q-K-G-G-I-F-K-Q-G-V
O 3	W-Q-K-G-G-I-F-K-Q-G-V-P
O 4	Q-K-G-G-I-F-K-Q-G-V-P-A
O 5	K-G-G-I-F-K-Q-G-V-P-A-F
O 6	G-G-I-F-K-Q-G-V-P-A-F-T
O 7	G-I-F-K-Q-G-V-P-A-F-T-V
O 8	I-F-K-Q-G-V-P-A-F-T-V-L
O 9	F-K-Q-G-V-P-A-F-T-V-L-Q

3.5.8.1. Anti FR-α Antibody Generation

An antibody to FR-α was successfully generated from mouse BN 3.2, surprisingly resulting from the FR-α pET 41 soluble recombinant protein construct which was found to contain large amounts of contaminating 60kDa protein. All 14 other fusions resulted in a weak response or the antibodies generated were found to be cross reactive. The initial five fusions generated a large number of positive hybridomas, however they were screened using protein containing the contaminant and it is likely that all hybridomas were recognising this rather than the target. Later fusions resulted in few positive wells when screened with the new FR-α pET32 refolded protein, despite the polyclonal bleeds appearing to recognise a band at 40 kDa when blotted. The FR-α 3 mice fusions were also unsuccessful with few positives resulting from fusions. The fusion which generated the successful antibody was the last of the FR-α pET41 soluble fusions performed and screened using the FR-α pET32 refolded protein, as at this stage the new protein had been generated. This fusion resulted in only one positive hybridoma from beginning to end. This is highly unusual as, typically fusions result in 50-100 positive hybridomas at fusion screen. Attempts to generate other positive clones were made, however no more surviving positive clones could be generated. Characteristic patterns of heterogeneous cytoplasmic and membrane immunostaining on sections of paraffin

wax embedded ovarian adenocarcinoma were observed during the development process (Figure 3-19).

Figure 3-19: FR-α bleed evaluation. Photograph of FR-α pET 41 NN polyclonal bleed on normal colon (top) and ovarian adenocarcinoma (bottom) x20. Note the membrane/ cytoplasmic staining and the difference between the staining seen with this bleed compared with the cross reactive bleed shown previously (Figure 3-8).

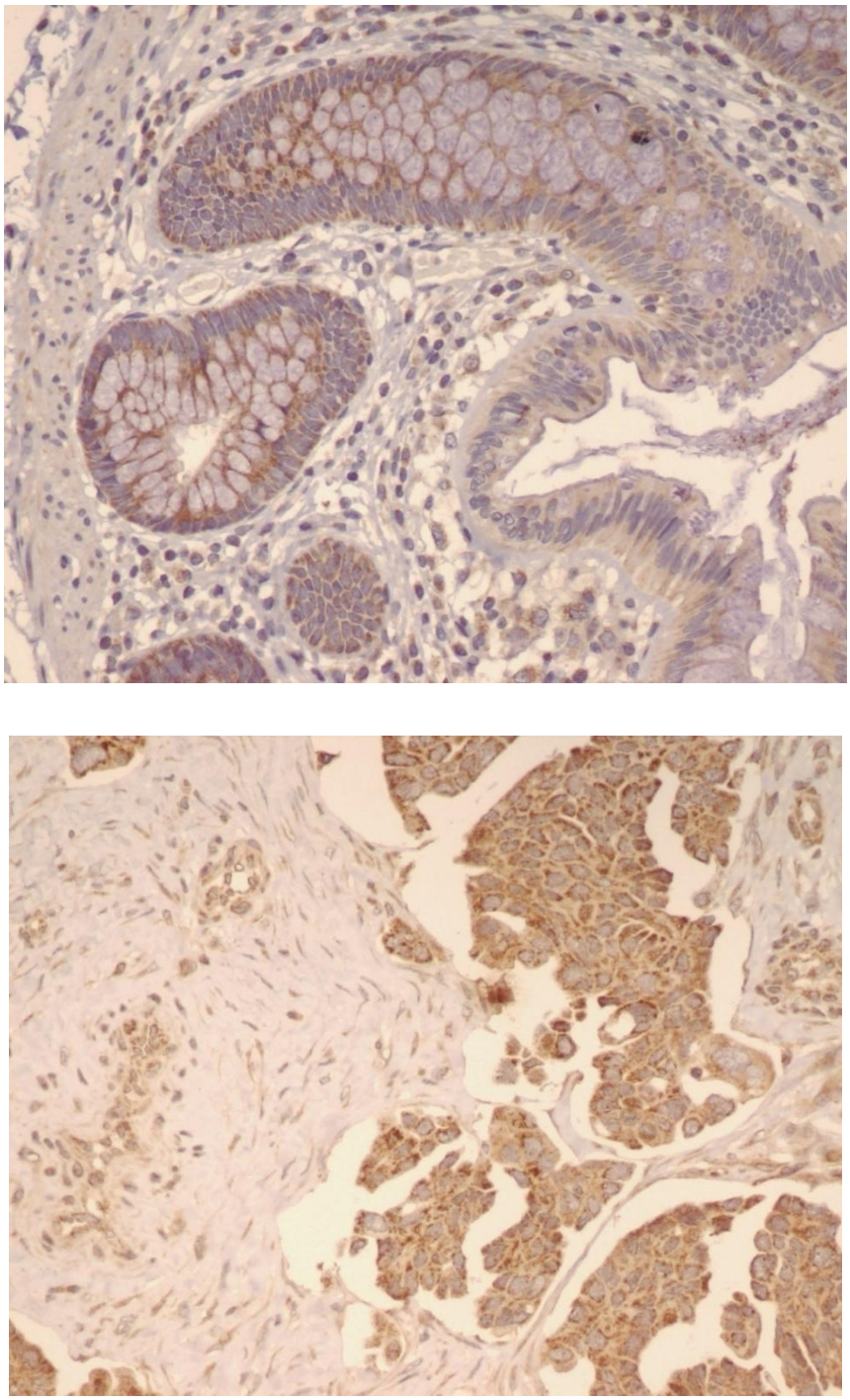

3.5.8.2. FR-α Expression via Western Blot Analysis

The selected FR-α antibodies were tested for their ability to react specifically with the human FR-α protein in a large panel of various different cell lines by WB as shown in figures 3-20, 3-21 and 3-22. The FR-α antibody produced from clone NN3.2 detected a single band of approximately 40 kDa in a limited number of cell lines tested (n=28) with varying levels of expression observed. An antibody to α -tubulin was used to correct for variations in loading between samples.

3.5.8.3. FR-α Extended Panel

Figure 3-20: FR-α extended panel WB. Representative WB (n=3) showing detection of FR-α WT protein by WB on a panel of cell lines via use of the generated FR-α BN3.2 antibody. An antibody to α-tubulin (56kDa) was used as a loading control to correct for variations in loading between samples.

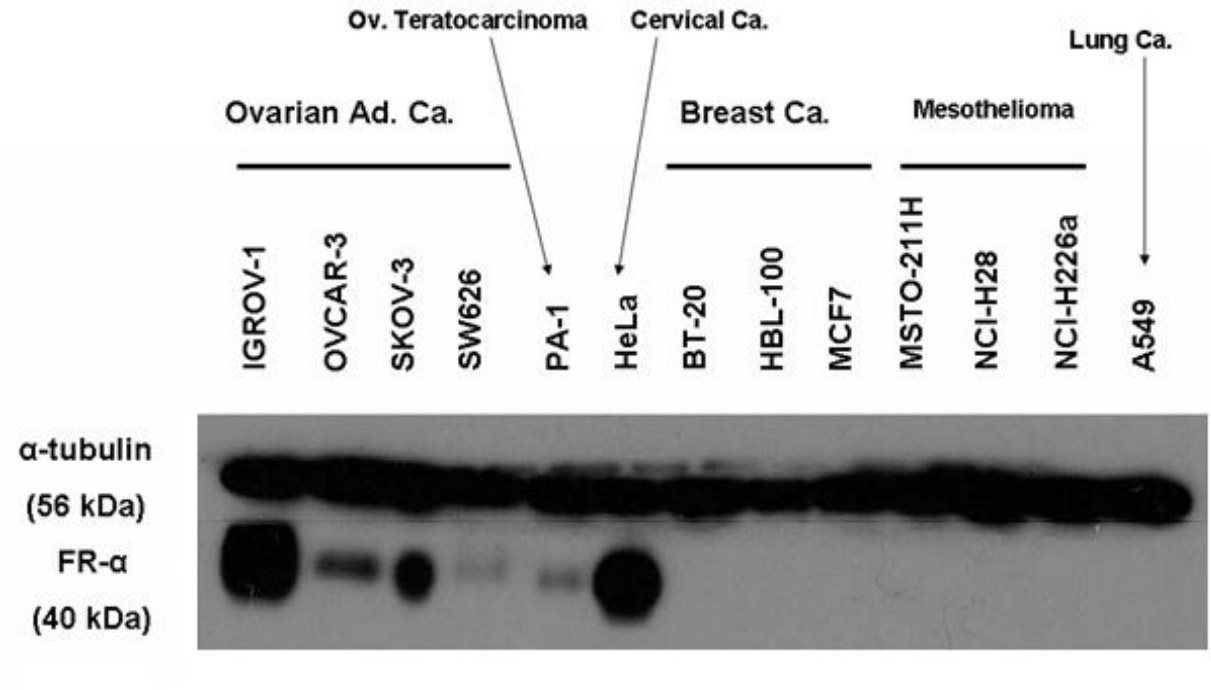

Varied expression was observed in the ovarian tumour samples ranging from strong (IGROV-1) to weak (SW626, PA-1). Strong expression was also observed in the cervical carcinoma cell line HeLa. No expression was observed in any of the breast carcinoma, mesothelioma or lung carcinoma samples tested. This image shows the overexposure as the SW626 and PA1 lanes were not demonstrated with lower exposures.

Figure 3-21: FR-α extended panel (2) WB. Representative WB (n=3) showing detection of FR-α WT protein by WB on a panel of cell lines via use of the generated FR-α BN3.2 antibody. An antibody to α-tubulin (56kDa) was used as a loading control to correct for variations in loading between samples.

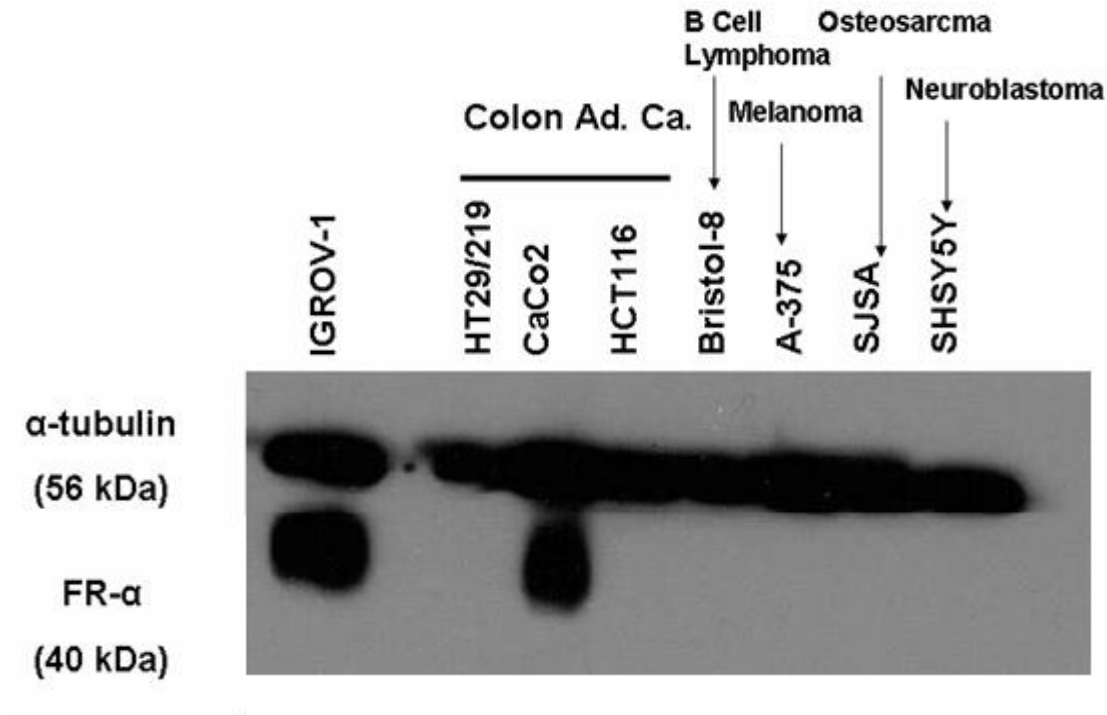

Expression was observed in one colon carcinoma cell line (CaCo2), and the ovarian carcinoma positive control IGROV-1. No expression was observed in two other ovarian adenocarcinoma samples, B-cell lymphoma, melanoma, osteosarcoma or neuroblastoma samples tested.

3.5.8.4. FR-α Leukaemia Panel

Figure 3-22: FR-α leukaemia panel WB. Representative WB (n=3) showing detection of FR-α WT protein by WB on a panel of cell lines via use of the generated FR-α BN3.2 antibody. An antibody to α-tubulin (56kDa) was used as a loading control to correct for variations in loading between samples.

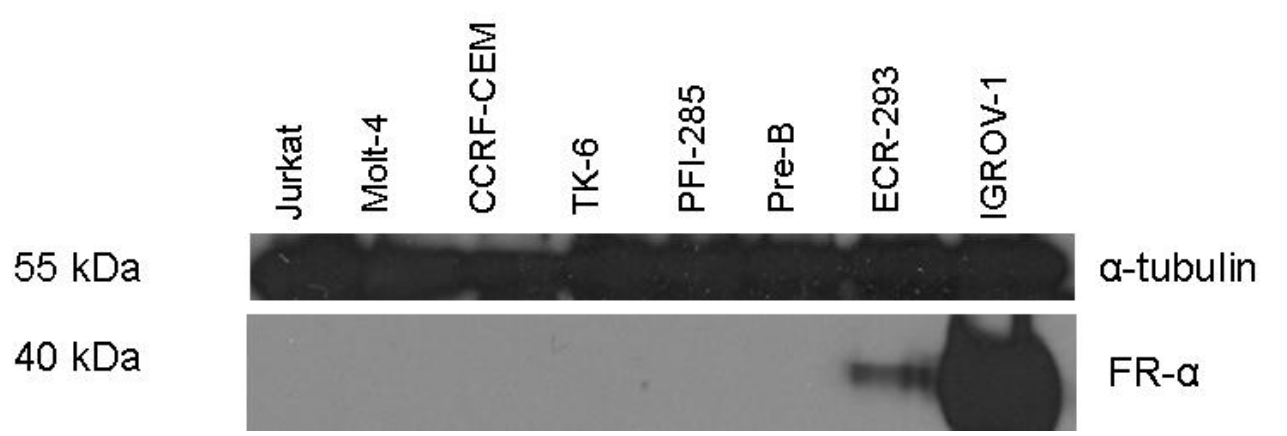

Expression was observed only in the ovarian carcinoma IGROV-1 positive control and ECR-293 embryonic kidney sample. No FR-α expression was seen in any of the leukaemia samples tested. Again the overexposure is shown to illustrate the reactivity seen in the ECR 293 which is not visible in lower exposures.

3.5.9. FR-α Expression in Normal and Inflamed Tissues

Immunoreactivity with the BN3.2 FR-α MAb was detected in a limited number of normal and inflamed human tissues. Syncitial trophoblasts of the placenta, the single layer of epithelium lining the ovary follicle and proximal kidney tubules were positive and the remaining samples were negative (Figure 3-23). The reactivity of FR-α antibody, clone BN 3.2, on a panel of normal and inflamed tissues is summarised below.

Table 3-5: Immunostaining for wild-type FR-α BN 3.2 on normal and inflamed tissues.

Tissue	Morphological Features	FR-α membrane/cytoplasmic staining intensity
Adrenal	All elements	Negative
Inflamed appendix	All elements	Negative
Bowel, large	All elements	Negative
Bowel, small	All elements	Negative
Brain, cerebellum	All elements	Negative
Cervix	All elements	Negative
Gall bladder	All elements	Negative
Kidney	Glomeruli Convoluted tubules Kidney vasculature	Negative Weak Negative
Kidney	Glomeruli Convoluted tubules Kidney vasculature	Negative Moderate Negative
Liver	All elements	Negative
Inflamed lung, peripheral	All elements	Negative
Muscle, skeletal	All elements	Negative
Myocardium	All elements	Negative
Ovary	Stroma/connective tissue Inner follicular epithelia Peritoneal surface epithelia Ovary vasculature	Negative Moderate-Strong Negative Negative
Placenta (term)	Syncito/Cytotrophoblasts Mesenchymal cells Placental vasculature	Moderate-Strong Negative Negative
Inflamed skin	All elements	Negative
Spinal cord	All elements	Negative
Testis	All elements	Negative
Inflamed tonsil	All elements	Negative
Ulcerative colitis	All elements	Negative
Umbilical cord	All elements	Negative
Uterus (endometrium)	All elements	Negative

Figure 3-23: FR-α normal panel. Membrane immunohistochemical staining for FR-α using clone BN 3.2 in paraffin embedded normal tissues: a) ovary (inclusion cyst); strong reactivity in debri contained within cyst and epithelia lining it (x4); b) strong reactivity in epithelia lining ovarian inclusion cyst (x10); c) kidney; weak reactivity in tubules (x20); d) placenta; strong reactivity in trophoblast layers (x20).

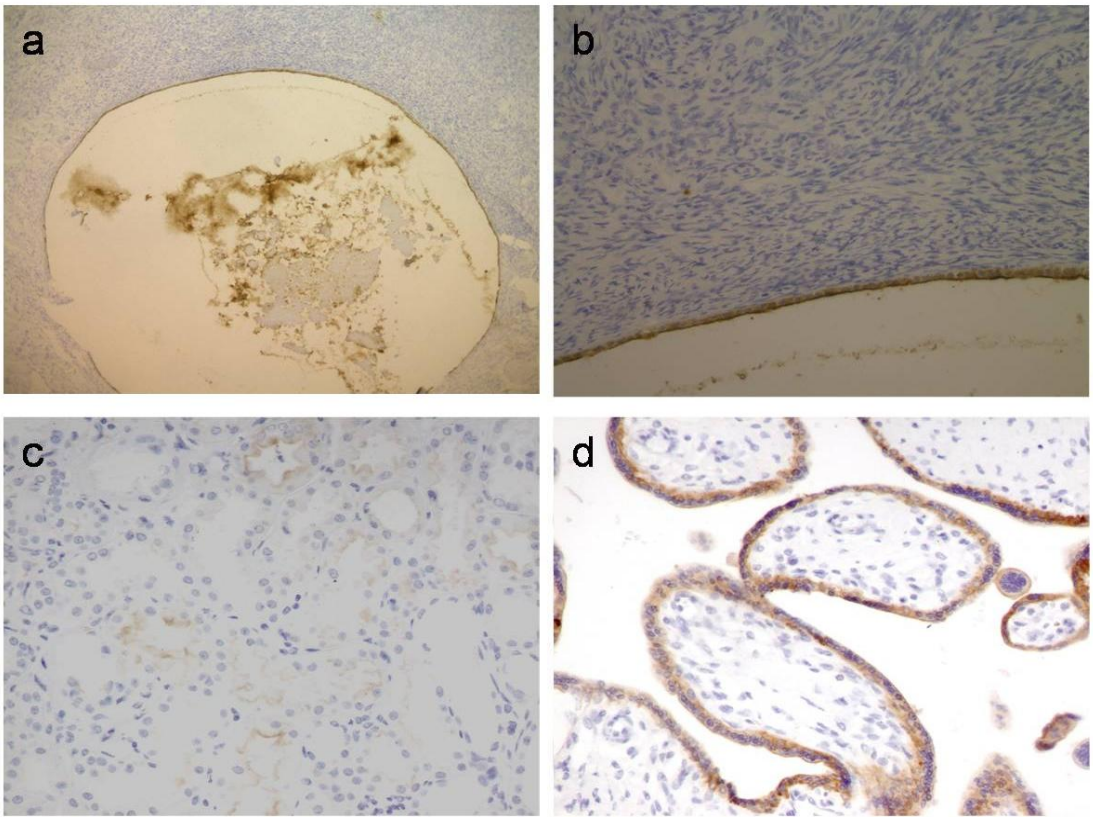

3.5.10. FR-α Expression in Benign and Malignant Tissues

The reactivity of the FR-α antibody, clone BN3.2, on a panel of formalin-fixed and paraffin-embedded tumour tissues samples is detailed in Table 3-5. The staining pattern of FR-α cytoplasmic/membrane positivity within each case was also heterogeneous. Strongly positive membrane/cytoplasmic staining for FR-α in tumour cells was noted in the majority of ovarian adenocarcinomas; low staining intensity was observed in endometrial adenocarcinoma, lung carcinoma, cholangiocarcinoma, thyroid papillary carcinoma, ovarian thecoma and granulosa and, less frequently in breast carcinomas (Figure 3-24).

Table 3-6: Immunostaining for FR-α on a range of benign and malignant tissues

Tissue	FR-α membrane/cytoplasmic staining intensity
Malignant melanoma	Negative (n=4)
Endometrial adenocarcinoma	Weak (tumour cells)
Pancreatic adenocarcinoma	Weak (normal ducts)
Lung carcinoma	Weak-Moderate (dysplastic epithelia/tumour)
Lung Squamous cell carcinoma	Weak (tumour)
Mesothelioma	Negative (n=6)
Breast sarcoma	Negative
Leiomyosarcoma	Negative
Ewings sarcoma	Negative
Rhabdomyosarcoma	Negative
Granulocytic sarcoma	Negative
Anaplastic lymphoma	Negative
Hodgkins lmphoma	Negative
Breast Carcinoma	Weak (tumour)
Breast Carcinoma	Negative (n=6)
Breast Carcinoma	Weak (tumour)
Ovary Serous carcinoma	Strong
Ovary Serous carcinoma	Moderate-Strong (n=4)
Ovary Serous carcinoma	Weak
Ovary Adenocarcinoma	Strong (n=4)
Ovary Adenocarcinoma	Weak
Ovary Adenocarcinoma	Weak-Moderate
Ovary Adenocarcinoma	Moderate
Ovary Adenocarcinoma	Moderate/strong
Ovary Clear cell	Negative
Ovary thecoma	Weak (tumour)
Ovary granulosa	Strong (tumour)
Cholangiocarcinoma	Weak (tumour)
GIST	Negative
Gastric adenocarcinoma	Negative
Bladder transitional cell carcinoma	Negative
Renal cell carcinoma	Negative (n=2)
Thyroid papillary carcinoma	Weak (inner luminal surfaces)
Thyroid follicular adenocarcinoma	Negative
Hepatoma	Negative
Liver cell adenocarcinoma	Negative
Prostate adenocarcinoma	Negative (n=2)

Figure 3-24: FR-α tumour panel (1). Membrane immunohistochemical staining for FR-α using clone BN 3.2 in paraffin embedded ovarian tumour tissues: a) adenocarcinoma of ovary 3c; strong membrane/cytoplasmic expression in tumour and absence of expression in adjacent normal stroma (x40); b) poorly differentiated adenocarcinoma of the ovary 3c (x20); c) serous carcinoma of ovary 3b; increased FR-alpha expression on inner luminal surfaces (x20); d) serous carcinoma of ovary 3c; strong membrane/cytoplasmic expression in tumour and no expression in normal surrounding stroma (x20); (e) poorly differentiated adenocarcinoma of ovary 3c (x20); f) serous carcinoma of ovary 3c (x40); g) poorly differentiated adenocarcinoma of the ovary 3c (x40); h) poorly differentiated adenocarcinoma of ovary 3c (x40). The majority of other tumours showed weak expression, thus ovarian adenocarcinomas were selected for use in the tumour panel.

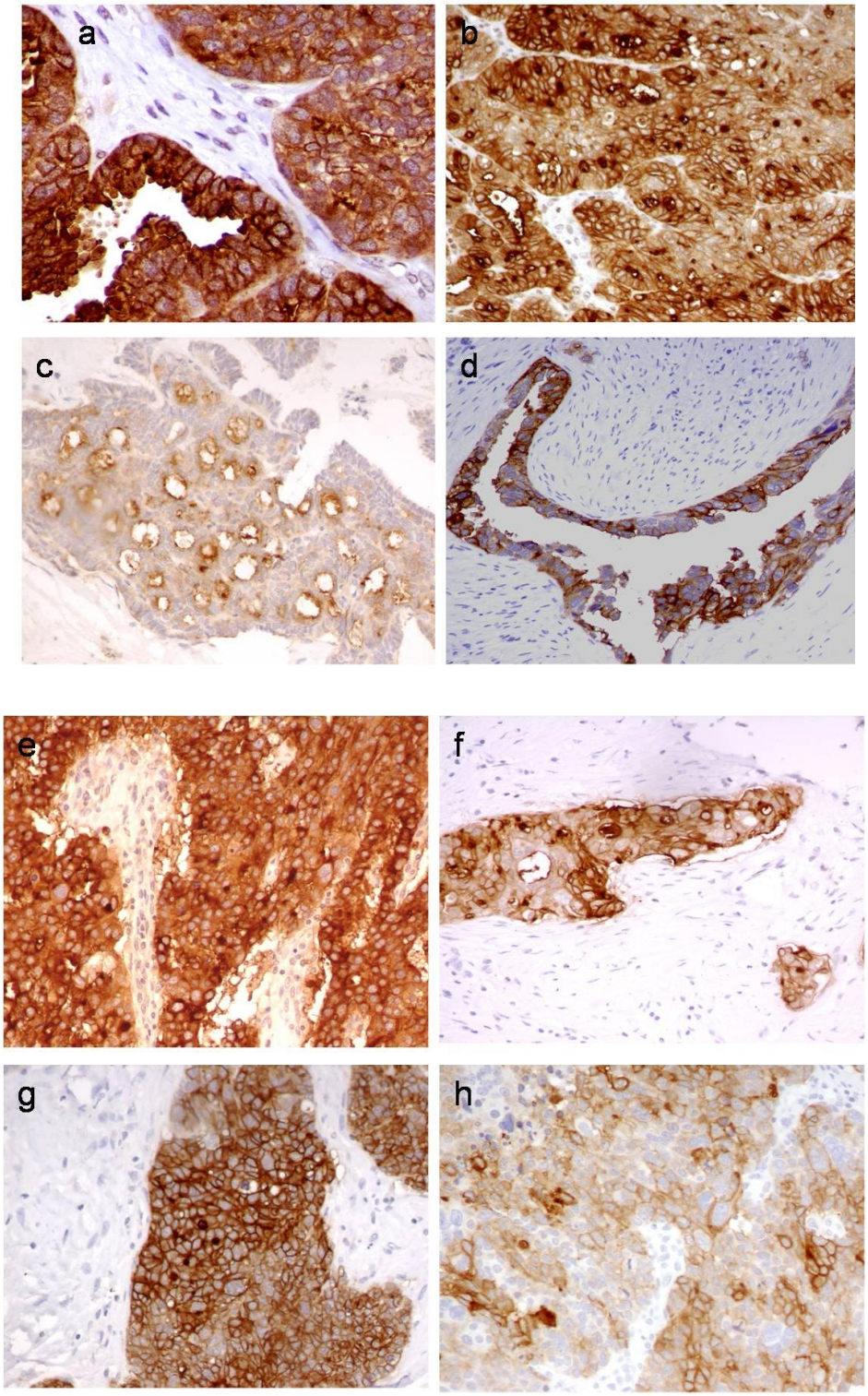

3.5.11. FR-α Further Characterisation

The FR-α antibody was found to suitable for use with both TBS and PBS buffers, it was also found to be suitable for use with both the ABC, Novolink™ polymer kit and the Bond Max immunostainer. Citrate was confirmed to be the best method of unmasking as although very similar in terms of staining intensity, Tris-EDTA gave cross reaction in areas of cell necrosis, however, both methods could be deemed suitable. Proteinase K failed to produce a signal. No unmasking was found to produce no signal in ovarian adenocarcinomas previously positive (Figure 3-25). The antibody isotype was determined to be Ig G1 κ (see 3.4.3 for method).

Figure 3-25: FR-α pre-treatment selection. Immunohistochemical staining for FR-α using clone BN3.2 in a selection of paraffin embedded ovarian adenocarcimoma samples with different pretreatments. Citrate (Cit) a,d&g (x40); Tris EDTA (TE) b,e&h; No pre-treatment (NP) c,f&i. Note the lack of staining in the NP samples, optimal staining in the CIT samples and staining seen in the TE treated samples with increased background.

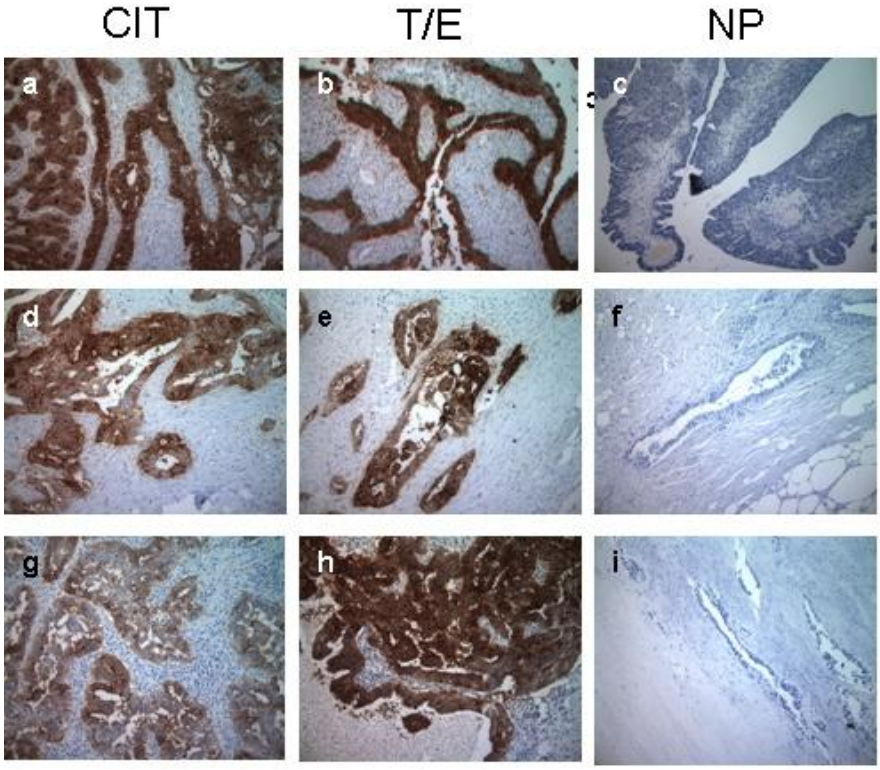

3.5.12. FR-α Epitope Mapping

Figure 3-26: FR-α epitope mapping. FR-α membrane (top) and the same membrane stained with ponceau-S (bottom) to observe the location on the peptide array recognised by clone BN 3.2.

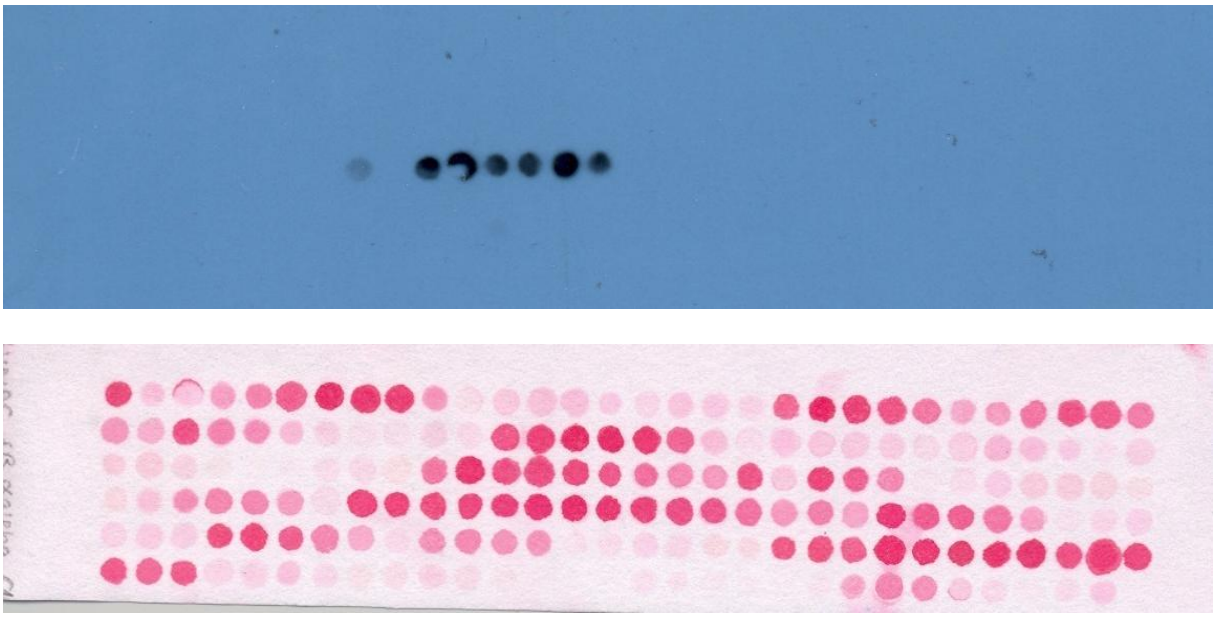

Seven peptides in total were highlighted by the BN 3.2 antibody, one peptide (A6) showed weak reactivity, followed by one negative peptide (A7), followed by six consecutive positive peptides (A8-A13) (Figure 3-27).

Figure 3-27: FR-α epitope. Peptide sequences corresponding to the spots showing reactivity with the FR-α BN 3.2 antibody. Positive sequences are shown in blue and negative adjacent peptides in red, epitope region is shown in green. Most likely epitope is shown in green.

A 5	P-E-D-K-L-H-E-Q-C-R-P-W
A 6	E-D-K-L-H-E-Q-C-R-P-W-R
A 7	D-K-L-H-E-Q-C-R-P-W-R-K
A 8	K-L-H-E-Q-C-R-P-W-R-K-N
A 9	L-H-E-Q-C-R-P-W-R-K-N-A
A10	H-E-Q-C-R-P-W-R-K-N-A-C
A11	E-Q-C-R-P-W-R-K-N-A-C-C
A12	Q-C-R-P-W-R-K-N-A-C-C-S
A13	C-R-P-W-R-K-N-A-C-C-S-T
A14	R-P-W-R-K-N-A-C-C-S-T-N

3.5.13. mOV 18 Epitope Mapping

Figure 3-28: mOV18 epitope mapping. FR-α membrane (top) and the same membrane stained with ponceau-S (bottom) to observe the location on the peptide array recognised by mOV18. This was performed to compare epitope recognition between the BN3.2 antibody and the other commercially available antibodies suitable for use on frozen tissue.

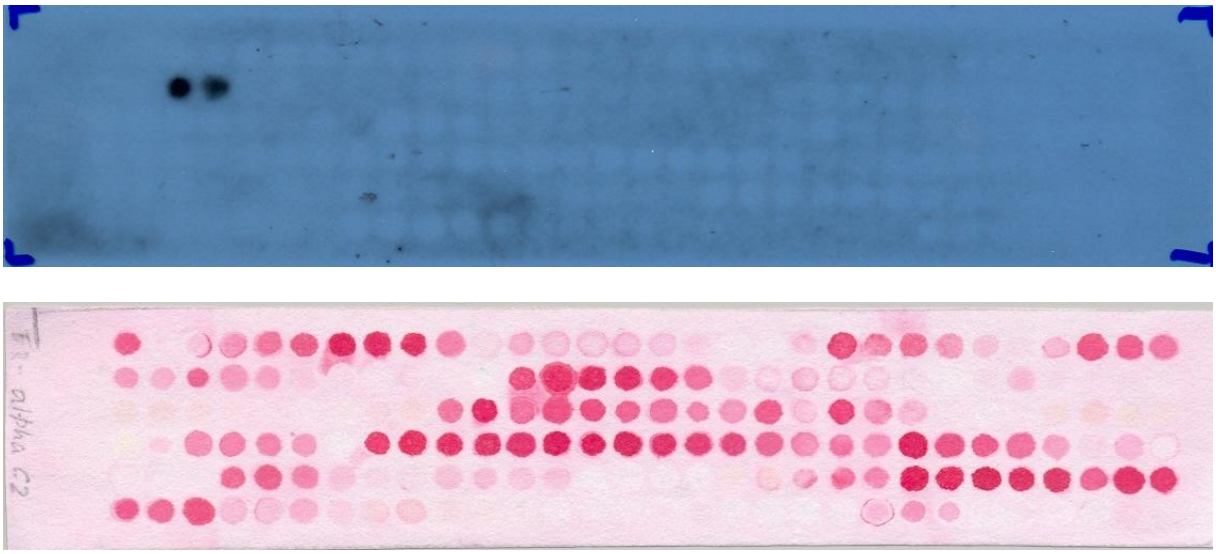

Only two peptides showed any reactivity with the mOV18 antibody (I3 & I4), these were consecutive (Figure 3-29).

Figure 3-29: mOV18 epitope. Peptide sequences corresponding to the spots showing reactivity with the mOV18 antibody. Positive sequences are shown in blue and negative adjacent peptides in red.

I 2	K-D-V-S-Y-L-Y-R-F-N-W-N
I 3	D-V-S-Y-L-Y-R-F-N-W-N-H
I 4	V-S-Y-L-Y-R-F-N-W-N-H-C
I 5	S-Y-L-Y-R-F-N-W-N-H-C-G

3.5.14. LK26 Epitope mapping

Figure 3-30: LK26 epitope mapping. FR-α membrane (top) and the same membrane stained with ponceau-S (bottom) to observe the location on the peptide array recognised by LK26.

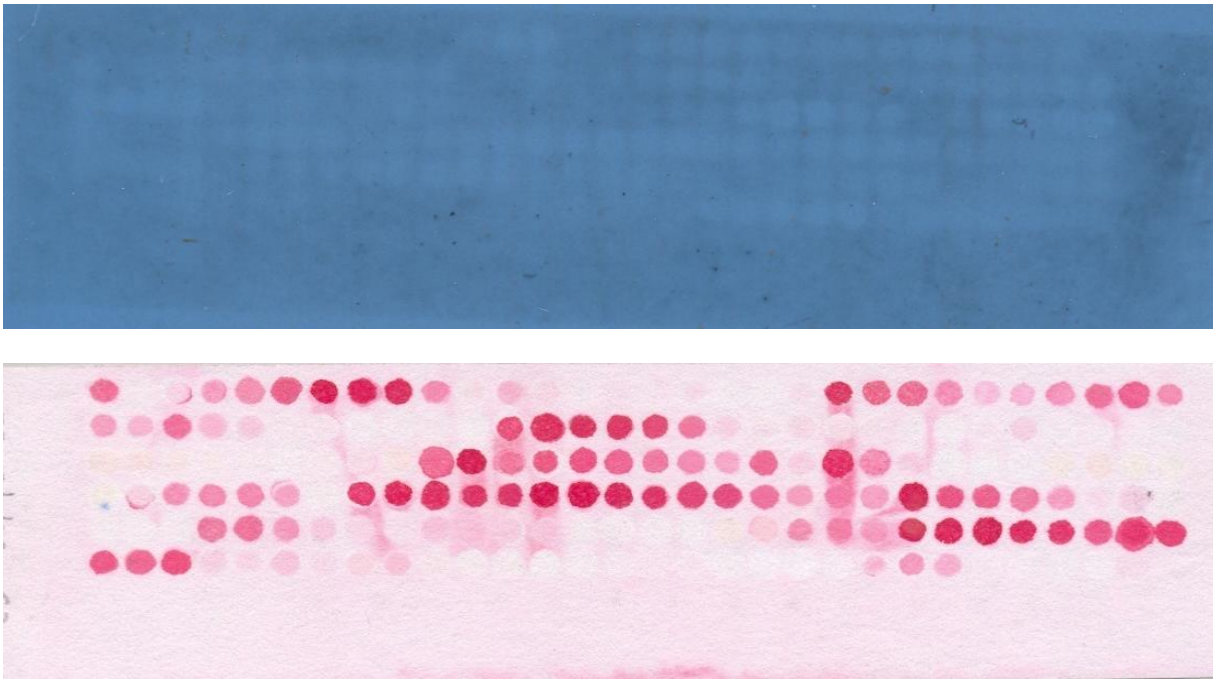

No peptides in the FR-α target sequence selected were found to react with the LK26 antibody.

3.6. Discussion

3.6.1. FPGS Antibody Development

A monoclonal antibody for the detection of FPGS in formalin-fixed, paraffin embedded tissues has been developed using established hybridoma technology techniques at Novocastra laboratories. Clone NN3.2 can also be used routinely in IHC using both ABC and the more sensitive Novolink Polymer kit. In addition it is also suitable for use in WB and ELISA. Its application for use on paraffin embedded samples enables expression profiles of various tissues to be evaluated with ease. It has also been characterised via WB analysis on a large panel of cell lysates from various tumour types. A large panel of cell lines (n=27) was used in order to fully characterise the expression of this protein and to determine specificity as there was little available data to compare it to. A single, 60kDa band was observed in the samples tested.

3.6.1.1. FPGS WB Analysis

The FPGS antibody was found to be highly specific and was found to produce a single, 60 kDa band on the extended panel. 27 cell lysates in total were tested and all samples showed some degree of positivity, ranging from strong to very weak.

FPGS mRNA expression in the ovarian cancer cell lines OVCAR3, SKOV 3 and IGROV-1, the mesothelioma cell line NCI-H226a, breast cancer cell line MCF-7 (Figure 3-11), the colon cancer cell lines HCT116 and HT29 (Figure 3-12) and the human T-cell ALL cell lines CCRF-CEM and MOLT-4 (Figure 3-13) have been previously reported and are consistent with the data seen in this study (Ross et al., 2000). Similarly, low mRNA expression in the lung carcinoma cell line A-549 has also been reported which is also consistent with the results seen as this cell line contained a low level of FPGS expression relative to the other cell lines tested (Ross et al., 2000).

Strongest expression was observed in the three MPM (Figure 3-11), colon adenocarcinoma (Figure 3-12), leukaemia and B-cell lymphoma samples tested (Figure 3-13). The findings for the leukaemia samples are supported by the observation that mRNA transcript levels have been found to be high in B-lineage leukaemias (Freemantle & Moran, 1997). A polyclonal antibody has also been used to detect the presence of FPGS in CCRF-CEM leukaemia cells and was found to specifically recognise distinct immunoreactive bands at 60 kDa via WB

analysis, further supporting the data seen in these validation experiments (Mc Guire, Russell, & Balinska, 2000). Stronger expression in Pre-B cells and lower expression in CCRF-CEM cells (Figure 3-13) was also observed and this finding is consistent with two studies assessing FPGS expression via gene reporter assays in B and T lineage leukaemia cells (Galpin et al., 1997; Leclerec, Leclerec, Kinser, & Barredo, 2006). Knowledge of lineage specific expression may assist in the predictive value of the antibodies as determinants of response to antifolates, particularly MTX which is commonly used in leukaemia patients. This may also be of value for pemetrexed as recent studies have indicated that this drug may be an effective antimyeloma agent (Ramirez, Ocio, San Miguel, & Pandiella, 2007). Studies have also noted high FPGS gene expression levels in colorectal tumour biopsies which supports the results seen by these WB studies, high FPGS expression in such tumours may explain the activity of raltitrexed in colorectal malignancies (Odin et al., 2003). The high expression of FPGS in the MPM samples tested (Figure 3-11) may explain the reason for the effectiveness of Pemetrexed in MPM, given that no detectable FR-α has yet been observed. This may offer a potential alternative determinant of response to pemetrexed, although only three samples were tested which is insufficient to draw any conclusion; further WB testing to assess FPGS expression in MPM may be valuable. Increased expression of FPGS activity in model cells has been found to lead to increased sensitivity to antifolate drugs whereas decreased FPGS activity has been shown to be a mechanism of resistance to such drugs in both model cells and clinical specimens (Chen et al., 1996). Mc Guire *et al* assessed FPGS expression in antifolate sensitive and resistant cell lines via the use of a rabbit polyclonal antibody, FPGS levels were found to be lower in the resistant cell lines, concluding that decreased FPGS activity is a mechanism of resistance to antifolates, particularly MTX (Mc Guire & Russell, 1998). FPGS expression may be key in the determination of response to some antifolates, particularly raltitrexed and pemetrexed; the route of entry of the drug into the cell has not been found to affect the rate of polyglutamation. Rates of polyglutamation, particularly MTX have not been found to be significantly different whether cells entered via the RFC or FR-α (Spinella, Brigle, Freemantle, Sierra, & Goldman, 1996).

3.6.1.2. FPGS IHC Analysis

From the available mRNA data the IHC results appear to be comparable with expression seen in a wide range of normal and inflamed tissues tested including colon, liver, kidney, tonsil, heart, skeletal muscle and bone marrow (Table 3-3, Figure 3-14) . These findings were consistent with previous published mRNA data (Freemantle & Moran, 1997; Leclerec & Barredo, 2001). Negative tissues included brain and spinal cord (Table 3-3). Again, this was as expected based on previous data (Leclerec & Barredo, 2001). Weak staining was observed in placental samples, consistent with the finding of a low level of placental mRNA (Freemantle et al., 1995). 19/22 normal samples tested showed some positivity, ranging from weak to strong staining and upon further testing via the use of a normal tissue panel microarray, 71/78 samples were found to display some positivity (Data not shown). Negative samples included cerebrum and cerebellum (Table 3-3).

Positivity was also observed in the majority of malignancies tested from the tumour panels, 200/206 samples tested showed some positivity, ranging from weak to strong staining (Table 3-4). Negative tumour samples included mixed germ cell choriocarcinoma, fibrothecoma, ganglioneuroma and solitary fibrous tumour omentum. Expression in these tumour subgroups has not been previously reported. Further studies would be required to validate these results fully as there was only a small area of tissue tested for each type which is not fully representative of this tumour subgroup.

Of particular note was staining in ovarian adenocarcinoma islands which appeared to be stronger than adjacent normal stromal tissue (Figure 3-15). This has been previously reported in bowel tumour biopsies with higher levels of FPGS mRNA than adjacent submucosa (Odin et al., 2003). Strong expression was also observed in one B-cell lymphoma sample tested, which again is consistent with previous data which reported high levels of FPGS mRNA in B-lineage leukaemias, but more WB and IHC studies are required to confirm this (Freemantle & Moran, 1997).

3.6.1.3. FPGS Epitope Mapping

Peptide array epitope mapping analysis has demonstrated specific reactivity of FPGS clone NN 3.2 with a linear target present within the FPGS sequence, confirming its monoclonal nature and single defined specificity. The epitope recognised has been determined to be

between the regions of amino acids 237-258 as elucidated from the peptide array data sheet; this region spans twenty one amino acids. Upon further analysis it was elucidated that the epitope was most likely to be in the region of amino acids 246-251, protein sequence IFKQGV as this is the region containing the most hydrophobic amino acids in sequence and reactivity appears to be lost when the C terminal hydrophobic isoleucine residue is lost from the peptide, indicating this is an important amino acid involved in antibody binding (Figure 3-18). The two adjacent negative peptides in the middle of the positive sequences may be due to a masking effect as the flanking amino acid is glutamine which is polar in nature and this may have blocked binding of the antibody. Conformational changes bridging one or more adjacent peptides together may also have affected the antibody binding as the peptides are attached to the membrane at one end only with the remaining peptides free to attach to each other; this may have masked the epitope causing negative results in between the positive spots (Figures 3-17, 3-18). Knowledge of the precise region within the FPGS sequence recognised by clone NN3.2 may be extremely valuable in future work as a recent study identified 34 single nucleotide polymorphisms in the FPGS gene, suggesting that these genetic variations in FPGS may alter the efficiacy of antifolate therapies (Leil et al., 2007).

It can be concluded that clone NN 3.2 is a sensitive tool for the detection of FPGS in paraffin embedded samples, the detection of a single band via WB together with the cytoplasmic IHC staining pattern are consistent with the known biology of FPGS and are evidence of the specific affinity of NN3.2 to FPGS. The information provided from these validation experiments may be useful as preliminary data in future IHC studies to assess FPGS expression as an indicator of response to antifolates, as FPGS is known to be key in the action of these drugs.

3.6.2. FR-α Antibody Development

A monoclonal antibody for the detection of FR-α in formalin-fixed, paraffin embedded tissues has been successfully developed. Clone BN3.2 can also be used routinely in IHC via both ABC and Novolink as described previously. In addition it is also suitable for use in WB and ELISA. Its application for use on paraffin embedded samples overcomes previous problems encountered with the mOV18 and 19 antibodies, which are only suitable for

immunohistochemical use on frozen tissue and its specificity has been further validated via WB analysis, an application for which mOV 18 and 19 are also unsuitable.

Clone BN 3.2 was raised to a 189 amino acid region of the FR-α protein containing sequences unique to the α isoform of the protein.

3.6.2.1. FR-α WB Analysis

The FR-α antibody was found to be highly specific and in the positive cell lysates produced a single, 40 kDa band on an extended panel. 27 cell lysates in total were tested and 8 samples showed some positivity, ranging from strong to weak. 5/5 ovarian cell lines showed some positivity, including one ovarian teratocarcinoma sample, with the strongest expression in the IGROV-1 cell line (Figure 3-20). Moderate expression was seen in the SKOV-3 and OVCAR-3 cell lines and weaker expression in the SW626 and PA-1 cell lines. Strong expression was also seen in the HeLa cervical carcinoma cell line (Figure 3-20) and the CaCo2 colon adenocarcinoma cell line (Figure 3-21). Expression via IHC in these tumours has been previously reported via the use of the LK26 antibody (Rettig et al., 1985). Weak expression was seen in the embryonic kidney cell line ECR-293 (Figure 3-22). No expression was seen in any of the remaining cell lines tested. FR-α mRNA expression has been previously reported in the ovarian cancer cell lines IGROV-1, SKOV-3 and OVCAR-3 (Ross et al., 2000) which is consistent with the results seen in this study, the relative levels of expression are also consistent with this study with IGROV-1 showing the highest FR-α expression, followed by SKOV-3 and OVCAR-3 (Figure 3-20). These results support the general observation that FR-α expression is extremely restricted, particularly to ovarian cancers which are known to express the protein most consistently (Toffoli et al., 1997), although the number of cell lines displaying positivity is still extremely limited. Negative expression has been previously reported in the CCRF-CEM leukaemia cell line, mesothelioma cell line NCI-H226a, lung adenocarcinoma cell line A549, colon adenocarcinoma cell line HCT116 and the breast cancer cell line MCF-7 (Ross et al., 2000). All cell lines were also found to be negative in our study which is consistent with this data (Figures 3-20, 3-21, 3-22) . Expression in embryonic kidney has not been previously reported, however normal human kidney is known to express FR-α (Mangiarotti et al., 2001). Of particular note is the lack of expression in the three malignant pleural mesothelioma cell lines and one lung carcinoma cell line tested (Figure 3-20). Although negative expression in the NCI-H226a and A-549 cells has been

previously reported there are no reports on the levels of expression in MSTO-211H and NCI-H28 cells. This data alone is insufficient to draw an accurate conclusion on the expression of FR-α in MPM as FR-α tissue expression patterns and mRNA transcripts have been extensively studied and it has been found that in many cases the FR expression patterns in cell lines do not reflect expression profiles *in vivo*. FR expression is commonly absent in cell lines derived from malignant tissue known to be consistently FR positive (Elnakat & Ratnam, 2004). In contrast to this a study by Tomassetti *et al* identified and purified both the soluble and membrane bound forms in the ovarian adenocarcinoma cell line IGROV-1, suggesting that some cell lines do express the protein *in vitro*. This study also supports the strong FR-α expression seen in the IGROV-1 cell line with clone BN 3.2 (Figure 3-20) (Tomassetti et al., 1993; Tomassetti et al., 2003). Expression of FR-α has also been reported in the colon adenocarcinoma cell line HT29 and the leukaemic cell line MOLT-4. Neither of these cells appeared to display FR-α expression in this study, although the colon adenocarcinoma cell line CaCo2 was found to be positive (Figure 3-21). This has not been previously reported. A potential problem with interpretation of these results may also be the culture conditions used to grow the cells, the majority of the cell lysates obtained were kindly donated and were cultured in commercial media. Standard RPMI contains supra-physiological concentrations of folic acid which is thought to downregulate the expression of FR-α in some cell lines and may be one of the reasons for the inconsistency of expression in cell lines often observed (Miotti et al., 1995). A more suitable media to use would have been folate free RPMI and dialysed FBS, supplemented with 20nM folinic acid which would have given folate levels approximating physiological concentrations in humans (Miotti et al., 1995). As it is time consuming to adapt cells to this type of media, this was not possible to perform within the time frame and cells cultured in standard media were used. This should be considered when interpreting these results as the level of FR-α expression may have been affected by this, although it has been previously reported that the extracellular folate concentration does not have an adverse effect on the expression of IGROV-1, OVCAR-3 and SW626 cells so this may also apply to other cell lines (Miotti et al., 1995). It may be that the HT29 and MOLT4 cell lines used in this study are, in fact positive but their expression has been downregulated via use of supra physiological concentrations of folate in the media.

The FR-α antibody produced from clone BN3.2 also detected a single band of approximately 40kDa in the ovarian adenocarcinoma cell extracts IGROV-1, OVCAR-3 and SKOV-3, which is consistent with previous published studies examining FR-α expression via mRNA, IHC on frozen tissue and radioligand binding assay (Figure 3-20) (Parker et al., 2005; Toffoli et al., 1997; Weitman et al., 1992b).

3.6.2.2. FRα IHC Analysis

Immunohistochemical studies using clone BN3.2 on formalin-fixed paraffin-embedded tissue sections have shown that the expression of FR-α is low-negative in the majority of normal and inflamed tissues, but its expression is seen to a varying degree and frequency in a range of different tumour types, in a manner consistent with previous published data (Campbell et al., 1991; Parker et al., 2005; Ross et al., 1994; Veggian et al., 1989). 3/22 normal samples tested were found to show positive staining. 5/6 placental samples showed positive staining upon further testing (Table 3-5, Figure 3-23).

Of particular interest is the strikingly high expression observed in the majority of ovarian malignancies tested. The detection of a single band via WB of cell and tissue extracts, together with the striking strong membrane and cytoplasmic staining are consistent with the known biology of FR-α and evidence of the specific affinity of the BN3.2 antibody to FR-α. Positive malignancies observed from the tumour panel (78 sections tested in total) included very strong staining in various ovarian adenocarcinoma samples, with 14/15 sections tested showing positivity. Less frequently, weaker staining was observed in endometrial adenocarcinomas (1/1), lung carcinomas (1/1) and breast carcinomas (2/8) (Table 3-5).

Moderate to weak staining was observed in endometrial adenocarcinoma, lung carcinoma, thyroid papillary carcinoma, ovarian thecoma and granulosa. Expression in these tissues has been previously reported (Evans et al., 2001; Ross et al., 1994; Wu et al., 1999). One recent study found 69% of frozen uterine serous carcinoma samples tested to express FR-α protein. As only 1 sample was assessed in this study, further analysis of FR-α expression in these tumours would be of interest (Dainty et al., 2007).

Weak expression in cholangiocarcinoma was also noted, which has not been previously reported. However, the result obtained was from one case on a tissue microarray and

further testing would need to be performed to validate this observation and assess the frequency of expression in this tumour type.

Also of interest was the lack of expression in both mesothelioma cell lines and paraffin embedded mesothelioma tissue (n=6 tumour samples), This result was surprising, as high expression in mesothelioma has been previously reported and cited as a possible explanation for the responsiveness of mesothelioma to the novel antifolate pemetrexed (Bueno, Appasani, Mercer, Lester, & Sugarbaker, 2001). However, other reports have cast doubt on both the expression of FR-α in mesothelioma and on the importance of FR-α as an uptake mechanism and determinant of response to pemetrexed (Chattopadhyay, Wang, Zhao, & Goldman, 2004). More samples would be required to investigate this further.

3.6.2.3. FR-α Epitope Mapping

Peptide array epitope mapping analysis has demonstrated specific reactivity of FR-α clone NN3.2 with a linear target present in the FR-α target sequence, which began at amino acid 45 and ended at amino acid 233. The epitope was found to map to amino acids 57-62 and is hypothesised to be contain the following amino acids; CRPWRK. Reactivity was found to be lost when the cysteine residue was lost from the peptide sequence, indicating the presence of this hydrophobic amino acid being significant for immunoreactivity to the peptide (Figure 3-27).

The epitope recognised contained a cysteine residue, when the protein is in its native conformation this cysteine is likely to be involved in a disulphide bridge, requiring breakage to expose the epitope, such as the antigen retrieval step required to expose this epitope in paraffin embedded tissues. This is supported by the lack of staining observed when no pre-treatment was assessed for antibody validation (Figure 3-25). However, the presence of this cysteine residue also led to the proposal that use of reducing agents such as DTT may break the bridges and allow the antibody to be used in applications such as IF and frozen IHC. The cysteine may also contribute to the negative adjacent peptide (A7, Figure 3-27) causing variable intensity of reactivity between peptide spots, this region of the sequence is relatively cysteine rich and the cysteine residues present in adjacent peptides may have formed disulphide bridges, linking the adjacent peptides and masking the epitope present in this part of the sequence. Another possible explanation for the variation in reactivity is the

location of the epitope towards the outer amino acids of the peptide; reactivity may not be as strong when the antibody binds to an epitope further from the site of attachment.

The mOV 18 epitope mapping experiment also supported this theory and demonstrated the opposite action occurring, only two peptides were found to display positive immunoreactivity, indicating that the epitope is likely to be conformational rather than linear in nature, the location of the epitope was also different to that of clone BN 3.2. For this reason it is not possible to determine the precise epitope sequence for mOV18 (Figures 3-28, 3-29). This also explains the reason for the epitope being destroyed by treatment with a reducing agent as the disulphide bridges would be broken, shearing the epitope and causing loss of binding affinity. Both the N-terminal and C terminal hydrophobic transmembrane alpha helices were missing from this target and it is likely that the conformational epitope bridges some of the target and one of the alpha helices missing from the peptide array.

No reactivity was observed on the peptide array treated with LK26 antibody, indicating that the epitope recognised by this antibody is different from that of the BN 3.2 clone and mOV 18 antibody and is likely to be located in a region not targeted by the peptide array, it can not be determined whether the epitope recognised is conformational or linear in nature as the peptide array does not cover the full sequence (Figures 3-30, 3-31). Although the staining was found to be comparable caution should be taken when using this antibody in IHC as it is a relatively insensitive method of interpreting protein expression when not supported by another application for confirmation. As learned previously from the cross reaction encountered it is advantageous for the antibody to be suitable for a number of applications to confirm its specificity. Despite this it has been reported that the LK26 antibody has been successfully humanised (MORAb-003) and in preclinical evaluation it has been found to possess novel, growth inhibitory properties both *in vitro* and *in vivo* and as a result has recently been advanced to clinical trials involving ovarian cancer patients (Ebel et al., 2007).

This antibody may be more suited to applications where the protein is present in its native conformation and this is supported by the results from this mapping experiment as there is no evidence to suggest that it recognises a linear target, unless it is in a region not covered by our target. It may also bridge one of the transmembrane alpha helices missing from the

target or the epitope may span a number of folded regions, fragmenting the epitope so it is not detected at all on a linear seqiuence.

It can be concluded that clone BN 3.2 is a sensitive tool for the detection of FR-α in paraffin embedded tissues and that this validation data supports its use in immunohistochemical studies to determine the role of FR-α as a tumour prognostic marker, potential predictive biomarker for response to antifolates and possible therapeutic target. This would be particularly useful in clinical trials of antifolates which are targeted to FR-α and may help to identify responsive subgroups of patients to whom such agents would be of particular benefit (Jackman et al., 2004).

Chapter Four

Chapter Four

4. Ovarian Tissue Microarray Analyses

Ovarian cancer is the major focus of this study largely due to its strikingly high frequency and level of expression of FR-α compared with other tumour types and other normal tissues. This offers an exciting target both for further studies assessing the frequency of expression in such tumours and also its relationships to survival and as a predictor of response to folate targeted therapies.

Few studies have investigated the relationship between tumour levels of FR-α and survival, largely due to limitations with the other commercially available antibodies, discussed in detail in section 1.8.3. However, due to the nature of FR-α and its role in folate transport and metabolism it is thought that high expression levels of FR-α are associated with poor prognosis and tumour progression (Toffoli et al., 1998). Similarly, its potential role in antifolate transport, coupled with its role in folate receptor targeted therapies may also indicate a role for FR-α in tumour targeted drug delivery as discussed in section 1.8.5. As indicated by the mOV18 and 19 antibodies by IHC on frozen tissue, ovarian cancer appears to be the major tumour type associated with overexpression of FR-α. It was thus the aim to obtain a TMA containing ovarian cancer cases to assess FR-α expression on a large scale in these samples. The data could then also be analysed in relation to FPGS expression. In addition, relationships between expression and survival could also be analysed to assess whether FR-α and FPGS expression may be independent prognostic markers for both overall and relapse free survival. The results observed were primarily part of the antibody validation process, to ensure the data generated from this larger study were consistent with previous published data in relation to both frequency of expression in ovarian cancer and its role as a marker of poor prognosis.

4.1. Ovarian TMA Study Aims and Objectives

- Obtain ovarian TMA slides, perform IHC using the Novolink polymer detection kit and accurately score based on intensity and % tumour cells stained by two independent observers.
- Obtain some statistical data via univariate and multivariate analysis on the TMA's to assess the relationship between the expression of FR-α, FPGS and other known prognostic markers in ovarian cancer.
- Identify whether FR-α and FPGS are independent markers of prognosis in ovarian cancer patients.
- Correlate the results obtained with previous published work to further confirm the validity of the antibodies.

4.2. Ovarian TMA Study Materials and Methods

A total of 167 ovarian cancer samples were collected over a period of five years, differing in stage, grade and tumour type. All samples used in the archival TMA had appropriate ethical approval and known patient clinical data collected from hospital records. Cell cores were taken from tumour–rich areas and assembled into a TMA, each core was duplicated to account for loss of tissue during processing. There were a total of four TMA's (designated OVCA 1, 2, 3 and 4), each containing ovarian carcinoma samples only with the exception of mouse liver cell cores placed on different edges of the slides used as markers to differentiate one TMA from another and a small panel of normal and tumour tissues on TMA four, which included breast, thyroid, liver, lung, colon, and kidney.

The TMA's were collected and prepared by Dr. Ann Fisher, Dr. Richard Edmondson and Dr. Ali Kucukmetin at Newcastle University.

IHC staining using the Novolink polymer kit was performed on the samples with the FR-α and FPGS antibodies employing the techniques described in section 3.3.6.

4.2.1. Assessment of TMA IHC Staining- Scoring System Used

The IHC staining of tissues was scored according to the proportion of tumour cells staining and the staining intensity. Reactivity was also determined to be cytoplasmic (C), nuclear (N), membrane (M) or any combination of the three. This gave a numerical result and was carried out by two observers independently. Tissues were visualised under a light microscope, the proportion and intensity of cytoplasmic/membrane staining for FR-α and cytoplasmic staining for FPGS were estimated, no nuclear reactivity was observed for either antibody. Inter scorer variablility was assessed by scoring independently, once scores were recorded they were then analysed together and in the event of a discrepancy an agreed score was decided upon further inspection of the core.

Intensity was assessed on a four point scale as follows:

0 = Negative

1= Weak

2 = Intermediate

3 = Strong

Concurrently the percentage of tumour cells stained was assessed on a four point scale as follows:

1 = 0-25%

2 = 25-50%

3= 50-75%

4= 75-100%

The scores for intensity and proportion were then multiplied to give a score intensity rating of between 0 and 12. Where staining was heterogeneous different intensity and proportion scores were multiplied, ensuring the total percentage of tumour cells equaled 100% (or four scale points) to give a score intensity, the different scores were then added together to give

an overall score. E.g. weak staining in 25% of tumour, intermediate staining in 50% of tumour and strong staining in the remaining 25% of tumour would be calculated as (1x1) + (2x2) + (3X1) = a total score of 8 (note the total percentage of tumour cells stained equaled 4 score points as 100% of the tumour was immunoreactive). As there were two cores representing one tumour per TMA an average score from both duplicate cores was also recorded.

4.2.2. Statistical Analysis

Statistical analysis was carried out by Mr M. Cole, NICR, Newcastle using Stata 10 software. Survival and time to recurrence were analysed by the construction of Kaplan Meier curves for patient overall survival, stage, grade, histology, CA125, residual disease, chemotherapy before surgery, FR-α and FPGS expression. Cox's proportional hazards model was used to compare survival curves to identify any statistically significant differences and was also used in a forward stepwise approach to perform multivariate analysis of the variables which on univariate analysis were significantly associated with clinical outcome to determine their utility as independent prognostic variables. In addition one way Anova and Bartletts tests were used to ensure equal variance across groups and to look for evidence of statistically significant relationships between FR-α and FPGS expression and some of the other variables including grade, histology and CA125 values.

4.2.2.1. Kaplan-Meier Survival Plots and Log-Rank Test

The relationship to survival was tested via the use of Kaplan-Meier survival plots and the the log-rank test to examine the significance of any differences in the rate of survival between patient subgroups defined by the variables under consideration taking into account the follow up time of the patients. Kaplan- Meier survival graphs are generated by estimation of conditional probabilities of events occurring at each time point when an event (such as death, relapse or loss of follow up) occurs and estimating the rate of survival at each time point taking this into consideration. The log-rank test employs logarithms of the ranks of the data to compare the survival curves and computes a p-value to indicate whether the overall differences between survival curves are statistically significant or if they could have been due to chance.

4.3. Ovarian TMA Study - Results

4.3.1. FR-α and FPGS Images and Scoring

Photographic images were taken from the TMA slides using the Aperio Scan Scope CS automated scanning and scoring system (Aperio Technologies Inc., Figure 4-1).

For FR-α, patterns of membrane/cytoplasmic heterogeneous staining were observed on all four TMA slides tested (Figure 4-2 and Figure 4-3). For FPGS, patterns of cytoplasmic heterogeneous staining were observed on all four TMA slides tested (Figure 4-5 and Figure 4-6). Staining for FR-α was predominantly membrane (Figure 4-8) and staining for FPGS was predominantly cytoplasmic (Figure 4-9). For both FR-α and FPGS the majority of samples were found to show some positivity ranging from strong (Figure 4-4 and Figure 4-7) to moderate/weak expression. Scores were recorded on a spreadsheet and statistical analysis performed to assess the relationship between expression of FR-α or FPGS and patient survival. Of 167 samples tested, 63 cases (38%) were found to have low FR-α expression (score 0.5-4), 46 (28%) were found to moderately express FR-α (score 4.5-8) and 57 (34%) were found to have high expression (8.5-12). Of 167 cases 30 (18%) were found to have low FPGS expression 70 (42%) were found to have moderate expression and 67 (40%) were found to have high FPGS expression.

Figure 4-1: Photograph of the OVCA TMA slides. Complete set of ovarian TMA's -OVCA1, 2, 3 and 4 stained with FR-α to illustrate the layout of the slides.

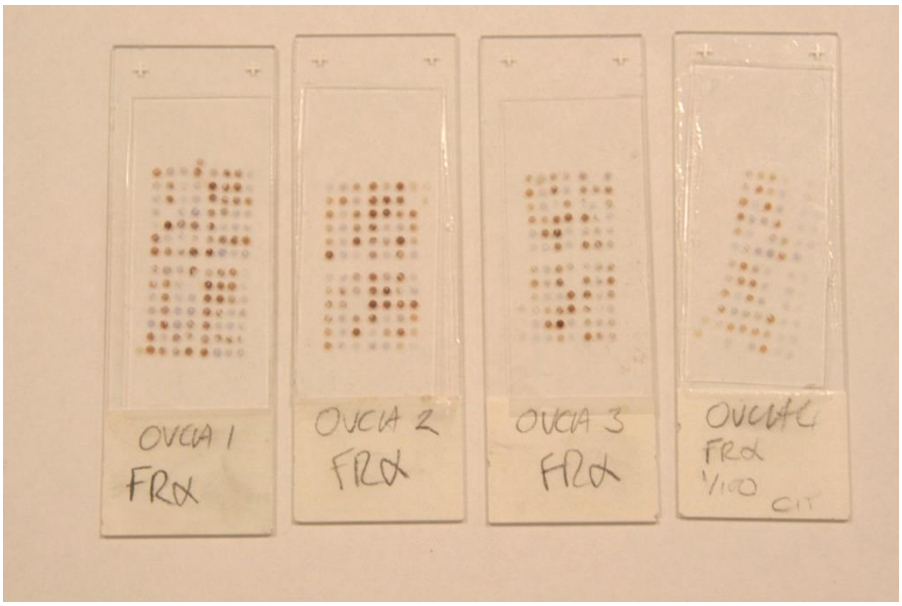

Figure 4-2: Photograph of OVCA1 stained with FR-α. Each core was assigned an identifier and linked to the corresponding patient data on an excel spreadsheet. Illustrates the layout of the TMA. Each TMA contains two cores taken from the same patient. FR-α gave variable intensity staining which was predominantly membrane and cytoplasmic.

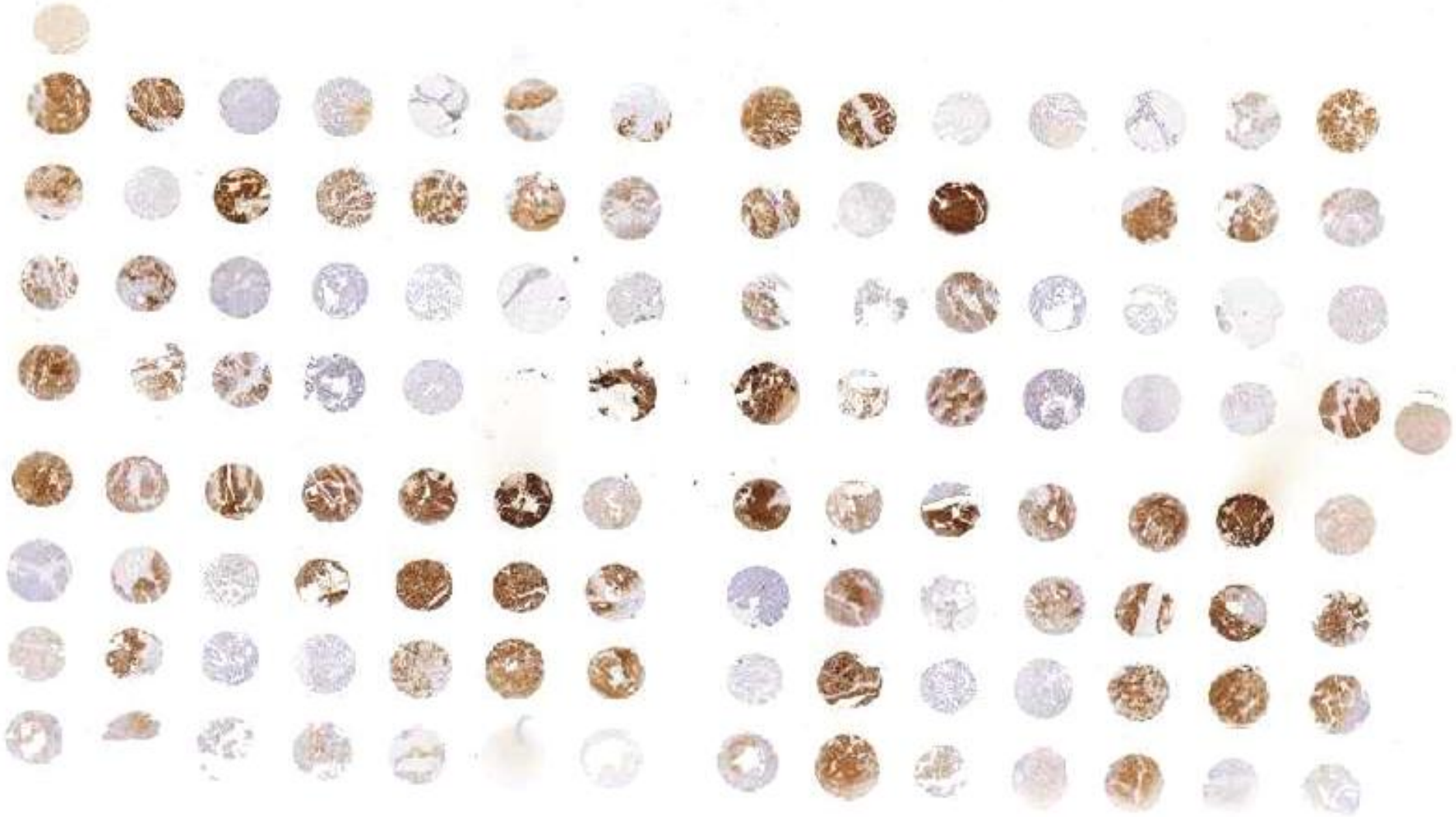

Figure 4-3: Photograph of twelve TMA cell cores (x1) stained with FR-α. Note the difference in staining intensity between cores Strong (3+) reactivity is represented by cores b, g, h and l,. Moderate (2+) reactivity is represented by cores c, d, e, f and j, weak (1+) reactivity is represented by cores a, i and k.

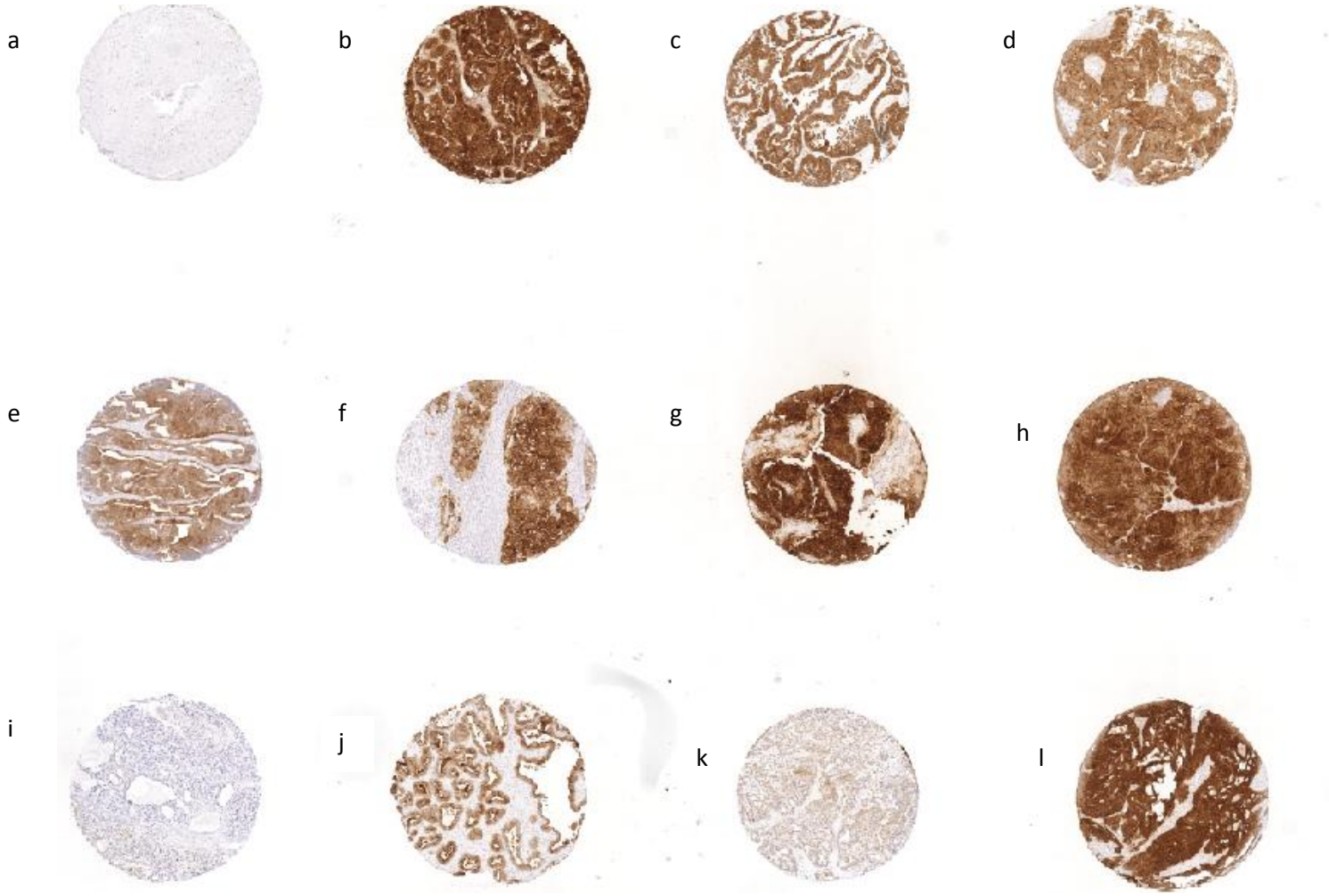

Figure 4-4: Photograph of eight TMA cores (x4) stained with FR-α. a,b and d represent four strongly reactive cores in 100% of the tumour, such cores would be given a score of 12 based on the scoring system used (3+ staining (3) x proportion of tumour cells stained 75-100% (4) = a score of12). C would be given a score of 10 (3+ in 50% of tumour 2+ in the remaining 50% of tumour = (3x2) + (2x2) = 10). f and h are moderately immunoreactive and would be given a score of 8 (2+ staining in 100% of tumour; 2x4 = 8). G is moderate-weakly immunoreactive and would be given a score of 6 (2+ staining in 25% of tumour, 1+ staining in 50% of tumour, remaining 25% negative;(2x1) + (2x2) = 6) e is weakly immunoreactive and would be given a score of 3; 1+ staining in 50-75% of tumour (1x3=3).

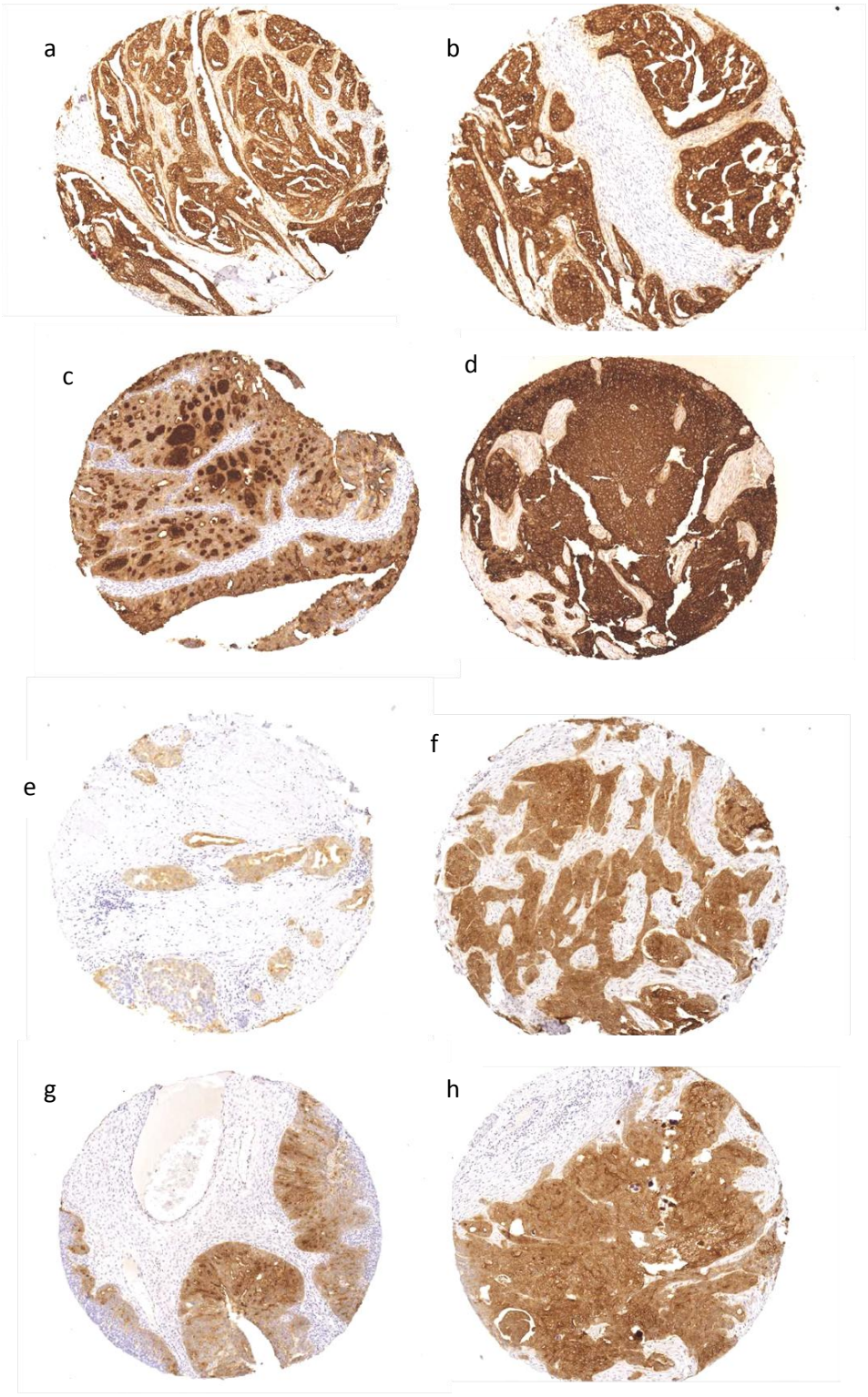

Figure 4-5: Photograph of OVCA1 stained with FPGS. Each core was assigned an identifier and linked to the corresponding patient data on an excel spreadsheet. Illustrates the layout of the TMA. Each TMA contains two cores taken from the same patient. FPGS gave variable intensity staining which was predominantly cytoplasmic.

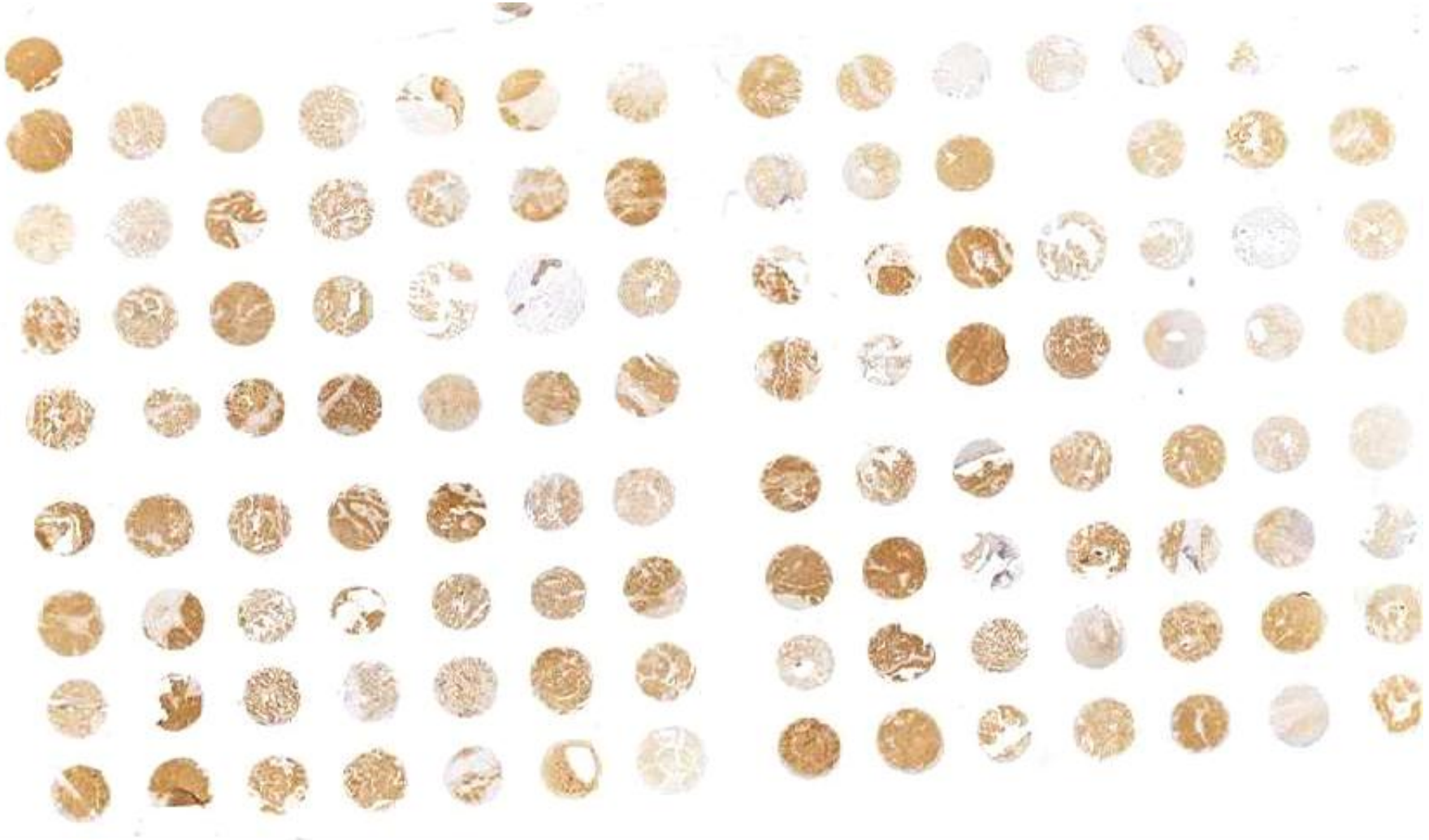

Figure 4-6: Twelve TMA cell cores (x1) stained with FPGS. Note the difference in staining intensity between cores Strong (3+) reactivity is represented by cores a,g,h and k. Moderate (2+) reactivity is represented by cores b,d,i,j and l,weak (1+) reactivity is represented by cores c,e, and f.

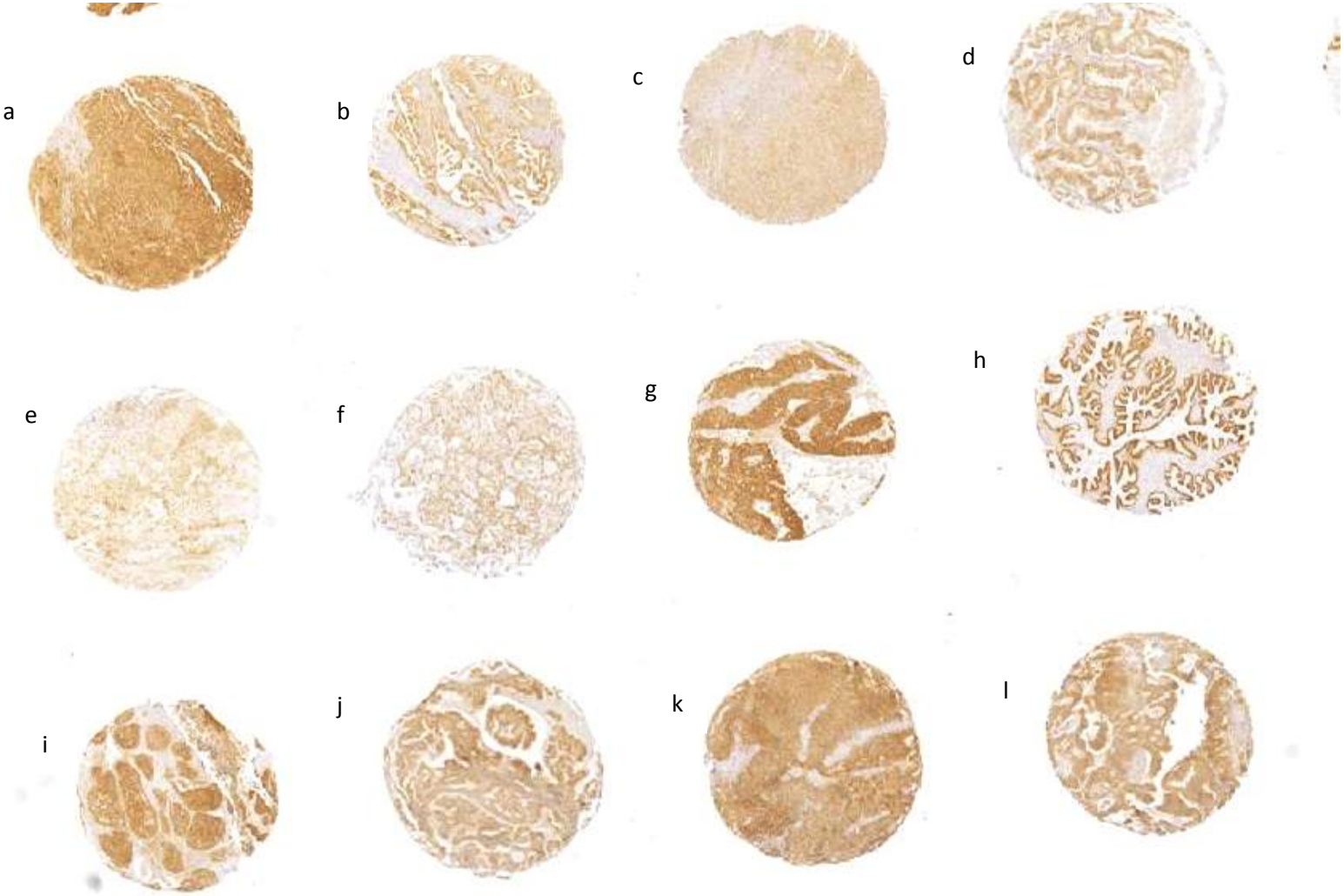

Figure 4-7: Photograph of eight TMA cores (x4) stained with FPGS. a,b and d represent four strongly reactive cores in 100% of the tumour, such cores would be given a score of 12 based on the scoring system used (3+ staining (3) x proportion of tumour cells stained 75-100% (4) = a score of12). C would be given a score of 10 (3+ in 50% of tumour 2+ in the remaining 50% of tumour = (3x2) + (2x2) = 10). f and h are moderately immunoreactive and would be given a score of 8 (2+ staining in 100% of tumour; 2x4 = 8). e is moderate-weakly immunoreactive and would be given a score of 6 (2+ staining in 25% of tumour, 1+ staining in 50% of tumour, remaining 25% negative;(2x1) + (2x2) = 6) g is moderate- weakly immunoreactive and would be given a score of 4; 2+ staining in 25% of tumour ,1+ staining in 50% of tumour, remaining 25% negative ((2x1) + (1x2) = 4)) .

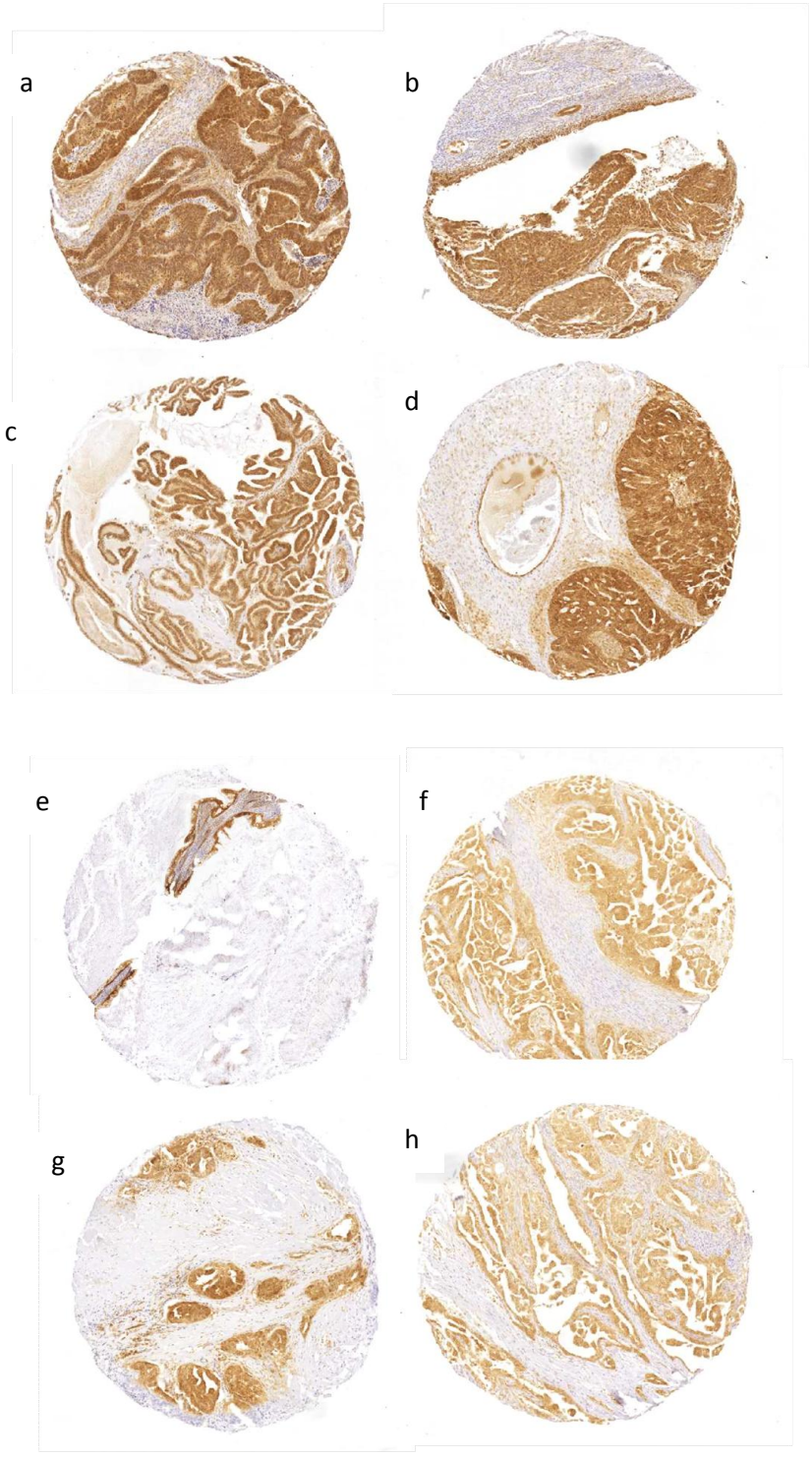

Figure 4-8: FR-α membrane staining. Image demonstrating strong membrane and cytoplasmic immunoreactivity of FR-α on one of the ovarian cancer cores (x20). Note the strong staining in tumour (brown)compared with adjacent stromal tissue (blue).

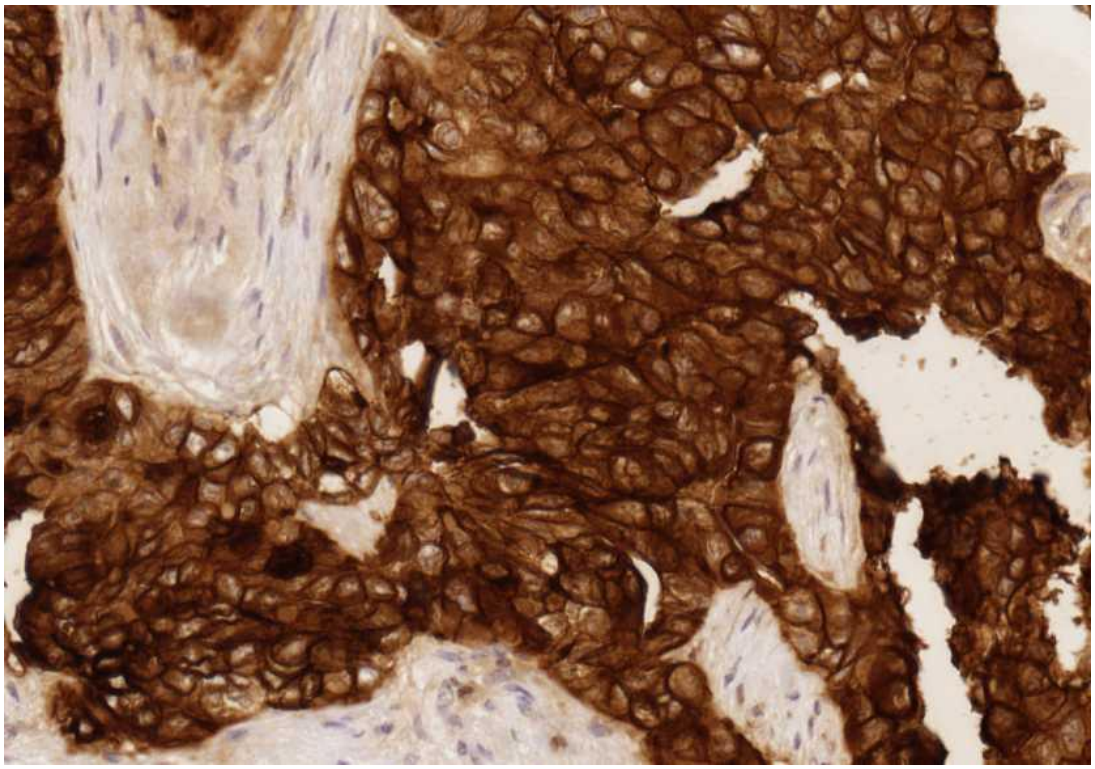

Figure 4-9: FPGS cytoplasmic staining. Image demonstrating moderate-strong cytoplasmic immunoreactivity of FPGS on one of the ovarian cancer cores (x20). Note the staining in tumour islands (brown) weaker reactivity in stromal tissue and negativity in lymphoid aggregates (blue).

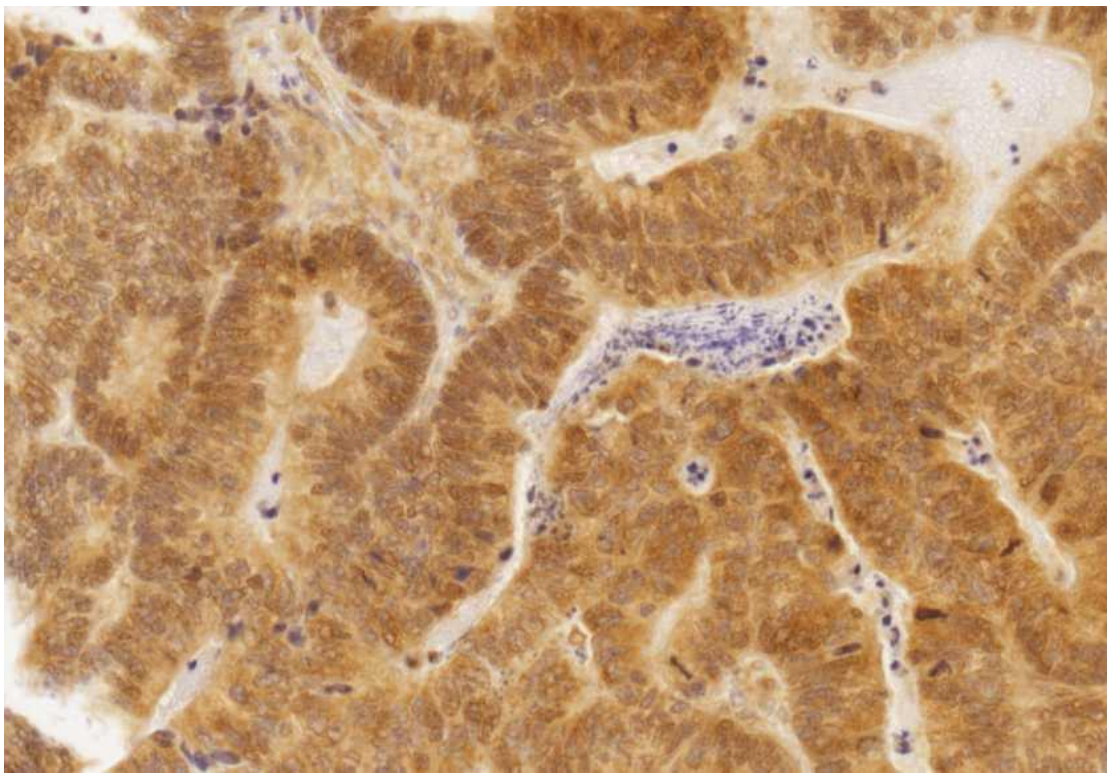

4.3.2. Statistical Analysis of Overall Survival

Statistical analysis of overall survival was performed to assess the association between all the variables and survival to ensure the data from this cohort of patients followed similar trends to those seen in patients with ovarian cancer.

For survival, no significant associations were found for age, chemotherapy before surgery or FPGS score. Statistically significant associations were found for stage, grade, histology, Log_{10} CA125, residual disease and FR-α IHC scores. (Table 4-1)

Table 4-1: Summary of statistical analysis of overall survival

Variable	Events (Total number) i.e. death	P value (Cox regression)	Hazard Ratio (HR)	95% CI
Age at operation				
<60 No	66 (108)	0.9359	1.00	0.98-1.01
<60 Yes	36 (58)			
Stage				
1	5 (27)			
2	6 (14)	0.180	2.25	0.69-7.38
3	67 (91)	< 0.000	6.99	2.80-17.44
4	17 (18)	< 0.000	22.41	8.04-62.44
Grade	Well diff vs rest	0.004	2.39	1.33-4.28
Poorly differentiated	56 (80)	0.003	0.40	0.22-0.73
Moderately differentiated	33 (45)	0.503	0.86	0.56-1.33
Well differentiated	13 (42)			
Histology	Endo vs rest	0.006	0.53	0.34-0.84
Adenocarcinoma	3 (3)	omitted	omitted	omitted
Endometrioid	25 (51)			
Papillary Serous	27 (41)	0.624	0.74	0.22-2.45
Clear Cell	12 (16)	0.930	0.94	0.27-3.36
Mucinous	7 (18)	0.206	0.42	0.11-1.62
Serous	28 (38)	0.796	0.85	0.26-2.82
CA125				
<480 No	50 (70)	0.157	1.00	0.99-1.00
<480 Yes	39 (70)			
Log10 CA125		0.040	1.36	1.01-1.83
Residual Disease				
Suboptimal cytoreduction	58 (64)	< 0.000	0.14	0.77-0.67
Optimal cytoreduction	18 (30)	0.001	0.39	0.76-0.24
Complete cytoreduction	18 (54)			
Chemo before surgery				
No	88 (138)			
Yes	4 (7)	0.522	1.39	0.51-3.80
FR-α 1				
Below median	36			
Above Median	63	0.044	0.655	0.43-0.98
Continuous variable	148	0.013	1.06	1.01-1.11
FR-α 2				
Below median	39			
Above median	59	0.030	0.64	0.424-0.958
Continuous variable	146	0.006	1.066	1.02-1.12
FR-α Mean				
Below median	39			
Above median	63	0.052	0.672	0.45-1.00
Continuous variable	152	0.009	1.06	1.02-1.12
FPGS 1				
Below median	28			
Above median	69	0.832	0.95	0.61-1.48
Continuous variable	145	0.81	1.00	0.95-1.08
FPGS 2				
Below median	30			
Above median	67	0.976	0.99	0.65-1.53
Continuous variable	143	0.802	1.01	0.94-1.07
FPGS Mean				
Below median	78			
Above median	24	0.713	0.91	0.58-1.45
Continuous variable	152	0.845	1.00	0.94-1.08

4.3.2.1. Overall Survival and FR-α Score 1, 2 and Mean

The FR-α analysis was performed three times, once for each individual score and also on the average score. FR-α was categorised into two groups based upon the median value. FR-α was also analysed when treated as a continuous variable. When categorised, scores 1 and 2 were found to have a statistically significant association with survival (p= 0.0419, 0.0288 respectively, Log-rank test, Figures 4-10, 4-11). The mean was found to be borderline significant (p=0.0502 Log-rank test, Figure 4-12). This indicated that high expression of FR-α is associated with shorter survival than low expression. When treated as a continuous variable all three scores were found to have a statistically significant association with survival (p= 0.013, 0.006, 0.009 respectively, Cox regression). All three scores were found to have a hazard ratio of 1.06 (95% CI 1.301-1.11), indicating a 1.6 fold increase in risk of death from the tumour for every score point increase.

Figure 4-10: FR-α Kaplan-Meier analysis (1). Demonstrating a significant difference in duration of survival between patient groups with tumours showing above and below median FR-α score 1 expression. Blue = high FR- α expression, Red = Low FR-α expression (p=0.0419, Log-rank test).

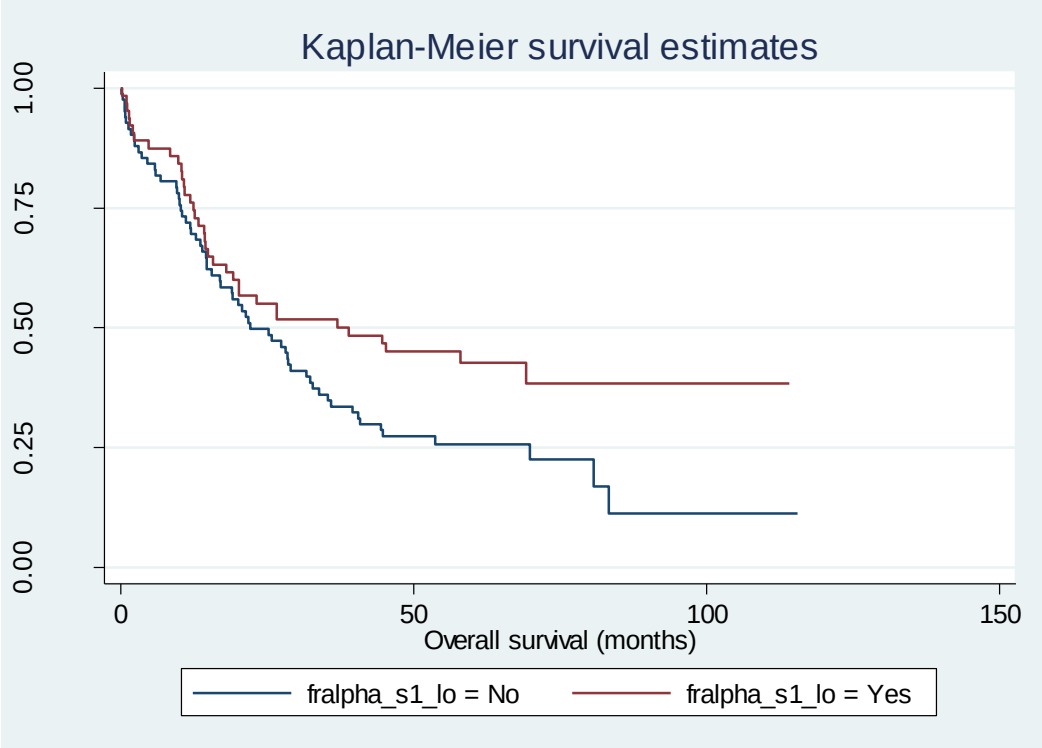

Figure 4-11: FR-α Kaplan-Meier analysis (2). Demonstrating a significant difference in duration of survival between patient groups with tumours showing above and below median FR-α score 2 expression. Blue = high FR- α expression, Red = Low FR-α expression (p=0.0288, Log rank test).

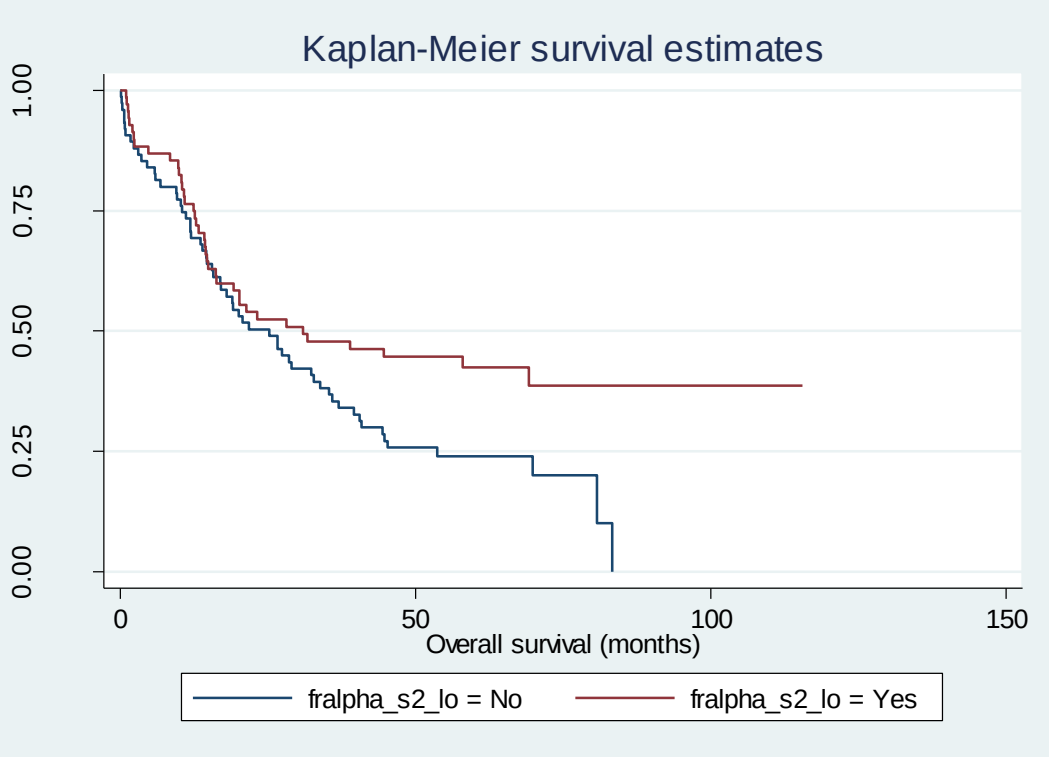

Figure 4-12: FR-α Kaplan-Meier analysis (3). Demonstrating a borderline significant difference in duration of survival between patient groups with tumours showing above and below median FR-α mean score expression. Blue = high FR- α expression, Red = Low FR-α expression (p=0.0502, Log-rank test).

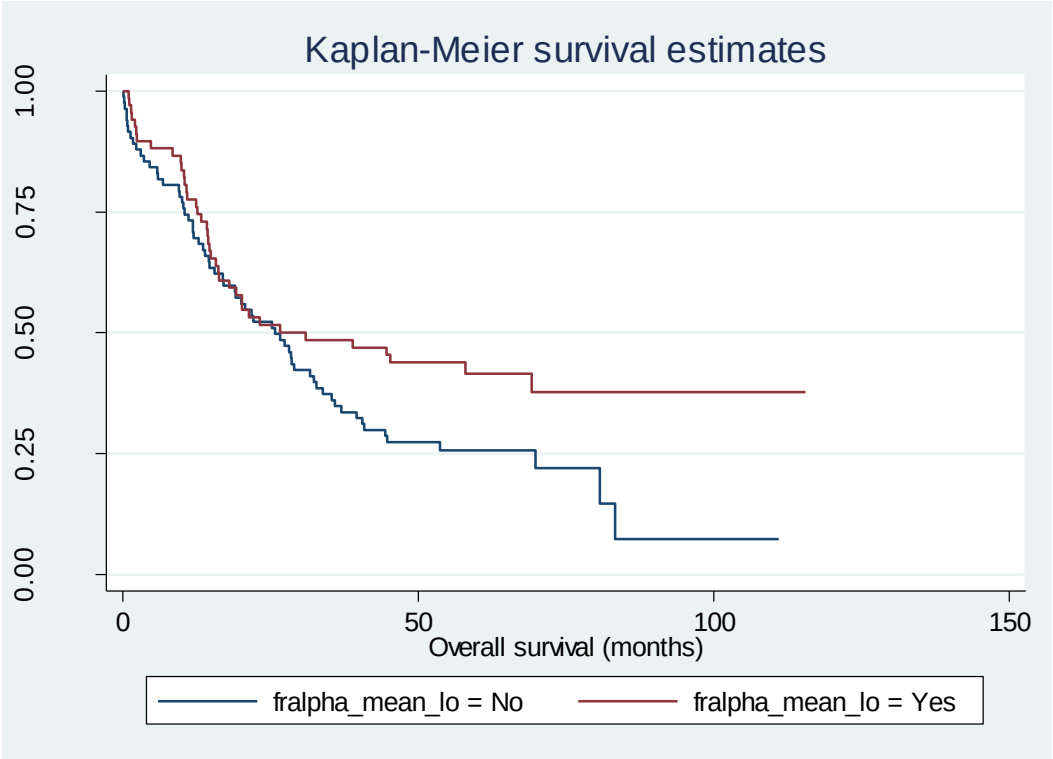

4.3.2.2. Overall Survival and FPGS Score 1, 2 and Mean

The FPGS analysis was also performed three times and categorised by the median value and treated as a continuous variable. When categorised, none of the three scores were found to have a significant association with survival. (p=0.8318, 0.9761 and 0.7124 respectively, Log-rank test (Figure 4-13). Treating FPGS as a continuous variable did not generate any difference with no significant association with survival (p= 0.013, 0.006, 0.009 respectively, Cox regression).

Figure 4-13: FPGS Kaplan-Meier analysis (1). Demonstrating no significant difference in duration of survival between patient groups with tumours showing above and below median FPGS score 1 expression. Blue = high FPGS expression, Red = Low FPGS expression. (p=0.08318, Log-rank test) Similar patterns were observed for score 2 and mean score (data not shown).

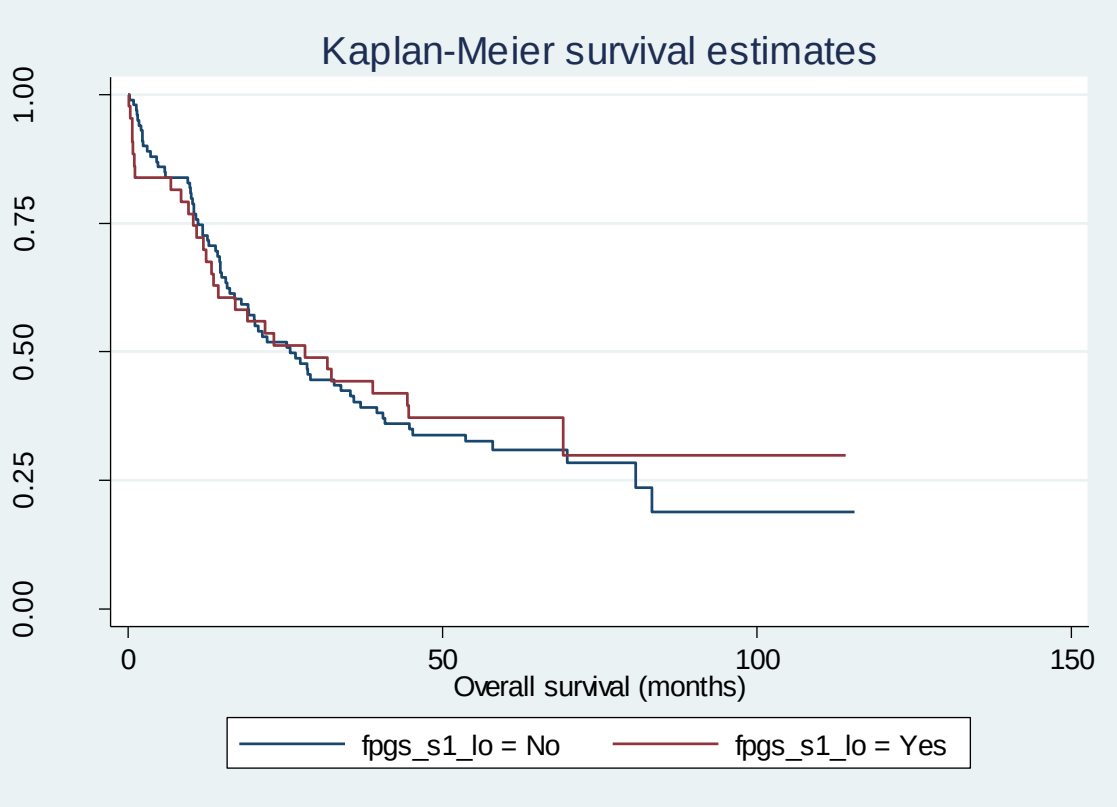

4.3.2.3. Overall Survival Multivariate Analysis

In a multivariate model performed in a forward stepwise approach, both FR-α and FPGS failed to retain significance independent of residual disease, histology and stage, the most statistically significant variables deduced from the overall survival analysis which dominated the model (p=0.000 Cox regression). Both significant FR-α scores were used in the analysis (p=0.486, 0.338, Cox regression). Both significant FPGS scores were also analysed (p=0.664, 0.445, Cox regression).

4.3.3. Statistical Analysis of Time to Relapse

For relapse free survival, no significant associations were found for age, chemotherapy before surgery or FPGS score. Statistically significant associations were found for stage, grade, histology, $\log_{10}$ CA125, residual disease and FR-α IHC scores. (Table 4-2) Results observed followed a similar pattern to that of the overall survival analysis and are consistent with previous published data on ovarian cancer survival (Yancik, 1993).

Table 4-2: Summary of statistical analysis of time to relapse

Variable	Events (Total number) i.e. death	P value	HR	95% CI
Age at operation				
<60 No	76 (119)	0.807	1.00	0.98-1.01
<60 Yes	38 (40)			
Stage				
1	5 (27)			
2	6 (14)	0.186	2.22	0.69-7.30
3	79(91)	< 0.00	9.18	3.68-22.83
4	18(18)	< 0.00	23.91	8.66-66.04
Grade				
Poorly Differentiated	65 (80)	0.132	0.72	0.47-1.10
Moderately Differentiated	33 (45)	< 0.000	0.361	0.20-0.64
Well Differentiated	16 (42)			
Histology	Endo vs rest	0.0087	0.57	0.37-0.87
Adenocarcinoma	3 (3)	0.993	1.00	0.61-1.65
Endometrioid	12 (51)	0.070	0.47	0.20-1.07
Papillary Serous	30 (41)	0.961	1.01	0.52-1.99
Clear Cell	8 (16)	0.993	1.00	0.61-1.65
Mucinous	31 (18)	0.013	0.53	0.32-0.88
Serous	30 (38)			
CA125				
<480 No	58 (70)	0.144	1.00	0.99-1.00
<480 Yes	43 (70)			
Log 10 CA125		0.011	1.44	1.09-1.90
Residual Disease				
Suboptimal cytoreduction	60 (64)	< 0.000	0.15	0.86-0.25
Optimal cytoreduction	25 (30)	0.029	0.59	0.37-0.95
Complete cytoreduction	22 (54)			
Chemo before surgery				
No	99 (138)			
Yes	6 (7)	0.268	1.60	0.70-3.65
FR alpha 1				
Below median	40			
Above Median	71	0.013	0.61	0.41-0.90
Continuous variable	111	0.003	1.06	1.02-1.11
FR alpha 2				
Below median	46			
Above median	63	0.053	0.68	0.46-1.00
Continuous variable	109	0.002	1.07	1.03-1.12
Mean Fr alpha				
Below median	44			
Above median	70	0.020	0.64	0.43-0.93
Continuous variable	114	0.003	1.07	1.02-1.12
FPGS 1				
Below median	29			
Above median	80	0.588	0.89	0.58-1.36
Continuous variable	109	0.62	1.01	0.96-1.08
FPGS 2				
Below median	31			
Above median	77	0.663	0.9121	0.60-1.38
Continuous variable	108	0.396	1.03	0.97-1.09
Mean FPGS				
Below median	26			
Above median	88	0.592	0.89	0.57-1.38
Continuous variable	114	0.524	1.02	0.96-1.09

4.3.3.1. Relapse Free Survival and FR-α Score 1, 2 and Mean

As for overall survival, FR-α analysis was performed for the three scores and also treated as a continuous variable. When categorised, scores 1 and mean were found to have a statistically significant association with survival (p= 0.0116, 0.0190 respectively, Log-rank test, Figures 4-14, 4-16). Score 2 was found to be borderline significant (p=0.0509 Log-rank test, Figure 4-15). This indicated that high expression of FR-α is associated with shorter survival than low expression. When treated as a continuous variable all three scores were found to have a statistically significant association with survival (p= 0.03, 0.002, 0.003 respectively, Cox regression). All three scores were found to have a hazard ratio of 1.07 (95% CI 1.02-1.12), indicating a 1.7 fold increase in risk of death from the tumour for every score point increase.

Figure 4-14: FR-α Kaplan-Meier analysis (4). Demonstrating a significant difference in duration of survival between patient groups with tumours showing above and below median FR-α score 1 expression. Blue = high FR- α expression, Red = Low FR-α expression (p=0.0116, Log-rank test).

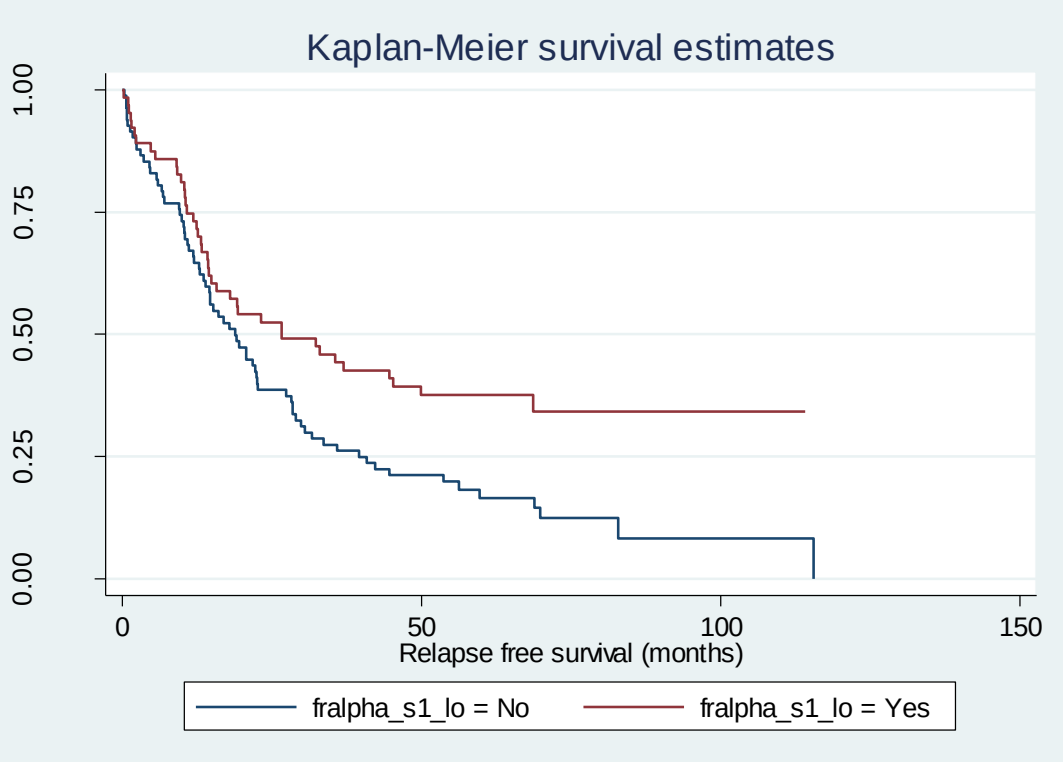

Figure 4-15: FR-α Kaplan-Meier analysis (5). Demonstrating a borderline significant difference in duration of survival between patient groups with tumours showing above and below median FR-α score 2 expression. Blue = high FR- α expression, Red = Low FR-α expression (p=0.0509, Log rank test).

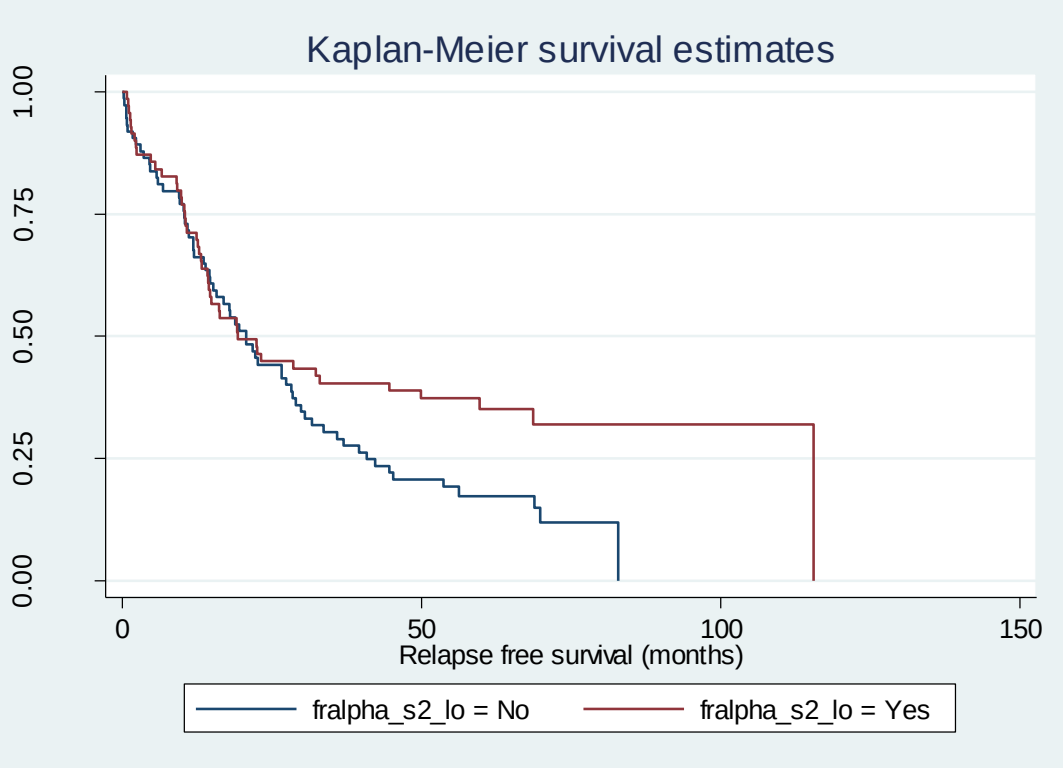

Figure 4-16: FR-α Kaplan-Meier analysis (6). Demonstrating a significant difference in duration of survival between patient groups with tumours showing above and below median FR-α mean score expression. Blue = high FR- α expression, Red = Low FR-α expression (p=0.0190, Log-rank test).

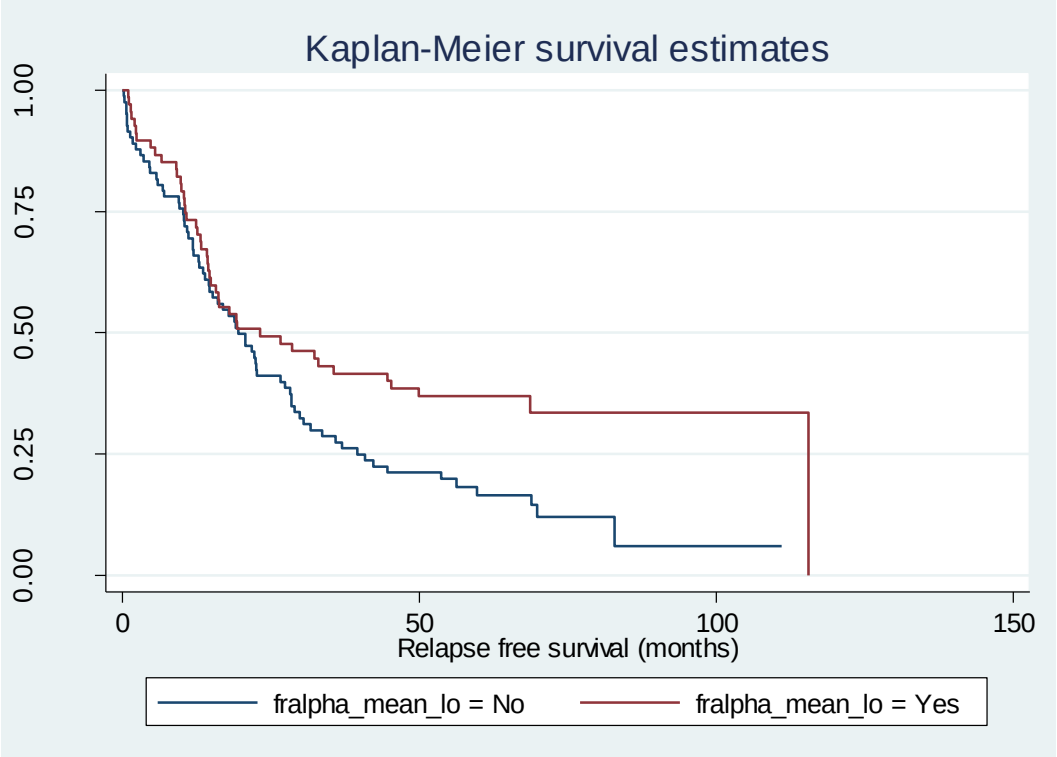

4.3.3.2. Relapse Free Survival and FPGS Score 1, 2 and Mean

The FPGS analysis was also performed three times and categorised by the median value and treated as a continuous variable. When categorised, none of the three scores were found to have a significant association with survival. (p=0.5879, 0.6629 and 0.5916 respectively, Log-rank test, Figure 4-17). Treating FPGS as a continuous variable did not generate any difference with no significant association with survival (p= 0.620, 0.396, 0.524 respectively, Cox regression).

Figure 4-17: FPGS Kaplan-Meier analysis (2). Demonstrating no significant difference in duration of survival between patient groups with tumours showing above and below median FPGS score 1 expression. (p=0.5879, Log-rank test) Blue = high FPGS expression, Red = Low FPGS expression. Similar patterns were observed for score 2 and mean score (data not shown).

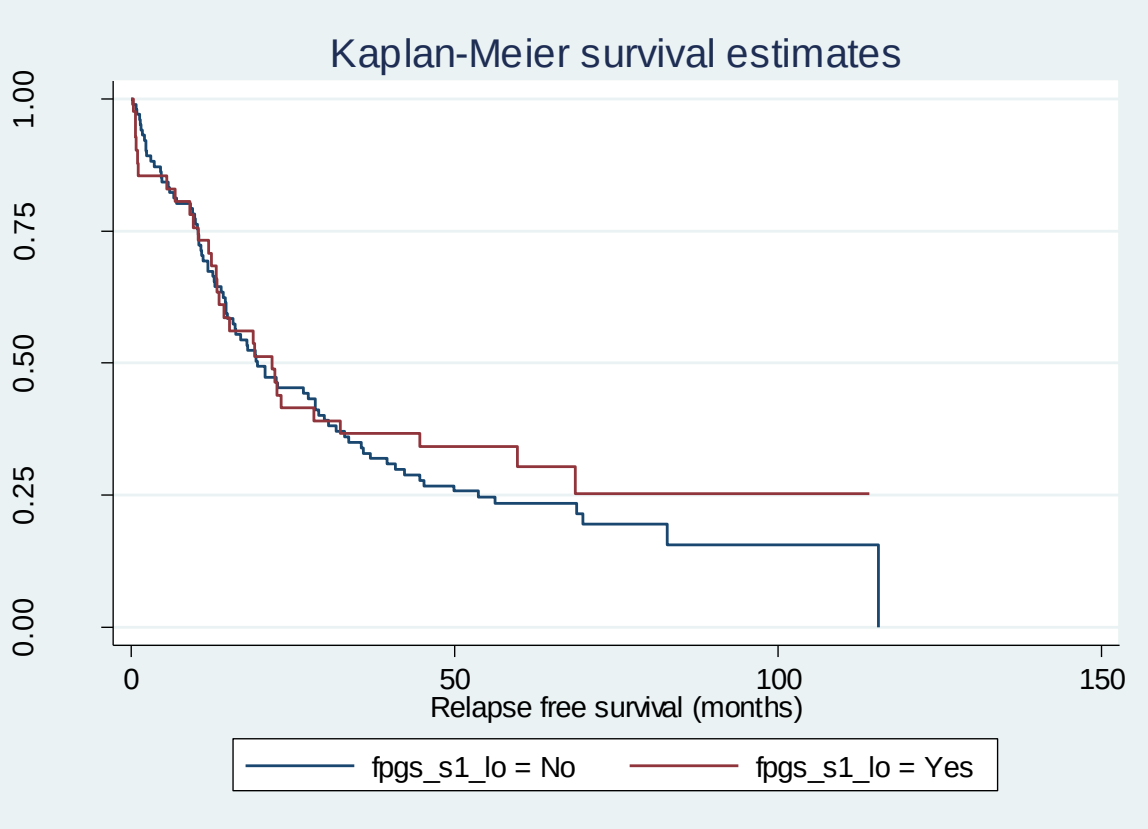

4.3.4. Relapse Free Survival Multivariate Analysis

In a multivariate model performed in a forward stepwise approach, both FR-α and FPGS failed to retain significance independent of residual disease, histology, grade and stage, the most statistically significant variables deduced from the relapse free survival analysis which dominated the model (p=0.000 Cox regression). Both significant FR-α scores were used in

the analysis (p=0.441, 0.303, Cox regression). Both significant FPGS scores were also analysed (p=0.506, 0.911, Cox regression).

4.3.4.1. Correlations between FR-α, FPGS and Other Prognostic Variables

In addition to the univariate and multivariate analyses, FR-α and FPGS scores were analysed to identify and correlation between them and the other prognostic variables using Bartletts test for equal variances. Significant correlations were found between FR-α and grade (p=0.0242), histology (p=0.0000), residual disease (p=0.0046), age (p=0.0205) and borderline significant association with CA125 (0.0549), no association was observed between FR-α and chemotherapy before surgery (p=0.2268) (Figure 4-18). The highest mean FR-α scores were observed in poorly differentiated tumours (7.12) of serous/papillary serous origin (7.16, 7.93 respectively). Patients over the age of 60, with suboptimal cytoreduction and CA125 levels of above 480 were also associated with a higher mean FR-α score (6.82, 7.82, 6.83 respectively). Significant correlations were found between FPGS and histology (p=0.0001), with the highest mean FPGS scores being observed in papillary serous tumours (8.74) (Figure 4-19). No significant associations were observed between FPGS and grade (p=0.8207), residual disease (p=0.0755), chemotherapy before surgery (p=0.7304), CA125 (p=0.1244) or age (0.2454).

Table 4-3: Summary of the correlations between FR-α/FPGS and the other prognostic variables.

Variable	Frequency	FR-α P value (one way Anova)	Mean FR-α Score	Std Dev	FPGS P value (one way Anova)	Mean FPGS Score	Std Dev
Grade		0.0242			0.8207		
Poorly Differentiated	77		7.12	4.06		7.68	3.10
Moderately Differentiated	45		6.09	4.32		7.32	3.36
Well Differentiated	41		4.88	4.42		7.67	3.22
Histology		< 0.0000			0.0001		
Adenocarcinoma	2		6.50	7.78		6.00	2.83
Endometrioid	49		6.33	4.46		7.63	3.10
Papillary Serous	41		7.93	3.66		8.74	2.98
Clear Cell	16		4.75	3.17		4.18	1.94
Mucinous	17		1.53	3.00		7.47	3.00
Serous	38		7.16	3.99		7.92	3.16
Residual Disease		0.0046			0.0755		
Suboptimal cytoreduction	62		7.28	4.30		7.92	3.26
Optimal cytoreduction	30		6.63	3.92		7.96	3.03
Complete cytoreduction	52		4.69	4.18		6.65	3.17
Chemo before surgery		0.2268			0.7304		
No	134		6.12	4.31		7.43	3.25
Yes	7		8.14	4.10		7.00	3.00
CA125		0.0549			0.1244		
<480 No	69		6.83	4.08		7.83	3.10
<480 Yes	67		5.40	4.49		6.99	3.18
Age at operation		0.0205			0.2454		
<60 No	106		6.82	4.10		7.80	3.15
<60 Yes	56		5.18	4.51		7.18	3.26

Figure 4-18: Statistical analysis of the relationship between FR-alpha IHC score 1 and the other prognostic variables. (p= 0.0242 grade; 0.000 histology; 0.0046 residual disease; 0.227 chemo before surgery, 0.0549 CA125 less than 480; 0.0205 age less than 60, Bartletts test).

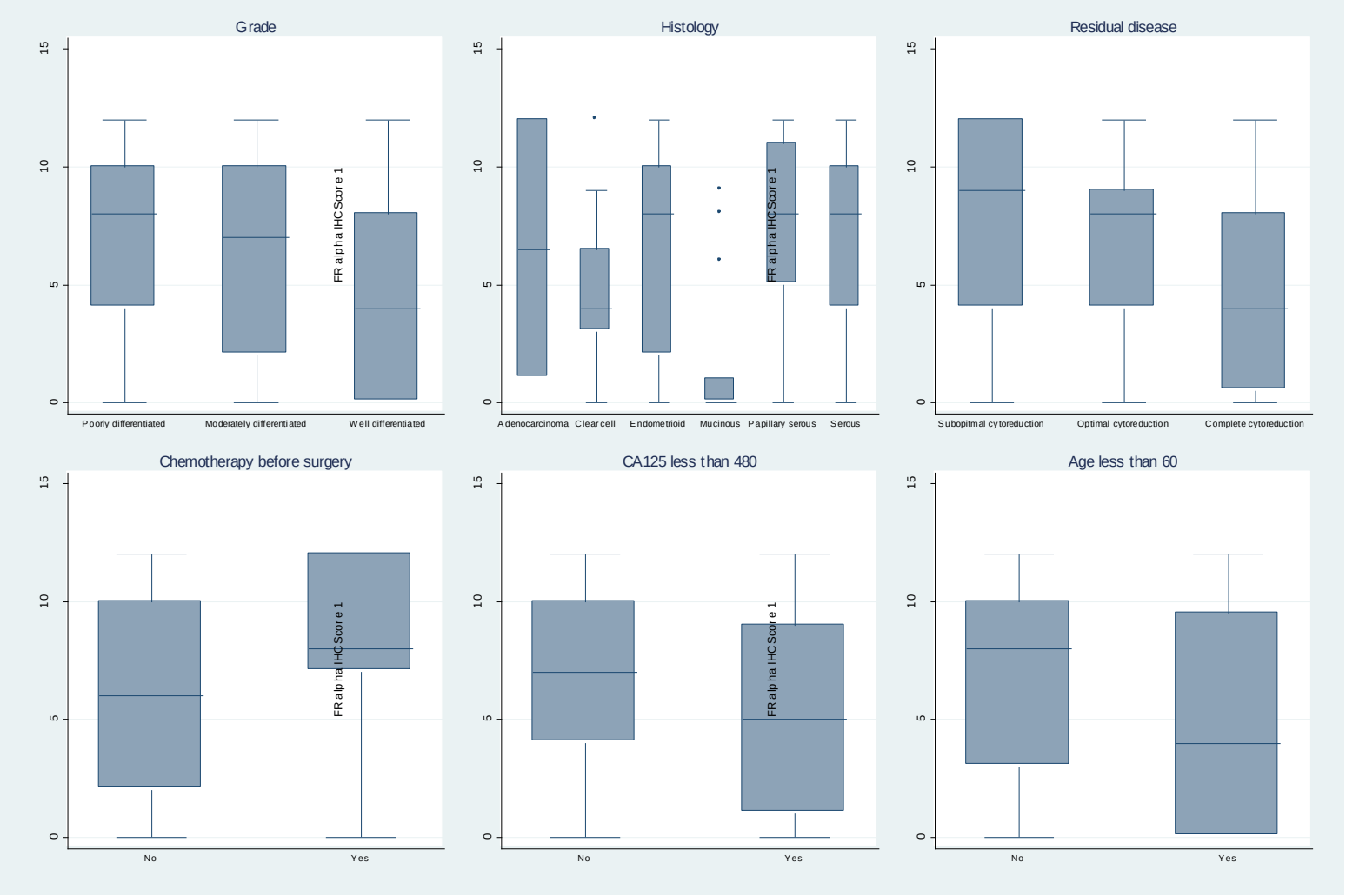

Figure 4-19: Statistical analysis of the relationship between FPGS IHC score 2 and the other prognostic variables. (p=0.821 grade; 0.001 histology; 0.076 residual disease; 0.730 chemo before surgery, 0.124 CA125 less than 480; 0.245 age less than 60, Bartletts test).

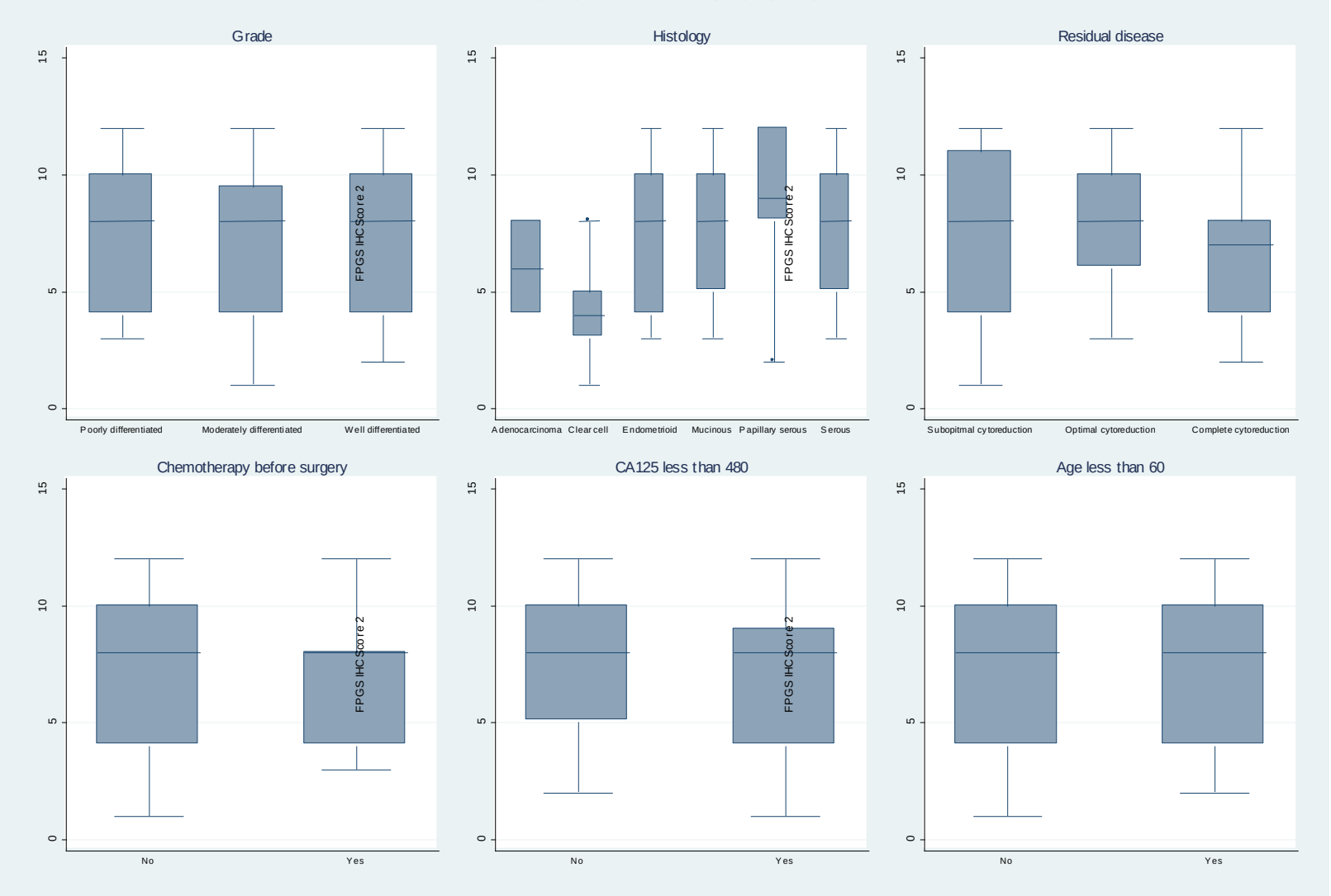

4.4. Discussion

The results of our study found FR-α expression in 89% of 167 ovarian cancer cases tested. This is in concordance with previous published data using LK26 and mOV18 antibodies on frozen tissue (Garin-Chesa et al., 1993; Miotti et al., 1987).

Significant correlation between FR-α expression and survival was observed, this is consistent with previous work, indicating a role for FR-α as a prognostic marker and potential therapeutic target for ovarian cancer (Toffoli et al., 1997). FR-α was found to be significantly associated with both overall survival (Figures 4-10 to 4-12) and relapse free survival (Figures 4-14 to 4-16), with patients with above median expression of FR-α having a significantly worse outcome than those with high expression. This indicates the role for high FR-α expression as an indicator of poor survival. Despite showing promising results in univariate analysis it did not, however retain its significance as a marker of prognosis independent of the other significant prognostic markers. When analysed in combination with grade, histology, residual disease, age and CA125 values it did retain its significance (Figure 4-18).

Toffoli et al (1997) found high expression of FR- α in 122 out of 136 (90%) ovarian tumour samples in a univariate analysis using the mOV18 monoclonal antibody and cytofluorometric analysis. FR-α was found to be overexpressed to a higher degree in ovarian neoplasms with a high histologic grade, advanced stage, serous histology and in a high percentage of cells in the S-phase (Toffoli et al., 1997). Our results support the results of this study as the frequency of expression is similar and the highest mean FR-α scores were observed in the serous and papillary serous histological subtypes. Strong FR-α expression was also associated with higher grade tumours with the poorly differentiated tumour group having the highest mean FR-α score. The lowest expression was observed in the mucinous tumour group, again this is consistent with previous published data suggesting non mucinous tumours have the lowest expression of FR-α (Elnakat & Ratnam, 2004; Mangiarotti et al., 2001).

More recently FR-α has been analysed in other tumour types including breast, colorectal and endometrial neoplasms with similar results (Brown Jones et al., 2008; Hartmann et al., 2007; Shia et al., 2008). All three of these studies were performed via the use of an antibody (mab343) developed by Wilbur Franklin and Philip Low, this antibody has not been previously described in the literature. It has recently been reported to be suitable for use on paraffin embedded tissue but is not commercially available. Shia *et al* tested mab343 on a

tissue microarray containing 152 normal colorectal mucosa samples, 42 adenomas, 152 primary and 52 metastatic colorectal carcinomas. Positive immunoreactivity was observed in 7% normal mucosa samples, 7% adenomas, 33% primary and 38% metastatic tumours. Positive expression was found to be significantly associated with age (<65 years, p=0.08) and presence of distant metastases (p=0.43), in addition univariate, but not multivariate analysis identified FR-α as a marker of poor 5 year disease specific survival (p=0.04) (Shia et al., 2008). Correlation between poor survival and high FR-α expression is consistent with the results observed in our study, however there is a contrast between age and survival with the highest expression observed in patients over the age of 60 in our study. The frequency of expression in colorectal cancer also appears to be higher than the results seen with the LK26 antibody where 6/27 (22%) cases were found to be positive, however this is inconclusive as our clone has not been tested on a cohort of this magnitude and it may be that FR-α expression is observed more frequently in colorectal carcinomas. Further work assessing the frequency of FR-α expression in colorectal carcinomas would be interesting.

Hartmann *et al (2007)* analysed FR-α expression using mab343 in breast cancer, a total of sixty three invasive breast cancer patient samples were analysed with divergent outcomes, thirty three had poor outcome with a median time to recurrence of 1.9 years. Thirty women comprised the good outcome group and were free of recurrence a minimum of seven years post diagnosis. High FR-α expression was found to be strongly associated with outcome (p=0.001). Staining was divided into two groups, strong (n=21) or weak (n=42). In the strong staining group 17 of 21 (81%) women had recurred compared with 16 of 42 women (38%) in the weak staining group (Hartmann et al., 2007). Again, the results of this study are consistent with the results observed in our study with the exception of the frequency of staining observed in breast cancer samples being significantly higher than our observations. 33% of breast cancer cases tested were found to display strong FR-α immunoreactivity, this is also in contrast to the results observed via the use of the LK26 antibody which reported strong FR-α immunoreactivity in 2/53 (3.4%) breast cancer samples tested with patchy staining observed in a further nine samples. This is more consistent with our results from our breast cancer case study where 2/49 (5%) of samples were found to be positive.

Finally, mab 343 was analysed on a TMA containing 310 evaluable cases of endometrial adenocarcinoma. Forty one percent were found to stain moderate/strongly. In addition to a

correlation with poor outcome this group were also found to be significantly associated with other poor prognostic factors such as advanced stage (p=0.028), nonendometreoid histology (p=0.001) and high grade (p=0.001). An association was also observed between moderate/strong staining and recurrence (p=0.0014) (Brown Jones et al., 2008). The results observed in this study were similar to the results observed in our study, with significant associations between FR-α being observed in relation to the same poor prognostic factors such as grade, stage and nonendometreoid histology. Similarly, in multivariate analysis, FR-α failed to retain its significance as an independent prognostic marker in both studies.

The results of these studies appear to correlate in the most part with the results observed in our study, despite this promise, studies using mab343 should be analysed with caution until more information is recorded, as the frequency of expression in all three tumour types analysed do not appear to be completely consistent with previous studies using mOV18 and LK26 antibodies on frozen tissues, nor are they completely consistent with the analysis performed using our antibody. There have also been reports of primarily cytoplasmic rather than membrane immunoreactivity and nuclear cross reaction with the use of mab343 which is inconsistent with the results of our study which clearly displays primarily membrane staining. It may be that mab343 is slightly cross reactive which may be the reason for the increased frequency of expression. This does not, however, appear to affect the survival results which appear to correlate well with the results of our study.

No significant associations were observed for FPGS expression and survival in either univariate or multivariate analysis (Figures 4-13, 4-17) and studies analysing this have not been previously reported. Despite this the expression of FPGS did follow similar trends to that of FR-α with the highest mean FPGS expression being observed in tumours of serous histology and lowest FPGS levels being observed in patients under the age of 60 with complete cytoreduction and CA125 values below 480 (Figure 4-19). The constitutive expression of FPGS in normal as well as tumour tissue may be the reason the correlations with survival are less obvious. Although a differential can be observed, with stronger immunoreactivity in tumour tissue than adjacent normal tissue the results may have been affected by this effect.

Age independently was not found to be a significant factor in prediction of survival in this cohort, although age is usually an important prognostic factor it may not be the most

important factor in ovarian cancer as the majority of women diagnosed are over the age of 40. Other factors may dominate in this disease such as stage and grade of tumour as often it is not diagnosed until later stages when disease has already advanced and spread beyond pelvic cavity. However when age is analysed in combination with FR-α scores it may be of more prognostic significance as patients over the age of 60 with high FR-α scores may be at a higher risk of death from the tumour than those patients with lower scores.

The results seen from this and the other studies described clearly indicate a role for high FR-α expression as an indicator of poor response and shorter survival when analysed taking into consideration the other significant prognostic variables. The reason for this is probably due to the cells conferring a growth advantage over other adjacent cells as the high affinity FR-α has for folic acid would allow maximal amounts of folate to be transported into the cell and used for the cells formation of new DNA and ultimately proliferation. Although this initially appears to be a negative attribute it may also be of great value in the determination of response of these patients to antifolates such as pemetrexed and additional studies using the antibody in combination with clinical data assessing response to pemetrexed would be extremely useful. As antifolates are not a first line therapy for the treatment of ovarian cancer the results of this study certainly warrant further analysis and investigation into the use of antifolates in this area and also in other tumours such as breast and colorectal cancers.

The Aperio Scan Scope CS system used for the generation of images can also be used for score analyses, producing computer generated scores. It would have been extremely interesting to use this software and use the results to compare the effectiveness of the automated system with manual scoring. Unfortunately, as this equipment was only recently purchased this was not possible and is beyond scope of this study, whose primary aim was not to test the effectiveness of a new technique, however this would be useful in future work.

In conclusion, FR-α but not FPGS shows great promise as both a prognostic marker of poor outcome and a potential determinant of response to both folate receptor targeted therapies and some antifolates such as pemetrexed which have a high affinity for FR-α, cells with high expression may take up the drug more readily, increasing the drug concentration in pathologic cells and reducing toxicity in normal tissue. Ovarian cancer was the main focus of

this study as it appears to express FR-α most consistently but use of our antibody to investigate expression in other tumour types would also be of great value, particularly as antifolates are already routinely used in various other solid tumours.

Chapter Five

Chapter Five

5. Cell Studies

After successful generation, characterisation and validation of anti-FR-α and FPGS MAbs at Novocastra laboratories via the methods described in chapters 2 and 3, it was the aim to exploit the novel antibodies via the generation of as much preliminary data as possible before the antibodies became commercially available. There were a number of different study ideas and paths to follow to generate interesting preliminary information to assess the potential of the antibodies for a number of different applications. Once the antibodies were submitted for approval by the consultant pathologist Dr. Hoffman and transferred to the production department at Novocastra all subsequent studies were carried out at the Northern Institute for Cancer Research (NICR) at Newcastle University.

As expression of both FR-α and FPGS may be important in the determination of response to antifolates and folate targeted therapies this was another area in which generation of data may be significant. A number of studies have identified potential modulators of FR-α expression including oestrogen regulation and extracellular folate concentration as reviewed in section 1.8.4, which would potentially increase the efficiacy of folate targeted therapies by selectively upregulating its expression (Kane et al., 1988; Kelemen, 2006; Kelley et al., 2003). Based on previous studies it is hypothesised that cells maintained in low folate conditions would express more FR-α than cells in high folate conditions (Kelley et al., 2003), detectable by WB using clone BN 3.2.

It is also hypothesised that cells treated with oestrogens may downregulate FR-α expression as oestrogen is thought to have a negative correlation with FR-α expression (Kane et al., 1988). The relationship between folate concentration, oestrogen regulation and FPGS were also investigated as an adjunct to the FR-α studies.

Comparative studies using the FR-α antibody generated in this project and the mOV18 antibody were also planned in order to determine whether the FR-α antibody was suitable for use on frozen tissue and to compare the staining with the only commercially available product.

During the work another antibody directed against FR-α was identified, known as the LK26 antibody. It was generated in 1985 to an antigen termed LK26 which was subsequently found to be FR-α (Garin-Chesa et al., 1993). Like the mOV 18 antibody this antibody is unsuitable for use on

paraffin embedded samples or for WB. It was decided that, where possible this antibody would also be used to generate extra data although not all samples could be tested due to limitations with tissue availability. Some IHC on frozen tissue was planned to observe any similarities or differences between the staining using all three antibodies. Like mOV18 and the data generated from initial FR-α experiments on paraffin embedded tissue panels, LK26 expression has been reported to be highly restricted in normal tissues with the exception of placenta and a subset of simple epithelia. Ovarian adenocarcinomas were also found to have high expression which is consistent with the data generated in this project and previous published data using mOV18. LK26 expression was not seen in normal adult ovary with the exception of the epithelial lining of some benign ovarian cysts (Garin-Chesa et al., 1993). This is consistent with the expression observed with the FR-α antibody clone BN 3.2. Mesothelioma samples were found to express little LK26, again this is consistent with the FR-α data generated from the BN3.2 antibody. Low/heterogeneous levels of expression were observed in endometrial, breast, lung and renal cell carcinomas, again this was consistent with the results seen with the BN3.2 antibody which is extremely encouraging (Garin-Chesa et al., 1993).

Assessment of the antibodies for other applications such as immunofluorescence (IF) and fluorescence activated cell sorting (FACS) may also be useful, it was planned to carry out preliminary studies to test the suitability of the antibodies for these applications. If successful it is likely that the antibody may have potential neutralising properties and it was planned to perform growth assays on cells known to express FR-α for any such properties it may possess, as the antibody alone may have direct therapeutic potential. In order to achieve this some FR-α antibody was purified in preparation for growth assays. This was achieved by column chromatography on a protein A sepharose (Prosep A, Millipore) column. The resultant purified antibody was stored in PBS in preparation for use in growth assays. This ensured that any growth factors present in the neat media would not have any effect on the cell growth and the effects observed would be due to the antibody alone.

As FR-α is already known to be highly expressed in the majority of ovarian tumours, these patients may all be selected for folate targeted therapies automatically without the need for a prior screening IHC test. It is hypothesised that use of the BN 3.2 antibody as a companion diagnostic may be more relevant in tumours overexpressing FR-α at a lower frequency in other tumour types. Breast cancer samples, collected in conjunction with clinical trials of the antifolate pemetrexed

were also analysed to observe the frequency of expression in these tumours as it may have a role in the prediction of response to pemetrexed where its expression is high.

5.1. Cell Studies - Aims and Objectives

- Generate some preliminary data on the potential applications of the antibodies generated.
- Investigate the effect of oestrogen modulation on expression of FR-α and FPGS proteins.
- Investigate the effect of folate modulation on expression of FR-α and FPGS protein.
- Assess suitability of FR-α antibody for IHC on frozen tissue and comparative studies with the commercially available mOV18 antibody.
- Assess expression of FR-α on a breast tumour panel provided by Eli-Lilly collected in conjunction with clinical trials of pemetrexed.
- Assessment of suitability of the FR-α antibody for application in IF and FACS.
- If IF and FACS successful perform cell growth assays for identification of any potential neutralising properties the FR-α antibody may possess.

5.2. Oestrogen Regulation Study – Materials and Methods

5.2.1. Culture and Treatment of Cells

The human ovarian cell lines OSEC2 (normal human ovarian surface epithelium), OVCAR-3 (human ovarian adenocarcinoma) and MDAH 2774 (human ovarian adenocarcinoma) were kindly grown and provided by Dr. Ann Fisher for use in this study. Cells were cultured in 96 well sterile culture plates in RPMI 1640 (Sigma) overnight, washed and grown for 72 hours in oestrogen depleted conditions in phenol red free (PRF) RPMI with dextran coated charcoal (DCC), the purpose of the DCC was to remove any steroid hormones from the media. Cells were then treated in PRF-RPMI-DCC for 48 hours.

Treatments were either;

- No treatment
- Vehicle (ethanol)
- Oestrogen (oestraidol) 10^{-6}, 10^{-8}, 10^{-9}, 10^{-12} M doses.

Cell pellets were then obtained and prepared for WB according to the methods previously described (section 3.3.4) to determine the effect of oestrogen treatment on the level of expression of FR-α. It is hypothesised that oestrogen treatment may downregulate the expression of FR-α. (Kelley et al., 2003; Rochman, Selhub, & Karrison, 1985, Kelley, 2003 #37) As the point at which FR-α expression is first initiated between normal and tumour cells and the mechanism by which this occurs is still unknown, normal human ovarian surface epithelial cells were also used in this study to observe any changes in expression which oestrogen treatment may cause in these cells.

5.3. Oestrogen Regulation Study - Results

Figure 5-1: FR-α oestrogen regulation WB. Detection of FR-α WT protein by WB on three cell lines; OVCAR-3; OSEC2 and MDAH treated with oestrogen via use of the generated FR-α BN3.2 antibody. 0= no treatment, V= vehicle. An antibody to α-tubulin (55kDa) was used as a loading control to correct for variations in loading between samples.

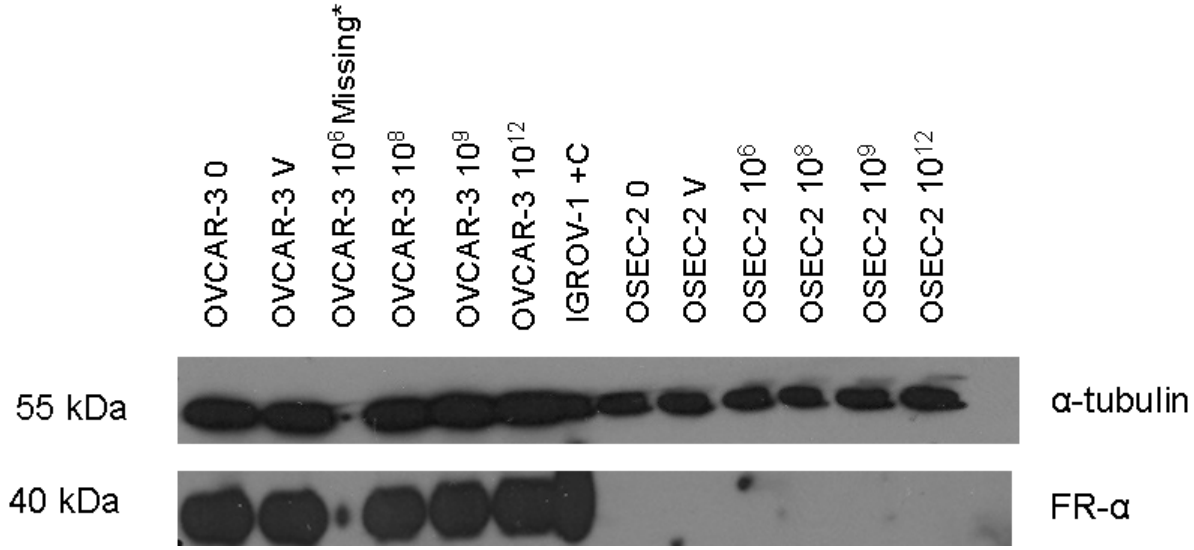

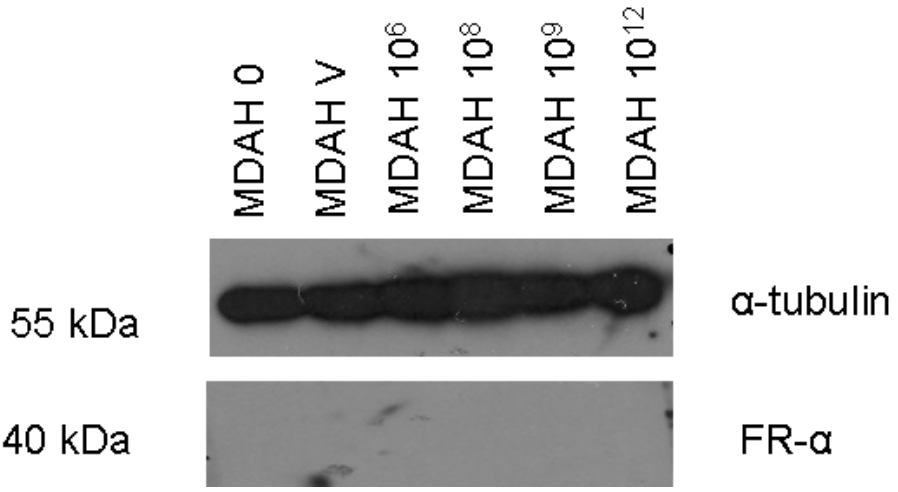

No FR-α expression was observed in the OSEC-2 or MDAH cell lines. Expression was observed in the OVCAR-3 cell line although this did not appear to alter with oestrogen treatment (Figure 5-1).

5.4. Oestrogen Regulation Study – Discussion

The results generated from the oestrogen regulation study were limited as only one cell line (OVCAR-3) showed any reactivity to FR-α and the expression did not appear to decrease with oestrogen treatment (Figure 5-1), as hypothesised and as has been previously reported in the literature (Kelley et al., 2003). It was planned to carry out an additional control experiment to ensure the system was working and to show that oestrogen treatment did have an effect by probing the membranes with a known oestrogen regulated protein. Western blotting to detect oestrogen receptor expression was initially planned as the control experiment, using an oestrogen receptor antibody (Novocastra Laboratories), however no specific reactivity was observed via WB in any of the cell lines used. A number of different antibodies to other oestrogen regulated proteins were also tested until availability of sample limited further tests, progesterone receptors A and B, PS2, cathepsin B and D, heat shock protein (HSP) 27 and C Myc were identified as oestrogen regulated proteins (Langdon et al., 1995; Nakopolou et al., 1995; Rochefort, 1995). Antibodies were located and tested via WB analysis, however, none of the antibodies tested appeared to show any reactivity with any of the cell lines. It may be that the cell lines selected for use in this work are not the optimal selection of cell lines to use for the control proteins tested, and the results of these studies cannot be relied on without a valid control antibody known to react with a protein regulated by oestrogen.

Unfortunately, due to time limitations it was not possible to culture these cells specifically for this experiment. The cells used were kindly donated by Dr. Ann Fisher and were unfortunately not optimal for use in this experiment. Additional experiments would need to be performed using different cell lines to clarify this result as these results are, at present inconclusive as FR-α does not appear to alter upon treatment with oestrogen. With the failure to generate any data at all in 2/3 cell lines and the absence of a valid control it is not possible to determine whether the results of this experiment are accurate and reproducible. To draw a conclusion different cell lines such as IGROV-1 ovarian cancer and HeLa cervical cancer cell lines should have been used as these are the cells reported to respond to oestrogen treatment in the literature and are both known to express high levels of FR-α (Kelley et al., 2003). In addition, these experiments were performed in media containing supra physiological levels of folate which may also have had an effect on FR-α expression. The media used in these experiments may have downregulated FR-α expression therefore even if there had been an effect on the expression it would not have been possible to determine if this was due to the oestrogen or the effect of the use of supra physiological levels of

folate in the media. Treatment of the cells with an antioestrogen such as Tamoxifen may have also been tested in addition to oestrogen treatment as this would have potentially upregulated FR-α and would be a useful additional experiment. Unfortunately as there was insufficient time available to carry out these experiments independently it had to be concluded at this point with a view to re-investigating this as future work, despite this the fact the experiment was performed was worth mentioning as there is much possibility for expansion and further investigation. Despite this the potential still remains to selectively upregulate FR-α expression to increase the efficiacy and frequency of tumours for folate receptor targeted therapies.

5.5. Extracellular Folate Concentration Study – Materials and Methods

Extracellular folate concentration is hypothesised to affect the level of expression of FR-α; as the requirement for folate is altered the expression of the receptor is thought to alter to reflect this change, with upregulation in folate depleted conditions and downregulation in high folate conditions where there is lesser need for a high intracellular folate concentration. *In vitro* studies have also demonstrated that this is the case (Kane, Elwood et al. 1988; Doucette and Stevens 2001).

The human ovarian carcinoma cell lines IGROV-1, SKOV-3 and SW626 and the cervical carcinoma cell line HeLa were selected for use in this study due to their known, varied levels of expression of FR-α as seen from previous WB data and as these cells have been used previously in the literature to investigate the effect of folate concentration on FR-α expression (Miotti et al., 1995).

Cell lines were cultured in normal conditions (2mM L-glutamine, 5% CO_2, 37 ^{o}C) using standard aseptic tissue culture techniques. The different culture conditions were as follows:

- High folate (HF) media – 500 mls RPMI 1640 (Sigma), 50 mls FBS, 5 mls penicillin/streptomycin. This media contains supra physiological concentrations of folate but the precise level of folate cannot be measured.
- Normal folate (NF) media – 500 mls folate free RPMI 1640 (Gibco cytogenetics), 50 mls dialysed FBS, 20μM folinic acid, 5mls penicillin/streptomycin. This media also contains

supra physiological concentrations of folate but the concentration can be more accurately determined via the use of folate free media.

- Low folate (LF) media – 500 mls folate free RPMI, 50 mls dialysed FBS, 20 nM folinic acid, 5mls penicillin/streptomycin. Although termed low-folate this media actually contains a concentration of folate approximating physiological levels in humans, for the purpsose of this study it was termed low folate media.

Once adapted to low folate media the cells were maintained for a period of one month before collection of cell pellets for subsequent protein estimation and WB using the methods described in section 3.3.4. All four cell lines were tested by WB for HF, NF and LF media to observe the effect of alteration of extracellular folate concentration on both FR-α and FPGS expression.

5.6. Extracellular Folate Concentration Study – Results

5.6.1. FPGS

Figure 5-2: FPGS extracellular folate concentration WB. Representative WB (n=3) showing detection of FPGS WT protein by WB on four cell lines (IGROV-1, SKOV-3, SW626 and HeLa) grown in LF, NF and HF media via use of the generated FPGS NN3.2 antibody. An antibody to β-actin was used as a loading control to correct for variations in loading between samples.

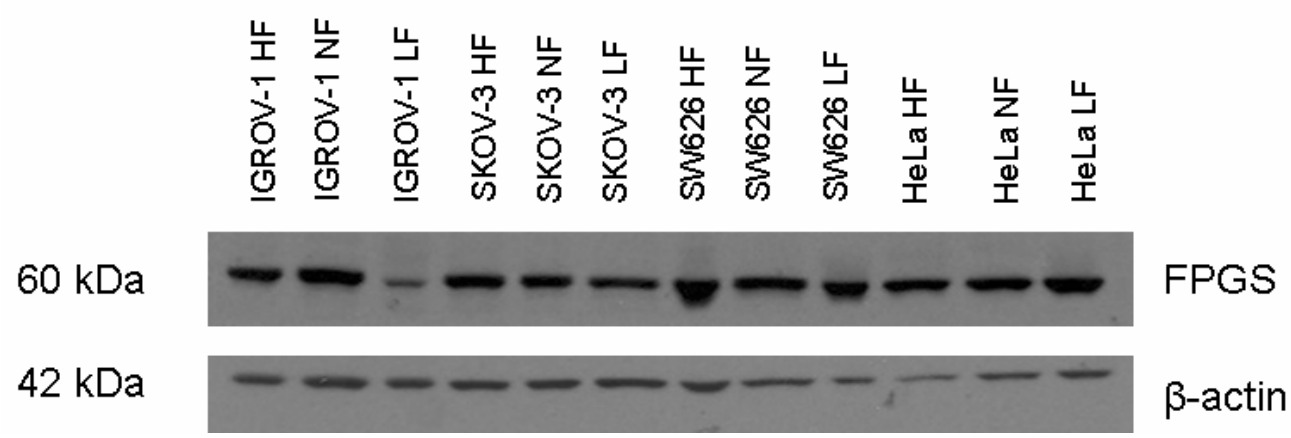

Slightly lower FPGS expression was observed in the IGROV-1 LF cell line relative to the NF and HF conditions. Similar expression was observed in all three of the SKOV-3 and SW626 cell lines. Similar expression was also observed in HeLa cells, although a little less sample was loaded in the

HF sample which may indicate that FPGS expression in the HF condition was slightly lower than in the NF and LF conditions (Figure5-2).

5.6.2. FR-α

Figure 5-3: FR-α extracellular folate concentration WB. Representative WB (n=3) showing detection of FR-α WT protein by WB on four cell lines grown in LF, NF and HF media via use of the generated FR-α BN3.2 antibody. An antibody to α-tubulin was used as a loading control to correct for variations in loading between samples.

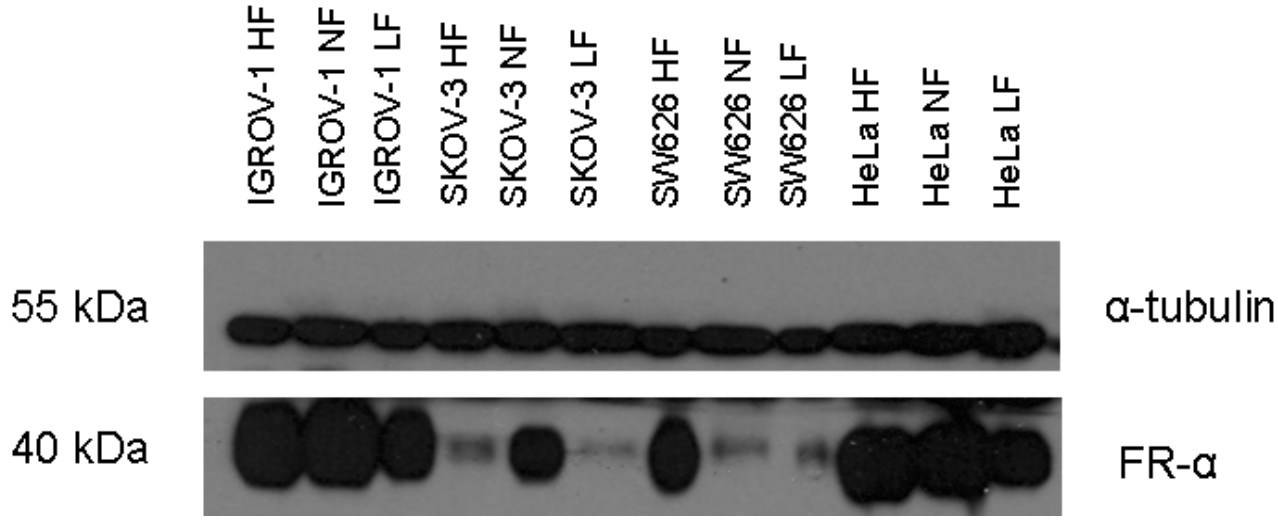

Slightly lower expression was observed in the IGROV-1 LF cell line. Lower expression was observed in the SKOV-3 HF and LF cells and higher expression in the NF cells. High expression was seen in the SW626 HF cells and lower expression in the NF and LF cells. Slightly lower expression was observed in the HeLa LF cells relative to the NF and HF cells (Figure5-3).

5.7. Extracellular Folate Concentration Study – Discussion

The results of this preliminary study indicate there was no significant correlation between folate concentration and FPGS expression, this is not consistent with the results from a previous study indicating that folate restriction significantly increases FPGS activity (Gates, Worzalla, Shih, Grindley, & Mendelsohn, 1996). In the IGROV-1 cells, a subtle difference was observed with lower FPGS expression in the LF cells in relation to HF and NF (Figure 5-2). This contradicts the results observed in this study as the LF condition appeared to have reduced the expression of FPGS. Little fluctuation between FPGS expression was observed in the SKOV-3 and SW626 cells, indicating

extracellular folate concentration does not affect FPGS expression in these cells. The result obtained from the HeLa cells, although very subtle also indicated that FPGS expression was slightly higher in cells grown HF media, although in this HF condition the exact level of folate present in the media is not measurable (Figure 5-2). Again these results appear to contradict the results seen in previous studies (Gates et al., 1996).

For FR-α expression both the IGROV-1 and HeLa LF cells appeared to have slightly lower expression compared to the HF and NF condition, again this is in contrast to the hypothesis (Figure 5-3). SKOV-3 NF was found to have significantly higher expression than the HF and LF conditions, again this does not support the hypothesis that FR-α is upregulated in response to lower concentrations of folate. For the SW626 cells the HF condition was found to have the highest FR-α expression. (Figure 5-3) None of the results from this preliminary study appear to support the hypothesis that low folate concentration increases FR-α expression, despite previous reports indicating that folate receptor function is regulated in response to altered folate concentration in culture (Doucette & Stevens, 2001; Kane et al., 1988; Kelemen, 2006). This may have been due to fluctuations in concentration of folate in the dFCS, although the same batch was used in all experiments. Although denoted LF, the lowest folate condition actually contained a concentration of folate (20nM) approximating physiological levels in humans. Future work may be focused upon repeating this experiment with a true low folate condition, i.e. containing 10nM folinic acid or below to observe any differences restricted folate has upon FR-α expression. As for the results observed in the oestrogen regulation experiment this is a useful initial experiment which is worthy of further investigations, although due to time limitations expansion was not possible in this project.

5.8. mOV18 Comparative Study –Materials and Methods

IHC on frozen placenta and normal, primary and metastatic ovarian tumour tissue sections, kindly donated by Dr. Jane Margetts was performed to generate results to satisfy two aims;

- To assess the suitability of the FR-α antibody for application on frozen tissue – if specific staining was observed it may have been likely that the antibody recognises the native conformation of the protein and may possess neutralising properties.
- To directly compare the expression and staining between FR-α and the commercially available mOV18 antibody to observe any correlation in the staining between them. As

no other known antibodies suitable for use on paraffin embedded tissue exist, much of the information on FR-α tissue expression had been elucidated by the use of the mOV18 antibody on frozen tissue. It would be expected that the staining would be similar in both intenstity, proportion of tumour stained and cellular localisation.

A total of 39 samples were available for testing, although there were limitations upon the amount of tissue which could be used. In addition to placenta and normal ovary, samples from 10 ovarian cancer patients were available for use, primary tumour samples and metastases from the same patient were collected. Each patient sample was numbered 1-10 and metastases were numbered with the patient number and M1,2 3 etc to identify metastases from each patient. The FR-α antibody only was used in this study.

Frozen sections were air dried under a fan for 1 hour prior to fixation. Initially a pilot test was performed to determine the optimal fixation method, no fixation, methanol, acetone and formalin were used and the sections were incubated for 10 minutes and air dried for 10 minutes post fixation. The remaining IHC was carried out using the same Novolink polymer method as used throughout the project and sections were treated in the same way as paraffin embedded samples, differing only in the initial steps and omitting the antigen retrieval step.

5.9. mOV18 Comparative Study - Results

Initial tests on ovarian sections showed little/ no correlation between the staining using the mOV18 antibody and the BN 3.2 antibody. As this study was not conclusive it was decided to discontinue this study as accurate comparisons could not be drawn from the data generated. The FR-α staining was not similar to the mOV 18 staining in intensity or pattern, although there was some staining seen it was weak and heterogeneous. It was decided that unless corresponding frozen and paraffin samples could be collected that accurate comparisons could not be made between the antibodies and that the generated BN 3.2 antibody was not suitable for use on frozen tissue. As it was the significance of the comparative study which was most important the data generated from use of the mOV18 antibody was not thought to be significant alone. As the BN 3.2 antibody was found to be unsuitable for use on frozen tissue it was also unlikely that it would have any neutralising properties and recognise the protein in its native conformation via growth assays,

although it was decided to assess the suitability for use in IF before deciding whether to proceed with growth assay experiments.

It was not until epitope mapping the BN 3.2 antibody that a significant development was observed which may enable the antibodies to be compared on frozen tissue, it was at this point that this experiment was revisited. Epitope mapping and the analysis is described in section 3.5.12. It was hypothesised that addition of a reducing agent to the tissue may denature the sample and expose a linear epitope recognised by the BN 3.2 antibody. The sections were treated with 5% DTT in protein block for 10 minutes prior to addition of the primary antibody. This additional step had not been previously reported as an IHC technique as it was thought this may destroy the antibody conformation; however the step appeared to restore the epitope recognised by the BN 3.2 antibody, allowing it to bind to the tissue in a similar manner to that of both the mOV18 and LK26 antibodies. Similarly treatment with DTT was also seen to destroy the epitope recognised by the mOV18 antibody causing a reduction in staining. In this study five sections only were used for each antibody and treatment due to limited supplies of tissue.

Figure 5-4: FR-α mOV18 comparative study. Immunohistochemical staining for FR-α using clone BN 3.2, mOV18 and LK26 antibodies on sections of freshly frozen placenta, normal ovary and ovarian adenocarcinoma primary and metastases. Note the similarities in staining between the mOV 18, LK 26 non reduced and the BN 3.2 reduced samples. Also of particular note is the atypical staining in the BN 3.2 non-reduced samples and reduction in staining in the mOV18 reduced samples.

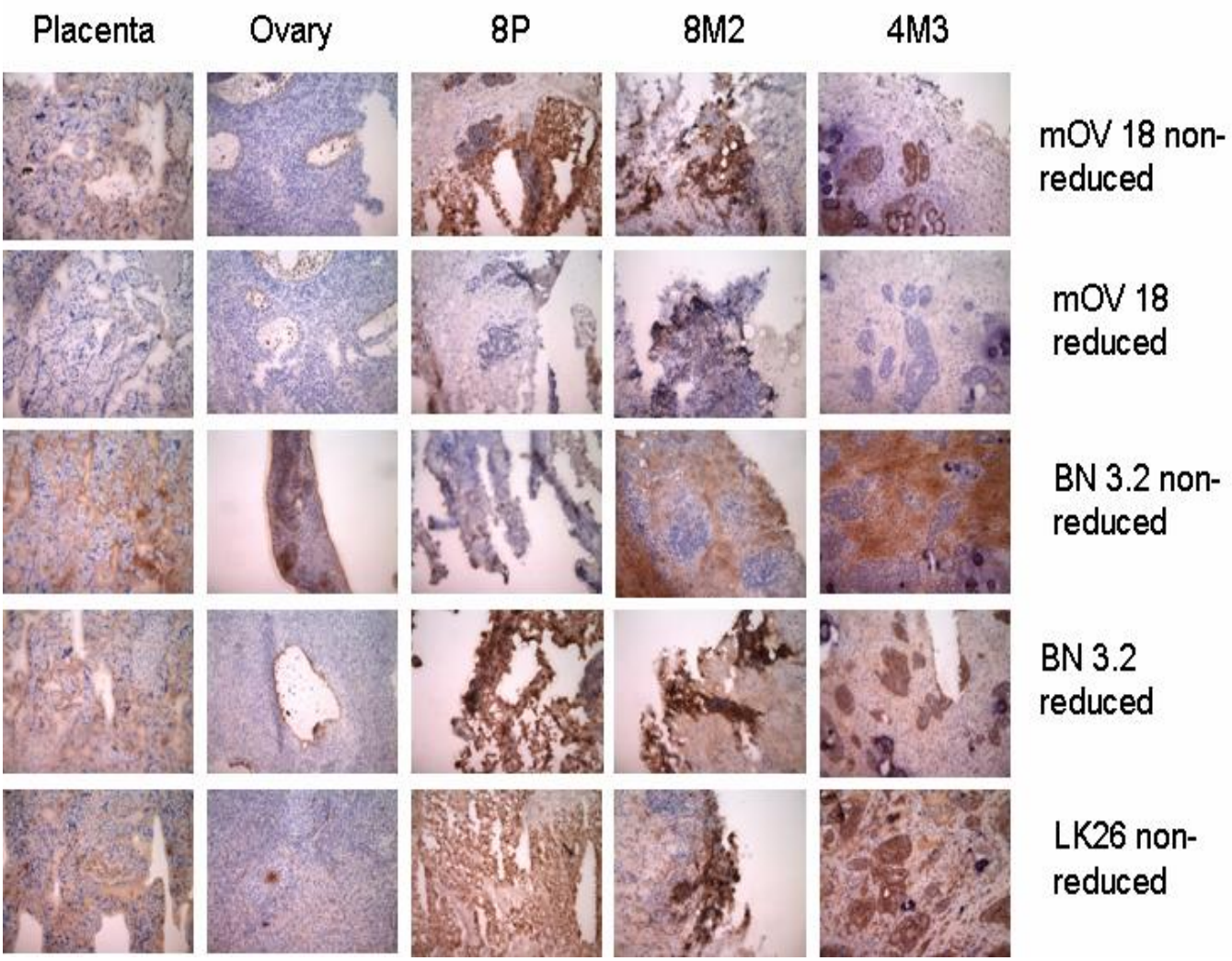

5.10. mOV18 Comparative Study – Discussion

When compared with the mOV18 antibody on frozen ovarian tumour tissue the staining did not appear to be comparable, BN3.2 did not stain any of the tissues as strongly as mOV18. The FR-α antibody may not be as effective in detection of the native conformation of the protein although it does, however appear to recognise an epitope linear in nature as it is suitable for WB. It is likely that the mOV18 antibody recognises a conformational epitope as it is unsuitable for WB analysis. Treatment of the tissue with DTT and IHC with mOV18 causes a reduction in staining, indicating that the epitope is destroyed by reduction, again supporting the theory that mOV18 recognises a conformational epitope (Figure 5-4). This was not performed on LK26 due to tissue limitations.

The data generated from this study has shown that treatment of frozen tissue with a reducing agent exposes the epitope recognised by BN 3.2, allowing more accurate comparisons between the staining seen from clone BN 3.2 compared with the other antibodies on the market, LK26 and mOV18. Although more studies were not carried out due to time limitations this would be an interesting experiment to perform and tissue may be easier to obtain than attempting to find corresponding frozen and paraffin embedded samples from the same patient. The technique of reducing samples before performing IHC is not commonly used, possibly due to the assumption that reduction of a sample may destroy the antibody structure. One report of use of reducing agents was found where paraffin embedded samples were treated with DTT and 2-mercaptoethanol before performing IHC, although in this case no effect was observed (Costa, Jacobsson, Collins, & Biberfeld, 1986). The results seen were comparable to that of the non-reduced LK26 and mOV18 samples, however, there were insufficient samples to score and perform statistical correlative analysis. A study using a larger number of samples and statistical analysis may be of value, although may not be necessary as sufficient data has been generated to fully validate the BN 3.2 antibody and to ascertain that is it specific for its target.

5.11. Breast Cancer Case Study – Materials and Methods

Samples of breast cancer cases collected in conjunction with clinical trials of Pemetrexed were provided by Eli Lilly to observe the frequency of expression of FR-α in breast cancer. Clinical data was not available so analysis of response could not be performed. Forty nine samples in total were provided and IHC was performed using the Novolink polymer kit as previously described in section 3.3.6.2.

5.12. Breast Cancer Case Study – Results

Of thirty eight evaluable cases only two (5.3%) displayed strong immunoreactivity, one section (2.6%) displayed moderate reactivity, ten (26%) displayed weak reactivity and the remaining twenty five samples (66%) were negative.

Figure 5-5: FR-α Breast cancer IHC case study. Immunohistochemical staining for FR-α on six breast cancer case studies using clone BN3.2. Negative/very weak staining was observed in the majority of samples (a,b,c), moderate staining (1+-2+) was observed in one sample (d) and strong staining (3+) observed in two samples tested. (e,f).

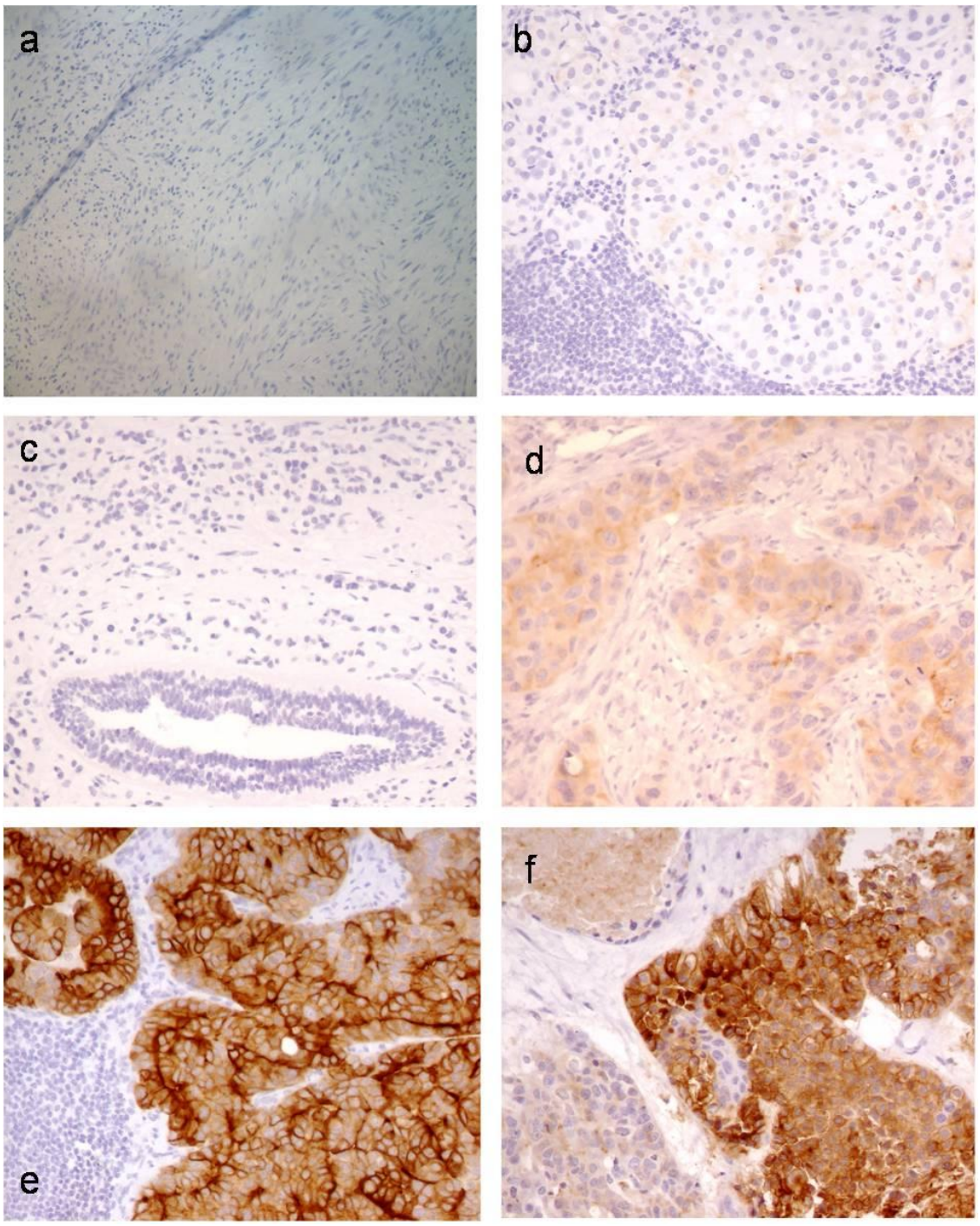

5.13. Breast Cancer Case Study - Discussion

Few samples showed FR-α expression, out of thirty eight evaluable samples tested only two (5.3%) displayed strong FR-α expression (Figure 5-5). These samples were collected in connection with clinical trials of Pemetrexed and it was inferred that this would be the key in determination of response, however this has not been found to be the case and unfortunately the clinical data has not been made available so no precise conclusions can be drawn from this study. Although only a small number of cases were found to be positive this may still be of significance as it may indicate a subset of breast cancer patients with tumours which may respond well to folate receptor targeted therapies. The striking difference between the weak and strongly immunoreactive samples would allow for a distinguishable positive or negative result. Unfortunately it is not known whether these tumours are primary or metastatic tumours. It would be interesting to observe the clinical information as it may be that the strong subset of tumours are oestrogen regulated or may even be be ovarian metastases. Such patients may benefit from other therapies aimed at modulating FR-α expression to increase the potential efficiacy of folate targeted therapies.

Despite the lack of clinical data this study has been useful as the results obtained are concomitant with the results previously seen via the use of the LK26 antibody on frozen breast cancer tissue, of fifty evaluable cases only two (4%) showed homogeneous LK26 expression with a further nine (18%) cases displaying weak, patchy expression.

Additional studies assessing the frequency of expression of FPGS may also be useful although in this study there were only sufficient samples to test FR-α.

Future testing on larger cohorts of breast cancer samples to further test the frequency of FR-α expression in breast cancers would be extremely interesting and this is a useful preliminary experiment demonstrating that investigation of FR-α expression in breast cancer is worthy of further investigation.

5.14. Immunofluorescence Studies – Materials and Methods

The suitability of the FR-α antibody for application in IF was assessed, if successful it was hypothesized that clone BN 3.2 may also possess potential neutralising properties as, like frozen tissue, the cells are in their native conformation. mOV 18 was also tested for comparison.

Multiple 8 well glass culture chamber slides (Nunc) were used for IF. The IGROV-1 ovarian carcinoma cell line was used in all IF studies as it has been found to express a high level of FR-α protein in previous studies. Initially a pilot study to determine the optimal cell seeding density, antibody concentration and cell fixation method was performed. 100, 1000, 2000 and 5000 cells were added to the first 4 wells of the 8-well chambers and repeated until a total of 10 chambers had been seeded. The cells were incubated for 48 hours at 37^{o}C to allow the cells to adhere and multiply, spreading over the surface of the slide. The chambers were then washed in ice cold PBS and fixed with either ice cold methanol at -20^{o}C or 10% formalin for 10 minutes. The methanol/formalin was aspirated and cells were rehydrated in PBS for 5 minutes then washed twice in PBS prior to blocking for 1 hour at RT or 4^{o}C overnight in blocking solution. (KCM buffer- [120mM KCl, 20 mM NaCl, 10 mM Tris/HCl pH 8, 1 mM EDTA] + 0.1% Triton-x-100 (Sigma) , 2% BSA, 10% dried milk powder). After incubation the blocking solution was removed and FR-α, FPGS and mOV 18 antibodies at 1/10, 1/20, 1/50 and 1/100 dilutions in blocking solution were added to the wells and incubated for 1-2 hours at RT or overnight at 4^{o}C. The cells were then washed three times for 15 minutes each time in washing solution (KCM buffer + 0.1% Triton-x-100) on a platform shaker. A fluorescent labelled antibody, Alexa fluor 594 (red) labeled goat-anti mouse IgG, (Invitrogen, Molecular Probes) at a dilution of 1/200 in blocking solution was then added to the cells and incubated in the dark for 1-2 hours at RT or 4^{o}C overnight. The cells were again washed three times in PBS, protected from the light, allowed to dry and mounted using hard set Vectashield mounting medium with DAPI to allow visualisation of the nucleus. The cells were analysed by fluorescence microscopy.

5.15. Immunofluorescence Studies - Results

The initial pilot studies were unsuccessful, fluorescence was observed via use of the mOV18 control antibody although no specific fluorescence could be seen with the FR-α antibody.

This experiment was discontinued but following epitope mapping it was decided to revisit the IF studies, discussed in detail in section 3.5.12. It was decided that another study would be performed as with the frozen study, this time reducing the samples with 5% DTT during the blocking step to observe the effect this may have on fluorescence.

The reducing agent appeared to alter the protein structure, allowing the FR-α antibody to bind to the membranes. The opposite effect occurred with the mOV18 antibody and after treatment with DTT the fluorescent signal was reduced (Figure 5-6).

Figure 5-6: IF comparative study WB. IF photographs comparing fluorescence between the mOV 18 antibody and the BN3.2 antibody. Blue reactivity illustrates the cell nuclei and red reactivity illustrates the reactivity of the antibody. A merged image was also taken to illustrate the location of the antibody reactivity in relation to the cell. Note the membrane fluorescence (red) in the mOV 18 non-reduced photographs and reduction in fluorescence when the cells are reduced. Also note the opposite occurring in the NN 3.2 antibody treated cells.

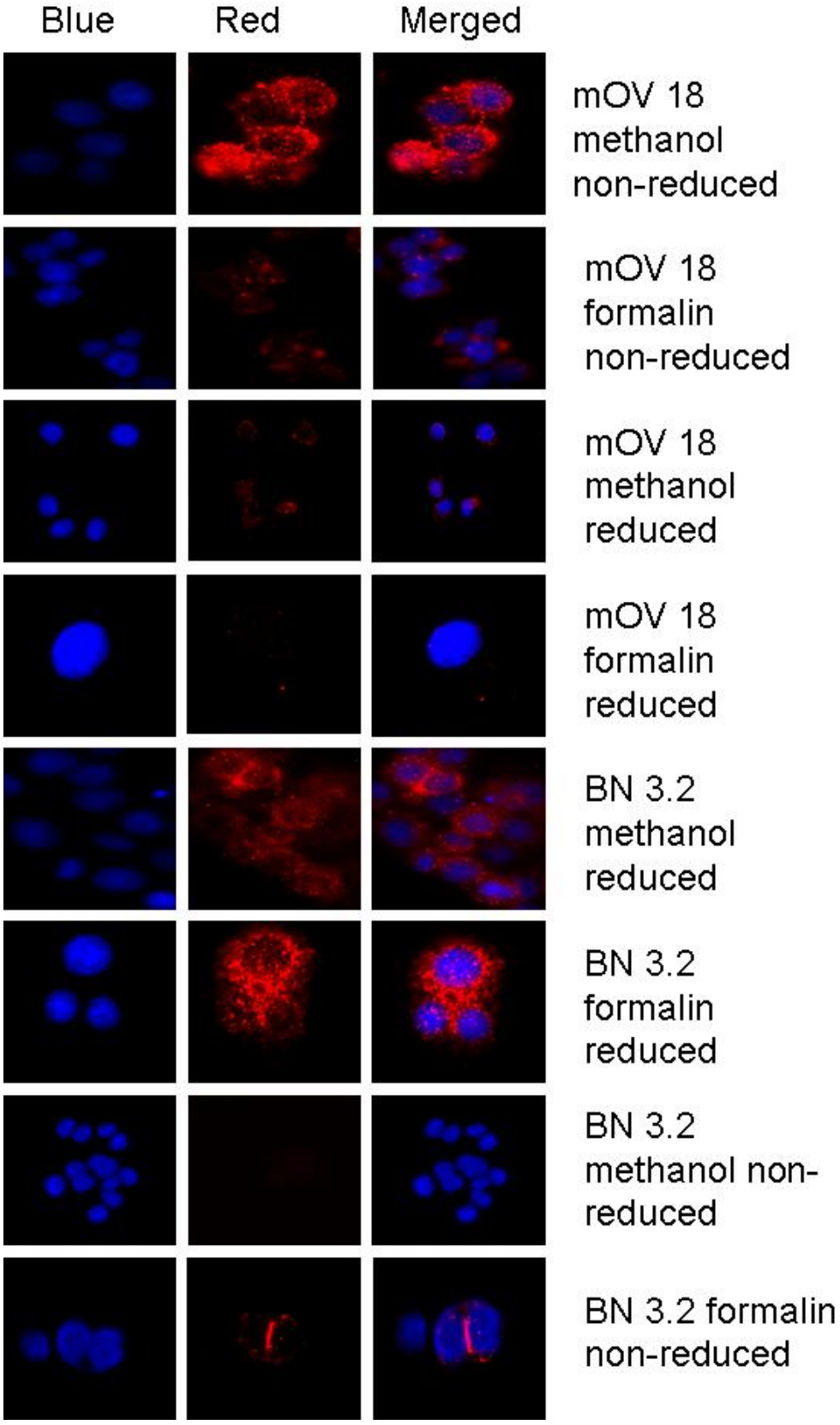

5.16. Immunofluorescence Studies - Discussion

The results seen for the IF studies are similar to that of the frozen studies as it was treatment with a reducing agent which allowed for comparison of fluorescence between the BN3.2 and mOV18 antibodies. The fluorescence observed with the reduced FR-α sample was similar to that of the non-reduced mOV18 control fixed in methanol. The fixation method used did not appear to have a significant effect on the epitope recognised by the BN 3.2 antibody, however, methanol was the only fixation method suitable for the mOV18 antibody (Figure 5-6). This suggests that the mOV 18 epitope is quite unstable and treatment of the cells easily destroys the epitope, this also supports the fact mOV 18 is unsuitable for use on FFPE samples.

Although these studies have provided interesting information on the applications of the BN 3.2 antibody the main focus of these studies has been proven to be unsuccessful. It was hoped that the BN 3.2 antibody, if suitable for use on frozen tissue and by IF may have potential neutralising properties, however these results have indicated that the epitope recognised, although linear is not exposed on the surface of cells in their native conformation. Although treatment with reducing agents caused epitope retrieval, this would be unsuitable for treatment of cells via growth assays *in vitro* and subsequent *in vivo* studies due to the toxic effects of reducing agents. For this reason it was decided not to perform FACS or growth assays as both these methods are dependent upon the antibody being able to recognize the protein in its native conformation.

It can be concluded that, although possible our antibody is not suited to IF, antibodies such as mOV18 and LK26 may have greater utility in this area as they detect the protein in its native conformation. This is not entirely bad news as there are already two antibodies potentially suitable for this application and the major aim was to generate something novel; these antibodies are also currently in trials as immunotherapeutic agents so the fact our antibody is unlikely to be suitable for this too is neither surprising or disappointing as there is still a gap in the market for antibodies suitable for use on FFPE samples.

Chapter Six

Chapter Six

6. Concluding Remarks and Future Direction

The major aim of this study, which was primarily to generate two monoclonal antibodies with specific reactivity for FR-α and FPGS, suitable for use on paraffin embedded samples, has been successfully achieved. In addition, both antibodies are suitable for use in WB analysis. Prior attempts to generate a specific antibody to FR-α suitable for this application have been unsuccessful. Valuable knowledge has been gained in overcoming problems associated with the generation of antibodies to difficult targets, including comprehensive screening protocols which could also be applied to other difficult targets.

In addition to successful generation of the antibodies, the ovarian TMA study and subsequent statistical analysis found a significant association between high FR-α expression and poor survival, which indicates a role for FR-α as a valuable prognostic marker of survival in ovarian cancer patients in combination with other independent markers of prognosis. Future studies using the FR-α antibody on paraffin embedded tissue may be extremely significant in the diagnosis, treatment and prognostic outcome of patients with ovarian cancer.

It was hypothesized that BN3.2 may also be of potential use in trials using pemetrexed as an indicator of response to this drug. It was disappointing to subsequently find no association between expression of FR-α and pemetrexed activity in MPM. Although this may not be the case for pemetrexed, there are now a number of small molecule therapies currently being evaluated which have been shown to have high affinity for FR-α over the RFC. BN3.2 may have a role to play as a companion disgnostic for these compounds if they are found to be effective antitumour agents.

Future work to carry out additional testing using FR-α on panels of tumours other than ovarian cancers or MPM such as colon carcinomas, breast, endometrial cancer and other solid tumour samples may also be of value. Although these tumours may not express FR- α as consistently, identification of subgroups of patients likely to respond to FR-α targeted therapies would also indicate a role for our antibody, again as a companion diagnostic.

A study assessing the expression of FPGS and response to pemetrexed in various tumours, particularly MPM would be extremely interesting as this protein may also be of importance in the determination of response since antifolates are polyglutamated. Although the FPGS statistical analysis did not find it to be a significant marker of prognosis it did follow a very similar trend to that of FR-α and use of the FPGS antibody as a predictor of response cannot be ruled out. This may not be restricted to ovarian cancer, particularly as it has a much wider pattern of expression than FR-α. Although it is constitutively expressed in the majority of proliferating cells its expression is higher in tumours and the difference in intensity can be easily observed via IHC analysis.

The cell studies discussed in this project provide useful preliminary data, investigation of the effect of oestrogen regulation, extracellular folate concentration and the expression of FR-α in breast cancer are worthy of further investigation and the results of our studies support this as there is much to learn in these areas.

The initial aim was to generate a panel of antibodies suitable for a number of different applications, however the problems encountered during molecular biology limited this and eventually only one successful antibody was generated for each protein. This is likely to be due to the extensive additional antibody screening protocol designed to ensure the antibodies generated were specific for the target alone which significantly reduced the number of clones handled at each stage. This was necessary to ensure there were no soluble stress proteins contaminating the samples to which antibodies could be generated. Despite this, the antibodies generated have now been proven to be highly specific for their targets and are suitable for use both on paraffin sections and via Western blot. Their specificity has been further confirmed by epitope mapping analysis which confirmed that both antibodies recognised a linear epitope present in their target sequence. The problems encountered in molecular biology may also explain the reason for previous unsuccessful attempts to generate an antibody to FR-α suitable for use on paraffin sections.

The frozen and IF studies have been able to provide valuable insight into the potential uses of the FR-α antibody, indicating uses not only for FFPE IHC and WB but, with modification of existing techniques, potential application in both IF and Frozen IHC. It is unlikely it will routinely

be utilised for such techniques when antibodies suitable for use in these applications are already commercially available and have been for a significant time.

It is disappointing that the application of BN3.2 in FACS and growth assays were found to be limited, however, it is not surprising as this antibody was specifically designed for use on FFPE sections. It is highly unlikely that one antibody be suitable for applications where the protein is both fixed and in its native conformation, as demonstrated previously by the mOV 18 and LK26 antibodies which carry unstable, conformational epitopes and are only suitable for IHC on frozen tissue. As these antibodies are unsuitable for routine applications it makes the work performed in this project novel, it also indicates a role for BN3.2 as a companion diagnostic to be used in combination with potential neutralizing antibodies as well as small molecule therapies. BN3.2 was not found to have any potential as a neutralising antibody, this is likely to be due to both the avoidance of key residues required for protein activity in order to comply with GMAG regulations and the cysteine rich sequence causing extensive folding of the protein. Neutralising antibodies are likely to recognise active residues and recognise epitopes in their native, conformational form. As these antibodies were specifically designed for use on paraffin sections, in hindsight, this is probably not the most appropriate method to use for neutralising antibody design. Generation of an antibody suitable for use on paraffin is probably of more value in this instance as there are already two potential neutralising antibodies on the market which are both undergoing trials.

The results of the oestrogen regulation study could also be expanded upon by repeating this experiment, assessing other potential modulators of FR-α expression such as caveolin 1 (Bagnoli et al., 2000; Sanna et al., 2007), the glucocorticoid receptor (Tran et al., 2005) or retinoic acid receptor would also be an interesting area of investigation, unfortunately in this particular study time limited further investigations in this area (Bolton et al., 1999). This is a particularly important area of research as modulation to selectively overexpress FR-α in malignant cells would be extremely advantageous in enhancing antifolates uptake by pathologic cells and reduction of toxicity in normal tissue. This ‘magic bullet’ approach is the major aim in the research of all types of cancer and the antibodies generated in this project will greatly assist such future studies.

Useful information on the antibody epitope recognition sites has also been elucidated, allowing future work to be directed appropriately. Both antibodies are also commercially available, filling the gap in the market and increasing the potential for further, large scale studies to be carried out.

In conclusion, both antibodies will be valuable tools for assessment of FR-α and FPGS expression in a variety of tumours, I confident that now they are commercially available they are an important tool and will play an extremely valuable role in both the diagnosis and treatment of not only ovarian malignancies but also subsets of other human cancers with high FR-α expression. Perhaps they may be even more important as companion diagnostics for tumours other than ovarian malignancies where the expression is less consistent and as determinants of response for all future FR-α directed therapies.

References

References

Alberts, B., Johnson, A., Lewis, J., Raff, M., Roberts, K., & Walter, P. 2002. ***Molecular Biology of the Cell*** (Fourth ed.): Garland Science Taylor and Francis Group.

Alkan, S. S. 2004. Monoclonal antibodies: The story of a discovery that revolutionised science and medicine. ***Nature Review Immunology***, 4: 153-156.

Antony, A. C. 1992. The biological chemistry of folate receptors. ***Blood***, 79: 2807-2820.

Antony, A. C. 1996. Folate Receptors. ***Annual Review of Nutrition***, 16: 501-521.

Antony, A. C., Kane, M. A., Portillo, R. M., Elwood, P. C., & Kolhouse, J. 1985. Studies of the role of a particulate folate binding protein in the uptake of 5-methyltetrahydrofolate by cultured human KB cells. ***Journal of Biological Chemistry***, 260: 14911-14917.

Antony, A. C., Tang, Y. S., Khan, R. A., Biju, M. P., Xiao, X., Li, Q. J., Sun, X. L., Jayaram, H. N., & Stabler, S. P. 2004. Translational upregulation of folate receptors is mediated by homocysteine via RNA-heterogenous nuclear riboprotein E1 interactions. ***Journal of Clinical Investigation***, 113(2): 285-301.

Armstrong, D. K. 2009. Efficacy and safety of farletuzumab, a humanized monoclonal antibody to folate receptor alpha, in platinum-sensitive relapsed ovarian cancer subjects: preliminary data from a phase-2 study. ***European Journal of Cancer***, 7(7): 449.

Bagnoli, M., Tomassetti, A., Figni, M., Flati, S., Dolo, V., Canevari, S., & Miotti, S. 2000. Downmodulation of caveolin-1 expression in human ovarian carcinoma is directly related to alpha folate receptor overexpression. ***Oncogene***, 19: 4754-4763.

Baneyx, F. 1999. Recombinant protein expression in Escherichia coli. ***Current Opinion in Biotechnology***, 10: 411-421.

Barredo, J. C., & Moran, R., . 1992. Determinants of antifolate cytotoxicity: folylpolyglutamate synthetase activity during cellular proliferation and development. ***Molecular Pharmacology***, 42: 687-694.

Basal, E., Eghbali-Fatourechi, G. Z., Kalli, K. R., Hartmann, L., Goodman, K., Goode, E. L., Kamen, B. A., Low, P. S., & Knutson, K. L. 2009. Functional folate receptor alpha is elavated in the blood of ovarian cancer patients. ***PLoS One***, 4(7): e6292.

Berg, J. M., Tymoczko, J. L., & Stryer, L. 2002. ***Biochemistry*** (5th ed.): W.H Freeman and Co New York.

Berry, J. D. 2005. Rational monoclonal antibody development to emerging pathogens, biothreat agents and agents of foreign animal disease: The antigen scale. ***The Veterinary Journal***, 170: 193-211.

Bolton, J. A., Wood, S. A., Kennedy, D., Don, R. H., & Mattick, J. S. 1999. Retinoic acid-dependent upregulation of mouse folate receptor alpha expression in embryonic stem cells, and conservation of alternate splicing patterns. ***Gene***, 230(215-224).

Brown Jones, M., Neuper, C., Clayton, A., Mariani, A., Konecny, G., Bijoy Thomas, M., Keeney, G., Hartmann, L., & Podratz, K. C. 2008. Rationale for folate receptor alpha targeted therapy in high risk endometrial carcinomas. ***International Journal of Cancer***, 123: 1699-1703.

Brzczinsca, A., Winska, P., & Balinska, M. 2000. Cellular aspects of folate and antifolate membrane transport. ***Acta Biochimica Polonica***, 47(3): 735-749.

Bueno, R., Appasani, K., Mercer, H., Lester, S., & Sugarbaker, D. 2001. The alpha folate receptor is highly activated in malignant pleural mesothelioma. ***Journal of Thoracic and Cardiovascular Surgery***, 121(2): 223-233.

Campbell, I. G., Jones, T. A., Foulkes, W. D., & Trowsdale, J. 1991. Folate binding protein is a marker for ovarian cancer. ***Cancer Research***, 51: 5329-5338.

Chattopadhyay, S., Wang, Y., Zhao, R., & Goldman, I. D. 2004. Lack of impact of the loss of constitutive folate receptor alpha expression, achieved by RNA interference, on the activity of the new generation antifolate Pemetrexed in HeLa cells. ***Clinical Cancer Research***, 10: 7986-7993.

Chen, L., Qi, H., Korenberg, J., Garrow, T., Choi, Y., J., & Shane, B. 1996. Purification and properties of human cytosolic folylpolyglutamate synthetase and organization, localization, and differential splicing of its gene. ***Journal of Biological Chemistry***, 271(22): 13077-13087.

Chen, V. J., Bewley, J. R., Andis, S. L., Schulz, R. M., Iversen, P. W., Shih, C., Mendelsohn, L. G., Seitz, D. E., & Tonkinson, J. L. 1998. Preclinical cellular pharmacology of LY231514 (MTA): A comparison with methotrexate, LY309887 and raltitrexed for their effects on intracellular folate and nucleoside triphosphate pools in CCRF-CEM cells. ***British Journal of Cancer***, 78: 27-34.

Coney, L. R., Tomassetti, A., Carayannopoulos, L., Frasca, V., Kamen, B. A., Colnaghi, M. I., & Zurawski, D. S. 1991. Cloning of a tumor-associated antigen: mOV18 and MOv19 antibodies recognize

a folate-binding protein. ***Cancer Research***, 51: 6125-6132.

Coons, A. H., Creech, H. J., & Jones, R. N. 1941. Immunological properties of an antibody containing a fluorescent group. ***Proceedings of the Society for Experimental Biological Medicine***, 47: 200-202.

Costa, P. P., Jacobsson, B., Collins, P., & Biberfeld, P. 1986. Unmasking antigen determinants in amyloid. ***Journal of Histochemistry and Cytochemistry***, 34(12): 1683-1685.

Crippa, F., Bolis, G., Seregni, E., Gavoni, N., Scarfone, G., Ferraris, C., Buraggi, G. L., & Bombardieri, E. 1994. Single-dose intraperitoneal radioimmunotherapy with the murine monoclonal antibody I-131 MOv18: Clinical results in patients with minimal residual disease of ovarian cancer. ***European Journal of Cancer***, 31a(5): 686-690.

Dainty, L. A., Risinger, J. I., Morrison, C., Chandramouli, G. V. R., Bidus, M. A., Zahn, C., Rose, S., Fowler, J., Berchuck, A., & Maxwell, G. L. 2007. ***Overexpression of folate binding protein and mesothelin are associated with uterine serous carcinoma***.

Doucette, M. M., & Stevens, V. L. 2001. Folate receptor function is regulated by response to different cellular growth rates in cultured mammalian cells. ***Biochemical and Molecular Action of Nutrients***, 14: 2819-2825.

Ebel, W., Routhier, E. L., Foley, B., Jacob, S., McDonough, J. M., Patel, R. K., Turchin, H. A., Chao, Q., Kline, B., Old, L. J., Phillips, M. D., Nicolaides, N. C., Sass, P., & Grasso, L. 2007. Preclinical evaluation of MORAb003, a humanized monoclonal antibody antagonising folate receptor alpha. ***Cancer Immunity***, 7: 6-12.

Egan, M. G., Sirlin, S., Rumberger, B. G., Garrow, T. A., Shane, B., & Sirotnak, F. M. 1995. Rapid decline in folylpolyglutamate synthetase activity and gene expression during maturation of HL-60 cells. ***Journal of Biological Chemistry***, 270: 5462-5468.

Elnakat, H., Gonit, M., Alincourt., D., Salazar, M., Zhang, J., Basrur, V., Gunning, W., Kamen, B. A., & Ratnam, M. 2009. regulation of folate receptor internalisation by protein kinase C alpha. ***Biochemistry***, 48: 8429-8260.

Elnakat, H., & Ratnam, M. 2004. Distribution, functionality and gene regulation of folate receptor isoforms: implications in targeted therapy. ***Advanced Drug Delivery Reviews***, 56: 1067-1084.

Elwood, P. C., Nachmanoff, K., Saikawa, Y., Page, S. T., Pacheco, P., Roberts, S., & Chung, K. N. 1997. The divergent 5 termini of the human folate receptor (hFR) mRNA's originate from two tissue specific promoters and alterative splicing: characterisation of the hFR gene structure. ***Biochemistry***, 36: 1467-1478.

Evans, C. O., Young, A. N., Brown, M. R., Brat, D. J., Parks, J. S., Neish, A. S., & Oyesiku, N. M. 2001. Novel patterns of gene expresison in pituitary adenomas identified by complementary deoxyribonucleic acid microarrays and quantitative reverse transcription polymerase chain reaction. ***Journal of Clinical Endocrinological Metabolism***, 86: 3097-3107.

Exinger, D., Exinger, F., Mennecier, B., Limacher, J. M., Dufour, P., & Kurtz, J. E. 2003. Multitargeted antifolate (Pemetrexed): A comprehensive review of its mechanisms of action, recent results and future prospects. ***Cancer Therapy***, 1: 315-322.

Fitzpatrick, A. 2003. Folate (Folic Acid): Implications for health and disease. In A. F. Industry (Ed.), May/June ed., Vol. 2003. Chatsworth, CA.

Freemantle, S. J., & Moran, R. 1997. Transcription of the human folylpolyglutamate synthetase gene. ***Journal of Biological Chemistry***, 272(40): 25373-25379.

Freemantle, S. J., Taylor, S., M., Krystal, G., & Moran, R., . 1995. Upstream organization of and multiple transcripts from the human folylpolyglutamate synthetase gene. ***Journal of Biological Chemistry***, 270(16): 9579-9584.

Freund, J. 1956. The mode of action of immunologic adjuvants. ***Bibl Tuberc***, 10: 130-148.

Freund, J., & Mc Dermott, K. 1942. Sensitization to horse serum by means of adjuvants. ***Proceedings of the Society for Experimental Biological Medicine***, 49: 548-553.

Galpin, A. J., Schuetz, J. D., Masson, E., Yanishevski, Y., Synold, T. W., Barredo, J. C., Pui, C. H., Relling, M. V., & Evans, W. E. 1997. Differences in folylpolyglutamate synthetase and dihydrofolate reductase expression in human B- lineage versus T- lineage leukaemic lymphoblasts: mechanisms for lineagic differences in methotrexate polyglutamation and cytotoxicity. ***Molecular Pharmacology***, 52: 155-163.

Garin-Chesa, P., Campbell, I. G., Saigo, P. E., Lewis, J. L. J., Old, L. J., & Rettig, W. J. 1993. Trophoblast and ovarian cancer antigen LK26. Sensitivity and specificity in immunopathology and molecular identification as a folate binding protein. ***American Journal of Pathology***, 142(2): 557-567.

Gates, S. B., Worzalla, J. F., Shih, C., Grindley, G. B., & Mendelsohn, L. G. 1996. Dietary folate and folylpolyglutamate synthetase activity in normal and neoplastic murine tissues and human tumour xenografts. ***Biochemical Pharmacology***, 52: 1477-1479.

Gibbs, D. D., Theti, D. S., Wood, N., Green, M., Raynaud, F., Valenti, M., Forster, M. D., Mitchell, F., Bavetsias, V., Henderson, E., & Jackman, A. L. 2005. BGC 945, a novel tumor-selective thymidylate synthase inhibitor targeted to alpha folate receptor overexpressing tumours. ***Cancer Research***, 65(24): 11721-11728.

Gish, W., & States, D. J. 1993. Identification of protein coding regions by database similarity search. ***Nature Genetics***, 3(3): 266-272.

Goldsby, R. A., Kindt, T. J., Osborne, B. A., & Kiuby, J. 2003. ***Immunology (Fifth Edition)***. New York.

Green, J. M., MacKenzie, R. E., & Matthews, R. G. 1988. Substrate flux through methylenetetrahydrofolate dehydrogenase: predicted effects on the concentration of methylenetetrahydrofolate on its partitioning into pathways leading to nucleotide biosynthesis or methionone regeneration. ***Biochemistry***, 27: 8014-8022.

Guyton, A. C., & Hall, J. E. 1997. ***Immunity, Allergy, Blood Groups and Infection: Human Physiology Mechanisms and Disease***. Philadelphia.

Hainsworth, J. D. 2000. Monoclonal antibody therapy in lymphoid malignancies. ***Oncologist***, 5: 376-384.

Hainsworth, J. D., Burris, H. A., Morrisey, L. H., Litchey, S., Scullin, D. L., Bearden, J. D., Richards, P., & Greco, F. A. 2000. Rituximab monoclonal antibody as initial systemic therapy for patients with low-grade non-Hodgkin lymphoma. ***Blood***, 95: 3052-3056.

Haller, D. G. 2001. Update of clinical trials with edrecolomab: a monoclonal antibody therapy for colorectal cancer. ***Seminars in Oncology***, 28: 25-30.

Hanauske, A., R., Eismann, U., Oberschmidt, O., Pospisil, H., Hoffman, S., Hanauske-Abel, H., Ma, D., Chen, V. J., Paoletti, P., & Niyikiza, C. 2007. In vitro chemosensitivity of freshly explanted tumour cells to pemetrexed is correlated with target gene expression. ***Invest New Drugs***, 10: 9060-9069.

Harris, H., & Watkins, J. F. 1965. Hybrid cells derived from mouse and man: Artificial heterokaryons of mammalian cells from different species. ***Nature***, 205: 640-646.

Hartmann, L. C., Keeney, G., Lingle, W. L., Christianson, T. J. H., Varghese, B., Hillman, D., Oberg, A., & Low, P. S. 2007. Folate receptor expression is associated with poor outcome in breast cancer. ***International Journal of Cancer***, 121: 938-942.

Henderson, G. B. 1990. Folate-binding proteins. ***Annual Review of Nutrition***, 10: 319-335.

Hernando, J. J., Park, T. W., Fishcher, H. P., Zivanovic, O., Braun, M., Polcher, M., Grunn, U., Leutner, C., Potszch, B., & Kuhn, W. 2007. Vaccination with dendritic cells transfected with mRNA encoded folate receptor alpha for relapsed metastatic ovarian cancer. ***The Lancet Oncology***, 8: 451-454.

Jackman, A. L., Theti, D. S., & Gibbs, D. D. 2004. Antifolates targeted specifically to the folate receptor. ***Advanced Drug Delivery Reviews***, 56: 1111-1125.

Jaton, J. C., & Riesen, W. 1976. The relationship between hypervariable regions, antigen binding specificity and the three dimensional structure of antibodies. ***Annals of Immunology***, 127(3-4): 273-283.

Kamen, B. A., & Smith, A. K. 2004. A review of folate receptor alpha cycling and 5-methyltetrahydrofolate accumulation with an emphasis on cell models in vitro. ***Advanced Drug Delivery Reviews***, 56: 1085-1097.

Kamen, B. A., Wang, M. T., Streckfuss, A. J., Peryea, X., & Anderson, R. 1988. Delivery of folates to the cytoplasm of MA104 cells ismediated by a surface receptor thay recycles. ***Journal of Biological Chemistry***, 263: 13602-13609.

Kane, M. A., Elwood, P. C., Portillo, R. M., Antony, A. C., Najfield, V., Finley, A., Waxman, S., & Kolhouse, J. 1988. Influence on immunoreactive folate binding proteins of extracellular folate concentration in cultured human cells. ***Journal of Clinical Investigation***, 81: 1398-1406.

Kaufmann, S. H. E., Schoel, B., van Embden, J. D. A., Koga, T., Wand-Wurtenburger, A., Munk, M. E., & Steinhoff, U. 1991. Heat shock protein 60: Implication for pathogenesis and protection against bacterial infection. ***Immunological Reviews***, 121: 67-90.

Kelemen, L. 2006. The fole of folate receptor alpha in cancer development, progression and treatment: Cause, consequence or innocent bystander? ***International Journal of Cancer***: 1-13.

Kelley, K. M. M., Rowan, B. G., & Ratnam, M. 2003. Modulation of the folate receptor alpha gene by the estrogen receptor: Mechanism and implications in tumour targeting. ***Cancer Research***, 63: 2820-2828.

Kiessling, R., Wasserman, K., & Horiguchi, S. 1999. Tumour induced immune dysfunction. ***Cancer Immunology and Immunotherapy***(48): 353-362.

Kohler, G., Howe, S., & Milstein, C. 1976. Fusion between immunoglobulin-secreting and non-secreting myeloma cell lines. ***European Journal of Immunology***, 6: 292-295.

Kohler, G., & Milstein, C. 1975. Continuous cultures of fused cells secreting antibody of pre-defined specificity. ***Nature***, 495-497.

Kohler, G., & Milstein, C. 1976. Derivation of specific antibody producing tissue culture and tumour lines by cell fusion. ***European Journal of Immunology***, 6: 511-519.

Konner, J. A., Bell-McGuinn, K. M., Sabbatini, P., Hensley, M. L., Tew, W. P., Pandit-Taskar, N., Vander Els, N., Phillips, M. D., Schweizer, C., Weil, S. C., Larson, S. M., & Old, L. J. 2010. Farletuzumab, a humanized monoclonal antibody against folate receptor alpha, in epithelial ovarian cancer: a phase I study. ***Clinical Cancer Research***, 16(21): 5288-5295.

Kranz, D. M., Partrick, T. A., Brigle, K. E., Spinella, M. J., & Roy, E. J. 1995. Conjugates of folate and anti T-cell-receptor antibodies specifically target folate receptor positive tumour cells for lysis. ***Proceedings of the National Academy of Sciences***, 92: 9057-9061.

Langdon, S. P., Rabiasz, G. J., Hirst, G. L., King, R. B., Hawkins, R. A., Smyth, J. F., & Miller, W. R. 1995. Expression of heat shock protein HSP 27 in human ovarian cancer. ***Clinical Cancer Research***, 1: 1603-1609.

Le Roy, C., & Wrana, J. 2005. Clathrin and non-clathrin mediated endocytic regulation of cell signalling. ***Nature Reviews Molecular Cell Biology***.

Leclerec, G. J., & Barredo, J. C. 2001. Folylpolyglutamate synthetase gene mRNA splice variants and protein expression in primary human leukaemia cells, cell lines and normal human tissues. ***Clinical Cancer Research***, 7: 942-951.

Leclerec, G. J., Leclerec, G. M., Kinser, T. T. H., & Barredo, J. C. 2006. Analysis of folylpolyglutamate synthetase gene expression in human B-precursor ALL and T-lineage ALL cells. ***Cancer***, 6: 132-143.

Leil, T. A., Endo, C., Adjei, A. A., Dv, G. K., Salavaggione, O. E., Reid, J. R., Ames, M. M., & Adjei, A. A. 2007. Identification and characterisation of genetic variation in the folylpolyglutamate synthetase gene. ***Cancer Research***, 67(18): 8772-8782.

Luckow, V. A., & Summers, M. D. 1988. Trends in the development of baculovirus expression vectors. ***Biotechnology***, 6: 47-55.

Lucock, M. 2000. Folic Acid: Nutritional Biochemistry, molecular biology, and role in disease processes. ***Molecular Genetics and Metabolism***, 71: 121-138.

Mangiarotti, F., Miotti, S., Galmozzi, E., Mazzi, M., Sforzini, S., Canevari, S., & Tomassetti, A. 2001. Functional effect of point mutations in the alpha folate receptor gene of CABA I ovarian carcinoma cells. ***Journal of Cellular Biochemistry***, 81: 488-498.

Mantovani, L. T., Miotti, S., Menard, S., Canevari, S., Raspaglesi, F., Bottini, C., Bottero, F., & Colnaghi, M. I. 1994. Folate binding protein distribution in normal tissues and biological fluids from ovarian carcinoma patients as detected by the monoclonal antibodies mOV18 and mOV 19. ***European Journal of Cancer***, 30A(3): 16-39.

Mattanovich, D., Gasser, B., Hohenblum, H., & Sauer, M. 2004. Stress in recombinant protein producing yeasts. ***Journal of Biotechnology***, 113: 121-135.

Matthews, R. G. 1984. ***Methionine biosynthesis: In folates and pterins***. New York: Wiley.

Mayor, S., & Reizman, H. 2004. GPI anchored protein precursor and anchor structure. ***Nature Reviews Molecular Cell Biology***, 5: 110-120.

Mayor, S., Rothberg, K. G., & Maxfield, F. 1994. Sequestration of GPI-anchored proteins in caveolae triggered by cross-linking. ***Science***, 264(1948-1951).

Mayor, S., Sabharanjak, S., & Maxfield, F. 1998. Cholesterol-dependent retention of GPI-anchored proteins in endosomes. ***EMBO Journal***.

Mc Guire, J. J., Russell, C., & Balinska, M. 2000. Human cytosolic and mitochondrial folylpolyglutamate synthetase are electrophoretically distinct. ***Journal of Biological Chemistry***, 275(17): 13012-13016.

Mc Guire, J. J., & Russell, C. A. 1998. Folylpolyglutamate synthetase expression in antifolate-sensitive and resistant human cell lines. ***Oncology Research***, 10(4): 193-200.

Miotti, S., Canevari, S., Menard, D., Mezzanzanica, D., Porro, G., Pupa, S. M., Regazzoni, M., Talgiabue, E., & Colnaghi, M. I. 1987. Characterisation of human ovarian carcinoma associated antigens defined by novel monoclonal antibodies with tumour restricted specificity. ***International Journal of Cancer***, 39: 297-303.

Miotti, S., Facheris, P., Tomassetti, A., Bottero, F., Bottini, C., Ottone, F., Colnaghi, M. I., Bunni, M. A., Priest, D. G., & Canevari, S. 1995. Growth of ovarian-carcinoma cell lines at physiological folate concentration: effect on folate-binding protein expression in vitro and in vivo. ***International Journal of Cancer***, 63(3): 395-401.

Mitchell, H. K., Snell, E. E., & Williams, R. J. 1941. The concentration of folic acid. ***Journal of the American Chemical Society***, 63: 2284.

Morshed, K. M., Ross, D. M., & McMartin, K. E. 1997. Folate transport proteins mediate the bidirectional transport of 5-methyltetrahydrofolate in cultured human proximal tubule cells. ***Journal of Nutrition***, 127: 1137-1147.

Mullis, K., Faloona, F., Scharf, S., Salki, R., Horn, G., & Erlich, H. 1986. Specific enzymatic amplification of DNA in vitro, The polymerase chain reaction. ***Cold Spring Harbour Symposium of Quantitative Biology***, 51: 263-273.

Nair, J. R., & Mc Guire, J. J. 2005. Submitochondrial localization of the mitochondrial isoform of folylpolyglutamate synthetase in CCRF-CEM human T-lymphoblastic leukaemia cells, ***Biochimica et Biophysica Acta***.

Nakopolou, L., Lazaris, A. C., Baltas, D., Giannopolou, I., Kanvantzas, N., & Tzonou, A. 1995. Prognostic evaluation of oestrogen regulated protein immunoreactivity in ductal invasive (NOS) breast cancer. ***Virchows Archiv***, 427(1): 33-40.

Nutt, J.E., Razak, A.R.A., O'Toole, K., Black, F., Quinn, A.E., Calvert, A.H., Plummer, E.R., & Lunec, J. (2010) The role of folate receptor alpha (FRα) in the response of malignant pleural mesothelioma to pemetrexed-containing chemotherapy. ***British Journal of Cancer***, 102: 553-560.

Odin, E., Wettergren, Y., Nilsson, S., Willen, R., Carlsson, G., Spears, C. P., Larsson, L., & Gustavvson, B. 2003. Altered gene expression of folate enzymes in adjacent mucosa is associated with outcome of colorectal cancer patients. ***Clinical Cancer Research***, 9: 6012-6019.

Parker, N., Turk, M. J., Westrick, E., Lewis, J. D., Low, P. S., & Leamon, C. 2005. Folate receptor expression in carcinomas and normal tissues determined by quantitative radioligand binding assay. ***Annals of Biochemistry***, 338: 284-293.

Polonen, L. 2000. http://ethesis.helsinki.fi/julkaisut/maa/kotie/vk/polonen/fig3.gif. In U. o. Helsinki (Ed.).

Qiu, A., Jansen, M., Sakaris, A., Min, S. H., Chattopadhyay, S., Tsai, E., Sandoval, C., Zhao, R., Akabas, M. H., & Goldberg, I. D. 2006. Identification of an intestinal folate transporter and the molecular basis for hereditary folate malabsorption. ***Cell***, 127(5): 917-928.

Ramaekers, V. T. H., & Blau, N. 2004. Cerebral folate deficiency. ***Developmental Medicine and Child Neurology***, 46(12): 843-851.

Ramirez, J. M., Ocio, E. M., San Miguel, J. F., & Pandiella, A. 2007. Pemetrexed acts as an antimyeloma agent by provoking cell cycle blockade and apoptosis. ***Leukaemia***, 21: 797-804.

Ramos-Vara. 2005. Technical aspects of immunohistochemistry. ***Vet Pathology***, 42(405-426).

Ratnam, M., Marquardt, H., Duhring, J. L., & Freisheim, J. H. 1989. Homologous membrane folate binding proteins in human placenta, cloning and sequence of cDNA. ***Biochemistry***, 28: 8249-8254.

Reddy, J. A., & Low, P. S. 1998. Folate mediated targeting of therapeutic and imaging agents to cancers. ***Critical Reviews in Therapeutic Drug Carrier Systems***, 15: 587-627.

Rettig, W. J., Cordon-Cardo, C., Koulos, J. P., Lewis, J. L., Oettgen, H. F., & Old, L. J. 1985. Cell surface antigens of human trophoblast and choriocarcinoma defined by monoclonal antibodies. ***International Journal of Cancer***, 35(4): 469-475.

Ritter, T. E., Fajardo, O., Matsue, H., Anderson, R. G. W., & Lacey, S. 1995. Folate receptors targeted to clathrin-coated pits cannot regulate vitamin uptake. ***Proceedings of the National Academy of Sciences***.

Rochefort, H. 1995. Oestrogen and anti-oestrogen regulated genes in human breast cancer. ***Ciba Found Symp***, 191: 254-265.

Rochman, H., Selhub, J., & Karrison, T. 1985. Folate binding protein and the estrogen receptor in breast cancer. ***Cancer Detection and Prevention***, 8(1-2): 71-75.

Romanoff, R. L., Ross, D. M., & Mc Martin, K. E. 2007. Acute ethanol exposure inhibits renal folate transport, but repeated exposure upregulates folate transport proteins in rats and human cells. ***Journal of Nutrition***, 137: 1260-1265.

Rosenberg, A. H., Lade, B. N., Chui, D., Lin, S., Dunn, J. J., & Studier, F. W. 1987. Vectors for selective expression of cloned DNA's by T7 RNA polymerase. ***Gene***, 56: 125-135.

Rosenblatt, D. S. 1995. ***Inherited disorders of folate transport and metabolism*** (7th ed.). New York: Mc Graw Hill book Co.

Ross, D. T., Scherf, U., Eisen, M. B., Perou, C. M., Rees, C., Spellman, P., Lyer, V., Jeffrey, S. S., Van de rijn, M., Waltham, M., Pergamenschikov, A., Lee, J. C., Lashkari, D., Shalon, D., Myers, T. G., Weinstein, J. N., Botstein, D., & Brown, P. O. 2000. Systematic variation in gene expression patterns in human cancer cell lines. ***Nature Genetics***, 24(3): 208-209.

Ross, J. F., Chaudhuri, P. K., & Ratnam, M. 1994. Differential regulation of folate receptor isoforms in normal and malignant tissues in vivo and in established cell lines. Physiologic and clinical implications. ***Cancer***, 73: 2431-2443.

Ross, J. F., Wang, H., Behm, F. G., Mathew, P., Wu, M., Booth, R., & Ratnam, M. 1999. Folate receptor type beta is a neutrophilic lineage marker and is differentially expressed in myeloid leukaemia. ***Cancer***, 85: 348-357.

Rothberg, K. G., Ying, Y. S., Kolhouse, J. F., Kamen, B. A., & Anderson, R. 1990. The glycophospholipid-linked folate receptor internalises folate without entering the clathrin-coated pit endocytic pathway. ***Journal of Cell Biology***, 110: 637-649.

Sabharanjak, S., & Mayor, S. 2004. Folate receptor endocytosis and trafficking. ***Advanced Drug Delivery Reviews***, 56: 1099-1109.

Sadlish, H., Williams, F. M. R., & Flintoff, W. 2002. Cytoplasmic domains of the reduced folate carrier are essential for trafficking, but not function. ***Journal of Biochemistry***, 364: 777-786.

Saiwaka, Y., Price, D., Hance, K. W., Chen, T. Y., & Elwood, P. C. 1995. Structural and functional analysis of the human KB cell folate receptor gene p4 promoter: co-operation of three clustered Sp-1 binding sites with initiator region for basal promoter activity. ***Biochemistry***, 34(9951-9961).

Salih, H. R., & Nussler, V. 2001. Immune escape versus tumour tolerance: how do tumours evade immune surveillance? ***European Journal of Medical Research***, 6: 323-332.

Sanghani, S. P., Sanghani, P. C., & Moran, R. G. 1999. Identification of three key active siteresidues in the c-terminal domain of human recombinant folylpolyglutamate synthetase by site-directed mutagenesis. ***Journal of Biological Chemistry***, 274(38): 27018-27027.

Sanna, E., Miotti, S., Mazzi, M., De Santis, G., Canevari, S., & Tomassetti, A. 2007. Binding of nuclear caveolin 1 to promoter elements of growth associated genes in ovarian carcinoma cells. ***Experimental Cell Research***, 313: 1307-1317.

Schroff, R. W., Foon, K. A., Beatty, S. M., Oldham, R. K., & Morgan, A. C. 1985. Human anti-murine immunoglobulin responses in patients receiving monoclonal antibody therapy. ***Cancer Research***, 45: 879-885.

Shi, S. R., Key, M. E., & Kalra, K. L. 1991. Antigen retrieval in formalin fixed, paraffin embedded tissues: An enhancement method for immunochemical stainingbased on microwave

oven heating of tissue sections. ***Journal of Histochemistry and Cytochemistry***, 39: 741-748.

Shia, J., Klimstra, D. S., Nitzkorski, J. R., Low, P. S., Gonen, M., Landmann, R., Weiser, M. R., Franklin, W. A., Prendergast, F. G., Murphy, L., Tang, L. H., Temple, L., Guillem, J. G., Wong, W. D., & Paty, P. B. 2008. Immunohistochemical expression of folate receptor alpha in colorectal carcinoma: patterns and biological significance. ***Human Pathology***, 39: 498-505.

Simons, K., & Ikonen, E. 1997. Functional rafts in cell membranes. ***Nature***, 387: 569-572.

Singh, S. M., & Panda, A. K. 2005. Solubilization and refolding of bacterial inclusion body proteins. ***Journal of Bioscience and Bioengineering***, 99(4): 303-310.

Smith, H. O. 1979. Nucleotide sequence specificity of restriction endonucleases. ***Science***, 205: 455-462.

Smith, H. O., & Nathans, D. 1973. A suggested nomenclature for bacterial host modification. ***Journal of Molecular Biology***, 81(419-423).

Sohn, K. J., Smirnakis, F., Moskovitz, D. N., Novakovic, P., Yates, Z., Lucock, M., Croxford, R., & Kim, Y. I. 2004. Effects of folylpolyglutamate synthetase modulation on chemosensitivity of colon cancer cells to 5-fluorouracil and methotrexate. ***Gut***, 53: 1825-1831.

Spinella, M. J., Brigle, K. E., Freemantle, S. J., Sierra, E. E., & Goldman, I. D. 1996. Comparison of methotrexate polyglutamation in L1210 leukaemia cells when influx is mediated by the reduced folatre carrier or folate receptor. ***Biochemical Pharmacology***, 52: 703-712.

Studier, F. W., & Moffatt, B. A. 1986. Use of bacteriophage T7 rNA polymerase to direct selective high level expression of cloned genes. ***Journal of Molecular Biology***, 189: 113-120.

Sun, X., Bognar, A. L., Baker, E. N., & Smith, C. A. 1998. Structural homologies with ATP and folate binding enzymes in the srystal structure of folylpolyglutamate synthetase. ***Proceedings of the National Academy of Sciences***, 95: 6647-6652.

Sun, X. L., Cross, J. A., Bognar, A. L., Baker, E. N., & Smith, C. A. 2001. Folate binding triggers the action of folylpolyglutamate synthetase. ***Journal of Molecular Biology***, 310: 1067-1078.

Takimoto, C. H. 1997. Antifolates in clinical development. ***Seminars in Oncology***, 24(18): 40-51.

Theti, D. S., & Jackman, A. L. 2004. The role of alpha-folate receptor-mediated transport in the antitumour activity of antifolate drugs. ***Clinical Cancer Research***, 10: 1080-1089.

Thompson-Hayner, N., Driscoll, J., Ferayorni, L., Spies-Karotkin, G., & Jauregui, H. O. 1982. Ponceau S: A sensitive method for protein determination in freshly isolated and cultured cells. ***Methods in Cell Science***, 7(2): 77-80.

Toffoli, G., Cernigoi, C., Russo, A., Gallo, A., Bagnoli, M., & Boiocchi, M. 1997. Overexpression of folate binding protein in ovarian cancers. ***International Journal of Cancer***, 74: 193-198.

Toffoli, G., Russo, A., Gallo, A., Cernigoi, C., Miotti, S., Sorio, R., Tumolo, S., & Boicchi, M. 1998. Expression of folate binding protein as a prognostic factor for response to platinum containing chemotherapy and survival in human ovarian cancer. ***International Journal of Cancer***, 79: 121-126.

Tomassetti, A., Coney, L. R., Canevari, S., Miotti, S., Facheris, P., Zurawski, V. R., & Colnaghi, M. I. 1993. Isolation and biochemcal characterisation of the soluble and membrane forms

of folate binding protein expressed in the ovarian carcinoma cell line IGROV-1. ***Federation of European Biochemical Societies***, 317(1,2): 143-146.

Tomassetti, A., Mangiarotti, F., Mazzi, M., Sforzini, S., Miotti, S., Galmozzi, E., Elwood, P. C., & Canevari, S. 2003. The variant hepatocyte nuclear factor 1 activates the P1 promoter of the human alpha folate receptor gene in ovarian carcinoma. ***Cancer Research***, 63: 696-704.

Tran, T., Shatnawi, A., Zheng, X., Kelley, K. M. M., & Ratnam, M. 2005. Enhancement of folate receptor alpha expression in tumour cells through the glucocorticoid receptor: a promising means to improved tumour detection and targeting. ***Cancer Research***, 65(10): 4431-4441.

Veggian, R., Fasolato, S., Menard, D., Minucci, D., Pizzetti, P., Regazzoni, M., Tagliabue, E., & Colnaghi, M. I. 1989. Immunohistochemical reactivity of a monoclonal antibody prepared against human ovarian carcinoma on normal and pathological female genital tissues. ***Tumori***, 75: 510-513.

Voet, D., & Voet, J. G. 2004. ***Biochemistry*** (3rd ed.): Wiley.

Wang, y., Zhao, R., & Goldman, I. D. 2003. Decreased expression of the reduced folate carrier and folylpolyglutamate synthetase is the basis for acquired resistance to the pemetrexed antifolate (LY231514) in an L210 murine leukaemia cell line. ***Biochemical Pharmacology***, 65(1163-1170).

Ward, R. L., Hawkins, N. J., Coomber, D., & Disis, M. L. 1999. Antibody immunity to the HER-2/neu oncogenic protein in patients with colorectal cancer. ***Human Immunology***, 60: 510-515.

Weitman, S. D., Lark, R. H., Coney, L. R., Fort, D. W., Frasca, V., Zurawski, V. R., & Kamen, B. A. 1992a. Distribution of the folate receptor GP38 in normal and malignant cell lines and tissues. ***Cancer Research***, 52: 3396-3401.

Weitman, S. D., Weinberg, L. R., Coney, L. R., Zurawski, D. S., Jennings, D. S., & Kamen, B. A. 1992b. Cellular localisation of the folate receptorpotential role in drug toxicity and folate homeostasis. ***Cancer Research***, 52: 6708-6711.

Whetstine, J. R., Flatley, R. M., & Matherley, L. H. 2002. The human reduced folate carrier gene is ubiquitously and differentially expressed in normal human tissues: identification of seven non-coding exons and characterisation of a novel promoter. ***Journal of Biochemistry***, 367: 629-640.

Wollack, J. B., Makori, B., Ahlawat, S., Koneru, R., Picinich, S. C., Smith, A. K., Goldman, I. D., Qiu, A., Cole, P. D., Glod, J., & Kamen, B. A. 2007. Characterization of folate uptake by choroid plexus epithelial cells in a rat primary culture model. ***Journal Of Neurochemistry***, 104(6): 1494-1503.

Wu, M., Gunning, W., & Ratnam, M. 1999. Expression of folate receptor type alpha in relation to cell type, malignancy and differentiation in ovary, uterus and cervix. ***Cancer Epidemiology***, 8: 775-782.

Yancik, R. 1993. Ovarian Cancer. Age contrasts in incidence, histology, disease sytage at diagnosis. ***Cancer***, 72(2): 517-523.

Yang, R., Kolb, A., Qin, J., Chou, A., Sowers, R., Hoang, B., Healey, J. H., Huvos, A. G., Meyers, P. A., & Gorlick, R. 2007. The folate receptor alpha is frequently overexpressed in

osteosarcoma samples and plays a role in the uptake of the physiologic substrate 5-methyl tetrahydrofolate. ***Clinical Cancer Research***, 13(9): 2557-2567.

Yasuda, S., Hasui, S., Yamamoto, C., Yoshioka, C., Kobayashi, M., Itagaki, S., Hirano, T., & Iseki, K. 2008. Placental Folate Transport during Pregnancy. ***Bioscience, Biotechnology, and Biochemistry***, 72(9): 2277-2284.

Zhao, R., & Goldman, I. D. 2007. The molecular identity and characterization of a proton-coupled folate transporter - PCFT; biological ramifications and impact on the activity of pemetrexed. ***Cancer Metastasis Reviews***, 26: 129-139.

Zhao, X., Li, H., & Lee, R. J. 2008. Targeted drug delivery via folate receptors. ***Expert Opinion in Drug Delivery***, 5(3): 309-319.

Appendices

Publications